

**Alternative Chelating Agents:  
Evaluation of Ready-Biodegradability, Complexation  
Properties and Suitability for Agricultural Practices**

Dissertation Presented to Faculty of Engineering, University of Porto for the Degree of  
Doctor in Environmental Engineering

João Pedro Costa Graça Martins

**Supervisor:** Doctor Helena Maria Vieira Monteiro Soares



Chemical Engineering Department  
Faculty of Engineering, University of Porto  
Portugal

July 2014



## Acknowledgments

I would like to acknowledge my supervisor, Professora Doutora Helena Soares, for giving me the opportunity to be part of this project and to provide all the conditions to develop my work. Especially, I would like to thank for the friendship, attention, encouragement, teaching and support.

I would also like to express my thanks to Professora Doutora Maria Teresa Barros, from the Faculdade de Ciências e Tecnologia, Universidade Nova de Lisboa, for the synthesis of the ligands, and also for receiving me in her laboratory, where I was easily integrated. Most of all, I want to thank for the friendship, teaching, and encouragement.

I would like to acknowledge to Professor Doutor Juan José Lucena, for receiving me in his research group at Universidad Autonoma de Madrid, for providing all the facilities to perform the biological experiments, and especially for the dedication, support and friendship. I would also like to thank to Professora Doutora Lourdes Hernandez-Apaolaza for the knowledge offered, to Clara Martin and Virginia Moreno, for helping me with the experiments, and to the entire research group at Departamento de Química Agrícola, for making my staying in Madrid so pleasant. Thank you for the kindness, friendship and support.

I am also grateful to “Fundação para a Ciência e a Tecnologia” for the financial support under the Project PTDC-AAC-AMB-111206-2009 and for a PhD scholarship with reference SFRH/BD/64718/2009.

To REQUIMTE – Rede de Química e Tecnologia, ICETA – Instituto de Ciência Agrária e Agro-Alimentares, and to Departamento de Engenharia Química, Faculdade de Engenharia da Universidade do Porto, I want to thank for providing me all the conditions to develop my work.

I would like to thank all my colleagues from laboratory 302B at FEUP (Isabel Pinto, Isabel Neto, Georgina Alves, Cristina Alves, Manuela Machado, Carlos Ferreira and Maryam Sadeghee), and also to Carina Machado and all those that over the time worked here. Thank you for the support, friendship and excellent work environment.

I want to express my gratitude to all my friends for being present in all moments.

Finally, a especial thanks to my parents, my sisters, to Sara, Rodrigo, Diogo and Constança, and all my Family, for being part of my life, with their love, and unconditional support.

## Abstract

Chelating agents are widely used in a variety of applications due to their ability to solubilize and/or masking metal ions. Thus, high amounts of these compounds are constantly released in the environment.

Many of the chelating agents used are non-degradable or degrade very slowly. In many applications, these compounds can be replaced by biodegradable ones with lower environmental impact.

In this work, the ready biodegradability of four chelating agents, N,N'-(S,S)-bis[1-carboxy-2-(imidazol-4-yl)ethylenediamine (BCIEE), N,N'-ethylene-di-L-cysteine (EC), N,N'-bis (4-imidazolymethyl)ethylenediamine (EMI) and 2,6-pyridine dicarboxylic acid (PDA) was tested according to the OECD guideline for testing of chemicals. Only PDA was found to be readily biodegradable. Chemical simulation was performed in order to understand the ability of the four compounds tested to complex with several metal ions [Ca(II), Cd(II), Co(II), Cu(II), Fe(III), Mg(II), Mn(II), Ni(II), Pb(II) and Zn(II)], and to discuss possible applications of each chelating agent. The applications found include food fortification, food processing, removal of Ca incrustations, soil remediation, and treatment of metal poisoning. Some of these chelating agents can also be used as additives in detergents, biocides, fertilizers and in pulp metal removal processes.

The use of iron chelates is the most efficient remedy to overcome and control iron chlorosis in plants, a common and complex nutritional disorder that affects plants growing under insufficient quantities of available iron.

The siderophore N,N'-2,6-bis(2,3-dihydroxybenzoyl)-L-lysine (azotochelin) and N,N'-Dihydroxy-N,N'-diisopropylhexanediamide (DPH), a siderophore analogue, were studied as potential iron chelators for iron nutrition in plants.

The stability in solution of the iron chelates in the presence of other metal cations, which may compete with iron for the chelating agent in nutrient solutions, is crucial for its effectiveness in supplying iron to plants. Azotochelin is produced by microorganisms, the soil bacterium *Azotobacter vinelandii*, as a mechanism to acquire iron in similar low iron availability conditions that also prevent plants to obtain this

essential nutrient. On the other hand, DPH is a biological and physicochemical model of the siderophore rhodotorulic acid produced by *Rhodotorula pilimanae* and related yeasts, and is not produced biologically. Therefore, the chelating properties of DPH were evaluated with the aim to assess its potentialities for being used as iron fertilizer. For this purpose, the complexation for the metal [Ca(II), Cu(II), Mg(II), Mn(II) or Zn(II)]–DPH–OH systems has been studied using pH-potentiometry, with the identification of the species formed in solution and determination of the overall stability constants. Additionally, the chemical stability of iron chelated with DPH in hydroponic conditions was assessed by computer chemical simulations. Under these conditions, DPH was found to form stable iron chelates in a wide pH range, that includes the agronomical pH range, and more important, the pH of calcareous soils.

The efficacy of the iron chelates of azotochelin and DPH to provide iron to cucumber (*Cucumis sativus*) (iron-efficient) plants was studied in hydroponic cultures, and compared with *o,o*-EDDHA/Fe<sup>3+</sup> and EDTA/Fe<sup>3+</sup>, which are used in iron fertilization. Because the reduction of iron(III) to iron(II) is an essential step for iron uptake by dicotyledonous plants, the ability of iron chelates of azotochelin or of DPH, to act as substrates in enzymatic reduction, at pH 7.5, was also assessed. However, it was only possible to determine the reduction rate of DPH/Fe<sup>3+</sup> by the ferric chelate reductase.

Both azotochelin/Fe<sup>3+</sup> and DPH/Fe<sup>3+</sup> chelates were effective in supplying iron to cucumber plants and can be considered as iron sources for cucumber plants when growing hydroponically. The recovery from chlorosis symptoms in the first 7 days after the application of the treatments with azotochelin/Fe<sup>3+</sup> or DPH/Fe<sup>3+</sup>, was similar to that observed when iron(III) chelates of *o,o*-EDDHA or EDTA were used. Additionally, the effect of the application of iron chelates in the uptake of other nutrients (Cu and Mn) was also evaluated. The results evidenced a good nutritional status of the plants treated with the iron(III) chelates of azotochelin and DPH.

The efficacy of the foliar application of the iron chelates of azotochelin and DPH, to deliver iron to soybean plants showing chlorotic symptoms, was also studied. The nutritional status of the plants treated with azotochelin/Fe<sup>3+</sup> and DPH/Fe<sup>3+</sup> was evaluated and the results were compared with plants treated with EDTA/Fe<sup>3+</sup> and *o,o*-EDDHA/Fe<sup>3+</sup>. Foliar sprays of DPH/Fe<sup>3+</sup>, EDTA/Fe<sup>3+</sup> and *o,o* – EDDHA/Fe<sup>3+</sup> were able to deliver Fe to soybean plants but for DPH/Fe<sup>3+</sup> and *o,o* - EDDHA/Fe<sup>3+</sup> only the

translocation of Fe to the roots was observed. The concentration of Mn measured in the roots of the plants was also affected by the foliar applications of iron chelate solutions. No evidences were found for the Fe uptake by the plants treated with foliar sprays of Azotochelin/Fe<sup>3+</sup>.





## Resumo

Os agentes quelantes são bastante usados numa grande variedade de aplicações devido à sua capacidade de solubilizar e/ou “mascarar” iões metálicos. Deste modo, grandes quantidades destes compostos são constantemente libertadas no meio ambiente.

Muitos dos agentes quelantes usados não são degradáveis ou são-no muito lentamente. Em muitas aplicações estes compostos podem ser substituídos por agentes quelantes biodegradáveis, conferindo um menor impacto ambiental.

Neste trabalho, foi testada a biodegradabilidade fácil de quatro agentes quelantes, N,N'-(S,S)-bis[1-carboxi-2-(imidazol-4-il)etilenodiamina (BCIEE), etileno-N,N'-di-L-cisteína (EC), N,N'-bis (4-imidazoilmetil)etilenodiamina (EMI) e o ácido 2,6-dicarboxílico-piridina (PDA), de acordo com as normas OCDE para testes de substâncias químicas. De entre estes compostos, apenas o PDA apresentou biodegradabilidade fácil. Foram também realizados estudos de simulação química com o objetivo de avaliar a capacidade dos quatro compostos para complexar com vários iões metálicos [Ca(II), Cd(II), Co(II) Cu(II), Fe(III), Mg(II), Mn(II), Ni(II), Pb(II) e Zn(II)] e prever possíveis aplicações para cada um dos agentes quelantes. As aplicações sugeridas incluem utilização em fortificantes alimentares, processamento de alimentos, remoção de incrustações de cálcio, remediação de solos e no tratamento de envenenamento por metais. Alguns dos agentes quelantes podem ainda ser usados como aditivos em detergentes, biocidas, fertilizantes e em processos de remoção de metais em pasta de papel.

O uso de agentes quelantes nas culturas é o método mais eficaz para evitar a clorose férrica nas plantas, uma doença comum que afeta o crescimento de plantas quando sujeitas a quantidades insuficientes de ferro disponível.

Neste trabalho, os compostos N,N'-2,6-bis(2,3-dihidroxibenzoil)-L-lisina (azotoquelina), e N,N'-Dihidroxi-N,N'-diisopropilhexanodiamida (DPH), um análogo sintético de um sideróforo, foram estudados como potenciais agentes quelantes de ferro na nutrição de plantas.

A estabilidade dos quelatos de ferro quando em soluções nutricionais e na presença de outros cátions metálicos, que podem competir com o próprio ferro para o agente quelante, é crucial para a sua eficiência no fornecimento de ferro às plantas. A azotoquelina é produzida por microorganismos, tais como a bactéria do solo *Azotobacter vinelandii*, como mecanismo para a remobilização de ferro em condições de baixa disponibilidade do mesmo. Por outro lado, o DPH é um modelo biológico e físico-químico do sideróforo ácido rodotorulico produzido por *Rhodotorula pilimanae* e outras leveduras, não sendo portanto produzido biologicamente. Neste trabalho, as propriedades quelantes do DPH foram avaliadas com o objetivo de determinar as suas potencialidades como fertilizante de ferro. Deste modo, foram efectuados estudos de complexação para vários sistemas M-DPH-OH [M= Ca(II), Cu(II), Mg(II), Mn(II) or Zn(II)] por potenciometria com eléctrodo de vidro, com vista à identificação das espécies formadas em solução e determinação das respectivas constantes de estabilidade globais. Adicionalmente, foi avaliada a estabilidade química do quelato DPH/Fe<sup>3+</sup>, em condições hidropónicas, através de simulações computacionais. Os resultados das simulações evidenciaram que o DPH forma quelatos de ferro estáveis numa ampla gama de pH. Este intervalo de pH inclui a gama de pH agronómico, incluindo o pH dos solos calcários.

Foi ainda estudada a eficácia dos quelatos de azotoquelina/Fe<sup>3+</sup> e DPH/Fe<sup>3+</sup> no fornecimento de ferro a plantas de pepino (*Cucumis sativus*) em culturas hidropónicas e comparada com a eficácia dos quelatos *o,o*-EDDHA/Fe<sup>3+</sup> e EDTA/Fe<sup>3+</sup>, os quais são usados frequentemente como fertilizantes de ferro. Uma vez que a redução do ferro (III) a ferro (II) é um passo importante na absorção do ferro por plantas dicotiledóneas, foi também avaliada a capacidade dos quelatos de azotoquelina/Fe<sup>3+</sup> ou DPH/Fe<sup>3+</sup> como substratos na redução enzimática a pH 7.5. Contudo, apenas foi possível determinar a velocidade de redução do quelato DPH/Fe<sup>3+</sup> pela enzima ferro reductase.

Ambos os quelatos, azotoquelina/Fe<sup>3+</sup> e DPH/Fe<sup>3+</sup>, mostraram ser eficazes no fornecimento de ferro a plantas de pepino e podem ser considerados fontes de ferro para as referidas plantas quando cultivadas em condições hidropónicas. A recuperação dos sintomas de clorose nos primeiros 7 dias após a aplicação dos tratamentos com azotoquelina/Fe<sup>3+</sup> e DPH/Fe<sup>3+</sup> foi semelhante à observada quando foram usados os quelatos de *o,o*-EDDHA/Fe<sup>3+</sup> e EDTA/Fe<sup>3+</sup>. Adicionalmente, também foi estudado o

efeito da aplicação de quelatos de ferro na absorção de outros nutrientes (Cu e Mn). Os resultados obtidos mostraram uma boa condição nutricional das plantas tratadas com os quelatos azotoquelina/ $\text{Fe}^{3+}$  e DPH/ $\text{Fe}^{3+}$ .

Neste trabalho, foi também estudada a eficácia da aplicação foliar dos quelatos de azotoquelina/ $\text{Fe}^{3+}$  e DPH/ $\text{Fe}^{3+}$  no fornecimento do ferro a plantas de soja que apresentavam sintomas de clorose. A condição nutricional das plantas tratadas com azotoquelina/ $\text{Fe}^{3+}$  e DPH/ $\text{Fe}^{3+}$  foi avaliada e comparada com os resultados obtidos para plantas tratadas com *o,o*-EDDHA/ $\text{Fe}^{3+}$  e EDTA/ $\text{Fe}^{3+}$ . Os *sprays* foliares de DPH/ $\text{Fe}^{3+}$ , *o,o*-EDDHA/ $\text{Fe}^{3+}$  e EDTA/ $\text{Fe}^{3+}$  mostraram capacidade de fornecer Fe a plantas de soja. No entanto, para os quelatos de DPH/ $\text{Fe}^{3+}$  e *o,o*-EDDHA/ $\text{Fe}^{3+}$  apenas se observou o transporte de Fe para as raízes. A concentração de Mn medida nas raízes das plantas também foi afetada pela aplicação foliar das soluções de quelatos de ferro. Não foram observadas quaisquer evidências da absorção de ferro por plantas tratadas com *sprays* foliares de azotoquelina/ $\text{Fe}^{3+}$ .



## **Preface**

### **Importance and Motivation**

The recognized importance of chelating agents motivates the constant research on these types of compounds either to take advantage of their chelation properties in different areas of application or to replace the chelating agents already in use by new, more environmental-friendly and/or more effective ones.

The development and/or application of new substances contributes to better understanding the features (chemical, structural) that have influence in the chelation process and also to understand the mechanisms in which chelating agents are involved.

Furthermore, the environmental fate of the large amounts of chelating agents used worldwide has been a matter of concern in the past decades. Thus, the search for more environmental friendly alternatives to the often non-degradable products in use, has also received great attention.

One of the vast applications of chelating agents (and other compounds with complexing properties) is in agriculture as fertilizer auxiliary materials, where they are used as source of several elements, such as Cu, Fe, Mn and Zn.

Chelating agents assume a particular interest in the case of iron fertilization, due to the low availability of iron for plants, which is a consequence of the low solubility of iron(III) even though iron is one of the most abundant elements in the earth. This low availability leads to iron chlorosis, a widespread agricultural problem responsible for decreasing chlorophyll, which reduces quality and yield in many crops, especially in calcareous and/or alkaline soils.

The application of iron chelates is the most effective practice to correct iron chlorosis. Among these compounds, EDDHA and its analogues are the most efficient. However, the properties of these products, based on polyaminocarboxylic acids, are not entirely satisfactory. Iron chlorosis in plants remains a huge problem because the performance of an iron chelate to supply iron to plants depends on innumerable factors such as i) the stability in solution in a wide range of pH, that must ascend up to pH 7.5-

8.5, if to be used in calcareous and/or alkaline soils, ii) the stability in the presence of other metal ions, mainly  $\text{Ca}^{2+}$  and  $\text{Mg}^{2+}$ , that due to their high concentrations in soils may displace  $\text{Fe}^{3+}$  from the chelates; iii) the type of soil and the reactivity with soil materials. Moreover, the efficiency of these types of compounds in iron nutrition depends on the plant species, and the strategy that the plant uses to acquire iron from the chelating agent. In addition to the environmental concerns already referred, EDDHA and other synthetic chelating agents, due to their high price, are mainly used in high-value crops.

Therefore, the search for suitable iron chelators, with specific properties to be used as iron fertilizers, taking into account the environmental impact of their application became a great challenge. Among a great number of compounds considered, the properties showed by microbial siderophores made them interesting objects of study.

Siderophores are known as effective iron chelators. Some microorganisms are able to produce siderophores in order to obtain iron from the environment under conditions that limit the acquisition of this element by plants. The way how plants utilize iron chelates, i.e., the uptake and transport of iron under different fertilization techniques, is not completely understood. Thus, additional investigation is needed in order to provide useful information about this issue.

The studies carried out in the present work had the objective of evaluating potential chelating agents with application as fertilizers and represent, at the same time, our intent to give a contribution to a better comprehension of the complex processes associated to iron transport and uptake by plants.

## **Outline**

This thesis is divided in six chapters. Chapter 1 includes a general introduction of chelating agents, as well as siderophores, a specific type of chelating agents produced biologically for transport and uptake of iron by several organisms. A bibliographic review on the use of chelating agents and siderophores in plant nutrition is also undertaken.

In Chapter 2, the ready-biodegradability of several chelating compounds will be investigated and the chelating properties for different metal ions will be assessed by computational methods in order to evaluate the potential applications of each compound.

Azotochelin, a siderophore produced by *Azotobacter vinelandii*, and N,N'-Dihydroxy-N,N'-diisopropylhexanediamide (DPH), a siderophore analogue of rhodotorulic acid produced by *Rhodotorula pilimanae* and related yeasts, were evaluated as potential alternative sources of iron to plants, including in alkaline conditions. Since DPH is not produced biologically, its chelating properties (stability constants) with other metal ions [Ca(II), Cu(II), Mg(II), Mn(II) or Zn(II)], that can restrict its effectiveness as iron fertilizer, was the subject of study in Chapter 3.

In Chapter 4, the ability of azotochelin and DPH as iron suppliers to plants was evaluated by the application of their iron chelates in hydroponic cultures of cucumber plants.

Chapter 5 complements the study of the suitability of azotochelin and DPH as iron suppliers to plants, by using foliar application of the iron chelates to soybean plants.

Finally, in Chapter 6, the main conclusions of this work are summarized, and suggestions for future work are addressed.





## Table of Contents

List of Figures.....	xxi
List of Tables.....	xxvii
Abbreviations and Symbols.....	xxix
<b>Chapter 1</b> .....	1
<b>1.1 Chelating Agents</b> .....	3
1.1.1 Definition and terminology.....	3
1.1.2 Chelating agents and applications.....	6
<b>1.2. Iron</b> .....	13
1.2.1 Bioavailability of iron.....	13
1.2.2 Iron in plant nutrition.....	15
1.2.2.1 Iron chelates in plant nutrition.....	20
<b>1.3 Siderophores</b> .....	26
1.3.1 Siderophores-Iron chelators.....	26
1.3.2 Siderophores in Iron Nutrition.....	37
<b>1.4 References</b> .....	44
<b>Chapter 2</b> .....	53
Abstract.....	55
<b>2.1 Introduction</b> .....	56
<b>2.2 Materials and Methods</b> .....	59
2.2.1 Chelating agents.....	59
2.2.2 Ready Biodegradation Tests.....	60
2.2.3 Complexation Modeling Study.....	61
<b>2.3 Results and Discussion</b> .....	62
2.3.1 Evaluation of the ready biodegradability of the chelating agents.....	62
2.3.2 Complexation modeling study.....	65
2.3.3 Possible applications for BCIEE, EC, EMI and PDA.....	69
<b>2.4. Conclusions</b> .....	71
2.5 References.....	72

<b>Chapter 3.....</b>	<b>77</b>
Abstract.....	79
<b>3.1 Introduction.....</b>	<b>80</b>
<b>3.2 Materials and Methods.....</b>	<b>81</b>
3.2.1 Potentiometric studies.....	82
3.2.2 Computer chemical simulations.....	87
<b>3.3 Results and Discussion.....</b>	<b>88</b>
3.3.1 Protonation and metal-complexation of DPH.....	88
3.3.2 Stability of Fe-DPH complexes under hydroponic conditions.....	104
<b>3.4 References.....</b>	<b>108</b>
<b>Chapter 4.....</b>	<b>111</b>
Abstract.....	113
<b>4.1 Introduction.....</b>	<b>114</b>
<b>4.2 Materials and Methods.....</b>	<b>116</b>
4.2.1 Preparation of Iron chelates.....	116
4.2.2 Effect of pH on the stability of azotochelin/Fe <sup>3+</sup> chelates, in Ca <sup>2+</sup> solutions.....	117
4.2.3 Azotochelin/Fe <sup>3+</sup> and DPH/Fe <sup>3+</sup> as substrate for FCR activity in stressed cucumber plants.....	118
4.2.4 Efficacy of azotochelin/Fe <sup>3+</sup> and DPH/Fe <sup>3+</sup> to provide Fe to cucumber plants in hydroponic culture. ....	121
4.2.5 Statistical analysis. ....	123
4.2.6 Computer chemical simulations.....	123
<b>4.3 Results.....</b>	<b>125</b>
4.3.1 Azotochelin/Fe <sup>3+</sup> and DPH/Fe <sup>3+</sup> chelates as substrate for FCR activity in stressed cucumber plants.....	125
4.3.2 Efficacy of azotochelin/Fe <sup>3+</sup> and DPH/Fe <sup>3+</sup> chelates to provide iron to cucumber plants in hydroponic culture. ....	128
<b>4.4 Discussion.....</b>	<b>136</b>
<b>4.5 References.....</b>	<b>146</b>

<b>Chapter 5.....</b>	<b>151</b>
Abstract.....	153
<b>5.1 Introduction.....</b>	<b>154</b>
<b>5.2 Materials and Methods.....</b>	<b>155</b>
5.2.1 Preparation of Iron chelates.....	155
5.2.2 Efficacy of azotochelin/Fe <sup>3+</sup> and DPH/Fe <sup>3+</sup> to provide Fe to soybean plants by foliar application.....	155
<b>5.3 Statistical Analysis .....</b>	<b>158</b>
<b>5.4 Results and Discussion .....</b>	<b>158</b>
<b>5.5 Conclusions .....</b>	<b>167</b>
<b>5.6 References .....</b>	<b>168</b>
<b>Chapter 6.....</b>	<b>171</b>
6.1 Main Conclusions and Future work.....	173



## List of Figures

### Chapter 1

<b>Figure 1.1</b> Schematic representation of a metal complex formed by a tetracoordinated metal bound to (A) four monodentate ligand or (B) two bidentate ligand.....	3
<b>Figure 1.2</b> Structure of EDTA (A), and schematic representation of a metal ion (M)-EDTA chelate with a five-membered ring highlighted (B).....	4
<b>Figure 1.3</b> Structural formulas of some important synthetically produced aminopolycarboxylate chelating agents (APCAs): $\beta$ -alanine diacetic acid (ADA), Diethylenetriaminepentaacetic acid (DTPA), Ethylenediaminedi(o-hydroxyphenylacetic) acid (EDDHA), Ethylenediaminedisuccinic acid (EDDS), and Nitriloacetic acid (NTA).....	7
<b>Figure 1.4</b> Structural formulas of phosphonate type chelating agents: Diethylenetriaminepentakis(methylene) phosphonic acid (DTPMP), 1,2-Diaminoethane-tetrakis(methylenephosphonic) acid (EDTMP), Hexamethylenediaminetetra(methylenephosphonic) acid (HDTMP), and Aminotrimethylenephosphonic acid (ATPM) .....	8
<b>Figure 1.5</b> Structural formulas of hydroxycarboxylate type chelating agents: N-(2-hydroxyethyl)iminodiacetic acid (HEIDA), N,N-bis(2-hydroxyethyl)glycine (DHEG), (Hydroxyethyl)etylenediaminetriacetic acid (HEDTA), and N,N,N',N'-tetrakis-2-hydroxyisopropylethylenediamine (Quadrol) .....	9
<b>Figure 1.6</b> Structural formula of a mixed carboxylate-phosphonate chelating agent:Phosphonobutane-tricarboxilic acid (PBTC).....	9
<b>Figure 1.7</b> Structural formula of some naturally occurring chelating agents.....	12
<b>Figure 1.8</b> Model for root responses to iron deficiency for Fe acquisition in Strategy I plants. i) Fe(III) solubilization, usually mediated by rhizosphere acidification, through proton extrusion (mediated by activation of plasmalemma $H^+$ -ATPase); ii) complexation with chelating compounds released; iii) reduction of Fe(III) to Fe(II) by ferric chelate reductase (FCR); iv) uptake into roots cells by a specific transporter for Fe(II): PM = plasma membrane; St = stimulated $H^+$ pumping ATPase; X = Production/release of chelators/reductants. (Adapted from Marschner and Römheld (1994)).....	17

<b>Figure 1.9</b> Model for root responses to iron deficiency for Fe acquisition in Strategy II plants, involving the synthesis of phytosiderophores that upon complexation with iron(III) with the formation of a $\text{Fe}^{3+}$ -PS chelate are taken up by a specific uptake system (Tr). (Adapted from Marschner and Römheld (1994)).....	18
<b>Figure 1.10</b> Structures of some phytosiderophores: Distichonic acid, 3-epi-hydroxymugineic acid (epi-HMA) and 3-dihydroxymugineic acid (HMA).....	19
<b>Figure 1.11</b> Structures of ethylenediamine-di(2-hydroxy-4-methylphenylacetic acid (EDDHMA), ethylenediamine-di(5-carboxy-2-hydroxyphenylacetic) acid (EDDCHA) and ethylenediamine-N,N'-bis(2-hydroxy-5-sulfonylphenyl) (EDDHSA).....	21
<b>Figure 1.12</b> Structures of N,N'-Bis(2-hydroxybenzyl)ethylenediamine-N,N'-diacetic acid (HBED), N,N'-Bis(2-hydroxy-5-methylbenzyl)ethylenediamine-N,N'-diacetic (HJB) and 2-(2-((2-hydroxybenzyl)amino)ethylamino)-2-(2-hydroxyphenyl)acetic acid (DCHA).....	22
<b>Figure 1.13</b> Model for the mechanism of action of Fe chelates in soils. $\text{FeY}=\text{Fe}^{3+}$ chelate; Y=Chelating agents; FCR= Ferric chelate reductase; Tr = Ferrous transporter. (Adapted from Lucena (2003)).....	24
<b>Figure 1.14:</b> Structure of N-(1,2-dicarboxyethyl)-D,L-aspartic acid (IDHA).....	25
<b>Figure 1.15</b> Most common siderophore binding groups (and $\text{pK}_{\text{as}}$ ): catechol, hydroxamic acid and $\alpha$ -hydroxycarboxylic acid.....	27
<b>Figure 1.16</b> Hydroxypyridione, carboxylic acid and amine binding groups.....	27
<b>Figure 1.17</b> Structures of some hydroxamate-based siderophores: desferrioxamine B (hexadentate, linear), Desferrichrome (hexadentate, Exocyclic), neurosporin (hexadentate, endocyclic) and rhodotorulic acid (tetradentate, linear).....	28
<b>Figure 1.18</b> Structure of the catechol-based siderophore Enterobactin (hexadentate, exocyclic), the $\alpha$ -hydroxycarboxylate-based siderophore, vibrioferrin, and the mixed-ligand siderophore, aerobactin.....	29
<b>Figure 1.19</b> Structure of desferrioxamine E.....	30
<b>Figure 1.20</b> Structure of Alcaligin.....	35

<b>Figure 1.21</b> Possible structures of iron(III)-tetradentate siderophore chelates. The structure assumed by the chelate depends on the pH, the length of the connecting chain between the hydroxamate groups and also of the metal to ligand ratio.....	35
<b>Figure 1.22</b> Structures of rhizoferrin, pseudobactin and agrobactin.....	40
<b>Figure 1.23</b> Structure of deferrichrome A.....	41
<b>Figure 1.24</b> Structure of coprogen and monohydroxamate and dihydroxamate products from hydrolysis.....	43
<b>Chapter 2</b>	
<b>Figure 2.1</b> Molecular structure of the chelating agents: N,N'-(S,S)-bis[1-carboxy-2-(imidazol-4-yl)ethyl]ethylenediamine (BCIEE), N,N'-ethylene-di-L-cysteine (EC), N,N'-bis(4-imidazolymethyl)ethylenediamine (EMI) and 2,6-pyridine dicarboxylic acid (PDA) .....	59
<b>Figure 2.2</b> Biodegradation assay of PDA according to OECD guidelines.....	63
<b>Figure 2.3.</b> Biodegradation assays of BCIEE, EC and EMI according to the OECD guidelines.....	64
<b>Figure 2.4.</b> Amount, in percentage, of each metal (Ca, Cd, Co, Cu, Fe, Mg, Mn, Ni, Pb or Zn) complexed with BCIEE (A), EC (B), EMI (C) and PDA (D). Chemical simulation were performed assuming one metal (M) and one chelating agent (L), with a [L]:[M] ratio of 2.5, [M] = 0.001 mol.L <sup>-1</sup> .....	66
<b>Figure 2.5.</b> Amount, in percentage, of metal complexed with EC (A), EMI (B) and PDA (C). Chemical simulations were performed assuming the simultaneous presence of the chelating agent ([L] = 0.02 mol.L <sup>-1</sup> ) and all metal ions ([Cd] = [Co] = [Cu] = [Fe] = [Mg] = [Mn] = [Ni] = [Pb] = [Zn] = 0.001 M) with an excess of Ca ([Ca] = 0.05 mol.L <sup>-1</sup> ).....	68
<b>Chapter 3</b>	
<b>Figure 3.1</b> Structure of N,N'-Dihydroxy-N,N'-diisopropylhexanediamide (DPH).....	81

<b>Figure 3.2</b> Representative pH titration curves for DPH and metal [Ca(II), Cu(II), Mg(II), Mn(II) or Zn(II)]-DPH-OH systems. Ca(II) and Mg(II): [L <sub>T</sub> ]:[M <sub>T</sub> ]=2 and 1, respectively, with [M <sub>T</sub> ]= 4.0 x 10 <sup>-3</sup> mol.L <sup>-1</sup> ; Cu(II) and Zn(II): [L <sub>T</sub> ]:[M <sub>T</sub> ]=2, [M <sub>T</sub> ]= 1.0 x 10 <sup>-3</sup> mol.L <sup>-1</sup> ; Mn(II): [L <sub>T</sub> ]:[M <sub>T</sub> ]=2, [M <sub>T</sub> ]= 2.5 x 10 <sup>-3</sup> mol.L <sup>-1</sup> ; For DPH alone: [L <sub>T</sub> ]=2.0 x 10 <sup>-3</sup> mol.L <sup>-1</sup> . μ=0.1 mol.L <sup>-1</sup> (KCl) and T=25 °C; a = moles of base (KOH) added per mole of ligand.....	88
<b>Figure 3.3</b> Z <sub>M</sub> function for Cu(II)-DPH-OH system. The computed function was calculated from the refinement operation performed for the models presented in Table 3.4. [L <sub>T</sub> ]: [Cu <sub>T</sub> ]=2, [Cu]= 1.0 x 10 <sup>-3</sup> mol.L <sup>-1</sup> .....	93
<b>Figure 3.4</b> Species distribution diagram computed for DPH (L <sup>2-</sup> ); [L <sub>T</sub> ] 2.0 x 10 <sup>-3</sup> mol.L <sup>-1</sup> .....	93
<b>Figure 3.5</b> Species distribution diagram computed, assuming the final model, for metal Cu(II)-DPH-OH system. Model III, Table 3.4, [L <sub>T</sub> ]: [M <sub>T</sub> ]=2, [M <sub>T</sub> ]= 1.0 x 10 <sup>-3</sup> mol.L <sup>-1</sup> . The dotted line indicates the pH value where precipitation was experimentally observed.....	94
<b>Figure 3.6</b> Z <sub>H</sub> and Z <sub>M</sub> (insert) functions for Zn(II)-DPH-OH system computed from the refinement operation performed for the models presented in Table 3.4; [L <sub>T</sub> ]: [Zn <sub>T</sub> ] = 2, [Zn <sub>T</sub> ] = 1.0 x 10 <sup>-3</sup> mol.L <sup>-1</sup> .....	95
<b>Figure 3.7</b> Species distribution diagram computed, assuming the final models, for Zn(II)-DPH-OH system: Model III, Table 3.4, [L <sub>T</sub> ]: [M <sub>T</sub> ]=2, [M <sub>T</sub> ]= 1.0 x 10 <sup>-3</sup> mol.L <sup>-1</sup> . The dotted line indicates the pH value where precipitation was observed.....	96
<b>Figure 3.8</b> Z <sub>M</sub> function for Mn(II)-DPH-OH system. The computed function was calculated from the refinement operation performed for the model presented in Table 3.5: [L <sub>T</sub> ]:[Mn <sub>T</sub> ]=2, [Mn]=2.5 x 10 <sup>-3</sup> mol.L <sup>-1</sup> .....	99
<b>Figure 3.9</b> Species distribution diagram computed, assuming the final models, for Mn(II)-DPH-OH system: Model II, Table 3.5, [L <sub>T</sub> ]:[Mn <sub>T</sub> ] = 2, [M <sub>T</sub> ] = 2.5 x 10 <sup>-3</sup> mol.L <sup>-1</sup> . The dashed line indicates Mn(II) oxidation.....	99
<b>Figure 3.10</b> Z <sub>M</sub> function for Ca(II)-DPH-OH system. The computed Z <sub>M</sub> function was calculated from the refinement operation performed for the models presented Table 3.5: Ca(II): [L <sub>T</sub> ]: [Ca <sub>T</sub> ] =2, [Ca <sub>T</sub> ]=4 x 10 <sup>-3</sup> mol.L <sup>-1</sup> .....	100
<b>Figure 3.11</b> Species distribution diagram computed, assuming the final models, for Ca(II)-DPH-OH system: Model III, Table 3.5, [L <sub>T</sub> ]: [M <sub>T</sub> ] = 2, with [M <sub>T</sub> ]= 4.0 x 10 <sup>-3</sup> mol.L <sup>-1</sup> .....	101



<b>Figure 3.12</b> $Z_M$ function for Mg(II)–DPH–OH system. The computed function was calculated from the refinement operation performed for the models presented in Table 3.5: $[L_T]: [Mg_T] = 1$ , $[Mg] = 4.0 \times 10^{-3} \text{ mol.L}^{-1}$ .....	102
<b>Figure 3.13</b> Species distribution diagram computed, assuming the final model, for Mg(II)–DPH–OH system: Model III, Table 3.5, $[L_T]: [M_T] = 1$ with $[M_T] = 4.0 \times 10^{-3} \text{ mol.L}^{-1}$ . The dotted line indicates the pH value where precipitation was observed.....	103
<b>Figure 3.14</b> Species distribution diagram of the DPH system in Hoagland nutrient solution (for detailed information about the composition of the solution see text): $[L] = 1.65 \times 10^{-4} \text{ mol.L}^{-1}$ ; $[Fe^{3+}] = 1.0 \times 10^{-4} \text{ mol.L}^{-1}$ . % is the percentage of species present, <b>(A)</b> with total ligand concentration set at 100%, or <b>(B)</b> with total Fe(III) concentration set at 100%; the dashed vertical line indicates $Fe(OH)_3$ precipitation.....	105
<b>Figure 3.15</b> Species distribution diagram of the <i>o,o</i> -EDDHA system in Hoagland nutrient solution (for detailed information about the composition of the solution see text): $[L] = 1.1 \times 10^{-4} \text{ mol.L}^{-1}$ ; $[Fe^{3+}] = 1.0 \times 10^{-4} \text{ mol.L}^{-1}$ . % is the percentage of species present <b>(A)</b> with total ligand concentration set at 100%, or <b>(B)</b> with total Fe(III) concentration set at 100%; the dashed vertical line indicates $Fe(OH)_3$ precipitation.....	106
<b>Chapter 4</b>	
<b>Figure 4.1</b> Structure of N, N'-2,6- Bis(2,3-dihydroxybenzoyl)-L-lysine (azotochelin).....	115
<b>Figure 4.2.</b> Fe chelate solutions formed with DPH and azotochelin, at pH 7.5.....	116
<b>Figure 4.3</b> Germination of cucumber seeds ( <i>Cucumis sativus</i> L. cv. Ashley) (A, B). Seedlings in holed plates (C) .....	118
<b>Figure 4.4</b> Cucumber plants growing in 12-L polypropylene bucket (12 pairs of plants per bucket) (A) .....	119
<b>Figure 4.5</b> Reductase assay.....	120
<b>Figure 4.6</b> Cucumber plants grown in hydroponic culture <b>(A;B)</b> , showing visible symptoms of iron deficiency at the time of application of the treatments (0 DAT) <b>(B)</b> .....	122
<b>Figure 4.7</b> Rate of $Fe^{3+}$ reduction from the iron chelates of DPH, EDDHA and EDTA, used for cucumber plants. Error bars represent standard deviations (SD, n=6). Different letters in the same period denotes significant differences among treatments for Duncan test ( $p < 0.05$ ).....	125

<b>Figure 4.8</b> Representative plots of the change of the absorbance over time, measured in the FCR assay with (A) azotochelin/ $\text{Fe}^{3+}$ , at 535 and 630 nm, (B) <i>o,o</i> -EDDHA/ $\text{Fe}^{3+}$ , at 535 and 480 nm, (C) DPH/ $\text{Fe}^{3+}$ , at 535 and 375 nm, (D) EDTA/ $\text{Fe}^{3+}$ , at 535 nm, and in blanks, respectively.....	127
<b>Figure 4.9</b> Effect of the different Fe chelate treatments on the SPAD index ( $\pm$ standard deviation; n = 5), measured in the first leaf level, of cucumber plants in hydroponic experiments.....	128
<b>Figure 4.10</b> Cucumber plants after 7 and 21 days of treatment, in hydroponic culture, with the iron chelates (10 $\mu\text{M}$ Fe) of Azotochelin, DPH, <i>o,o</i> -EDDHA, EDTA and control plants (2 $\mu\text{M}$ Fe) .....	137
<b>Figure 4.11</b> Species distribution diagrams of the EDTA system in (A) aqueous solution and in (B,C) Hoagland nutrient solution (for detailed information about the composition of the solution see Chapter 3): [L]=1.1 x 10 <sup>-4</sup> mol.L <sup>-1</sup> ; [ $\text{Fe}^{3+}$ ]=1.0 x 10 <sup>-4</sup> mol.L <sup>-1</sup> . % is the percentage of species present (A,B) with total Fe(III) concentration set at 100% or (C) with total ligand concentration set at 100%,; the dashed vertical line indicates $\text{Fe}(\text{OH})_3$ precipitation.....	140
<b>Figure 4.12</b> Soluble Fe, at different pH, measured in Azotochelin/ $\text{Fe}^{3+}$ ( $[\text{Fe}^{3+}] = 1.5 \times 10^{-4}$ mol.L <sup>-1</sup> ) solutions after 3 and 7 days of interaction with $\text{Ca}^{2+}$ , 1.6 x 10 <sup>-3</sup> mol.L <sup>-1</sup> . Mean value from two replicates for obtained for each pH.....	141
<b>Figure 4.13</b> Representative UV-Vis absorption spectra of a azotochelin/ $\text{Fe}^{3+}$ ( $[\text{Fe}^{3+}] = 50 \mu\text{mol.L}^{-1}$ ) solution at pH 7.5; and two proposed structures, for possible bis(catecholate)-iron(III) complex species, ML (A) and $\text{M}_2\text{L}_2$ (B) formed by azotochelin and iron(III) at pH 7.5.....	142
<b>Figure 4.14</b> Coordination shift from catecholate to the salicylate mode upon protonation.....	143
<b>Chapter 5</b>	
<b>Figure 5.1</b> Germination of soybean seeds (Glycine max L. cv. Stine 0408) (A). Seedlings in holed plates (B); Plants in 2 L vessels (C).....	156
<b>Figure 5.2</b> Nebulizer system (A) used to spray first leaf levels of each plant (B) in foliar application treatments. ....	157
<b>Figure 5.3</b> Examples of soyben plants after 7 days after foliar application with the iron chelates (5 mmol.L <sup>-1</sup> Fe) of Azotochelin, DPH, <i>o,o</i> -EDDHA, EDTA and control plants (- Fe).....	160

## List of tables

### Chapter 1

<b>Table 1.1</b> Estimated production/use of chelating agents (tons/year).....	10
--	----

<b>Table 1.2</b> Overall stability constants with $\text{Fe}^{3+}$ and $\text{Fe}^{2+}$ , $\text{pFe}^{3+}$ , and redox potential of several siderophores, siderophore analogues, and synthetic chelating agents.....	31
---	----

### Chapter 3

<b>Table 3.1</b> Protonation constants for water and overall stability constants for M(II) complexes with $\text{OH}^-$ , at 25.0 °C (Martell and Smith, 2004).....	86
---	----

<b>Table 3.2</b> Protonation and overall stability constants (as $\log \beta$ ) for <i>o</i> , <i>o</i> -EDDHA complexes formed with Ca(II), Mg(II), Cu(II) and Fe(III) (Yunta, et al., 2003) .....	87
---	----

<b>Table 3.3</b> Overall DPH protonation constants and overall stability constants (as $\log \beta$ ) for DPH with Cu(II), Zn(II), Mn(II), Mg(II) and Ca(II), refined simultaneously for all titrations in ESTA, determined by GEP in 0.1 M KCl at 25 °C (charges were omitted for simplicity) .....	90
--	----

<b>Table 3.4</b> Overall stability constants (as $\log \beta$ values) for M-DPH systems determined by GEP for one titration in 0.1 mol.L <sup>-1</sup> KCl at 25° C; M = Cu(II) or Zn(II), $[\text{M}_\text{T}] = 1.0 \times 10^{-3} \text{ mol.L}^{-1}$ .....	92
--	----

<b>Table 3.5</b> Overall stability constants (as $\log_{10}\beta$ values) for M-DPH systems determined by GEP for one titration in 0.1 mol L <sup>-1</sup> KCl at 25° C; M = Mn(II), Mg(II) or Ca(II) .....	98
---	----

### Chapter 4

<b>Table 4.1</b> Protonation and overall stability constants (as $\log \beta$ ) for EDTA complexes formed with Ca(II), Cu(II), Mg(II), Mn(II) and Zn(II) (Martell and Smith, 2004).....	124
---	-----

<b>Table 4.2</b> Effect of the different Fe -chelate treatments on the SPAD index ( $\pm$ standard deviation; n = 5 for iron chelates tested and n=3 for control) in most recently developed leaves of cucumber plants formed in different levels after the application of the Fe-chelates treatments in hydroponic experiments.....	130
--	-----

<b>Table 4.3.</b> Effect of the different Fe chelate treatments on the dry weight (g; $\pm$ standard deviation; n = 5 for iron chelates tested and n=3 for control) of leaf, root and stem in cucumber plants grown in hydroponic experiments.....	131
<b>Table 4.4</b> Effect of the different Fe chelate treatments on the leaf Fe concentration ( $\mu\text{mol g}^{-1}$ DW; $\pm$ standard deviation; n = 5 for iron chelates tested and n=3 for control) and Fe content ( $\mu\text{mol plant}^{-1}$ ; $\pm$ standard deviation; n = 5 for iron chelates tested and n=3 for control) in cucumber plants grown in hydroponic experiments.....	132
<b>Table 4.5.</b> Effect of the different Fe chelate treatments on leaf Mn and Cu concentrations ( $\mu\text{mol g}^{-1}$ DW; $\pm$ standard deviation; n = 5 for iron chelates tested and n=3 for control) and Fe/Mn ratio in cucumber plants grown in hydroponic experiments.....	133
<b>Table 4.6</b> Effect of the different Fe chelate treatments on the Fe concentration ( $\mu\text{mol g}^{-1}$ DW; $\pm$ standard deviation; n = 5 for iron chelates tested and n=3 for control) in the stems at 7 and 21 DAT in cucumber plants grown in hydroponic experiments.....	135
<b>Table 4.7</b> Stability constants (as $\log\beta$ ) of $\text{Fe}^{3+}$ with DPH, <i>o,o</i> -EDDHA and EDTA and pFe calculated for $[\text{L}_\text{T}] = 1.0 \times 10^{-5} \text{ mol.L}^{-1}$ , $[\text{Fe}_\text{T}] = 1.0 \times 10^{-6} \text{ mol.L}^{-1}$ , at pH 7.5. $\text{Fe}(\text{OH})_3$ (s) [ $\log \beta = -2.74$ (Martell and Smith, 2004)] was introduced as precipitation controller.....	135
<b>Chapter 5</b>	
<b>Table 5.1.</b> Effect of the foliar application of the different Fe chelate treatments on the Fe content ( $\mu\text{mol plant}^{-1}$ DW; $\pm$ SE, n=5) in untreated leaves, stems and roots, of soybean plants grown in hydroponics conditions (DAT 7). .....	159
<b>Table 5.2</b> Effect of the foliar application of the different Fe chelate treatments on the SPAD values ( $\text{SPAD} \pm \text{SE}$ , n=5) measured in the first and second leaf levels, in soybean plants grown in hydroponic conditions.....	162
<b>Table 5.3.</b> Effect of the foliar application of different Fe chelate treatments on leaves, stems and roots dry weight ( $\pm$ SE, n=5), in soybean plants grown in hydroponic conditions.....	164
<b>Table 5.4</b> Effect of the foliar application of the different Fe chelate treatments on the concentration of Fe, Mn, Zn and Cu ( $\mu\text{mol g}^{-1}$ DW $\pm$ SE, n=5) measured in the roots of soybean plants grown in hydroponic conditions.....	166

## Abbreviations and Symbols

ABS - Absorbance

ADA -  $\beta$ -alanine diacetic acid

APCAs – Aminopolycarboxylic acids

ATPM - Aminotrimethylenephosphonic acid

Azotochelin - N,N'-2,6-bis(2,3-dihydroxybenzoyl)-L-lysine

BCIEE - N,N'-(S,S)-bis[1-carboxy-2-(imidazol-4-yl)ethylenediamine

BPDS - Bathophenanthroline disulfonic acid

CAPSO – 3-(Cyclohexylamino)-2-hydroxy-1-propanesulfonic acid

DAT - Days after treatment application

DCHA - 2-(2-((2-hydroxybenzyl)amino)ethylamino)-2-(2-hydroxyphenyl)acetic acid

DHEG - N,N-bis(2-hydroxyethyl)glycine

DPH – N',N-Dihydroxy-N,N'-diisopropylhexanediamide

DTPA - Diethylenetriaminepentaacetic acid

DTPMP - Diethylenetriaminepentakis(methylene) phosphonic acid

DW – Dry weight

EC – N,N'-ethylene-di-L-cysteine

EDDCHA - Ethylenediaminedi(5-carboxy-2-hydroxyphenylacetic) acid

EDDHA - Ethylenediamine-N,N'bis(2-hydroxyphenylacetic) acid

EDDHMA - Ethylenediamine-di(2-hydroxy-4-methylphenylacetic acid

EDDHSA - Ethylenediamine-N,N'-bis(2-hydroxy-5-sulfonylphenyl)

EDDS - Ethylenediaminedisuccinic acid

EDTA - Ethylenediaminetetraacetic acid

EDTMP - Diaminoethane-tetrakis(methylenephosphonic) acid

EMI - N,N'-bis (4-imidazolymethyl)ethylenediamine

epi-HMA - 3-epi-hydroxymugineic acid

FCR - Ferric chelate reductase

GEP – Glass Electrode Potentiometry

HBED - N,N'-Bis(2-hydroxybenzyl)ethylenediamine-N,N'-diacetic acid

HEDTA - Hydroxyethylenediaminetriacetic acid

HEIDA - N-(2-hydroxyethyl)iminodiacetic acid

HEPES - 4-(2-hydroxyethyl)piperazine-1-ethanesulfonic acid  
 HDTMP - Hexamethylenediaminotetra(methylenephosphonic) acid  
 HJB - N,N'-Bis(2-hydroxy-5-methylbenzyl)ethylenediamine-N,N'-diacetic acid  
 HMA - 3-dihydroxymugineic acid  
 IDHA - N-(1,2-dicarboxyethyl)-D,L-aspartic acid  
 IRT1 - Iron-regulated transporter 1  
 IUPAC – International Union of Pure and Applied Chemistry  
 MES – 2-(N-morpholino)ethanesulfonic acid  
 MS – Microbial siderophore  
 NTA - Nitrilotriacetic acid  
 OECD - Organization for Economic Co-operation and Development  
 o,o-EDDHA - Ethylenediamine-N,N'-bis(o-hydroxy-phenylacetic) acid  
 PBTC - Phosphonobutane-tricarboxylic acid  
 PDA - 2,6-pyridine dicarboxylic acid  
 PDTA – Propylenediamine tetra-acetic acid  
 PM – Plasma membrane  
 PS - Phytosiderophore  
 PSB - Pseudobactin  
 Quadrol - N,N,N',N'-tetrakis-2-hydroxyisopropylethylenediamine  
 SE – Standard error  
 SPAD - Soil-Plant Analysis Development  
 a - moles of base (KOH) added per mole of ligand  
 $\beta_{n0l}$  – Formation constants of  $M_nL_0H_l$  species  
 $\beta_{MLH}$  – Overall stability constant for the Metal-Ligand complexes  
 $E^0$  – Electrode intercept  
 $E_n^{obs}$  – Observed electrode potential at  $n^{th}$  data point  
 $E_n^{calc}$  - Calculated electrode potential at  $n^{th}$  data point  
 $[H^+]$  – proton concentration  
 K – Stability constant for the metal-Ligand complexes  
 k – Electrode calibration slope  
 Ka – Ligand protonation constant  
 [L] – Free ligand concentration

$[L_T]$  – Initial or total ligand concentration (in the cell)  
 $[L_T]:[M_T]$  - Ligand total to metal total concentration ratio  
 $[M]$  – Free metal concentration  
 $[M_T]$  – Initial or total metal concentration  
 $N$  – Number of experimental points recorded on a system  
 $n_p$  – Number of parameters simultaneously optimized  
 $[OH]$  – Hydroxide concentration  
 $R^H$  – Hamilton R-factor, Statistical parameter generated by ESTA  
 $T$  – Temperature  
 $U$  – ESTA objective function  
 $Z_H$  – Proton formation functions generated by ESTA  
 $Z_M$  – Metal formation function generated by ESTA  
 $\lambda$  – Wavelength  
 $\lambda_{max}$  – Wavelength of maximum absorbance.  
 $\mu$  - Ionic strength





# Chapter 1

---

Introduction



## 1.1 Chelating Agents

### 1.1.1 Definition and terminology

Coordinating compounds, also called ligands (from the latin ligare = to bind), are molecules or anions containing free electrons pairs with the ability to interact with (metal)-cations (Figure 1.1) (Nowack and VanBriesen, 2005).

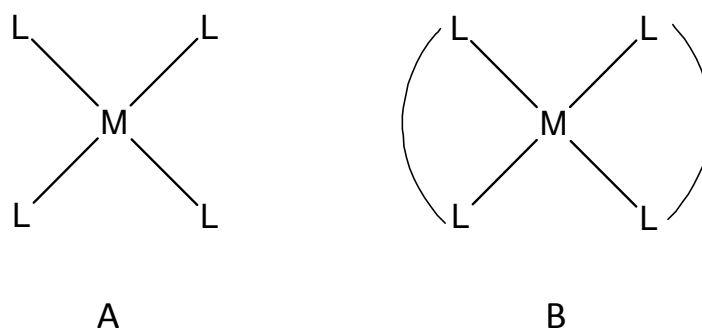


**Figure 1.1** Schematic representation of a metal complex formed by a tetracoordinated metal bound to (A) four monodentate ligand or (B) two bidentate ligand.

When each coordination compound is able to occupy only one position in the inner coordination sphere of the central ion, it is referred as monodentate (Nowack and VanBriesen, 2005) (Figure 1.1A) and a metal-complex (not a chelate) is formed by the interaction with the metal ion (Howard and Wilson, 2000). On the other hand, chelating agents are multidentate ligands, and the interaction with a single multiply-charged metal ion occurs by two (bidentate ligands), three (tridentate), or more binding sites, with the formation of a chelate ring (Knepper, 2003) (Figure 1.1B). This ring formation usually leads to species with higher stability than metal-ligand complexes in which such ring is not present (Bucheli-Witschel and Egli, 2001). The complex formation with chelating agents is called chelation (from the greek, chelè = claw) (Howard and Wilson, 2000), and the complexes formed are chelates (Nowack and VanBriesen, 2005). The term chelate was first applied by Morgan and Drew (1920). The main donor atoms found in chelating agents are N, O, S and P (Howard and

Wilson, 2000), and chelates are usually highly stable because of the shear-like enclosure of the central ion by the chelating agent. The chelating effect, but also the size of the chelate ring, plays an important role on determining the stability of the chelate. Chelate rings with six or five members, as those formed with the well-known ethylenediaminetetraacetic acid (EDTA), Figure 1.2, are usually extremely stable, when the central ion are bivalent or trivalent ions (e.g.  $\text{Mg}^{2+}$ ,  $\text{Ca}^{2+}$ ,  $\text{Zn}^{2+}$ ,  $\text{Ni}^{2+}$ ,  $\text{Cu}^{2+}$  or  $\text{Fe}^{3+}$ ) (Knepper, 2003).

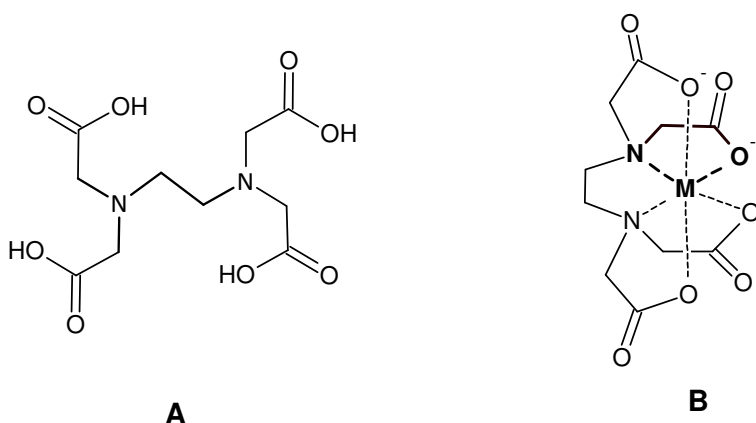


**Figure 1.2** Structure of EDTA (A), and schematic representation of a metal ion (M)-EDTA chelate with a five-membered ring highlighted (B).

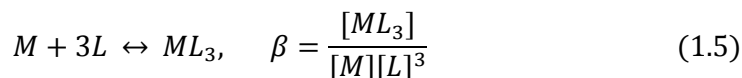
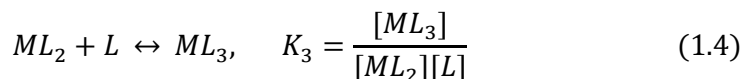
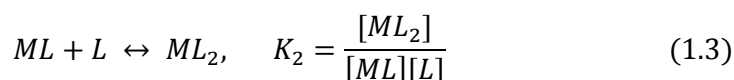
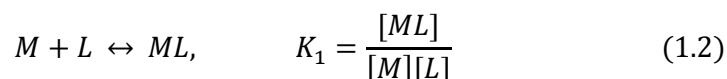
Chelation is an equilibrium system, involving the chelating agent, the solvated metal ion (the solvent molecules do not generally enter into equations), and the chelate (Howard and Wilson, 2000); the stability of a metal complex is expressed as a complex formation constant, that can also be referred as stability constant,  $K$  (IUPAC, 1997), and is defined in Equation 1.1,

$$M + L \leftrightarrow ML, \quad K = \frac{[ML]}{[M][L]} \quad (1.1)$$

where  $K$  is the complex formation constant, usually expressed as a logarithm,  $\log K$ ,  $[M]$  is the free metal ion concentration,  $[L]$  is the free ligand concentration, and  $[ML]$  is the concentration of metal complex or chelate.

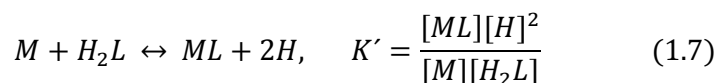
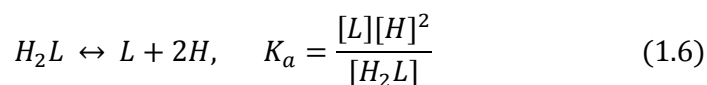
The stability constant is “an equilibrium constant that expresses the propensity of a substance to be formed from its component parts. The larger the stability constant, the more stable is the species” (IUPAC, 1997). The stability constants of chelates are usually greater than those involving the complexation of metal atoms by monodentate ligands (Howard and Wilson, 2000).

Metals are characterized by coordination numbers that corresponds to the number of donor atoms directly linked to the metal (IUPAC, 1997). When more than one ligand complexes with a single metal atom, the reaction usually proceeds stepwise. Equations 1.2-1.4 represent the equilibrium between a metal with a coordination number of six and a bidentate chelating agent, where  $\beta$  in Equation 1.5, is the overall stability constant, consisting in the product of the various step stability constants,  $\beta = K_1K_2K_3$ .

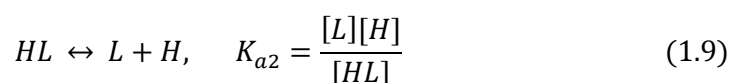
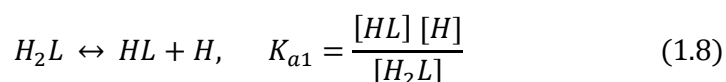


Donor atoms of chelating agents are Lewis bases, and in solution, many of the chelating agents can exist in equilibrium in the protonated or unprotonated forms. Thus, the stability constant depends on the pH of the solution, due to the competition between the metal ions and the hydrogen ions for the available donor atoms.

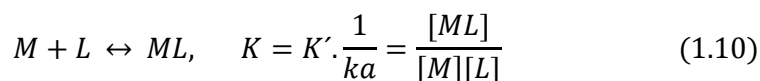
Considering  $H_2L$ , as the protonated form of a divalent ligand, L (charges are omitted for simplicity), the stability constant for metal chelation given by Equation 1.1, is the sum of the acid dissociation reaction (Equation 1.6), and the chelate formation from the protonated ligand (Equation 1.7)



$K_a$  in Equation 1.6 refers to the overall protonation constant,  $K_a = K_{a1}K_{a2}$ , obtained from



and thus the constant for the chelate formation,  $K$  (equation 1.1), from the fully dissociated form of the ligand is given by:



### 1.1.2 Chelating agents and applications

The major chemical property of chelating agents is their ability to form stable, water-soluble species with many metal ions (Bucheli-Witschel and Egli, 2001). The properties of both the uncomplexed metal ion and the chelating agent are markedly different from the chelate formed. For that, chelating agents are used to manipulate metal ions to avoid harmful, unwanted reactions. In some cases, however, they are used to take advantages from specific properties of the chelated metal ion (Howard and Wilson, 2000; Bucheli-Witschel and Egli, 2001).

In biological and synthetic processes, chelating agents are mainly used for metal solubilization and/or transport of metal cations (Knepper, 2003). Furthermore,

they are also used due to their ability to mask metal ions, which, upon chelation, lose their original chemical properties (Knepper, 2003).

In industrial processes and products, chelating agents are largely used when the presence of free metal ions causes problems such as the formation of insoluble metal salt precipitates or the catalysis of the decomposition of organic compounds (Bucheli-Witschel and Egli, 2001).

The first chelating agent to be synthesized was nitrilotriacetic acid (NTA) (Figure 1.3) in 1862 (Nowack and VanBriesen, 2005). NTA was also the first chelating agent industrially manufactured, in 1926, followed by EDTA (Figure 1.2A) in 1939 (Knepper, 2003).

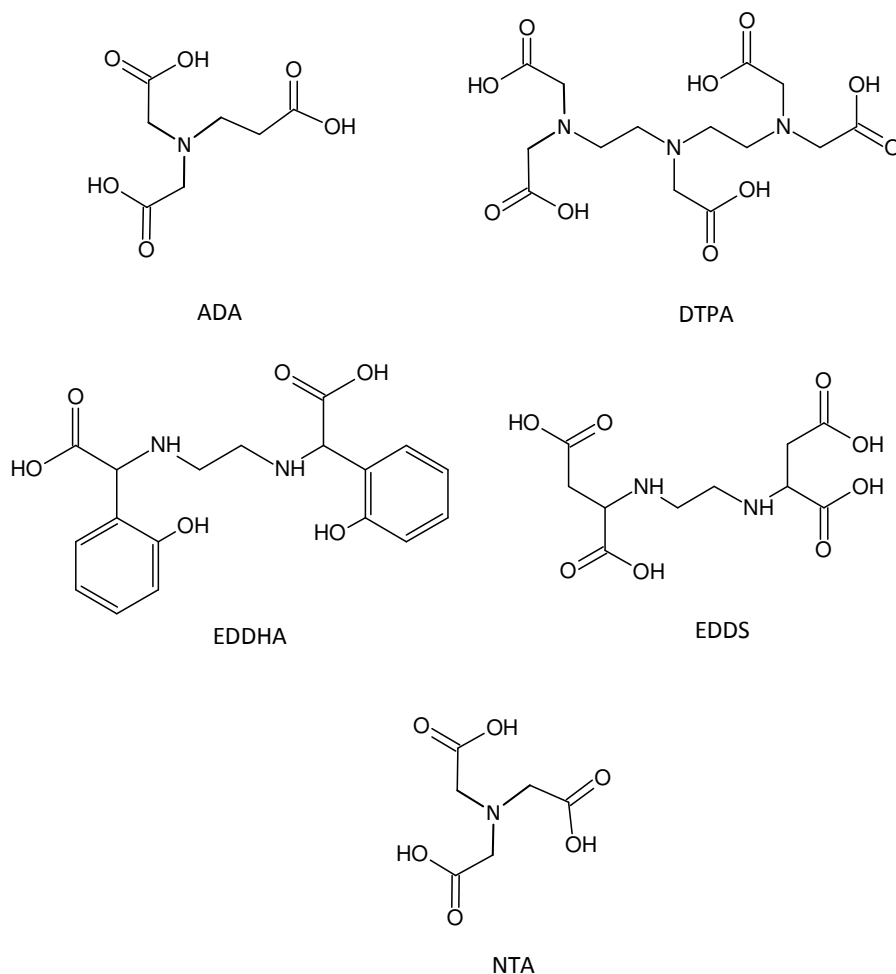


**Figure 1.3** Structural formulas of some important synthetically produced aminopolycarboxylate chelating agents (APCAs): β-alanine diacetic acid (ADA), Diethylenetriaminepentaacetic acid (DTPA), Ethylenediaminedi(o-hydroxyphenylacetic) acid (EDDHA), Ethylenediaminedisuccinic acid (EDDS), and Nitriloacetic acid (NTA).

Both EDTA and NTA belong to a large group of chelating agents called aminopolycarboxylic acids (APCAs). APCAs are characterized by one or more tertiary and secondary amines and two or more carboxylic acid groups (Nowack and VanBriesen, 2005). Some of the most important APCAs produced synthetically are shown in Figure 1.3. Besides APCAs, two more groups of chelating agents are usually considered: the phosphonates and the hydroxycarboxylates (Knepper, 2003). The group of phosphonates include compounds containing the phosphonic acid moiety  $\text{-C-PO(OH)}_2$  (Figure 1.4) that are, in many cases, structure-analogues of the aminopolycarboxylates (Nowack and VanBriesen, 2005). Some hydroxycarboxylates also differ from APCAs only from the replacement of the carboxylate group by a hydroxyl group (Knepper, 2003). Examples of phosphonate and hydroxycarboxylates chelating agents are represented in Figure 1.4 and Figure 1.5, respectively. Phospho butanetricarboxylic acid (PBTC) (Figure 1.6) is an example of a mixed carboxylate-phosphonate chelating agent.

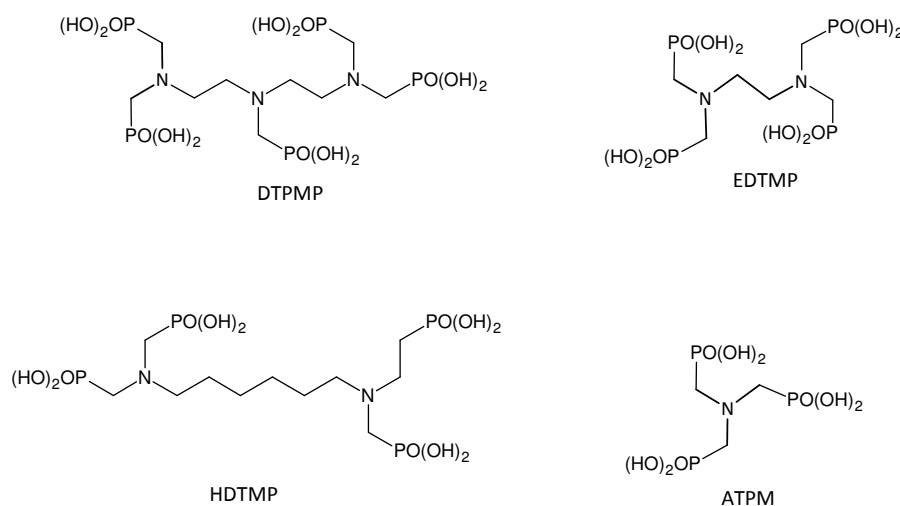


**Figure 1.4** Structural formulas of phosphonate type chelating agents: Diethylenetriaminepentakis(methylene) phosphonic acid (DTPMP), 1,2-Diaminoethane-tetrakis(methylenephosphonic) acid (EDTMP), Hexamethylenediamino tetra(methylenephosphonic) acid (HDTMP), and Aminotrimethylenephosphonic acid (ATPM).



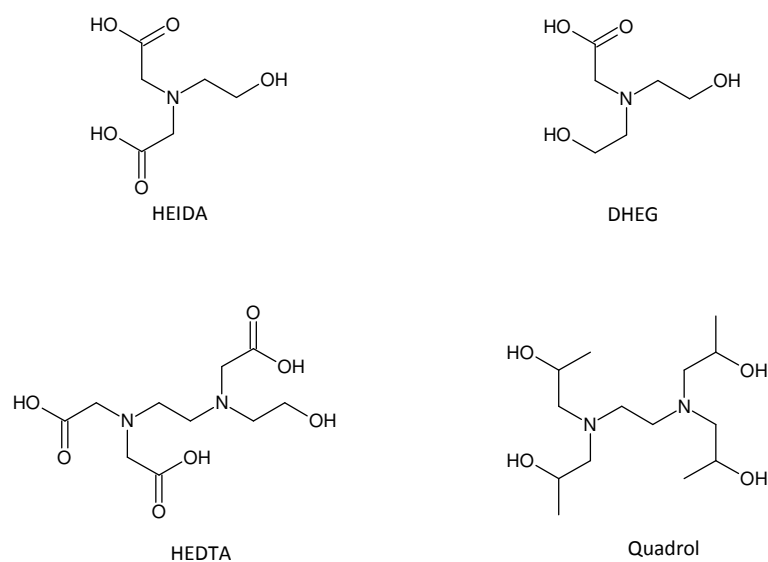


**Figure 1.5** Structural formulas of hydroxycarboxylate type chelating agents: N-(2-hydroxyethyl)iminodiacetic acid (HEIDA), N,N-bis(2-hydroxyethyl)glycine (DHEG), (Hydroxyethyl)etylenediaminetriacetic acid (HEDTA), and N,N,N',N'-tetrakis-2-hydroxyisopropylethylenediamine (Quadrol).

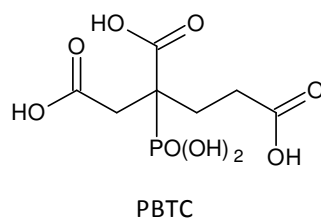


**Figure 1.6** Structural formula of a mixed carboxylate-phosphonate chelating agent: Phosphonobutane-tricarboxylic acid (PBTC).

The importance of the chelating agents is demonstrated by the estimated values reported for their production and consumption in USA and Europe (Table 1.1). EDTA is the most widely used chelating agent in the world. In 1999, about 34 000 tons of EDTA were used in Europe, and in 2000 the total use of APCAs was of 200 000 tons (Nowack and VanBriesen, 2005).

**Table 1.1** Estimated production/use of chelating agents (tons/year).

	Europe	Year	US	Year
EDTA	13 600 <sup>(a)</sup>	1981	42 000 <sup>(a)</sup>	1981
	34 500 <sup>(b)</sup>	1999	50 000 <sup>(b)</sup>	1987
NTA	8 300 <sup>(a)</sup>	1981	32 000 <sup>(a)</sup>	1981
	19 890 <sup>(b)</sup>	1999		
DTPA	500 <sup>(a)</sup>	1981	4 000 <sup>(a)</sup>	1981
	14 350 <sup>(b)</sup>	1999		
HEDTA	2 000 <sup>(a) (b)</sup>	1981	18 000 <sup>(a)</sup>	1981
Other APCAs	2 000 <sup>(a)</sup>		2 500 <sup>(a)</sup>	
(Organo)phosphonates	16 000 <sup>(b)</sup>	1999	30 000 <sup>(b)</sup>	1991
Hydroxycarboxilic acids	15 000 <sup>(a)</sup>	1981	110 000 <sup>(a)</sup>	1981

a) Europe, based on consumption; USA, based on production (Bucheli-Witschel, 2001)

b) Based on consumption (Nowack and VanBriesen, 2005)

Chelating agents are mainly used to avoid interferences by metal ions (Knepper, 2003) in industrial processes; this is accomplished by preventing the formation of metal precipitates by removing metal ions from the systems and hindering metal ions catalysis of unwanted chemical reactions. Nevertheless, in some cases they are also used to make metal ions more available by keeping them in solution (Bucheli-Witschel, 2001).

Some of the areas and application of chelating agents are listed below (Knepper, 2003; Nowack and VanBriesen, 2005):

- In textile, pulp and paper industry, to mask heavy-metal ions. Phosphonates, for example, are used to complex heavy metals in chlorine-free bleaching solutions that could inactivate the peroxide.
- As additives in washing and cleaning agents, where they are important for binding  $\text{Ca}^{2+}$  and  $\text{Mg}^{2+}$  ions, to prevent the deposition of scale on textiles, and washing machine parts; as well as for the stabilization of bleach during the storage and washing.
- As dispersion and corrosion inhibiting agents; the formation of water-soluble metal complexes leads to the elimination of deposits (metallic oxides of copper and iron) and water incrustations. Chelating agents are used in industrial cleaning agents, cooling waters, desalination systems and in oil fields to inhibit scale formation, e.g. barium sulfate and calcium carbonate precipitation.
- In the photo industry as oxidizing agents, where  $\beta$ -ADA and PDTA are being used as substitutes for EDTA.
- In plating enterprises, as inhibitors during the elimination of nickel from galvanic wastewater, and to mask  $\text{Ca}^{2+}$  and  $\text{Mg}^{2+}$  ions and dissolve their oxides. Quadrol (Figure 1.5) is used in copper-separation processes.
- In nuclear industry for decontamination of reactors and equipment, due to the formation of water soluble complexes with radionuclides.
- In surface treatment and in pretreatment baths, as intermediaries in dissolving heavy metals, metals and their oxides.
- In dairies and milk-processing enterprises, to support the elimination and/or prevention of the formation of milk-stone linings. Among other compounds, NTA and MGDA are being proposed to replace the predominantly used EDTA.
- In remediation of contaminated soils or sludges.
- In agriculture: Fe(III) chelates of EDTA, HEDTA, DTPA, EDDHA, and Cu(II), Zn(II) and Mn(II) chelates of EDTA are present in fertilizers.
- In the pharmaceutical, cosmetics and foodstuffs industries, as stabilizers for formulations and as antioxidants. EDTA is used to sequester trace metals to prevent metal-catalyzed reactions responsible for loss of flavor, rancidity, and discoloration in food products and vitamins, and to control metals that destabilize cosmetics and pharmaceuticals.

Chelates and chelation reactions are also abundant in nature, and are involved in biochemical processes such as photosynthesis, oxygen transport by blood, enzymatic reactions, and ion transport through membranes (Howard and Wilson, 2000). Chlorophyll, hemoglobin and hemecyanin are examples of natural chelatin agents (Knepper, 2003). Several naturally occurring chelating agents, Figure 1.7, are produced by plants and microorganisms and are involved in the metal uptake by these organisms (Bucheli-Witschel and Egli, 2001).

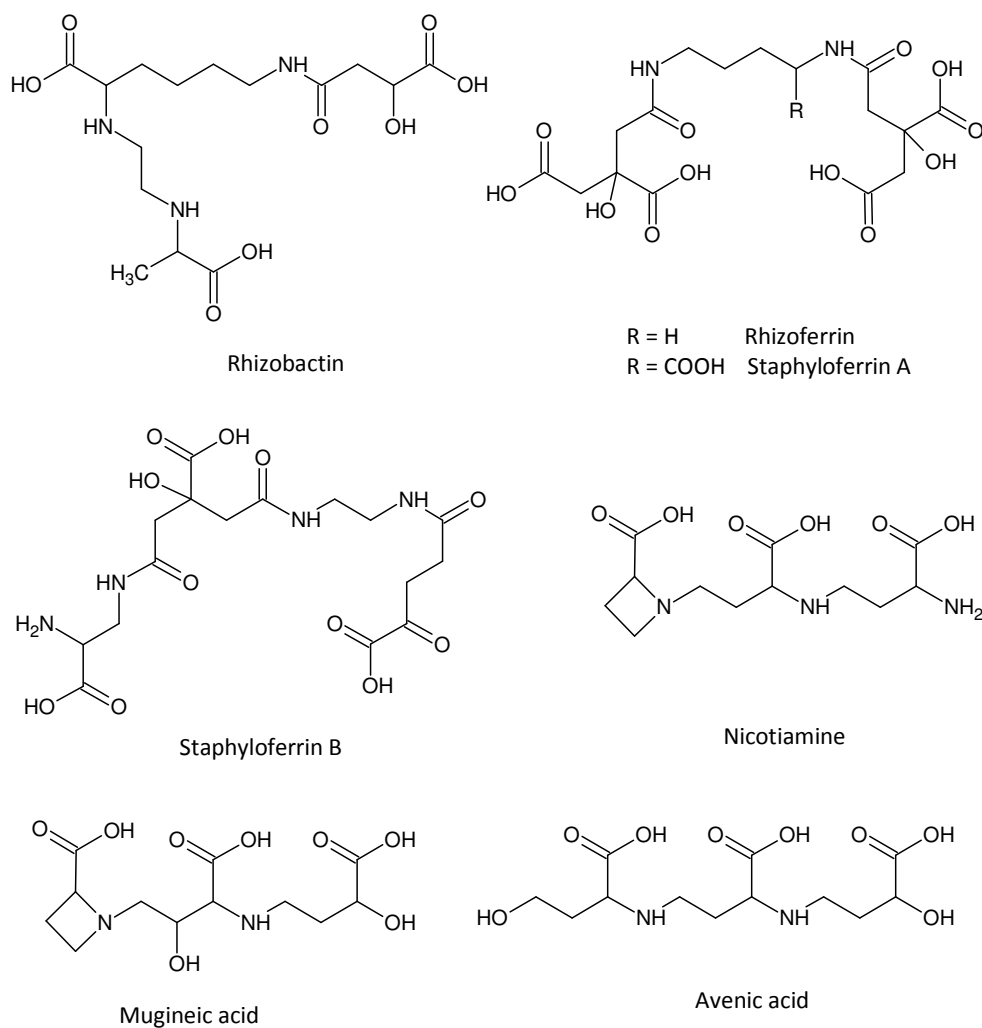


**Figure 1.7** Structural formula of some naturally occurring chelating agents.

For example, rhizobactin and rizoferin (Figure 1.7), which are produced by *Rhizobium meliloti* and *Rhizopus microspores*, respectively, under low-iron conditions, are able to deliver iron to the producing organism and in some cases to other organisms as well. Also mugineic and avenic acids are known to play a role in the iron uptake by some plants. (Bucheli-Witschel and Egli, 2001).

In the last decade, the environmental fate of chelating agents has received considerable attention and the use of synthetic chelating agents non-degradable became a matter of concern. Much investigation has been performed in order to find environmental friendly alternatives to replace such compounds. From this, several naturally chelating agents have been studied and mass production was suggested for the application in different areas such as agriculture, medical science and pharmacy (Bucheli-Witschel and Egli, 2001).

Environmental concerns regarding to the persistence in the environment of slowly or non-biodegradable chelating agents arise specially from their potential to perturb the natural speciation of metals and to influence metal availability. Their presence at high concentrations may lead to the remobilization of metals from sediment, aquifers, and wastewater sludges, creating a risk to ground water and drinking water (Nowack and VanBriesen, 2005).

## **1.2 Iron**

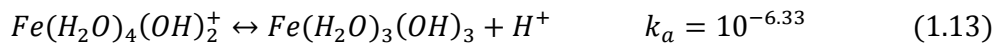
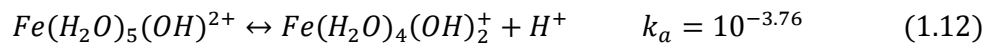
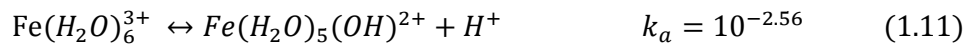
### **1.2.1 Bioavailability of iron**

Iron (Fe) is an essential element for the growth and development of nearly all living organisms, including bacteria, fungi and plants. It acts as a catalyst in some of the most fundamental enzymatic processes including oxygen metabolism, electron transfer, DNA and RNA synthesis, playing an ubiquitous role in redox enzymes, especially in the context of respiration and photosynthesis (Amin, et al., 2009; Barberon, et al., 2011; Schalk, et al., 2011).

It is the fourth most abundant element in the earth's crust, after oxygen, silicon and aluminium, and occurs in excess in most types of soil (Loper and Buyer, 1991; Lemanceau, et al., 2009; Radzki, et al., 2013). However, under aerobic conditions at neutral pH, iron is present only in the form of extremely insoluble hydroxides, oxyhydroxides and oxides. The formation of such species severely restricts the bioavailability of this metal for plants and microbes. It has been estimated that nearly approximately one third of the earth soil can be considered iron deficient (Tagliavini and Rombola, 2001; Lemanceau, et al., 2009; Bao, et al., 2010; Radzki, et al., 2013).

Iron exists in a wide range of oxidation states, but the ferrous ( $\text{Fe}^{2+}$ ) and ferric ( $\text{Fe}^{3+}$ ) are the most common (Miethke, 2013). In primary minerals, iron occurs in its ferrous state, that, upon weathering, is oxidized to  $\text{Fe}^{3+}$ , in a process that depends on the redox and pH conditions of the soil environment. Under aerobic conditions and at pH values in the range of 5 to 8,  $\text{Fe}^{2+}$  is readily oxidized to  $\text{Fe}^{3+}$ , which after release from mineral lattices precipitates, and forms ferric oxides and hydroxides (Colombo, et al., 2014).

In aqueous aerobic environment, iron is present as the ferric ion that is a moderately strong Brønsted acid with  $\text{pK}_a$ 's of 2.56, 3.56 and 6.33 (Eqs: 1.11-1.13) (Crumbliss and Harrington, 2009,)



and upon deprotonation, a variety of insoluble hydroxides such as  $\text{Fe}(\text{OH})_3$  ( $K_{\text{sp}} = 4 \times 10^{-38}$ , Equation 1.14) (Colombo, et al., 2014) can be formed.



Iron(II) has higher solubility than iron(III) due to the lower charge density and consequently much less acidic coordinated water ligands. However, iron(II) is much less stable than iron(III), and is oxidized upon exposure to oxygen.

In most minerals, iron(III) occurs in octahedral coordination with oxygen. Crystalline Fe (hydro)oxides, goethite ( $\alpha$ -FeOOH) and hematite ( $\alpha$ -Fe<sub>2</sub>O<sub>3</sub>) are the most stable and abundant minerals in well-drained soil. Other Fe oxides may exist in poorly drained soil as crystalline minerals (lepidocrocite, maghemite, and magnetite), short-range-ordered crystalline minerals (ferrihydrite and ferroxite), or noncrystalline precipitates (Colombo, et al., 2014).

It has been estimated that the total concentration of inorganic Fe species in the soil solutions is around  $10^{-10}$  mol.L<sup>-1</sup> (Crumbliss and Harrington, 2009), that is much lower than that required for organisms (microorganisms, fungi and plants) (Loper and Buyer, 1991; Hider and Kong, 2010; Colombo, et al., 2014). In order to overcome the low availability of iron, these organisms developed specific mechanisms to obtain iron from the environment. The particular case of plants will be discussed in section 1.3.

### 1.2.2 Iron in plant nutrition

Iron is one of the most studied element in mineral nutrition of plants and was first recognized as essential for plant growth by Griss in 1843 (Shenker and Chen, 2005; Ma and Ling, 2009).

In cultivated soils solutions at pH range relevant to plant growth, the solubility of iron is controlled, as referred in section 1.2.1, at extremely low levels by stable hydroxides, oxyhydroxides and oxides (Lemanceau, et al., 2009). The minimum concentration of soluble Fe required in soil solution for plants ( $10^{-9}$  to  $10^{-4}$ M) is above the maximal value in the pH range of 7.4 to 8.5 (common in calcareous soils), which is less than  $10^{-10}$  (Loper and Buyer, 1991; Crowley, et al., 1992; Shenker and Chen, 2005). This iron limitation (often associated with alkaline, calcareous soils) frequently leads to iron deficiency in plants, manifested as leaf chlorosis (Shenker and Chen, 2005; Weger, et al., 2009).

In plants, Fe is involved in the synthesis of chlorophyll and is essential for the maintenance of chloroplast structure and function (Bao, et al., 2010). Iron chlorosis is a

nutritional disorder that is caused by a reduction in leaf photosynthetic pigment concentration, and intervenial leaf yellowing is the most characteristic visual symptom in chlorotic plants. Fe-deficiency is a worldwide problem that leads to yield loss and reduced quality and size in crops (Alvarez-Fernandez, et al., 2003; Lemanceau, et al., 2009; Rodriguez-Lucena, et al., 2010; Jin, et al., 2014).

Iron deficiency in plants is often a matter of availability rather than quantity of iron. This widespread nutritional disorder occurs in well aerated soils, especially but not only in alkaline and calcareous soils, and limits crop production. In this type of soils, calcium carbonate buffers soil solution pH at 7.5–8.5 range, and there is a high bicarbonate concentration. It is estimated that calcareous soils cover about 30% of world's land surface (Alvarez-Fernandez, et al., 2003; Shenker and Chen, 2005; Lemanceau, et al., 2009; Ma and Ling, 2009; Rodriguez-Lucena, et al., 2010).

Cultivated plants differ on their susceptibility to Fe deficiency. Many of the most important horticultural and agronomic crops are susceptible to Fe deficiency. Peach, pear, kiwifruit and citrus are among the most susceptible crops to suffer from Fe chlorosis (Tagliavini and Rombola, 2001; Lucena, 2003).

Some plant species have developed efficient strategies for acquiring Fe from low solubility sources (Ma and Ling, 2009). At least two distinct strategies of iron assimilation have been identified, that differ in the way how to solubilize and transport Fe: Strategy I found in dicotyledonous and non-graminaceous monocotyledonous species, and Strategy II found only in graminaceous species (Colombo, et al., 2014; Ma and Ling, 2009).

Strategy I (Figure 1.8) (dicotyledonous and non-graminaceous monocotyledonous) involves i) Fe(III) solubilization, usually by rhizosphere acidification, through proton extrusion, mediated by activation of plasmalemma  $H^+$ -ATPase; ii) enhanced release of reductants and chelating compounds (organic acids containing carboxylates, and mostly phenolic groups) for Fe(III) complexation and mobilization, and iii) reduction of Fe(III) to the more soluble Fe(II) form by a NADPH-ferric chelate reductase (FCR), before iv) uptake into roots cell by a specific transporter for Fe(II), (Holden, et al., 1991; Marschner and Römheld, 1994; Lucena, 2003; Shenker and Chen, 2005; Günter and Volker, 2007; Ma and Ling, 2009; Bao, et al., 2010; Jin, et al., 2014).



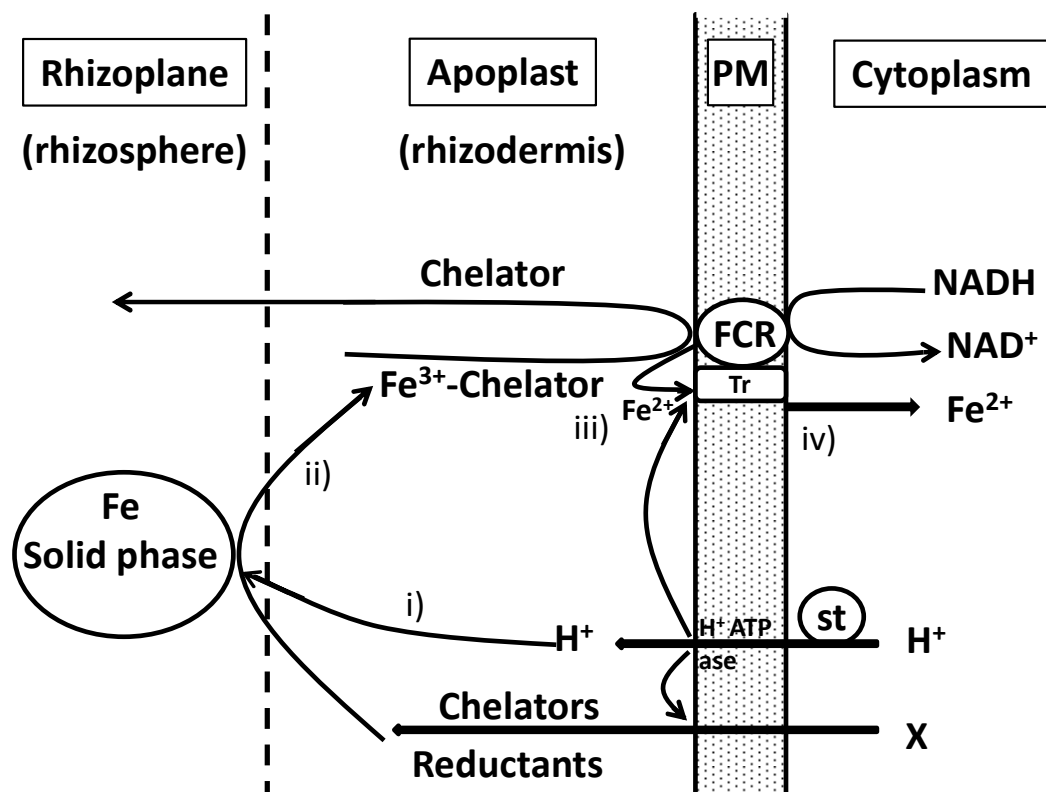


**Figure 1.8** Model for root responses to iron deficiency for Fe acquisition in Strategy I plants. i) Fe(III) solubilization, usually mediated by rhizosphere acidification, through proton extrusion (mediated by activation of plasmalemma  $H^+$ -ATPase); ii) complexation with chelating compounds released; iii) reduction of Fe(III) to Fe(II) by ferric chelate reductase (FCR); iv) uptake into roots cells by a specific transporter for Fe(II): PM = plasma membrane; St = stimulated  $H^+$  pumping ATPase; X = Production/release of chelators/reductants. (Adapted from Marschner and Römheld (1994)).

This high affinity iron transporter at the root surface is appointed to be the iron-regulated transporter 1 (IRT1), from the model plant *Arabidopsis*. IRT1 homologs have also been characterized in other plants, such as in Pea and tomato (Lemanceau, et al., 2009; Barberon, et al., 2011). The release of phenolic acids and compounds containing the carboxylate group is responsible for Fe(III) complexation, and also, at some extent, for Fe(III) reduction in the rhizosphere.

Fe deficiency also induces the accumulation of organic acids (citrate, malate) in the root tissue. These compounds not only provide protons for the  $H^+$ -ATPase-mediated rhizosphere acidification, but the related metabolism, also provides electrons for Fe deficiency-induced plasma membrane-bound reductase system (Günter and Volker, 2007).

Strategy II (Figure 1.9) (graminaceous species) is characterized by the synthesis and secretion of highly effective chelators for Fe(III) (phytosiderophores (PS), also known as mugineic acids (MAs), which are derived from nicotiamine.

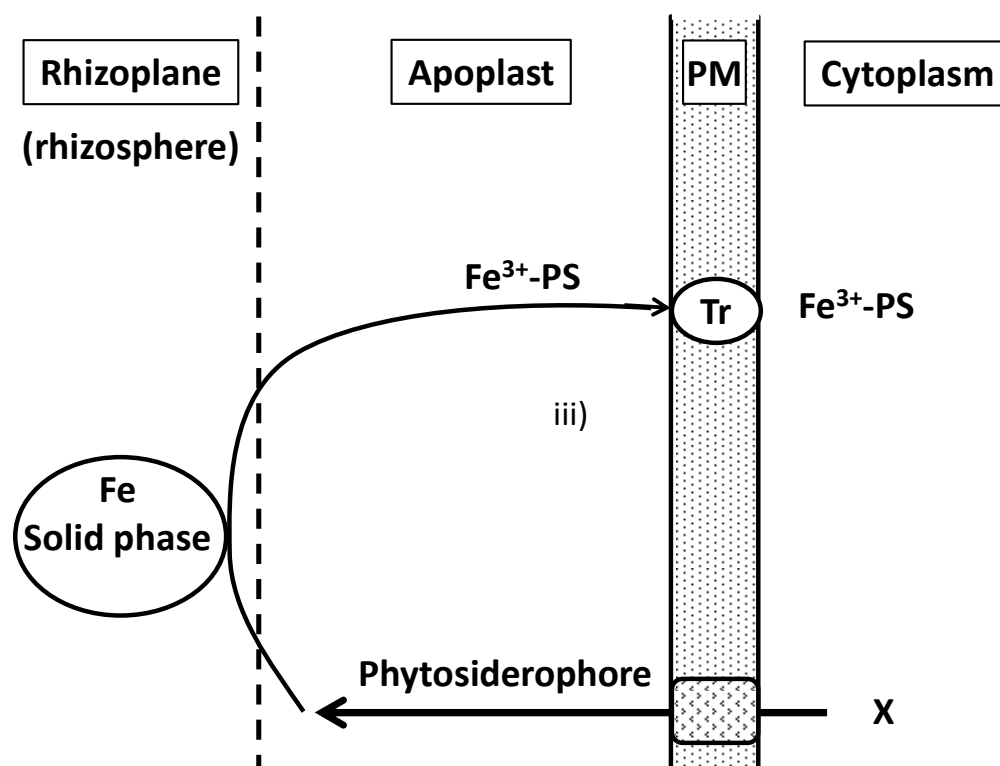


**Figure 1.9** Model for root responses to iron deficiency for Fe acquisition in Strategy II plants, involving the synthesis of phytosiderophores that upon complexation with iron(III) with the formation of a  $Fe^{3+}$ -PS chelate are taken up by a specific uptake system (Tr). (Adapted from Marschner and Römheld (1994)).

$Fe^{3+}$ -PS complexes are taken up by a specific uptake system, located at the plasma membrane in roots of graminaceous plants. The best characterized of this transporters is YS1 (Yellow stripe 1) (or YSL1, yellow stripe-like), named after the

phenotypic appearance of a maize mutant, deficient in phytosiderophore uptake (Crichton, 2007).

After entering the cytosol, the behavior of Fe-PS complexes is still unknown, but Fe liberation occurs probably via reduction by common physiologically available reductants such as NAD(P)H and glutathione (Jurkevitch, et al., 1993; Morrissey and Guerinot, 2009; Shenker and Chen, 2005; Günter and Volker, 2007; Ma and Ling, 2009; Namba and Murata, 2010).

Mugineic acid (MA), avenic acid (Figure 1.7), Hydroxymugineic acid (HMA), epihydroxymugineic acid (epi-HMA) and distichonic acid A (Figure 1.10) are examples of PS identified in barley, rye and oat (Günter and Volker, 2007; Kobayashi, et al., 2008).

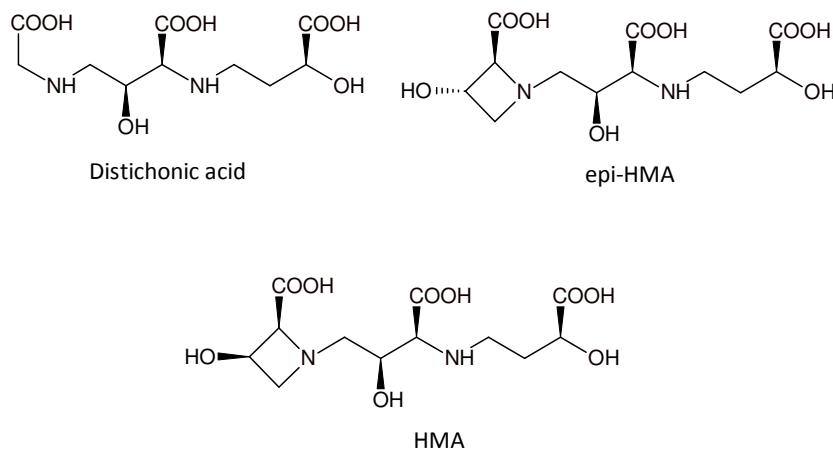


**Figure 1.10** Structures of some phytosiderophores: distichonic acid, 3-epi-hydroxymugineic acid (epi-HMA) and 3-dydroxymugineic acid (HMA).

Plant strategies to acquire iron are often not efficient enough to meet the needs of the plants growing especially in calcareous and alkaline soils (Radzki, et al., 2013). Fe availability to plants and its uptake, transport and accumulation in plants is of great concern and several agronomical approaches to alleviate Fe deficiency considered are based on: i) increasing the availability of indigenous soil-Fe; ii) supplying the plant with external sources of available Fe; and iii) increasing plant efficiency in Fe uptake and translocation (Shenker and Chen, 2005).

### 1.2.2.1 Iron chelates in plant nutrition

Different types of iron fertilizers can be used to overcome Fe chlorosis. These fertilizers can be grouped in three main classes: inorganic Fe-compounds, natural Fe-complexes, and synthetic Fe-chelates (Lucena, et al., 2010; Abadia, et al., 2011).

Inorganic Fe-compounds include soluble Fe salts (e.g.,  $\text{Fe}_2(\text{SO}_4) \cdot 7\text{H}_2\text{O}$ ), insoluble compounds such as Fe oxide-hydroxides and other (cheap) Fe minerals, and industrial by-products (e.g. low grade pyrite ( $\text{FeS}_2$ ) from mining residues, Fe-dust from steel industry and coal slurry solids). These compounds are quite inefficient, especially when applied to high pH soils (i.e. calcareous soils) and are commonly used in foliar fertilization (Shenker and Chen, 2005; Abadia, et al., 2011).

Natural Fe complex fertilizers may have different origins and derive generally from natural products, such as peat, manure and composted organic residues or by-products of wood processing wastes. This group includes a large number of substances such as humates, lignosulfonates, amino acids, gluconate, citrate. Due to the low stability in soils, natural Fe-complexes are recommended only in soil-less horticulture and also for foliar applications (Abadia, et al., 2011).

Currently, fertilization with synthetic chelates [e.g. EDTA (Figure 1.2 in section 1.1.1) and EDDHA (Figure 1.3 in section 1.1.2)] is the most effective agricultural practice to prevent or correct Fe deficiencies in crops and the most widely distributed. Synthetic Fe-chelate fertilizers are obtained from polyaminocarboxylic acids, which have high affinity for Fe(III) and can be classified as nonphenolic chelates, such as EDTA, and phenolic chelates such as EDDHA (Villen, et al., 2007; Lucena, et al., 2010; Radzki, et al., 2013; Abadia, et al., 2011).

Besides EDTA and EDDHA, some of the main chelating agents used to prepare commercial Fe fertilizers are diethylenetriaminepentaacetic acid (DTPA), hydroxyethylethylenediaminetriacetic acid (HEDTA) (Figures 1.3 and 1.4 in section 1.1.2), ethylenediamine-di(2-hydroxy-4-methylphenylacetic acid (EDDHMA), ethylenediaminedi(5-carboxy-2-hydroxyphenylacetic) acid (EDDCHA) and ethylenediamine-N,N'-bis(2-hydroxy-5-sulfonylphenyl) (EDDHSA) (Figure 1.11) (Lucena, 2003).

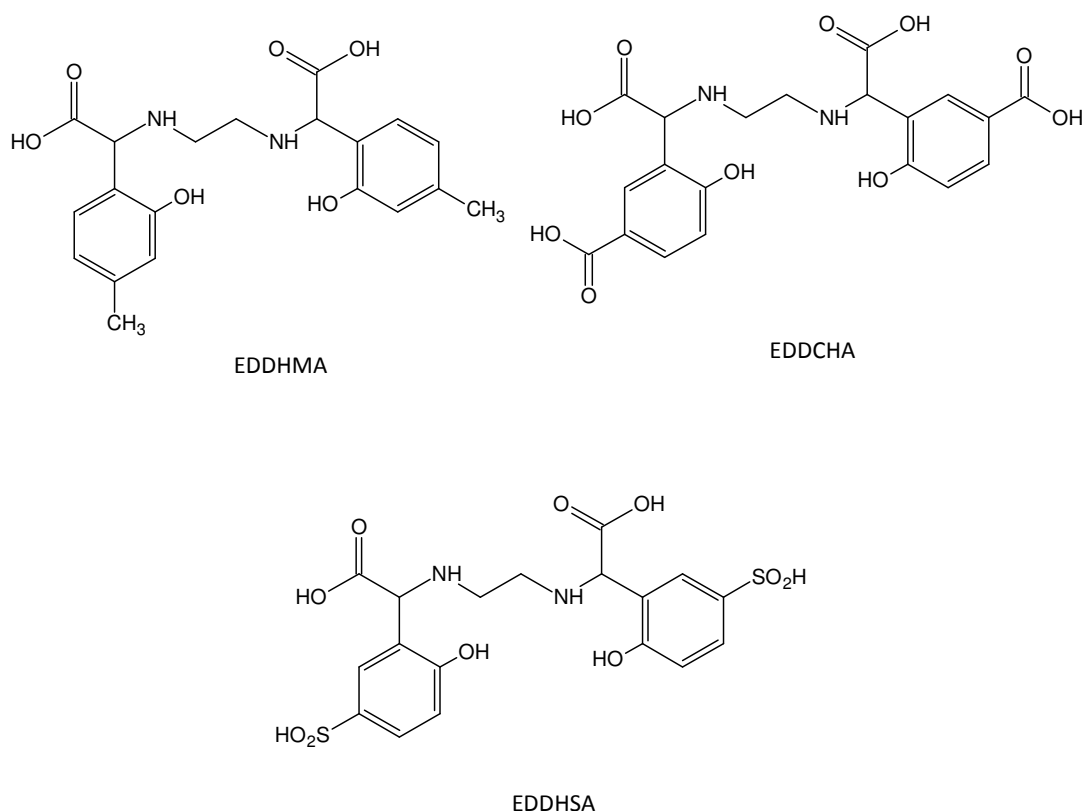


**Figure 1.11** Structures of ethylenediamine-di(2-hydroxy-4-methylphenylacetic acid (EDDHMA), ethylenediamine-di(5-carboxy-2-hydroxyphenylacetic) acid (EDDCHA) and ethylenediamine-N,N'-bis(2-hydroxy-5-sulfonylphenyl) (EDDHSA).

The first description of the use of synthetic chelating agents in plant nutrition dates back to 1951 when Fe(III)EDTA was firstly used as iron fertilizer for chlorotic plants (Jacobson, 1951). EDDHA, one of the most efficient iron fertilizers, was synthesized also in 1951 (Jacobson, 1951; Nowack, 2008).

In the particular case of calcareous soils, synthetic Fe(III)-chelates from chelating agents with phenolic groups are very effective Fe fertilizers while the efficacy of the nonphenolic chelates lowers considerably when applied in alkaline soils (Abadia, et al., 2011; Yunta, et al., 2013). Recently, the Fe(III)-chelates of three chelating agents, N,N'-Bis(2-hydroxybenzyl)ethylenediamine-N,N'-diacetic acid (HBED), N,N'-Bis(2-hydroxy-5-methylbenzyl)ethylenediamine-N,N'-diacetic (HJB) and 2-((2-hydroxybenzyl)amino)ethylamino)-2-(2-hydroxyphenyl)acetic acid (DCHA) (Figure

1.12), structurally similar to *o,o*-EDDHA, have been proposed for Fe-fertilization (Abadia, et al., 2011).

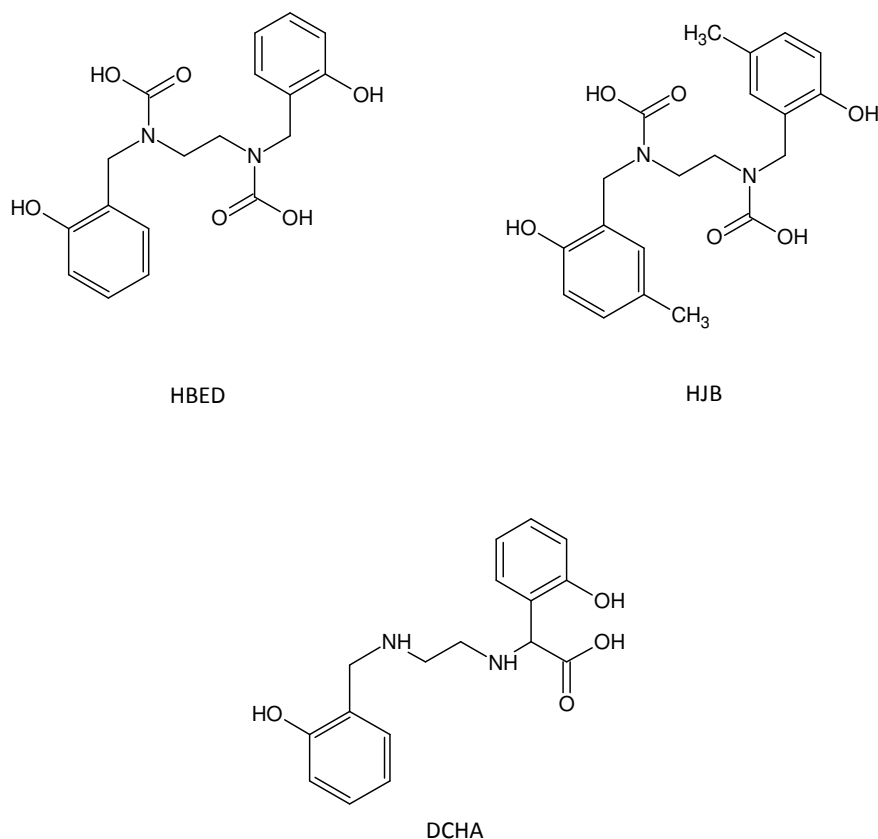


**Figure 1.12** Structures of N,N'-Bis(2-hydroxybenzyl)ethylenediamine-N,N'-diacetic acid (HBED), N,N'-Bis(2-hydroxy-5-methylbenzyl)ethylenediamine-N,N'-diacetic (HJB) and 2-(2-((2-hydroxybenzyl)amino)ethylamino)-2-(2-hydroxyphenyl)acetic acid (DCHA).

The ability of chelating agents to keep Fe in soluble form depends on their stability. Chelating agents (e.g. HEDTA, EDTA, DTPA), that form low stability chelates can maintain Fe in solution but not in calcareous soil conditions (Lucena, 2003). EDTA, for example, sustains Fe in a soluble form effectively in moderately acid to near neutral soils, but loses its Fe chelating ability above pH 7. At this pH, DTPA is still able to chelate significant amounts of Fe. Fe-EDDHA is stable in a wider pH range (from pH 4 up to 9) and is able to maintain Fe in soil solution and transport it to the plant root in high calcareous soils (Ylivainio, et al., 2006; Colombo, et al., 2014).

To be effective for improving Fe nutrition, a good chelating agent must also be able to maintain large amounts of Fe in solution without being displaced by other cations (Lucena, 2003). However, excessively high stability constant of a Fe-chelate might make the iron poorly available for the FCR and hence impair root Fe uptake in Strategy I plants (Tagliavini and Rombola, 2001). In this case, the redox potential must not be low (i.e.  $E_o > -500\text{mV}$ ) to enable the ferric complex to be easily reduced (Shenker and Chen, 2005). In Strategy II, the Fe uptake system, based on  $\text{Fe}^{3+}$ -phytossiderophores, does not work for strong chelates such as  $\text{Fe}^{3+}$ -EDDHA (Lucena, et al., 1988), and if the chelate is to be used in Strategy II plants, lower affinity for  $\text{Fe}^{3+}$  might be required to facilitate iron exchange with the phytossiderophores. On the other hand, the direct uptake by plants of other chelating agents than PS have been proposed by several authors, specially for the particular case of microbial siderophores ( $\text{MS}_s$ ), but the existence of a specific Fe uptake mechanism has not been proven so far (Bar-Ness, et al., 1992; Hördt, et al., 2000; Vansuyt, et al., 2007).

When applied to Strategy I plants, once the Fe has been released to the plant, the re-use of the chelating agent may occur with the ligand going back, by the concentration gradient, and take more native iron from the solid phase (Figure 1.13). This hypothesis is called “the “shuttle effect”. It depends on the reactivity and degradation (microbial, chemical and photochemical) of the free anion (chelating agent), and to occur it is important that the rate of chelation of the native iron allows a rapid reformulation of the chelate (Lucena, 2003; Shenker and Chen, 2005). Fe-EDTA, Fe-EDDHA and Fe-DTPA are the most widely-evaluated Fe chelates (Goos and Germain, 2001). Occasionally, new products are proposed as Fe fertilizers, especially for application in alkaline soils.

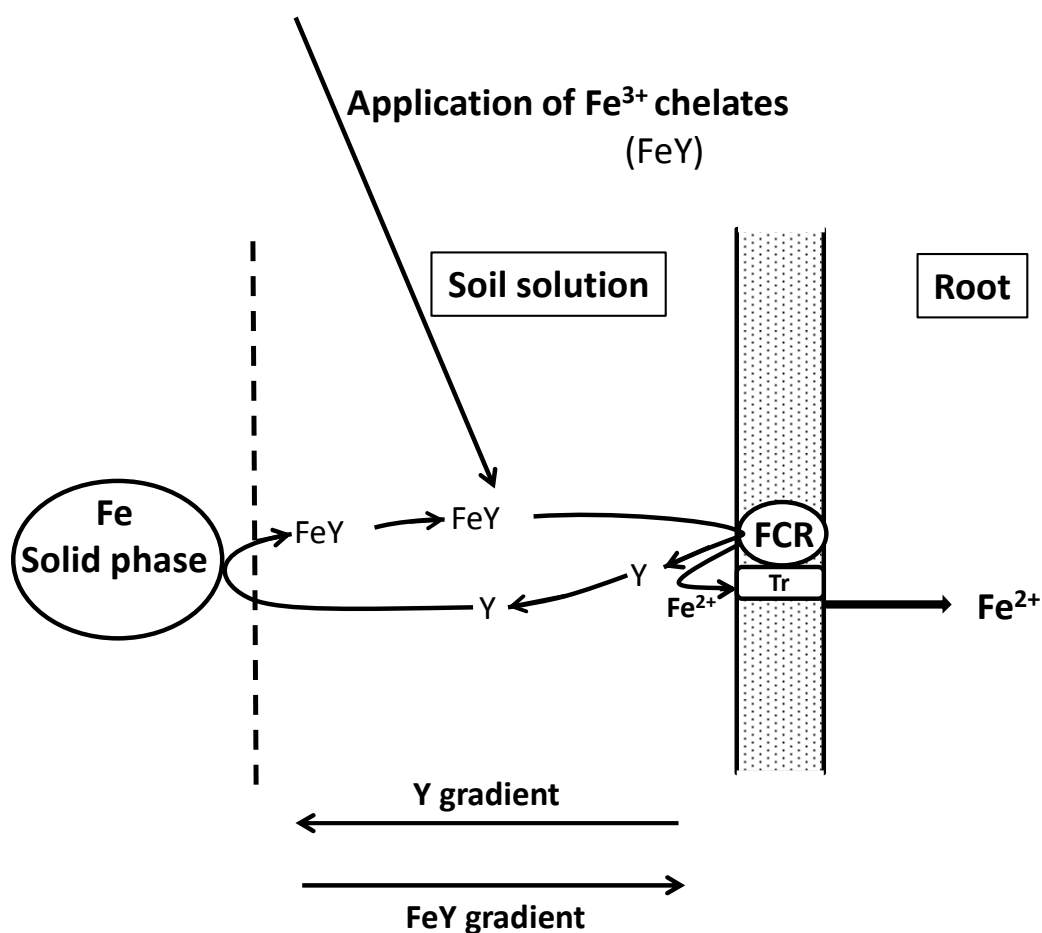


**Figure 1.13** Model for the mechanism of action of Fe chelates in soils.  $\text{FeY}=\text{Fe}^{3+}$  chelate;  $\text{Y}$ =Chelating agents; FCR= Ferric chelate reductase; Tr = Ferrous transporter. (Adapted from Lucena (2003)).

Many of the poly aminocarboxylate chelating agents used in Fe-fertilization, including both EDTA and EDDHA, are poorly biodegradable. After the chelate splitting (dechelation) this ligands remain in soil which leads to environmental concerns, arising from their persistence in the environment especially in ground water and drinking water. Thus, the behaviour of chelating agents in the environment has received much attention in the last decades (Nowack, 2008). EDTA, for example, occurs at higher concentration in European surface water than other anthropogenic organic compound (Nowack, 2008; Abadia, et al., 2011). Although high concentrations of EDTA are not toxic for humans, it is not easily removed during wastewater treatment and the main risk remains in its ability to bind heavy and toxic metals and rend them water soluble



and thus contaminating drinking water. EDTA has been found to increase plant uptake of Pb and Cd, and to leach these heavy metals (Ylivainio, et al., 2006; Radzki, et al., 2013).

Biodegradable chelating agents, such as ethylenediaminedisuccinic acid (EDDS) (Figure 1.3 in section 1.1.2), have been studied with variable results, markedly dependent of the soil pH (Abadia, et al., 2011). Recently, the degradable chelating agent, N-(1,2-dicarboxyethyl)-D,L-aspartic acid (Figure 1.14), commonly known as iminodisuccinic acid, IDHA have been proposed as Fe fertilizers (Villen, et al., 2007) but the use of this product also showed limitations. Lucena et al. (2008) showed that IDHA can be used instead of EDTA chelates in hydroponics and fertigation cultures; however, its use at high pH conditions or with highly Fe sensitive crops is not recommended (Lucena, et al., 2008). On the other hand, foliar application of Fe(III)-EDTA to peach trees showed to be more efficient than Fe(III)-IDHA (Abadia, et al., 2011).

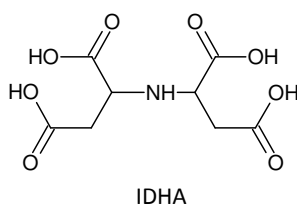


**Figure 1.14:** Structure of N-(1,2-dicarboxyethyl)-D,L-aspartic acid (IDHA).

Alternatives to the iron chelators in use are being studied either to enhance the effectiveness as iron fertilizers or to be replaced by more environmental friendly compounds. The use of biological chelators for more environmental friendly practices is under evaluation. Since  $\text{Fe}^{3+}$ -siderophores are considered efficient Fe carriers within the soil solution up to the root cells and through the cell wall, they have been considered as good iron fertilizers (Colombo, et al., 2014). The potential use of microbial siderophores as iron fertilizers will be discussed in section 3.2.

The potential market for Fe chelators in 2006 was estimated to be 200-400 €  $\text{ha}^{-1} \text{ year}^{-1}$  (Radzki, et al., 2013). However, the alleviation of Fe-chlorosis remains a major agronomic problem that stimulates the study of new methods and products for fertilizing soils; this includes the use of new biological iron chelators.

## 1.3 Siderophores

### 1.3.1 Siderophores-Iron chelators

Siderophores (Greek for "iron carriers") are defined as relatively low molecular weight (<1500 Da) organic chelating agents with very high and specific affinity for Fe(III). These compounds are produced by bacteria and fungi growing under low iron availability (consequence of the minimal solubility of Fe hydroxides) in order to acquire, transport and process the metal ion (Neilands, 1995; Amin, et al., 2009; Jin, et al., 2014).

There are several excellent review articles in the literature regarding to the structure, chemistry and function of siderophores as microbial iron transport compounds (Raymond, et al., 1984; Neilands, 1995; Roosenberg, et al., 2000; Liu and Hider, 2002; Boukhalfa and Crumbliss, 2002; Kraemer, 2004; Dhungana and Crumbliss, 2005; Crumbliss and Harrington, 2009; Hider and Kong, 2010). In this section, the main features of this class of compounds will be presented.

The insolubility of iron(III) hydroxides and the low equilibrium concentrations of iron in biological environments are inconsequential compared to the enormous stability and selectivity of the iron(III)-microbial siderophore complexes [Fe(III)-MS]. The 1:1 stability constant of Fe(III)-MS complexes ranges from  $10^{23}$  to  $10^{52}$ . These complexes stay in solution and enhance thereby the diffusion of iron to the cell surface (Hider, et al., 1981; Kraemer, 2004; Colombo, et al., 2014). On the other hand, the affinity for all divalent ions is substantially lower; thus, the siderophore ligand can be said to be "virtually specific" for Fe(III) in the presence of other environmental prevalent metal ions. Siderophores also possess, without exception, a higher affinity for iron(III) than for iron(II) (Neilands, 1995; Dhungana and Crumbliss, 2005; Hider and Kong, 2010).

Almost 500 siderophore structures are known to date. As all of them increase the concentration of total soluble iron, it is not surprising that they use similar tools and strategies. These similar strategies are reflected in analogous structures (Boukhalfa and Crumbliss, 2002).

The most common siderophores found in nature are classified as catecholates, hydroxamates and hydroxycarboxylates, according to the binding sites present: catechol, hydroxamic acid and  $\alpha$ -hydroxycarboxylic acid, respectively (Figure 1.15). Upon chelation, these groups form five membered chelate rings, which are considered effective for iron complexes, due to the size of the chelate ring, and the angles that are formed (Roosenberg, et al., 2000; Winkelmann, 2002; Dhungana and Crumbliss, 2005; Winkelmann, 2007; Hider and Kong, 2010).

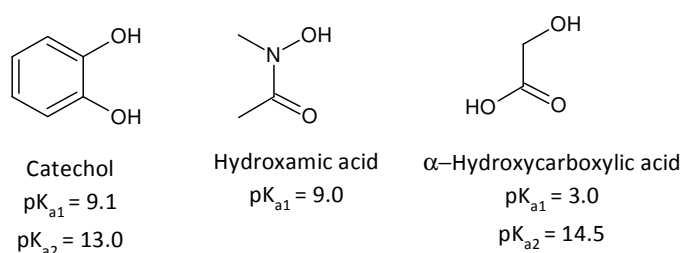


**Figure 1.15** Most common siderophore binding groups (and  $pK_{as}$ ): catechol, hydroxamic acid and  $\alpha$ -hydroxycarboxylic acid.

In general, the order of iron(III) affinity for these common donor groups has been found to be catechol > hydroxamic acid >  $\alpha$ -hydroxycarboxylic acid > single-atom donor groups. Multidentate siderophores may also consist in mixed donor group systems that may include other less-frequently observed binding groups, such as the hydroxypyridinone, the carboxylic acid and amine moieties (Figure 1.16) (Winkelmann, 2007; Crumbliss and Harrington, 2009).

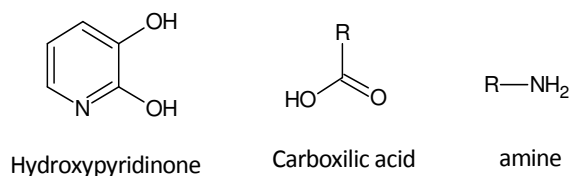


**Figure 1.16** Hydroxypyridinone, carboxylic acid and amine binding groups.

The hydroxamate donor group is particularly prevalent in fungal siderophores such as the hexadentate siderophores desferrioxamine B, desferrichrome, neurosporin, and rhodotorulic acid, a tetradentate ligand (Figure 1.17). Three main architectures are assumed by natural multidentate siderophores: linear, exocyclic, and endocyclic (Crumbliss and Harrington, 2009).

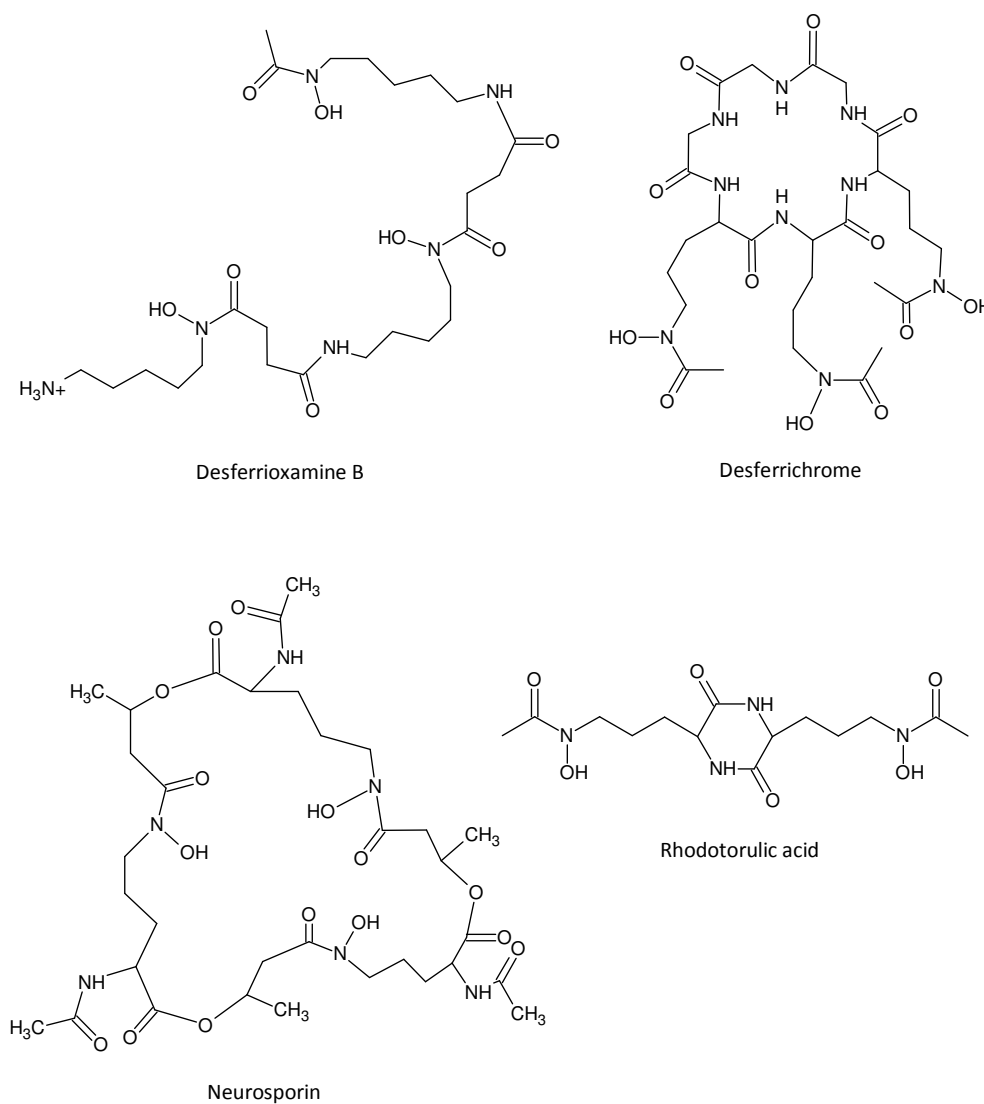


**Figure 1.17** Structures of some hydroxamate-based siderophores: desferrioxamine B (hexadentate, linear), desferrichrome (hexadentate, exocyclic), neurosporin (hexadentate, endocyclic) and rhodotorulic acid (tetradentate, linear).

Most desferrioxamines (e.g., desferrioxamine B, Figure 1.17) are linear siderophores. In exocyclic siderophores, the donor groups are attached to pendant arms radiating from a central ring system, such as in ferrichrome (Figure 1.17), and in the catecholamine siderophore, enterobactin (Figure 1.18).

In endocyclic siderophores, the donor groups are part of macrocyclic molecules (e.g, neurosporin, Figure 1.17). Vibrioferrin and aerobactin (Figure 1.18) are examples of a  $\alpha$ -hydroxycarboxylate-based, and a mixed-donor siderophore, respectively (Roosenberg, et al., 2000; Crumbliss and Harrington, 2009).

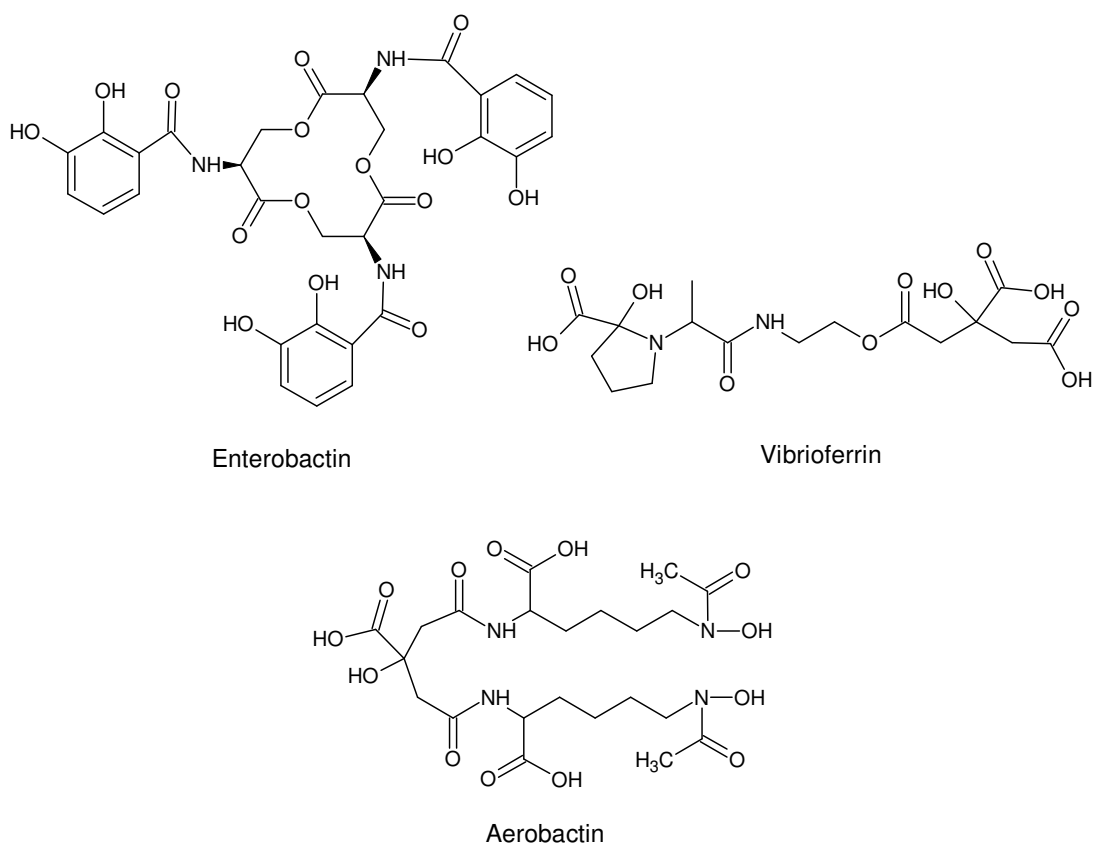
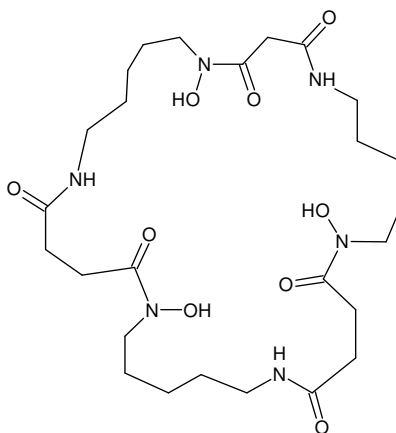


**Figure 1.18** Structure of the catechol-based siderophore enterobactin (hexadentate, exocyclic), the  $\alpha$ -hydroxycarboxylate-based siderophore, vibrioferrin, and the mixed-ligand siderophore, aerobactin.

A favorable entropic contribution is obtained in the formation of ferric chelates with hexadentate siderophores when compared to tris(bidentate) analogues, which can be observed in the case of desferrioxamine E (Figure 1.19) ( $\beta_{11}^{Fe(III)} = 32.5$ ) and of tris(acetohydroxamic acid) ( $\beta_{13}^{Fe(III)} = 28.3$ ) (Table 1.2). Higher differences can be observed, especially in the case of tricatechololate siderophores (Hider and Kong, 2010).



Desferrioxamine E

**Figure 1.19** Structure of desferrioxamine E.

The stability of microbial siderophores is often higher than most common synthetic chelating agents used for agricultural purposes (section 2.2). The overall stability constant with iron(III) for several siderophores and, some known synthetic chelating agents, is presented in Table 1.2.

**Table 1.2** Overall stability constants with  $\text{Fe}^{3+}$  and  $\text{Fe}^{2+}$ ,  $\text{pFe}^{3+}$ , and redox potential of several siderophores, siderophore analogues, and synthetic chelating agents.

Name	$\log \beta (\text{Fe}^{3+})^{1)}$	$\text{pFe}^{3+} *$	$\log \beta (\text{Fe}^{2+})^{1)}$	$E_{1/2} \text{ vs NHE}$ (mV)**
<b>Cathecolate</b>				
Enterobactin	49.0 <sup>a) b) c)</sup>	35.5 <sup>a) b)</sup> 34.3 <sup>c)</sup>	23.91 <sup>a)</sup>	-750 <sup>a)</sup>
Bacilibactin	47.6 <sup>c)</sup>	33.1 <sup>c)</sup>		
MECAM	45.9 <sup>a) b)</sup>	29.1 <sup>a) b)</sup>		
<b>Hydroxamate</b>				
Coprogen	29.35 <sup>c)</sup>	25.6 <sup>c)</sup>		
Desferricrocin	30.4 <sup>d)</sup>	26.5 <sup>c)</sup>	11.6 <sup>d)</sup>	-412 <sup>d)</sup>
Desferrichrome	29.1 <sup>a) b)</sup>	25.0 <sup>a) b)</sup> 25.2 <sup>c)</sup>	9.9 <sup>d)</sup>	-400 <sup>d)</sup>
Desferrichrome A	32 <sup>a) b)</sup>	25.2 <sup>a) b) c)</sup>	9.91 <sup>a)</sup>	-440 <sup>a)</sup>
Desferrioxamine B	30.5 <sup>a) b)</sup> 30.6 <sup>c) d) e)</sup>	26.6 <sup>a) c)</sup> 25.0 <sup>b)</sup>	10.3 <sup>a)</sup>	-468 <sup>b) d)</sup> -470 <sup>f)</sup>
Desferrioxamine E	32.5 <sup>a) b)</sup> 32.21 <sup>c)</sup>	27.7 <sup>a) c)</sup> 26.6 <sup>b)</sup>	11.6 <sup>a)</sup>	-447 <sup>a)</sup>
Rhodotorulic acid	21.55 <sup>a)</sup> ; 21.99 <sup>c)</sup> 62.2 <sup>2) a)</sup> ; 62.3 <sup>2) c)</sup>	21.9 <sup>c)</sup>	21.1 <sup>2) c)</sup>	-359 <sup>a)</sup>
Alcaligin	23.5 <sup>c) d)</sup> 64.6 <sup>2) c)</sup>	23.0 <sup>c)</sup>	22.6 <sup>d)</sup>	-446 <sup>d)</sup>
Bisucaberin	23.5 <sup>c)</sup> 64.3 <sup>2) c)</sup>	22.5 <sup>c)</sup>		

**Table 1.2 (Cont.)** Overall stability constants with  $\text{Fe}^{3+}$  and  $\text{Fe}^{2+}$ ,  $\text{pFe}^{3+}$ , and redox potential of several siderophores, siderophore analogues, and synthetic chelating agents.

Name	$\log \beta (\text{Fe}^{3+})^1$	$\text{pFe}^{3+*}$	$\log \beta (\text{Fe}^{2+})^1$	$E_{1/2} \text{ vs NHE (mV)}^{**}$
<b><math>\alpha</math>-Hydroxycarboxylate</b>				
Rhizoferrin	25.3 <sup>a)</sup>	20.0 <sup>a)</sup>		-82 <sup>b)</sup>
Mugineic acid	32.5 <sup>c)</sup>	19.7 <sup>c)</sup>		
<b>Mixed siderophores</b>				
Aerobactin	27.6 <sup>c)</sup> 22.5 <sup>c)</sup>	23.3 <sup>c)</sup>	4.86 <sup>a)</sup>	-336 <sup>a)</sup>
Pseudobactin				-482 <sup>f)</sup>
Pyoverdin PaA	30.8 <sup>a) c)</sup>	27.0 <sup>a) c)</sup>	9.78 <sup>a)</sup>	-510 <sup>a)</sup>
Pyoverdin Pp	31.06 <sup>c)</sup>	25.13 <sup>c)</sup>		
<b>Other compounds</b>				
N,N'-Dimethyl-2,3-dihydroxybenzenamide	40.2 <sup>3) a) b)</sup>	15.0 <sup>a) b)</sup>		
Acetohydroxamic acid	28.3 <sup>3) a) b) d)</sup>	14.8 <sup>a) b)</sup>	11.2 <sup>3) d)</sup>	-293 <sup>a)</sup>
N-methylacetohydroxamic acid	29.4 <sup>3) d)</sup>		11.2 <sup>3) d)</sup>	-348 <sup>a)</sup>



**Table 1.2 (Cont.)** Overall stability constants with  $\text{Fe}^{3+}$  and  $\text{Fe}^{2+}$ ,  $p\text{Fe}^{3+}$ , and redox potential of several siderophores, siderophore analogues, and synthetic chelating agents.

Name	$\log \beta (\text{Fe}^{3+})^{1)}$	$p\text{Fe}^{3+} *$	$\log \beta (\text{Fe}^{2+})^{1)}$	$E_{1/2} \text{ vs NHE (mV)}^{**}$
<b>Other compounds (cont.)</b>				
EDDHA	35.54 <sup>e)</sup>			-230 <sup>f)</sup>
DTPA	27.6 <sup>e)</sup>		16.2 <sup>e)</sup>	
EDTA	25.1 <sup>a) b) e)</sup>	23.4 <sup>a) b)</sup>	14.30 <sup>e)</sup>	-110 <sup>b)</sup>
EDDS	22.0 <sup>e)</sup>			
HEDTA	19.7 <sup>e)</sup>		12.2 <sup>e)</sup>	
NTA	16.0 <sup>e)</sup>		8.90 <sup>e)</sup>	

<sup>1)</sup>  $\beta = \beta_{110}$  using the  $\beta_{MLH}$  notation

<sup>2)</sup>  $\beta = \beta_{230}$

<sup>3)</sup>  $\beta = \beta_{130}$ ;

\*  $p\text{Fe} = -\log[\text{Fe}_{aq}^{3+}]$  (Equation 3.4; see text), at pH 7.4,  $1\mu\text{M}$  total  $\text{Fe}^{3+}$  and  $10\mu\text{M}$  total ligand

\*\* Reduction midpoint potentials, not standard reduction potentials, as the potential are not measured at standard conditions

<sup>a)</sup> Boukhalfa and Crumbliss, 2002

<sup>b)</sup> Hider and Kong, 2010

<sup>c)</sup> Crumbliss and Harrington, 2009

<sup>d)</sup> Dhungana and Crumbliss, 2005

<sup>e)</sup> Martell and Smith, 2004

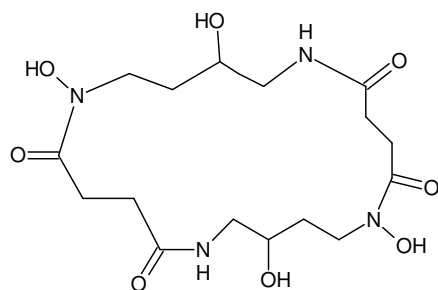
<sup>f)</sup> Bar-Ness, et al., 1991

The stability constant,  $\beta$  in table 1.2, refers to overall formation constant of the chelate, from the fully deprotonated ligand L. However, the binding sites for iron(III) of many chelating agents and siderophores in particular, are acidic. Therefore in aqueous solution there is a competition between  $H^+$  and  $Fe^{3+}$  binding, as already referred in section 1.1. Thus, the stability constant is strongly dependent on the pH, due to deprotonation reactions (Equation 1.7, section 1.1).

This fact limits the comparison using the stability constant, when comparing chelating agents with different binding sites. The  $pK_a$  of catechol, hydroxamic acid and  $\alpha$ - hydroxycarboxylic acid are indicated in Figure 1.15. The negative logarithm of the free aqueous iron(III) concentration ( $pFe$  value, equation 1.15) is usually used for comparing iron-siderophores, when the ligand and the metal are used at fixed concentrations and a fixed pH value, usually  $[Fe^{3+}]_{tot}=1 \mu mol.L^{-1}$ ,  $[L]_{tot}=10 \mu mol.L^{-1}$ , at pH 7.4.

$$pFe = -\log[Fe_{aq}^{3+}] \quad (1.15)$$

The  $pFe$  value is especially useful to compare ligands with different denticities, which are able to form chelates with different stoichiometry (Crumbliss and Harrington, 2009). Most siderophores are hexadentate ligands, that are able to satisfy the six coordination sites of ferric ions with the formation of very stable 1:1 ligand:metal chelates. On the other hand, tetradentate siderophores, also common in nature [e.g. rhodotorulic acid (Figure 1.17) and alcaligin (Figure 1.20)], can form complexes with different stoichiometries, including the formation of multimetallic assemblies, to ensure full iron coordination (Raymond, et al., 1984; Boukhalfa and Crumbliss, 2002; Hider and Kong, 2010).



Alcaligin

**Figure 1.20** Structure of Alcaligin

In solution, rhodotorulic acid (Figure 1.17) and alcaligin, for example, are known to form  $\text{FeL}$  and the  $\text{Fe}_2\text{L}_3$  species (Table 1.2). However other species are possible to be formed in other tetradentate ligands, such as  $\text{M}_2\text{L}_2$  and protonated species (Figure 1.21).

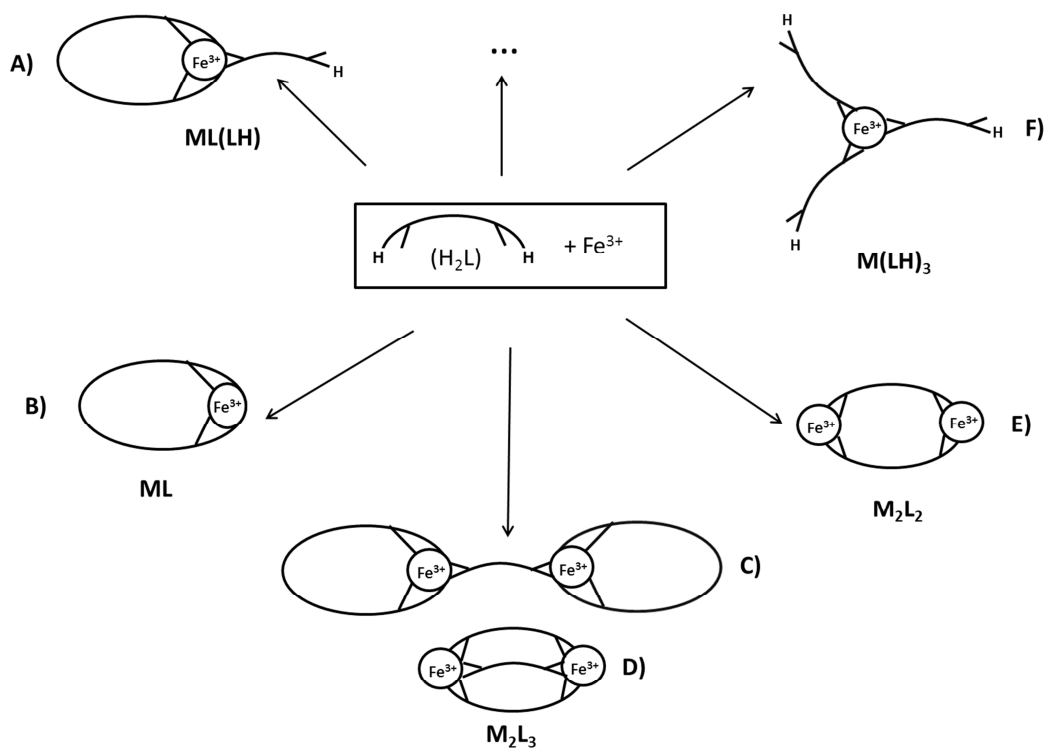


**Figure 1.21** Possible structures of iron(III)-tetradentate siderophore chelates. The structure assumed by the chelate depends on the pH, the length of the connecting chain between the hydroxamate groups and also of the metal to ligand ratio.

The formation of such species depends on the pH, the length of the connecting chain between the binding groups, and also on the metal to ligand ratio.  $\text{FeL(LH)}$  and  $\text{Fe(L)}_3$  species, for example, may be formed when the ligand is present in excess in relation to the amount of iron (Boukhalfa and Crumbliss, 2002; Hider and Kong, 2010).

Hexadentate siderophores, that usually contain the hydroxamate and/or catecholate units, have much higher affinity for  $\text{Fe(III)}$  than for  $\text{Fe(II)}$ . For example, the affinity of desferrioxamine B for  $\text{Fe(III)}$  ( $\beta_{11}^{\text{Fe(III)}} = 30.6$ ) is 20 orders of magnitude higher than for  $\text{Fe(II)}$  ( $\beta_{110}^{\text{Fe(II)}} = 10.0$ ).

The selectivity of siderophores for iron(III) over iron(II) leads to extremely low redox potentials. The stability constant for chelation with  $\text{Fe(II)}$ , and the redox potentials for several siderophores, are shown in table 1.2.

Equation 3.5 describes the relationship between the redox potential of a  $\text{Fe(III)}$ -siderophore complex ( $E_{\text{complex}}$ ) and the selectivity for  $\text{Fe(III)}$ , measured by the ratio of the overall siderophore (L) stability constant for  $\text{Fe}^{3+}(\beta_{110}^{\text{Fe(III)}})$  and  $\text{Fe}^{2+}(\beta_{110}^{\text{Fe(II)}})$ .  $E_{\text{aq}}^0$  represents the redox potential for the  $\text{Fe(H}_2\text{O)}_6^{3+}/\text{Fe(H}_2\text{O)}_6^{2+}$  couple.

$$E_{\text{complex}} = E_{\text{aq}}^0 - 59 \log \frac{\left(\beta_{110}^{\text{Fe(III)}}\right)}{\left(\beta_{110}^{\text{Fe(II)}}\right)} \quad 3.5$$

The stability of the  $\text{Fe(III)}$ -siderophore lowers with the decrease of the denticity of the ligand. It has been suggested that tetradentate siderophores may have advantages over hexadentated ones because they form a variety of species (e.g.,  $\text{Fe}_2\text{L}_3$ ,  $\text{FeL(OH)}_2^{2+}$ ), which are labile with respect to ligand exchange. Furthermore, the chelates formed are thermodynamically easier to reduce, which facilitate the removal of iron via reductive processes (Boukhalfa and Crumbliss, 2002)

### 1.3.2 Siderophores in Iron Nutrition

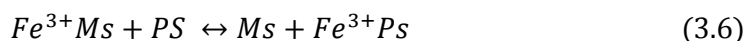
As referred in section 1.2.2, in Strategy II plants (monocots), the Fe uptake is based on chelation of  $Fe^{3+}$  by strong ligands (phytosiderophores,  $PS_s$ ) belonging to the mugineic acids (MAs) family (Colombo, et al., 2014).

On the other hand, the importance of iron in the interactions among microorganisms and plants has long been recognized and competitive or collaborative relationships occur between plant roots and bacteria. The production of siderophores has been proposed as the key microbial activity that benefits plant iron acquisition (Neema, et al., 1993; Radzki, et al., 2013; Colombo, et al., 2014; Jin, et al., 2014).

Although several studies have already demonstrated that plants use iron provided by microbial siderophores, plant strategies I or II do not consider a transport system involving this type of compounds. A third Strategy for iron uptake involving the use of microbial siderophores was first suggested by Bienfait in 1989 (Crowley, et al., 1991; Crowley, et al., 1992; Johnson, et al., 2002; Fernandez, et al., 2005; Radzki, et al., 2013).

The mechanism of Fe(III)-siderophore acquisition by plants and their subsequent utilization within plants remain largely unknown. Despite its major importance, the ability of plants to acquire Fe from microbial siderophores is only one component of the multi-component complex system that controls the rhizosphere (Shenker and Chen, 2005; Jin, et al., 2014).

It has been suggested that Strategy I and Strategy II plants may transport Fe from microbial Fe(III) siderophores by a reduction-based mechanism, or by ligand exchange with phytosiderophores (Equation 3.6), respectively (Loper and Buyer, 1991; Bar-Ness, et al., 1992; Radzki, et al., 2013)



However, in some cases, due to the very high stability constants of  $Fe^{III}$ - $MS_s$  complexes, which are the case of trishydroxamates and triscathecolates, the iron exchange between  $Fe(III)$ - $MS_s$  and  $PS_s$  can be very limited. Thus, the contribution of

microbial Fe complexes to the Fe acquisition of grasses (Strategy II plants) via the “ligand exchange” can be very low (Colombo, et al., 2014).

On the other hand, it was argued that due to the low redox potential, the Fe(III) chelated by microbial siderophores is not readily reduced by the reductase system on plant roots (Chen, et al., 2000; Colombo, et al., 2014).

Therefore, the direct uptake of microbial siderophores by Strategy I and II plants was proposed as Strategy III. Evidences of the the direct uptake of the Fe-siderophores, by root cell via an unidentified component, that is independent of the IRT1 transporters in Strategy I plants and YS1 transporters in Strategy II plants, have been reported by several authors (Shenker, et al., 1992; Chen, et al., 2000), and more recently by Vansuyt et al. (2007). However, as previously referred (section 2.4), the existence of a specific Fe uptake mechanism is still controversial (Loper and Buyer, 1991; Marschner and Römheld, 1994, Hördt, et al., 2000; Jin, et al., 2014). On the other hand, the results obtained by Bar-Ness et al. (1992), using a fluorescent ferrioxamine analogue, did not support such mechanism in both Strategy I and Strategy II plants.

Vansuyt et al. (2007) suggested that the reductase activity was not involved in the iron uptake by *Arabidopsis thaliana*, a Strategy I plant species, from a siderophore, a pyoverdine, produced by *Pseudomonas fluorescens*, nor that iron was incorporated through the IRT1 transporter. The iron uptake would occur through a different (unknown) Strategy, as first proposed by Bienfait (1989) (Vansuyt, et al., 2007). Such Strategy should involve the incorporation of the bacterial siderophore, by analogy to the iron uptake Strategy II, based on phytosiderophores, through their incorporation in roots when chelated with iron.

Moreover, not all siderophores may be used by plants and individual plant species and varieties have different abilities to use specific siderophore types (Crowley, et al., 1988).

Nevertheless, several studies have already demonstrated that a variety of plant species such as peanut, cotton (Bar-Ness, et al., 1991), oat (Crowley, et al., 1988), sorghum and sunflower (Cline, et al., 1984), and also cucumber, tomato, pea and maize have the ability to acquire Fe from MS<sub>s</sub> (Stutz, 1964; Yehuda, et al., 1996; Loper and Buyer, 1991).

Pseudobactin (PSB) of *Pseudomonas putida*, Figure 1.22, served as a Fe source for both dicots and monocots. In short term experiments, sorghum (monocot) exhibited significantly higher uptake from FePSB than from FeEDDHA. On the other hand, in peanuts, cotton and sunflower (dicots) the Fe uptake rate from FePSB was relatively low when compared to FeEDDHA (Bar-Ness, et al., 1991). Fe-rhodotorulic acid of *Rhodotorula pilimanaea* (Figure 1.17) was used by tomato, and Fe-aerobactin (Figure 1.18) is taken up directly as a complex by soybean and oat (Chen, et al., 1998; Chen, et al., 2000).

Rhizoferrin of *Rhizopus arrhizus* (Figure 1.22) was found to provide Fe for barley and corn by ligand exchange with phytosiderophores (Yehuda, et al., 1996) and to be also an efficient Fe source for tomato and cucumber (Strategy I plants) (Shenker, et al., 1992; Yehuda, et al., 2000). In tomato, uptake rates of Fe from rhizoferrin were as high as from EDDHA/Fe<sup>3+</sup>. It was suggested that due to its size, this siderophore is more likely to be transported directly across the plasma membrane of root cells than hydroxamate and catecholate-type siderophores (Marschner and Römheld, 1994).

Higher Fe levels were found in plants supplied with Fe in the form of Fe-siderophores, when compared with plants supplied with the same concentration of Fe-EDTA, as observed by Vansuyt et al. (2007) in the case of the Strategy I plant *Arabidopsis thaliana* supplied with Fe-pyoverdine. It has been shown that this compound also increased the iron content of other Strategy I plants, such as peanut, cotton and cucumber (Crowley, et al., 1991; Bar-Ness, et al., 1991; Vansuyt, et al., 2007; Jin, et al., 2014).

As referred in section 1.3.1, hydroxamate and catecholate groups are the most common in siderophores. The importance of phenolic and catecholate compounds in plant nutrition is well known. Reductants and iron chelators are released by Strategy I plants under Fe deficiency that includes phenolic compounds together with flavins and organic acids, depending on the plant species. Phenolic compounds represent the major component of root exudates from Fe-deficient red clover plants (Jin, et al., 2014). Agrobactin (Figure 1.22), a linear catechol siderophore, showed to enhance the uptake of iron in pea and bean plants (Becker, et al., 1985; Bar-Ness, et al., 1992; Jin, et al., 2014).

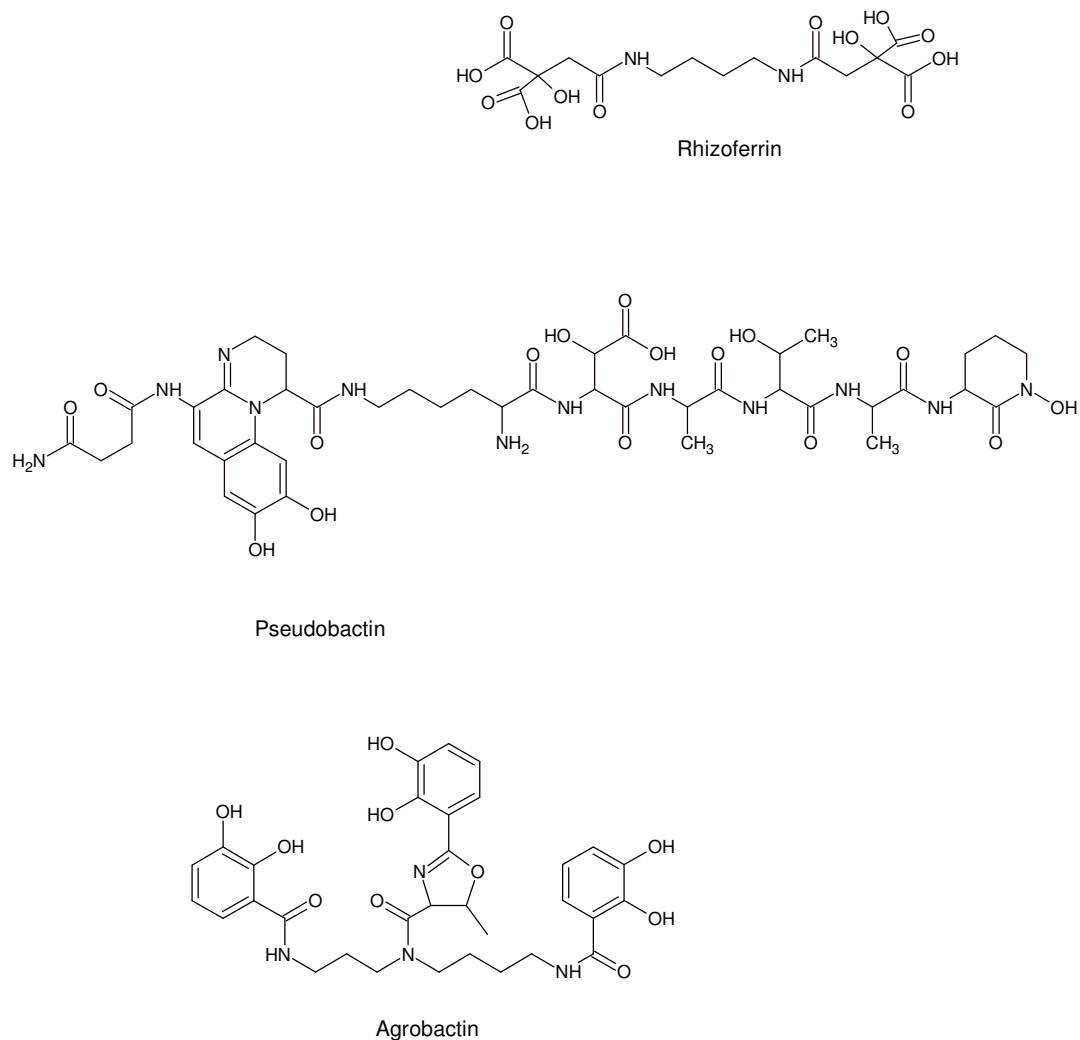
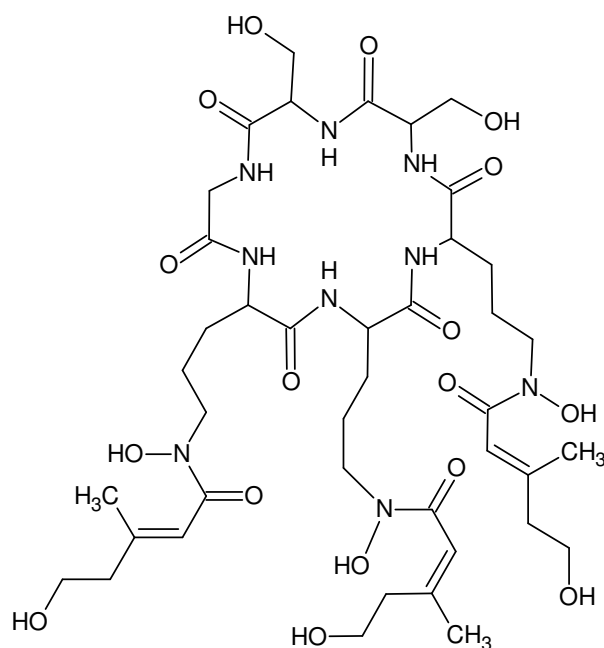


**Figure 1.22** Structures of rhizoferrin, pseudobactin and agrobactin.

It has been shown that plants also use iron from hydroxamate siderophores, such as desferrichrome, rhodotorulic acid, desferrioxamine B (Figure 1.17) and desferrichrome A, Figure 1.23, (Crowley, et al., 1988; Crowley, et al., 1991; Yehuda, et al., 1996), and also from a mixed ligand, catechol-hydroxamate-hydroxi-acid siderophore produced by *Pseudomonas* (Crowley, et al., 1988). Also, organic amendments, that contain catechol and hydroxamates siderophores, among other organic compounds capable of chelating Fe (e.g., humic acids, amino acids) are able to correct Fe deficiency of corn and sorghum grown in calcareous soils (Chen, et al., 1998).





Desferrichrome A

**Figure 1.23** Structure of deferrichrome A.

Different results were obtained when iron was supplied to different plants with the iron chelates of the trihydroxamate desferrioxamine B. While oat plants remained green in nutrient solution containing 5  $\mu\text{M}$  ferrioxamine B (Crowley, et al., 1988), maize became chlorotic even when grown in 10  $\mu\text{M}$  ferrioxamine B (Hördt, et al., 2000). Additionally, ferrioxamine B was found to be able to provide Fe for cucumber, sunflower and sorghum (Chen, et al., 1998) and to be better used by oat than ferrichrome, ferrichrome A, and coprogen (Crowley, et al., 1991).

On the other hand, many published uptake/translocation rates of Fe supplied by stable trihydroxamate siderophores are low, when compared to other Fe chelates (e.g.,  $\text{Fe}^{3+}$ -EDTA) in Strategy I plants, or to Fe-Phytosiderores (FePs), in Strategy II plants (Bar-Ness, et al., 1991; Römheld, 1991; Zhang, et al., 1991; Crowley, et al., 1992; Hördt, et al., 2000).

Such results must be related, as referred earlier, to the high stability constant of the  $\text{MS}_s$  for Strategy II plants, or to the low reduction by the Ferric reductase (FCR), in Strategy I plants (Jin, et al., 2014). In plants, the redox potential E(mV) of most biological reductants (e.g. E=-320 mV for NADPH, which is suggested to be the electron

donor for Fe(III) reduction for ferric chelate reductase in Strategy I plants) is higher than the redox potential of siderophore-Fe<sup>3+</sup> chelates, usually within the range of -330 to -750 mV (Boukhalfa and Crumbliss, 2002; Jin, et al., 2014; Robinson, et al., 1999). In the case of Strategy II plants, the higher stability of the MS<sub>s</sub> (10<sup>23</sup> to 10<sup>52</sup>) limits the ligand exchange with PS<sub>s</sub> (10<sup>18</sup>) (Colombo, et al., 2014). Moreover, the specific transporter for Fe(III)-phytosiderophores probably does not work efficiently for other Fe(III)-chelates (Romheld and Marschner, 1986).

It was suggested that less stable chelates may be more efficient in supplying iron to plants, than the very stable iron chelates formed by trihydroxamates (Hördt, et al., 2000). This fact can be related to the higher reduction rate of the mono- and dihydroxamates iron chelates when supplied to Strategy I plants (e.g. cucumber), and to higher ligand exchange rate, when supplied to Strategy II plants (e.g. maize). In fact, Hördt et al. (2000) reported that ferric monohydroxamates (fusarinines) and dihydroxamate (dimerum acid) siderophores obtained from the decomposition of coprogen (log  $\beta_{110}$ =29.35, Table 3.2), a trihydroxamate (Figure 1.24), were more efficient in providing iron to plants than the ferric chelates of coprogen or ferrioxamine B.

Thus, siderophores, or siderophore analogues, with lower stability constants than the usually released by microorganisms, might be more efficient iron supplier for plants and must be considered as potential iron chelators for more environmental friendly practices. However, it must be noted, as already referred, that the acquisition of Fe(III)-siderophore chelates by the roots of Strategy II plants may be achieved via an yet unidentified plasmalemma pathway and it is possible that endocytosis is involved in Fe-siderophore incorporation into root cells (Lemanceau, et al., 2009; Jin, et al., 2014).

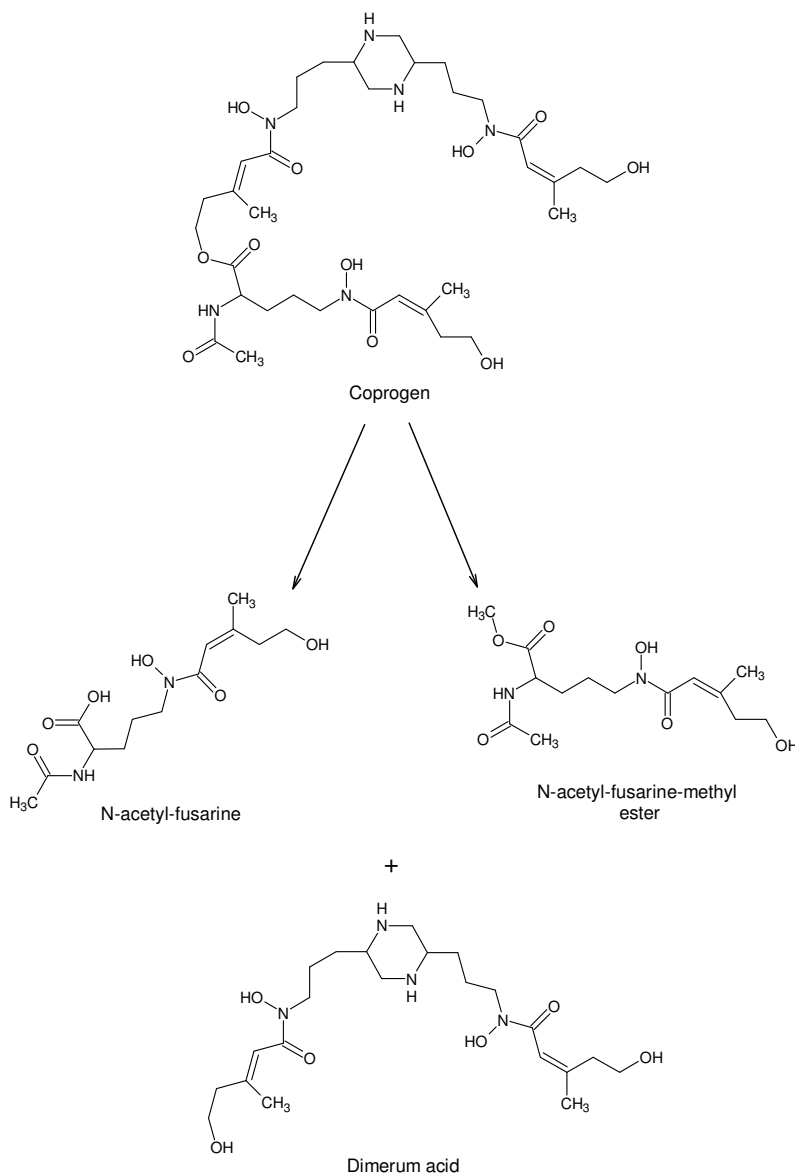


**Figure 1.24** Structure of coprogen and monohydroxamate and dihydroxamate products from hydrolysis.

From the discussed above, it is notorious that the way how soil microorganisms, and the siderophores that they exudate, promote plant Fe acquisition is largely unknown. Thus, research on new compounds, siderophores and analogues, surely will help to understand this important mechanism.

“Once siderophores are found to be efficient Fe mediators for plant roots in soil, as observed in nutrient culture, commercial bio-production of this siderophores as a new source of Fe-chelates will be of interest” (Shenker and Chen, 2005).

## 1.4 References

Abadia, J.; Vazquez, S.; Rellán-Alvarez, R.; El-Jendoubi, H.; Abadia, A.; Alvarez-Fernandez, A.; Flor Lopez-Millan, A., Towards a Knowledge-Based Correction of Iron Chlorosis. *Plant Physiology and Biochemistry* **2011**, *49* (5), 471-482.

Alvarez-Fernandez, A.; Paniagua, P.; Abadia, J.; Abadia, A., Effects of Fe Deficiency Chlorosis on Yield and Fruit Quality in Peach (*Prunus Persica* L. Batsch). *Journal of Agricultural and Food Chemistry* **2003**, *51* (19), 5738-5744.

Amin, S. A.; Green, D. H.; Kuepper, F. C.; Carrano, C. J., Vibrioferrin, an Unusual Marine Siderophore: Iron Binding, Photochemistry, and Biological Implications. *Inorganic Chemistry* **2009**, *48* (23), 11451-11458.

Bao, T.; Sun, L. N.; Sun, T. H., Evaluation of Iron on Cadmium Uptake by Tomato, Morel and Leaf Red Beet in Hydroponic Culture. *J. Plant Nutr.* **2010**, *33* (5), 713-723.

Bar-Ness, E.; Chen, Y.; Hadar, Y.; Marschner, H.; Romheld, V., Siderophores of *Pseudomonas*-Putida as an Iron Source for Dicot and Monocot Plants. *Plant Soil* **1991**, *130* (1-2), 231-241.

Bar-Ness, E.; Hadar, Y.; Chen, Y.; Shanzer, A.; Libman, J., Iron Uptake by Plants from Microbial Siderophores - a Study with 7-Nitrobenz-2 Oxa-1,3-Diazole-Desferrioxamine as Fluorescent Ferrioxamine B-Analog. *Plant Physiol.* **1992**, *99* (4), 1329-1335.

Barberon, M.; Zelazny, E.; Robert, S.; Conejero, G.; Curie, C.; Friml, J.; Vert, G., Monoubiquitin-Dependent Endocytosis of the Iron-Regulated Transporter 1 (Irt1) Transporter Controls Iron Uptake in Plants. *Proceedings of the National Academy of Sciences of the United States of America* **2011**, *108* (32), E450-E458.

Becker, J. O.; Messens, E.; Hedges, R. W., The Influence of Agrobactin on the Uptake of Ferric Iron by Plants. *Fems Microbiology Ecology* **1985**, *31* (3), 171-175.

Boukhalfa, H.; Crumbliss, A. L., Chemical Aspects of Siderophore Mediated Iron Transport. *Biometals* **2002**, *15* (4), 325-339.

Bucheli-Witschel, M.; Egli, T., Environmental Fate and Microbial Degradation of Aminopolycarboxylic Acids. *Fems Microbiology Reviews* **2001**, 25 (1), 69-106.

Chen, L. M.; Dick, W. A.; Streeter, J. G.; Hoitink, H. A. J., Fe Chelates from Compost Microorganisms Improve Fe Nutrition of Soybean and Oat. *Plant Soil* **1998**, 200 (2), 139-147.

Chen, L. M.; Dick, W. A.; Streeter, J. G., Production of Aerobactin by Microorganisms from a Compost Enrichment Culture and Soybean Utilization. *J. Plant Nutr.* **2000**, 23 (11-12), 2047-2060.

Cline, G. R.; Reid, C. P. P.; Powell, P. E.; Szaniszlo, P. J., Effects of a Hydroxamate Siderophore on Iron-Absorption by Sunflower and Sorghum. *Plant Physiol.* **1984**, 76 (1), 36-39.

Colombo, C.; Palumbo, G.; He, J. Z.; Pinton, R.; Cesco, S., Review on Iron Availability in Soil: Interaction of Fe Minerals, Plants, and Microbes. *J. Soils Sediments* **2014**, 14 (3), 538-548.

Crichton, R., *Biological Inorganic Chemistry: An Introduction*. Elsevier, Amsterdam, **2007**.

Crowley, D. E.; Reid, C. P. P.; Szaniszlo, P. J., Utilization of Microbial Siderophores in Iron Acquisition by Oat. *Plant Physiol.* **1988**, 87 (3), 680-685.

Crowley, D. E.; Wang, Y. C.; Reid, C. P. P.; Szaniszlo, P. J., Mechanisms of Iron Acquisition from Siderophores by Microorganisms and Plants. *Plant Soil* **1991**, 130 (1-2), 179-198.

Crowley, D. E.; Romheld, V.; Marschner, H.; Szaniszlo, P. J., Root-Microbial Effects on Plant Iron Uptake from Siderophores and Phytosiderophores. *Plant Soil* **1992**, 142 (1), 1-7.

Crumbliss, A. L.; Harrington, J. M., Iron Sequestration by Small Molecules: Thermodynamic and Kinetic Studies of Natural Siderophores and Synthetic Model Compounds. In *Advances in Inorganic Chemistry, Vol 61: Metal Ion Controlled*

*Reactivity*, VanEldik, R.; Hubbard, C. D., Eds. Elsevier Academic Press Inc: San Diego, **2009**; Vol. 61, pp 179-250.

Dhungana, S.; Crumbliss, A. L., Coordination Chemistry and Redox Processes in Siderophore-Mediated Iron Transport. *Geomicrobiology Journal* **2005**, 22 (3-4), 87-98.

Fernandez, V.; Ebert, G.; Winkelmann, G., The Use of Microbial Siderophores for Foliar Iron Application Studies. *Plant Soil* **2005**, 272 (1-2), 245-252.

Goos, R. J.; Germain, S., Solubility of Twelve Iron Fertilizer Products in Alkaline Soils. *Communications in Soil Science and Plant Analysis* **2001**, 32 (13-14), 2317-2323.

Günter, N.; Volker, R., The Release of Root Exudates as Affected by the Plant Physiological Status. In *The Rhizosphere*, CRC Press: **2007**; pp 23-72.

Hider, R. C.; Mohdnor, A. R.; Silver, J.; Morrison, I. E. G.; Rees, L. V. C., Model Compounds for Microbial Iron-Transport Compounds .1. Solution Chemistry and Mossbauer Study of Iron(II) and Iron(III) Complexes from Phenolic and Catecholic Systems. *Journal of the Chemical Society-Dalton Transactions* **1981**, (2), 609-622.

Hider, R. C.; Kong, X., Chemistry and Biology of Siderophores. *Natural product reports* **2010**, 27 (5), 637.

Holden, M. J.; Luster, D. G.; Chaney, R. L.; Buckhout, T. J.; Robinson, C., Fe<sup>3+</sup>-Chelate Reductase-Activity of Plasma-Membranes Isolated from Tomato (*Lycopersicon-Esculentum* Mill) Roots - Comparison of Enzymes from Fe-Deficient and Fe-Sufficient Roots. *Plant Physiol.* **1991**, 97 (2), 537-544.

Hördt, W.; Romheld, V.; Winkelmann, G., Fusarinines and Dimerum Acid, Mono- and Dihydroxamate Siderophores from *Penicillium Chrysogenum*, Improve Iron Utilization by Strategy I and Strategy II Plants. *Biometals* **2000**, 13 (1), 37-46.

Howard, W. L.; Wilson, D., Chelating Agents. In *Kirk-Othmer Encyclopedia of Chemical Technology*, John Wiley & Sons, Inc.: **2000**; Vol. 5, p 708.

IUPAC, Compendium of Chemical Terminology, 2nd Ed. (the "Gold Book"). Compiled by A. D. McNaught and A. Wilkinson. Blackwell Scientific Publications, Oxford (1997). Xml on-Line Corrected Version: [Http://Goldbook.Iupac.Org](http://Goldbook.Iupac.Org) (2006-) Created by M. Nic, J. Jirat, B. Kosata; Updates Compiled by A. Jenkins. Isbn 0-9678550-9-8. Doi:10.1351/Goldbook.

Jacobson, L., Maintenance of Iron Supply in Nutrient Solutions by a Single Addition of Ferric Potassium Ethylenediamine Tetra-Acetate. *Plant Physiol.* **1951**, 26 (2), 411-413.

Jin, C. W.; Ye, Y. Q.; Zheng, S. J., An Underground Tale: Contribution of Microbial Activity to Plant Iron Acquisition Via Ecological Processes. *Annals of Botany* **2014**, 113 (1), 7-18.

Johnson, G. V.; Lopez, A.; Foster, N. L., Reduction and Transport of Fe from Siderophores - Reduction of Siderophores and Chelates and Uptake and Transport of Iron by Cucumber Seedlings. *Plant Soil* **2002**, 241 (1), 27-33.

Jurkevitch, E.; Hadar, Y.; Chen, Y.; Chino, M.; Mori, S., Indirect Utilization of the Phytosiderophore Mugineic Acid as an Iron Source to Rhizosphere Fluorescent Pseudomonas. *Biometals* **1993**, 6 (2), 119-123.

Knepper, T. P., Synthetic Chelating Agents and Compounds Exhibiting Complexing Properties in the Aquatic Environment. *Trens in Analytical Chemistry* **2003**, 22 (10), 708-724.

Kobayashi, T.; Nakanishi, H.; Takahashi, M.; Mori, S.; Nishizawa, N. K., Generation and Field Trials of Transgenic Rice Tolerant to Iron Deficiency. *Rice* **2008**, 1 (2), 144-153.

Kraemer, S., Iron Oxide Dissolution and Solubility in the Presence of Siderophores. *Aquat. Sci.* **2004**, 66 (1), 3-18.

Lemanceau, P.; Bauer, P.; Kraemer, S.; Briat, J. F., Iron Dynamics in the Rhizosphere as a Case Study for Analyzing Interactions between Soils, Plants and Microbes. *Plant Soil* **2009**, 321 (1-2), 513-535.

Liu, Z. D.; Hider, R. C., Design of Iron Chelators with Therapeutic Application. *Coordination Chemistry Reviews* **2002**, 232 (1-2), 151-171.

Loper, J. E.; Buyer, J. S., Siderophores in Microbial Interactions on Plant-Surfaces. *Mol. Plant-Microbe Interact.* **1991**, 4 (1), 5-13.

Lucena, J. J.; Gárate, A.; Carpena, O., Lolium Multiflorum Uptake of Iron Supplied as Different Synthetic Chelates. *Plant Soil* **1988**, 112 (1), 23-28.

Lucena, J. J., Fe Chelates for Remediation of Fe Chlorosis in Strategy I Plants. *J. Plant Nutr.* **2003**, 26 (10-11), 1969-1984.

Lucena, J. J.; Sentis, J. A.; Villen, M.; Lao, T.; Perez-Saez, M., Idha Chelates as a Micronutrient Source for Green Bean and Tomato in Fertigation and Hydroponics. *Agronomy Journal* **2008**, 100 (3), 813-818.

Lucena, J. J.; Garate, A.; Villen, M., Stability in Solution and Reactivity with Soils and Soil Components of Iron and Zinc Complexes. *J. Plant Nutr. Soil Sci.* **2010**, 173 (6), 900-906.

Ma, J. F.; Ling, H.-Q., Iron for Plants and Humans. *Plant Soil* **2009**, 325 (1-2), 1-3.

Marschner, H.; Römheld, V., Strategies of Plants for Acquisition of Iron. *Plant Soil* **1994**, 165 (2), 261-274.

Martell, A. E.; Smith, R. M., *Nist Standard Reference Database 46 Version 8.0, Nist Critically Selected Stability Constants of Metal Complexes Database*. US Department of Commerce: National Institute of Standards and Technology, 2004.

Miethke, M., Molecular Strategies of Microbial Iron Assimilation: From High-Affinity Complexes to Cofactor Assembly Systems. *Metallomics* **2013**, 5 (1), 15-28.

Morgan, G. T.; Drew, H. D. K., Researches on Residual Affinity and Coordination Part II Acetylacetonates of Selenium and Tellurium. *Journal of the Chemical Society* **1920**, 117, 1456-1465.



Morrissey, J.; Guerinot, M. L., Iron Uptake and Transport in Plants: The Good, the Bad, and the Lonome. *Chemical Reviews* **2009**, *109* (10), 4553-4567.

Namba, K.; Murata, Y., Toward Mechanistic Elucidation of Iron Acquisition in Barley: Efficient Synthesis of Mugineic Acids and Their Transport Activities. *Chemical Record* **2010**, *10* (2), 140-150.

Neema, C.; Laulhere, J. P.; Expert, D., Iron-Deficiency Induced by Chrysobactin in Saintpaulia Leaves Inoculated with Erwinia-Chrysanthemi. *Plant Physiol.* **1993**, *102* (3), 967-973.

Neilands, J. B., Siderophores - Structure and Function of Microbial Iron Transport Compounds. *J. Biol. Chem.* **1995**, *270* (45), 26723-26726.

Nowack, B.; VanBriesen, J. M., Chelating Agents in the Environment. In *Biogeochemistry of Chelating Agents*, ACS Symposium Series 910; American Chemical Society: Washington, DC, **2005**; Vol. chap. 1.

Nowack, B., Chelating Agents and the Environment. *Environmental Pollution* **2008**, *153* (1), 1-2.

Radzki, W.; Manero, F. J. G.; Algar, E.; Garcia, J. A. L.; Garcia-Villaraco, A.; Solano, B. R., Bacterial Siderophores Efficiently Provide Iron to Iron-Starved Tomato Plants in Hydroponics Culture. *Antonie Van Leeuwenhoek* **2013**, *104* (3), 321-330.

Raymond, K. N.; Muller, G.; Matzanke, B. F., Complexation of Iron by Siderophores - a Review of Their Solution and Structural Chemistry and Biological Function. *Topics in Current Chemistry* **1984**, *123*, 49-102.

Robinson, N. J.; Procter, C. M.; Connolly, E. L.; Guerinot, M. L., A Ferric-Chelate Reductase for Iron Uptake from Soils. *Nature* **1999**, *397* (6721), 694-697.

Rodriguez-Lucena, P.; Hernandez-Apaolaza, L.; Lucena, J. J., Comparison of Iron Chelates and Complexes Supplied as Foliar Sprays and in Nutrient Solution to Correct Iron Chlorosis of Soybean. *J. Plant Nutr. Soil Sci.* **2010**, *173* (1), 120-126.

Römheld, V.; Marschner, H., Evidence for a Specific Uptake System for Iron Phytosiderophores in Roots of Grasses. *Plant Physiol.* **1986**, *80* (1), 175-180.

Römheld, V., The Role of Phytosiderophores in Acquisition of Iron and Other Micronutrients in Gramineous Species - an Ecological Approach. *Plant Soil* **1991**, *130* (1-2), 127-134.

Roosenberg, J. M.; Lin, Y. M.; Lu, Y.; Miller, M. J., Studies and Syntheses of Siderophores, Microbial Iron Chelators, and Analogs as Potential Drug Delivery Agents. *Current Medicinal Chemistry* **2000**, *7* (2), 159-197.

Schalk, I. J.; Hannauer, M.; Braud, A., New Roles for Bacterial Siderophores in Metal Transport and Tolerance. *Environmental Microbiology* **2011**, *13* (11), 2844-2854.

Shenker, M.; Oliver, I.; Helmann, M.; Hadar, Y.; Chen, Y., Utilization by Tomatoes of Iron Mediated by a Siderophore Produced by *Rhizopus-Arrhizus*. *J. Plant Nutr.* **1992**, *15* (10), 2173-2182.

Shenker, M.; Chen, Y., Increasing Iron Availability to Crops: Fertilizers, Organo-Fertilizers, and Biological Approaches. *Soil Sci. Plant Nutr.* **2005**, *51* (1), 1-17.

Stutz, E., Aufnahme Von Ferrioxamin B Durch Tomatenpflanzen. *Experientia* **1964**, *20* (8), 430.

Tagliavini, M.; Rombola, A. D., Iron Deficiency and Chlorosis in Orchard and Vineyard Ecosystems. *European Journal of Agronomy* **2001**, *15* (2), 71-92.

Vansuyt, G.; Robin, A.; Briat, J.-F.; Curie, C.; Lemanceau, P., Iron Acquisition from Fe-Pyoverdine by *Arabidopsis Thaliana*. *Mol. Plant-Microbe Interact.* **2007**, *20* (4), 441-447.

Villen, M.; Garcia-Arsuaga, A.; Lucena, J. J., Potential Use of Biodegradable Chelate N-(1,2-Dicarboxyethyl)-D,L-Aspartic Acid/ $\text{Fe}^{3+}$  as an Fe Fertilizer. *Journal of Agricultural and Food Chemistry* **2007**, *55* (2), 402-407.

Weger, H. G.; Lam, J.; Wirtz, N. L.; Walker, C. N.; Treble, R. G., High Stability Ferric Chelates Result in Decreased Iron Uptake by the Green Alga *Chlorella Kessleri* Owing to Decreased Ferric Reductase Activity and Chelation of Ferrous Iron. *Botany* **2009**, *87* (10), 922-931.

Winkelmann, G., Metal Transport - Microbial Siderophore-Mediated Transport. *biochemical society transactions* **2002**, *30* (4), 691-696.

Winkelmann, G., Ecology of Siderophores with Special Reference to the Fungi. *Biometals* **2007**, *20* (3-4), 379-392.

Yehuda, Z.; Shenker, M.; Romheld, V.; Marschner, H.; Hadar, Y.; Chen, Y. N., The Role of Ligand Exchange in the Uptake of Iron from Microbial Siderophores by Gramineous Plants. *Plant Physiol.* **1996**, *112* (3), 1273-1280.

Yehuda, Z.; Shenker, M.; Hadar, Y.; Chen, Y. N., Remedy of Chlorosis Induced by Iron Deficiency in Plants with the Fungal Siderophore Rhizoferrin. *J. Plant Nutr.* **2000**, *23* (11-12), 1991-2006.

Ylivainio, K.; Jaakkola, A.; Aksela, R., Impact of Liming on Utilization of <sup>59</sup>Fe-Chelates by Lettuce (*Lactuca Sativa* L.). *Journal of Plant Nutrition and Soil Science-Zeitschrift Fur Pflanzenernahrung Und Bodenkunde* **2006**, *169* (4), 523-528.

Yunta, F.; Martin, I.; Lucena, J. J.; Garate, A., Iron Chelates Supplied Foliarly Improve the Iron Translocation Rate in Tempranillo Grapevine. *Communications in Soil Science and Plant Analysis* **2013**, *44* (1-4), 794-804.

Zhang, F. S.; Romheld, V.; Marschner, H., Role of the Root Apoplasm for Iron Acquisition by Wheat Plants. *Plant Physiol.* **1991**, *97* (4), 1302-1305.



## **Chapter 2**

---

Alternative chelating agents: evaluation of the  
ready-biodegradability and complexation  
properties



## **Alternative chelating agents: Evaluation of the ready biodegradability and complexation properties\***

### **Abstract**

The ready biodegradability of four chelating agents, N,N'-(S,S)-bis[1-carboxy-2-(imidazol-4-yl)ethyl]ethylenediamine (BCIEE), N,N'-ethylene-di-L-cysteine (EC), N,N'-bis(4-imidazolymethyl)ethylenediamine (EMI) and 2,6-pyridine dicarboxylic acid (PDA), was tested according to the Organization for Economic Co-operation and Development (OECD) guideline for testing of chemicals. PDA proved to be a readily biodegradable substance. However, none of the other three compounds were degraded during the 28 days of the test. Chemical simulations were performed for the four compounds in order to understand their ability to complex with some metal ions (Ca, Cd, Co, Cu, Fe, Mg, Mn, Ni, Pb, Zn) and discuss possible applications of these chelating agents. Two different conditions were simulated: (i) in the presence of the chelating agent and one metal ion; (ii) in the simultaneous presence of the chelating agent and all metal ions with an excess of Ca. For those compounds, which revealed not to be ready biodegradable (BCIEE, EC and EMI), applications, where this property was not fundamental or even not required, were evaluated.

Chemical simulations pointed out that possible applications for these chelating agents are: food fortification, food process, fertilizers, biocides, soil remediation and treatment of metal poisoning.

Additionally, chemical simulations also predicted that PDA is an efficient chelating agent for Ca incrustations removal, detergents and for pulp metal ions removal process.

---

*\*Journal of Environmental Science and Health Part a-Toxic/Hazardous Substances & Environmental Engineering* **2014**, 49 (3), 344-354.

## 2.1 Introduction

Aminopolycarboxylates are well-known effective chelators and, due to their excellent binding capacity, they have been widely used as chelating agents in many industrial processes and products for years. Among the most commonly chelating agents used are EDTA (Figure 1.2A in section 1.1.1) and DTPA (Figure 1.3 in section 1.1.2). The main requirements for a chelating agent are: (i) the ability to complex with metals, essentially heavy metals at a wide range of pH; (ii) to have a good quality/price ratio; and (iii) do not cause damage to the environment (Bucheli-Witschel and Egli, 2001).

Chelating agents are used in a wide variety of situations, such as food processing, agriculture, prevention/inhibition of the growth of microorganisms, soil remediation, treatment of metal poisoning, management of calcium precipitates scale, detergents, pulp and paper, metal electroplating and tanning processes, mainly with two different purposes: (i) to remove critical metals that could be harmful to the efficient function of the process or (ii) to avoid metals precipitation and to ensure an essential amount to the good function of the process (Bucheli-Witschel and Egli, 2001).

In the case of food processing, chelating agents are used in food fortification to increase the concentration of Fe and Zn (Salgueiro, et al., 2002; Greffeuille, et al., 2011) and in food preservation as an antioxidant by sequestering harmful metal (mainly Fe and Cu) ions. The chelating agent can also act as an antimicrobial, binding to Fe ions and suppress bacterial growth by producing a Fe deficient environment (Al-Nabulsi and Holley, 2006).

Chelated micronutrients are widely used in agriculture in order to reduce mineral deficiencies on soil that cause problems on crops growth. Fe, Mn and Zn ions are the main cause of concern. Specific chelating agents to provide Fe ions to plants were already described; EDDHA (Figure 1.3 in section 1.1.2) is an example of a chelating agent used as a commercial fertilizer (Lucena, 2003).

Chelating agents associated to specific metal ions can be used as biocidal for stabilization, inhibition or reduction of the growth of microorganisms. Metal ions possess broad biocidal properties (Borkow, et al., 2010). For example, Cu ions are used



as a biocidal in a wide variety of applications; water purification, crops protection or antiviral are just a part of all possibilities. In contrast to the low sensitivity of human tissue (skin or other) to Cu ions, microorganisms are highly susceptible. Cu ions have a broad-spectrum effect on microorganisms, disrupting the cell membrane integrity, displacing essential metals within cells, interfering with the oxidative phosphorylation and the conformational structure of nucleic acids and proteins (Borkow and Gabbay, 2005). Other metal ions, like Zn or Co, can also be used as biocidal.

Heavy metals, like Cu, Zn, Ni and Cr, which could be toxic to human health, are the most frequently contaminants of soils. There are many approaches to soil remediation, but when the main aim is to remove heavy metals, washing with a strong acid or with a chelating agent is normally used because it is a rapid method and turns possible the heavy metals recovery (Xie and Marshall, 2001; Lin, et al., 2012). The chelating agent for this process should be able to form soluble metal complexes over a wide pH range and should not be adsorbed onto the soil surface (Lin, et al., 2012). The separation of metals from the chelating agent could be performed by precipitation with a pH adjustment (Xie and Marshall, 2001; Tandy, et al., 2004). Since large quantities of chelating agent are needed for remediation of soils, the recovery and reuse of the chelating agent should be an attractive objective in this process.

For chelating treatment of metal poisoning, particularly with Fe, Hg, Cd or Pb, it is fundamental that the chelating agent is highly selective for the metal ion(s) causing the poisoning, in the presence of Ca ions (Aposhian, et al., 1995; Johri, et al., 2010). Ideally, the metal chelate should be more soluble than the offending metal ion and thus increases its excretion by the kidney.

Ca ions can precipitate on the form of calcium oxalate, calcium sulphate or calcium carbonate and provoke the formation of Ca incrustations on the equipment surfaces; this is an operational problem that occurs at many mills, which is directly linked with significant production losses and increased maintenance costs (Rudie and Hart, 2005). For the management of calcium precipitates scale, chelating agents are also used to remove Ca incrustations.

Other important applications of the chelating agents are: (i) detergents, where chelating agents are used, mainly, for avoiding the precipitation of salts during the washing process (Knepper, 2003), by inactivating hardness minerals (Ca and Mg)

(Dixon and Giles, 2012); (ii) in the pulp and paper or textile industries, where chelating agents should be able to remove metal ions (Fe, Mn and Cu) that catalyze the decomposition of the bleaching agents (Zeronian and Inglesby, 1995; Wuorimaa, et al., 2006); (iii) in metal electroplating, where chelating agents are used in an aqueous solution contacting with a metal surface for avoiding undesirable precipitation or removing/re-dissolving salts normally of Cu, Ni or Zn (Hanna, et al., 2004; Pereira, et al., 2010); (iv) at tanning process to solubilize metal ions (Zn, Cr and Fe), that are necessary to improve the process (Sreeram and Ramasami, 2003).

The biodegradability of the chelating agents has been of particular concern due to the risk of causing environmental damage. Even though, nowadays, it is desirable, whenever possible, to use biodegradable compounds, the use of non-readily biodegradable chelating agents can also be wanted. This is the case of some type of applications where it is necessary that the chelating agent remains available for a certain period of time. In these circumstances, the use of readily biodegradable compounds should be avoided as they can be easily degraded by the permanent contact with microorganisms. Examples of these situations are the use of chelating compounds in the agriculture or as biocides where readily biodegradation is not required. In these cases, chelating agents with slightly low biodegradation are preferred in order to increase the period of action of fertilizers or biocides. In other situations, the amount of compound used is low and does not have significant impact on the environment, like in food processing or in the treatment of metal poisoning. In other applications, like in soil remediation, the reuse of the chelating agent is desirable; so, in this case, the chelating agent should not be quickly degraded in order to be used several times.

In the last years, we proved that EC, EMI and BCIEE (Figure 2.1) are efficient chelating agents for many metal ions (Barros, et al., 2009; Martins, et al., 2010a; Martins, et al., 2010b; Martins, et al., 2011). Additionally, PDA (Figure 2.1) is also described in the literature (Martell and Smith, 2004) as a potential chelating agent.

The present work aims to evaluate the potential ready-biodegradability of these four chelating agents (BCIEE, EC, EMI and PDA) and discuss some possible applications for them, according to the results of the ready biodegradability tests and the metal complexation capability of each one.

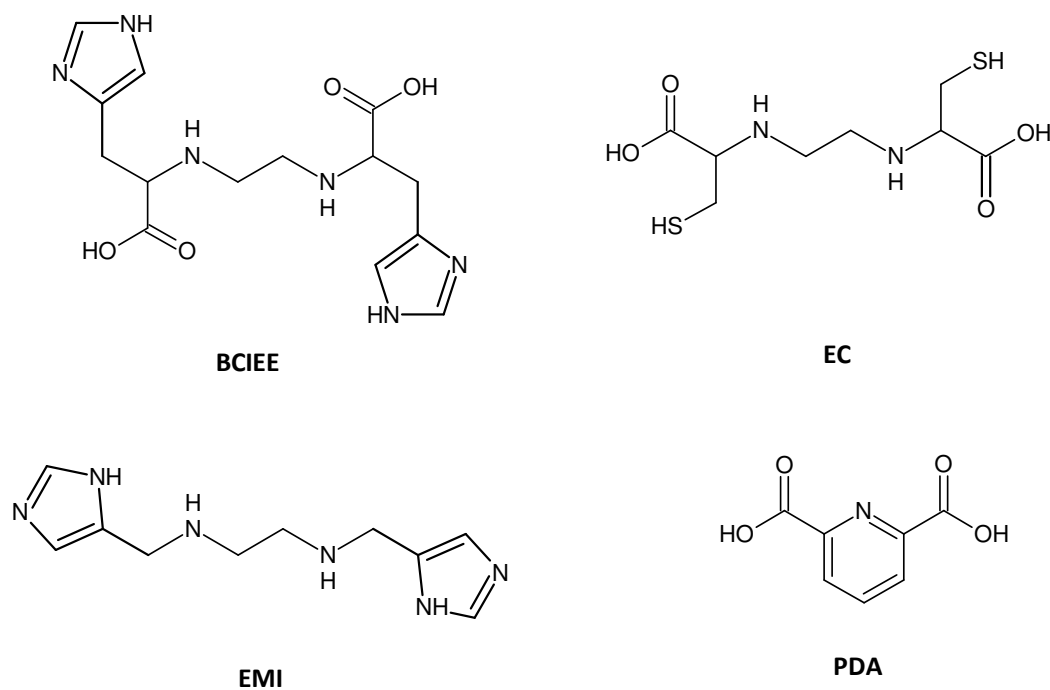


**Figure 2.1** Molecular structure of the chelating agents: N,N'-(S,S)-bis[1-carboxy-2-(imidazol-4-yl)ethyl]ethylenediamine (BCIEE), N,N'-ethylene-di-L-cysteine (EC), N,N'-bis(4-imidazolymethyl)ethylenediamine (EMI) and 2,6-pyridine dicarboxylic acid (PDA).

## 2.2 Materials and Methods

### 2.2.1 Chelating agents

All tested chelating agents were synthesized by the research group headed by Professor Maria Teresa Barros, REQUIMTE, Faculdade de Ciências e Tecnologia, Universidade Nova de Lisboa. EC and PDA were prepared as reported by Barros et al. (2009) and Pinto et al. (2014), respectively.

BCIEE was obtained in the form of N,N'-(S,S)bis[1-carboxy-2-(imidazol-4-yl)ethyl]ethylenediamine tetrahydrochloride based on the method described by Miyake et al. (2002).

EMI was obtained in the form of N,N'-Bis(4-(5)-imidazolylmethyl)ethylenediamine tetrahydrochloride, based on the method described by Gruenwed.Dw (1968).

### 2.2.2 Ready Biodegradation Tests

Ready biodegradation of the chelating agents was tested according to the OECD guidelines (301A: DOC-Die Away method) (OECD, 1992). Mineral medium and respective stock solutions were prepared according to the OECD guidelines (OECD, 1992). Tests were performed with distilled water with previous total organic carbon (TOC) control; additionally, each lot of membrane filters were tested in order to confirm that membranes did not release soluble organic carbon.

Inoculum was collected from the aeration tank of a domestic sewage treatment plant and aerated for 12 hours. Subsequently, it was centrifuged (1,100xg, 10 minutes), washed with mineral medium, in order to remove any possible inhibitor substances, and homogenized. Finally, inoculum was prepared by suspending 0.3 g of the sludge in 100 mL of mineral medium.

The assays (biodegradation and control tests) were carried out in 250 mL conical flasks, with a total volume of 150 mL. Biodegradation tests contained mineral medium, substance test and the inoculum. All flasks, except abiotic control (see below), were inoculated with 1.5 mL of inoculum, prepared as described above. Conical flasks were agitated at 150 rpm, in an orbital incubator (Infors HT, Ecotron), at a temperature of  $22 \pm 2$  °C. Sodium acetate was used as reference substance.

As described by the OECD guidelines (OECD, 1992), for dissolved organic carbon (DOC) method, the compound to be tested must be soluble, not volatile nor adsorbed by glass or sludge. Thus, solubility tests were previously performed and several controls were carried out: blank inoculum (without test substance), procedure control (the test substance was replaced by reference substance), abiotic control [with test substance and mercury (II) chloride], adsorption control [like biodegradation assay with mercury (II) chloride] and toxicity control (containing test and reference substances). Biodegradation tests and inoculum blanks were performed in duplicate, while the other controls were performed in a single assay.

At defined periods of time, indicated in the figures, samples were withdrawn from biodegradation tests and controls, centrifuged at 4,000xg for 5 minutes, and the supernatant filtered with a 0.45  $\mu\text{m}$  membrane. DOC measurements were performed in the supernatants of each sample, in duplicate, using a TOC analyser (TOC-5000A – Total Organic Carbon Analyzer, Shimadzu).

Degradation percentage was calculated considering the mean of the value obtained for two different flasks of the substance test, each one based on duplicate DOC measurements.

### 2.2.3 Complexation Modeling Study

Metal chemical speciation calculations between each chelating agent and metal(s) were performed using MINEQL+ Version 4.5 (Schecher and McAvoy, 2003), a computer program that generates chemical equilibrium concentrations of all species being considered in the model by the program reactions. The stability constants for BCIEE, EC, EMI and PDA with the metal ions considered in chemical simulations were obtained from the literature (Martell and Smith, 2004; Barros, et al., 2009; Martins, et al., 2010a; Martins, et al., 2010b; Martins, et al., 2011). Computational simulations were performed in aqueous medium in the pH range between 0 and 14.

For each chelating agent, at least two different conditions were simulated. For the first condition, complexation between one metal (M) and one chelating agent (L), with a  $[L]/[M]$  ratio of 2.5,  $[M] = 0.001 \text{ M}$ , was simulated. For the second condition, the presence of all the metals (Ca, Cd, Co, Cu, Fe, Mg, Mn, Ni, Pb and Zn) and the chelating agent, in a situation of excess of Ca, was assumed. The concentration of the chelating agent was 0.02 M, approximately twice of the sum of the concentration of all metals (for each metal,  $[M] = 0.001\text{M}$ ), except Ca. The concentration of Ca ions was 0.05M.

## 2.3 Results and Discussion

### 2.3.1 Evaluation of the ready biodegradability of the chelating agents

In the present work, the biodegradability of four chelating agents (BCIEE, EC, EMI and PDA) was assessed. For this purpose, the 301 A: DOC Die-Away method, recommended by the OECD for the screening of chemicals for ready biodegradability in aerobic aqueous conditions (OECD, 1992), was used.

As it can be seen in Figure 2.2, the PDA biodegradation started after the first day of the test and reached a degradation of 69 and 86%, after 7 and 14 days, respectively. The difference of replicates values of DOC removal, at the end of the test, was less than 20% (data not shown). The biodegradability of PDA is, apparently, in contradiction with the results presented in the literature, which describes that PDA is not biodegraded by unacclimated (microorganisms not previously exposed to PDA) mixed cultures (Banerji and Regmi, 1998); the results previously described can be, most likely, explained by the low time (36h) used, by the authors, in the biodegradation assay. Consistent with this possibility, in our assay, no biodegradation occurred in the first 24h; however, once the biodegradation started it occurred in a very fast way (Figure 2.2). The absence of degradation in the adsorption control shows that the observed reduction of PDA was not due to any adsorption of the chelating agent to the glass of the flask or to the sludge (inoculum). The values of degradation of the abiotic control were close to zero, which proves that PDA was not degraded by other processes like photochemical or chemical reactions over the assay period. Reference substance reached the “pass level” (70% of DOC degradation) after the fifth day (data not shown). In addition, the results of the toxicity control are in agreement with PDA biodegradability since over 90% of degradation (after 14 days) was accomplished when half of the initial DOC was due to the reference compound and the other half to the test substance (Figure 2.2). Together, these results prove that PDA can be classified as a readily biodegradable substance by the OECD criteria: a reduction of DOC > 70% was achieved for a 10 day window within the 28 days of the test (OECD, 1992).

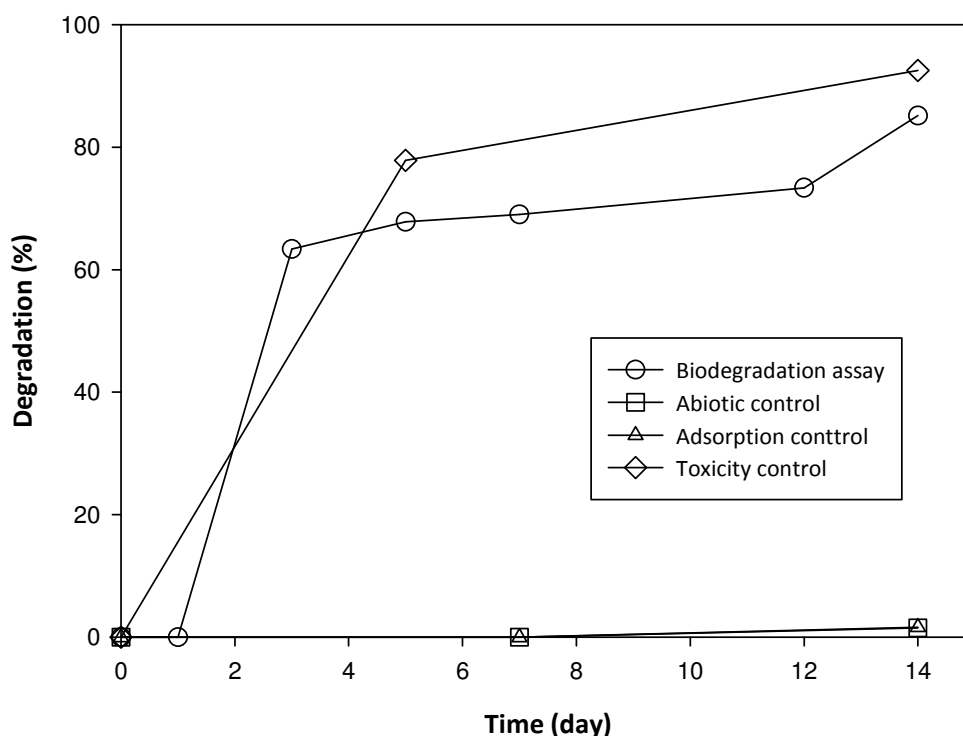


**Figure 2.2** Biodegradation assay of PDA according to OECD guidelines.

In the case of BCIEE, EC and EMI, no DOC decrease was observed over the assay time period (Figure 2.3). However, a biodegradation >35%, occurred in less than 14 days, in all toxicity controls, which are composed by equal amounts of the reference and the test substance (Figure 2.3). These results strongly suggest that none of these compounds is toxic, since they did not impair the biodegradation of the reference substance. Additionally, the abiotic and adsorption controls revealed that no degradation or adsorption of BCIEE, EC and EMI occurred, because no DOC decrease was noticed during the test (data not shown). Since BCIEE, EC and EMI were not biodegradable within the 28 days established by the OECD guidelines, these compounds cannot be considered as readily biodegradable, even though they were not toxic to the microorganisms.

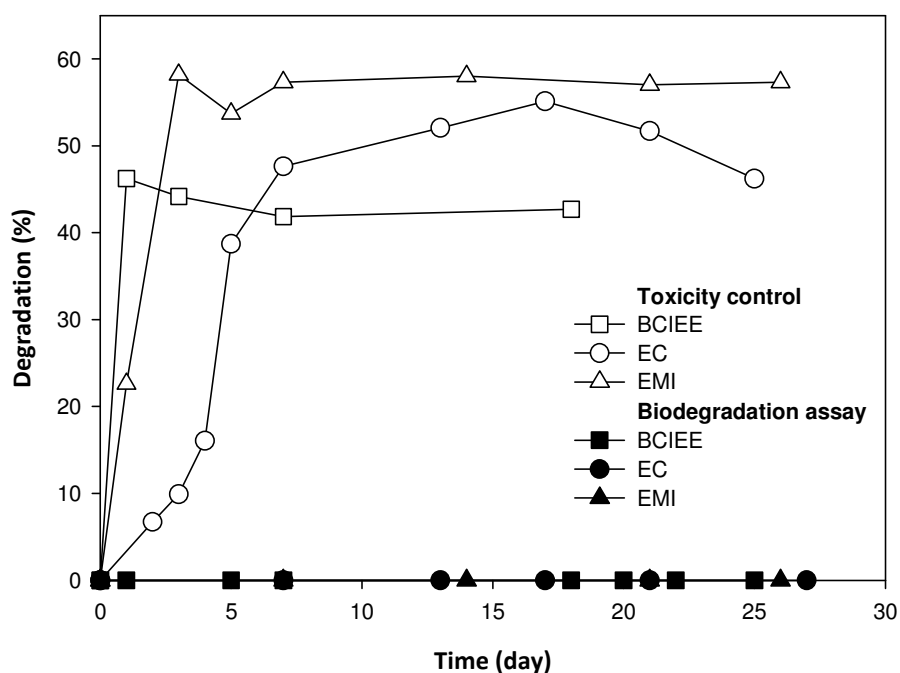


**Figure 2.3.** Biodegradation assays of BCIEE, EC and EMI according to the OECD guidelines.

Sykora et al. (2001) reported that the susceptibility of ethylenediamine derivatives containing two secondary nitrogen atoms are readily to potentially biodegradable. The fact that none of the three compounds evaluated in this work (BCIEE, EC and EMI), which present secondary amines (Figure 2.1), were degraded during the tests demonstrates that potential biodegradability of the chelators with secondary nitrogen atoms did not apply in any of these cases. Nevertheless, this fact does not imply that these compounds are not biodegradable at all because factors like acclimation time and microorganisms species used in biodegradation tests influence the degradation of substances.

In conclusion, among the four chelating agents studied, PDA was the only one that exhibited considerable degradation under the studied conditions, and thus, can be classified as a readily biodegradable substance by the OECD criteria (OECD, 1992).



### 2.3.2 Complexation modeling study

Application of chelating agents for a specific purpose, such as in industrial or agriculture applications is based on solving a problem of a multicomponent system (Jones and Williams, 2001).

Thus, in a first attempt and in order to understand the ability of each chelating agent to complex with a specific ion, metal chemical simulations were performed and the total amount of each metal complexed with each chelating agent was calculated (Figure 2.4). Figure 2.4A evidences that BCIEE complex strongly with Cd, Co, Cu, Ni and Zn ions in a large range of pH (at least between pH 6 and 11.5), but not with Pb ions, although in the presence of an excess of chelating agent. In a similar way, as it was described for BCIEE, EC complexes totally with several metal (Ca, Cd, Co, Cu, Mg, Ni, Pb and Zn) ions throughout a wider pH range (at least between pH 4 and 13), except with Mn ions, which total complexation is predicted in the pH range between 8.0 and 12.5 (Figure 2.4B).

EMI has a low affinity for Ca and Mg ions, as it is shown by the percentage (about 40%) of complexes formed in a higher and narrower pH range (Figure 2.4C), and a moderate affinity for Mn and Pb ions, which is evidenced by the total complexation in a narrower pH range (7-10 and 5-8, respectively). On the other hand, EMI evidences a high affinity for Cd, Cu, Ni and Zn ions, which is reflected by the total complexation in a wider pH range (5.5-12, 3-12.5, 3.5-13 and 5-11, respectively).

Figure 2.4D evidences that PDA complex almost totally with Cd, Co, Cu, Ni and Zn ions throughout a wider pH range (3-11, 2.5-11, 0-11, 2.5-11, 2.5-11, respectively). PDA exhibits a very weak affinity with Mg, complexes totally Fe under acidic conditions ( $\text{pH} < 5.5$ ) and Pb in the pH range between 1.5 and 8.5. For higher pH values ( $\text{pH} > 4.5$ ), PDA evidences high affinity for Mn and Ca ions.

The overall analysis of these results suggest the following conclusions: (i) all four compounds can be used to chelate Cd, Cu, Ni and Zn ions in a wider range of pH; (ii) BCIEE, EC and PDA can be used to chelate Co ions; (iii) EC and PDA can be used to chelate Ca and Pb ions; (iv) EC can be used to complex Mg ions and PDA can be used to chelate Fe ions; (v) EC, EMI and PDA can also be used to chelate Mn ions.

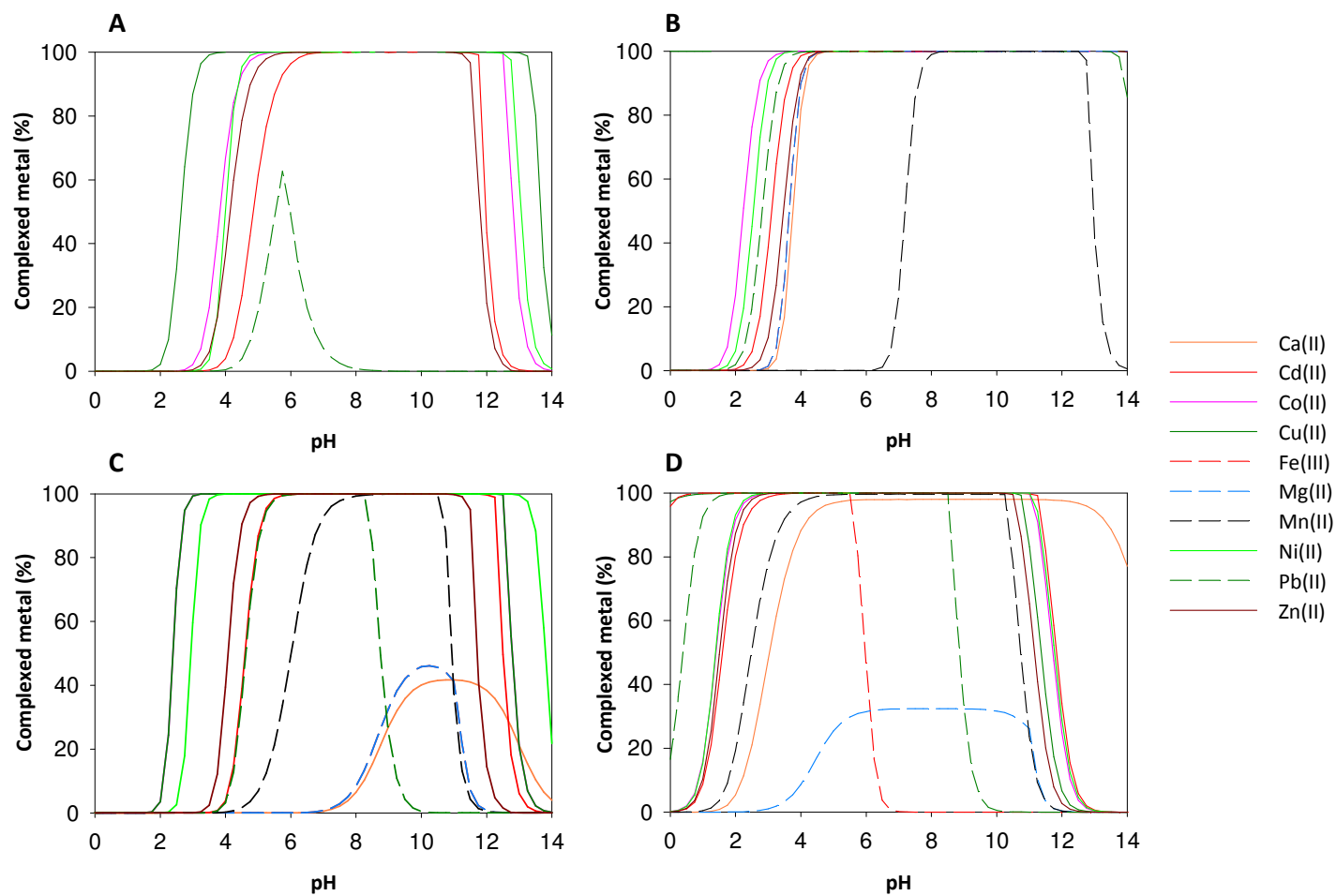


**Figure 2.4.** Amount, in percentage, of each metal (Ca, Cd, Co, Cu, Fe, Mg, Mn, Ni, Pb or Zn) complexed with BCIEE (A), EC (B), EMI (C) and PDA (D). Chemical simulation were performed assuming one metal (M) and one chelating agent (L), with a [L]:[M] ratio of 2.5, [M] = 0.001 M.

Usually, the major concern on the application of chelating agents is in the removal of heavy metals. But in some cases, other metal ions, like Ca and Mg, are also present, generally at much higher concentrations than the heavy metal ions, which may lead to undesirable complexation (Lanham, et al., 2011).

The presence of Ca ions, at a higher concentration than the other metal ions, is unavoidable (bleaching, dyeing or tanning process, food products or metal scale removal) or even essential (remediation of soils) for a wide kind of processes (Heinzman, et al., 1999). Therefore, in order to predict the chelating behavior of each compound under conditions of excess of Ca, metal chemical speciation were simulated in aqueous solution considering a concentration of chelating agent approximately half of the concentration of Ca ions and twice the total concentration corresponding to the sum of all other metal (Cd, Co, Cu, Fe, Mg, Mn, Ni, Pb and Zn) ions. The percentage of each metal complexed with each chelating agent was calculated and is presented in Figure 2.5.

The comparative analysis between figures 2.5A and 2.4B evidences that, in the presence of excess of Ca, EC is not able to complex Mn in all range of pH; in addition, Mg is only partially (~ 40%) complexed in the pH range 4 and 10. In the same way, complexation between Cd and Zn ions and EC is also diminished up to pH 6.5. However, total complexation of Cd and Zn ions is predicted for pH higher than 6.5 and between pH 6.5-10, respectively. Figure 2.5A shows that EC remains an extremely efficient chelating agent (~100%) for Cu, Co and Ni ions, even in presence of excess of Ca ions. Relatively to EMI, heavy metals complexation seems not to be affected by the presence of excess of Ca ions (Figure 2.5B). On the other hand, PDA is not able to complex Mg in all range of pH and complexes Mn in a less extent (about 40-50% in the pH range 3-9) (Figure 2.5C). For the other metal ions, complexation with PDA remains high (~100%), but until a slightly lower pH value than without excess of Ca ions.

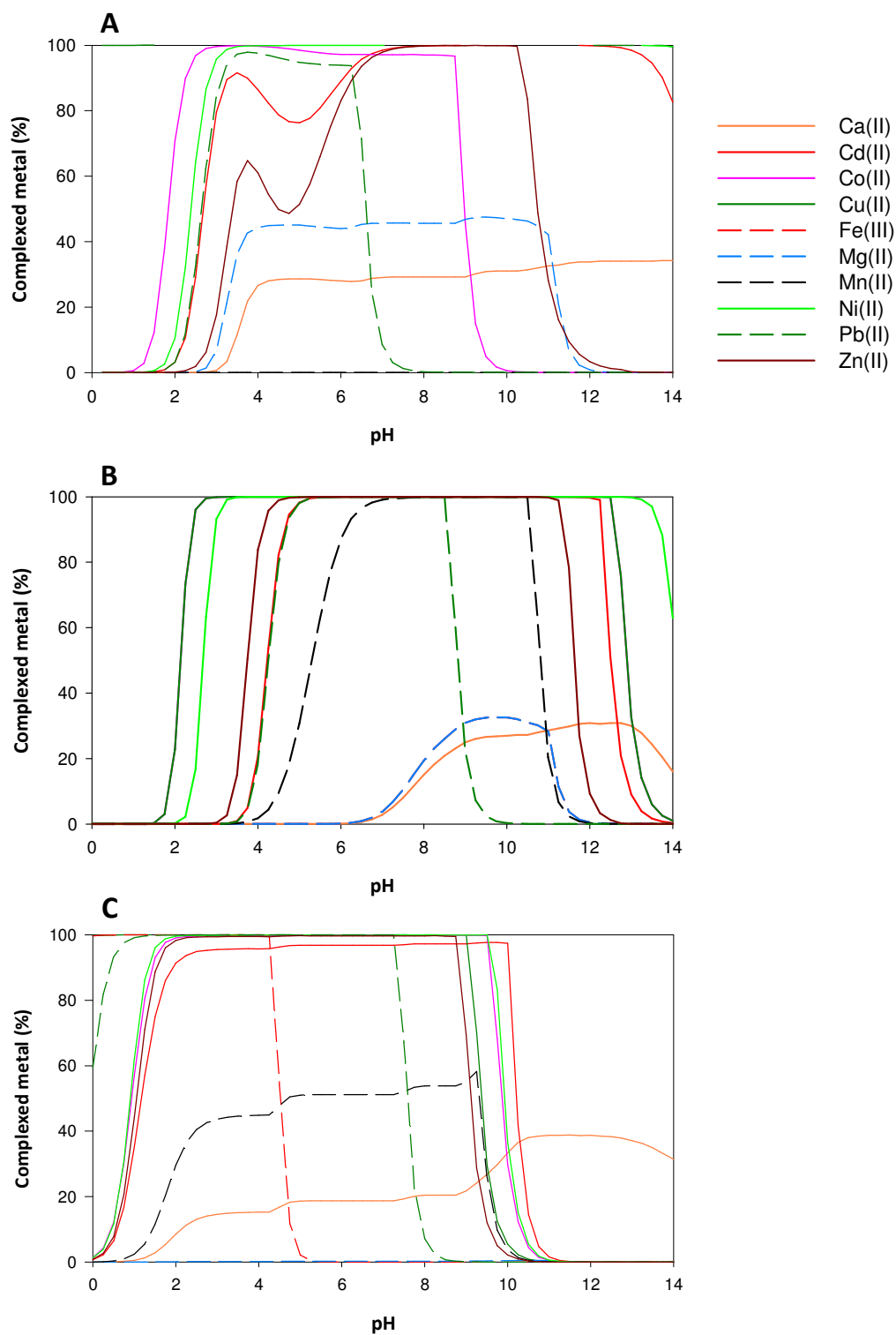


**Figure 2.5.** Amount, in percentage, of metal complexed with EC (A), EMI (B) and PDA (C). Chemical simulations were performed assuming the simultaneous presence of the chelating agent ( $[L] = 0.02 \text{ M}$ ) and all metal ions ( $[Cd] = [Co] = [Cu] = [Fe] = [Mg] = [Mn] = [Ni] = [Pb] = [Zn] = 0.001 \text{ M}$ ) with an excess of Ca ( $[Ca] = 0.05 \text{ M}$ ).

### 2.3.3 Possible applications for BCIEE, EC, EMI and PDA

According to the metal chemical simulations previously described, BCIEE, EC, EMI and PDA seem to be possible alternative chelating agents for being used as: food fortifiers and on food process. BCIEE, EC and EMI could be possible alternatives to combat Zn deficiencies, and PDA to combat Zn and Fe deficiencies. BCIEE, EC, EMI and PDA seem to be also an interesting alternative to sequester Cu in order to avoid oxidative degradation or enzymatic browning on food (Bendini, et al., 2006; Li, et al., 2008). PDA can also be suitable for sequestering Fe in food process and food fortification.

The use of chelating agents to make micronutrients (mainly Fe; Mn and Zn are used) available to agriculture process was already mentioned (Lopez-Rayó, et al., 2012). Figure 2.5B shows that EMI form stable complexes with Mn and Zn without Ca ions competitions in the pH range 7 and 10, which includes the typical pH of calcareous soils. Thus, EMI can be a potential alternative chelating agent for preparing Zn and Mn soils fertilizers.

The complexing properties of BCIEE show the capability to be used as biocidal, when associated to Co, Cu and Zn. EC can also be used as biocidal, complexed with Co or Cu, like EMI when complexed with Cu or Zn. PDA, as a readily biodegradable compound, remains to be an interesting option. Readily biodegradable compounds should be used in situations that the biocidal action must be quickly and nonpersistent. PDA could be used as a biocidal associated to Co, Cu, Zn and Fe. For example, PDA could be used to depleting Fe concentration on media to very low levels and inhibit the bacteria growth (Feng, et al., 1997).

PDA has already been used in soil remediation (Banerji and Regmi, 1998); however, this compound is ready biodegradable and thus it will be fastly biodegraded under field conditions. To keep the treatment at low cost, the chelating agent must be reused for further extraction cycles (Xie and Marshall, 2001; Tandy, et al., 2004). When it is recycled during consecutive extraction operations, the chelating agent remains in solution for a long period of time; so, the biodegradation of compounds during metal extraction from soil would be unwanted. As soil extractions are carried out at favorable conditions for biodegradation of the chelates, readily biodegradable

chelating agents may not be the better option. The degree of biodegradability of a particular chelate is an important factor in their selection and in estimation of its reuse frequency. EC and EMI appear to be more adequate to be used on soil remediation processes due to their ability to complex Cu, Zn and Ni ions, in the presence of Ca ions, and do not remove Fe ions, both present on soils.

Another possible application for the chelating agents studied in this work is for the treatment of metal poisoning with Cd or Pb ions. For this type of application, chelating agent must be highly selective for the metal poisoning ion, in the presence of Ca ions (Aposhian, et al., 1995; Johri, et al., 2010) at physiological pH. EC, EMI and PDA can be possible alternatives for the treatment of Cd poisoning, but for Pb poisoning treatment, only EMI and PDA can be considered.

EC and PDA have high affinity for Ca ions in a large range of pH. Since high amounts of chelating agent are needed to remove Ca from the incrustations, the use of a readily biodegradable compound is more suitable. Due to its biodegradability, PDA can be an interesting possibility for this application.

Considering the fact that large amounts of chelating agent are needed for some applications, such as is the case of metal electroplating, detergents, tanning process or pulp and textile industries, PDA must be regarded as a possible alternative. PDA is not suitable for metal electroplating because extremely alkaline pH values, higher than 12.5, are used (Hanna, et al., 2004; Pereira, et al., 2010) and PDA does not chelate Cu, Ni or Zn at so high pH range. However, PDA can be an alternative for pulp industry, where the detrimental metal ions are Fe, Mn and Cu. Chemical simulations showed that PDA complex Fe ions until pH 4, but the [L]:[M] ratio should be increased at least ten times, which is enough to ensure complexation of Fe until a pH of 5.5 (data not shown); this pH value is within the pH range used for metals removal from pulp (Khristova, et al., 2002). Since PDA is a good Ca chelating agent, this compound can also be used on pulp industry, or in others industries, not only for the detrimental metal ions removal, but with the aim of joining the ability of PDA to remove heavy metal ions and to reduce Ca incrustations. It is well known that Ca incrustations are often a cause of concern at this kind of process (Rudie and Hart, 2005); so, the application of PDA in this direction can be an interesting option. Some authors had already showed that PDA can be used in detergents application, as a builder in

dishwashing (De Ridder, et al., 1983; Frankena, 1988) and laundry (Boskamp, 1990) compositions, due to its ability to sequester Ca ions.

## **2.4. Conclusions**

In the present work, we demonstrated that the chelating agent PDA is ready-biodegradable according to the OECD criteria. Due to its high biodegradability, this compound can be used on Ca incrustations removal and on pulp metal ions removal processes. In these industrial processes, the biodegradability of PDA is of paramount importance taking into account the large amounts of complexing agent used and its possibility to reach the environment. Although the three other tested compounds (BCIEE, EC and EMI) did not demonstrate to be ready-biodegradable during the 28 days of the test, none of them provided evidence of being toxic to microorganisms. The non-ready biodegradability of BCIEE, EC and EMI compounds should not be a factor of exclusion; on the contrary, this characteristic can be advantageous, particularly when no environmental damage occurs or if it is required that the chelating agent remains available during a certain period of time. Food fortification, food process, fertilizers, biocides, soil remediation and treatment of metal poisoning are examples of possible applications for these chelating agents.

## 2.5 References

Al-Nabulsi, A. A.; Holley, R. A., Enhancing the Antimicrobial Effects of Bovine Lactoferrin against Escherichia Coli O157 : H7 by Cation Chelation, NaCl and Temperature. *Journal of Applied Microbiology* **2006**, *100* (2), 244-255.

Aposhian, H. V.; Maiorino, R. M.; Gonzalezramirez, D.; Zunigacharles, M.; Xu, Z. F.; Hurlbut, K. M.; Juncomunoz, P.; Dart, R. C.; Aposhian, M. M., Mobilization of Heavy-Metals by Newer, Therapeutically Useful Chelating-Agents. *Toxicology* **1995**, *97* (1-3), 23-38.

Banerji, S. K.; Regmi, T. P., Biodegradation of the Chelator 2,6-Pyridine Dicarboxylic Acid (Pda) Used for Soil Metal Extraction. *Waste Management* **1998**, *18* (5), 331-338.

Barros, M. T.; Martins, J.; Pinto, R. M.; Santos, M. S.; Soares, H., Complexation Studies of N, N'-Ethylenedi-L-Cysteine with Some Metal Ions. *Journal of Solution Chemistry* **2009**, *38* (12), 1504-1519.

Bendini, A.; Cerretani, L.; Vecchi, S.; Carrasco-Pancorbo, A.; Lercker, G., Protective Effects of Extra Virgin Olive Oil Phenolics on Oxidative Stability in the Presence or Absence of Copper Ions. *Journal of Agricultural and Food Chemistry* **2006**, *54* (13), 4880-4887.

Borkow, G.; Gabbay, J., Copper as a Biocidal Tool. *Current Medicinal Chemistry* **2005**, *12* (18), 2163-2175.

Borkow, G.; Zhou, S. S.; Page, T.; Gabbay, J., A Novel Anti-Influenza Copper Oxide Containing Respiratory Face Mask. *Plos One* **2010**, *5* (6).

Boskamp, J. V. Detergent Compositions. EP 0358472 A2, May 14, 1990.

Bucheli-Witschel, M.; Egli, T., Environmental Fate and Microbial Degradation of Aminopolycarboxylic Acids. *Fems Microbiology Reviews* **2001**, *25* (1), 69-106.



De Ridder, J. J. M.; Hollingsworth, M. W.; Robb, I. D. Dishwashing Composition. EP 0082564 A2, June 29, 1983.

Dixon, N. J.; Giles, M. R. Automatic Dishwashing Composition. WO/2012/038755A1, March 29, 2012.

Feng, M. H.; Lalor, B.; Hu, S. W.; Mei, J.; Huber, A.; Kidby, D.; Holbein, B., Inhibition of Yeast Growth in Grape Juice through Removal of Iron and Other Metals. *International Journal of Food Science and Technology* **1997**, 32 (1), 21-28.

Frankena, H. Machine Dish Washing Composition Containing Dipicolinic Acid. EP 0266904 A2, May 11, 1988.

Grefeuille, V.; Kayode, A. P. P.; Icard-Verniere, C.; Gnimadi, M.; Rochette, I.; Mouquet-Rivier, C., Changes in Iron, Zinc and Chelating Agents During Traditional African Processing of Maize: Effect of Iron Contamination on Bioaccessibility. *Food Chemistry* **2011**, 126 (4), 1800-1807.

Gruenwed.Dw, Multidentate Coordination Compounds . Chelating Properties of Aliphatic Amines Containing Alpha-Pyridyl Residues and Other Aromatic Ring Systems as Donor Groups. *Inorganic Chemistry* **1968**, 7 (3), 495-501.

Hanna, F.; Hamid, Z. A.; Aal, A. A., Controlling Factors Affecting the Stability and Rate of Electroless Copper Plating. *Materials Letters* **2004**, 58 (1-2), 104-109.

Heinzman, S. W.; Ingram, B. T.; Simpson, A. J. Aqueous Compositions Comprising Complexing Agents and Uses Therof. WO/1999/039045 A1, August 5, 1999.

Johri, N.; Jacquillet, G.; Unwin, R., Heavy Metal Poisoning: The Effects of Cadmium on the Kidney. *Biometals* **2010**, 23 (5), 783-792.

Jones, P. W.; Williams, D. R., Speciation Efficiency Indices (Sei) and Readily-Biodegradable Indices (Rbi) for Optimising Ligand Control of Environmental and Associated Industrial Processes. *International Journal of Environmental Analytical Chemistry* **2001**, 81 (1), 73-88.

Khristova, P.; Tomkinson, J.; Valchev, I.; Dimitrov, I.; Jones, G. L., Totally Chlorine-Free Bleaching of Flax Pulp. *Bioresource Technology* **2002**, 85 (1), 79-85.

Knepper, T. P., Synthetic Chelating Agents and Compounds Exhibiting Complexing Properties in the Aquatic Environment. *Trac-Trends in Analytical Chemistry* **2003**, 22 (10), 708-724.

Lanham, A. B.; Carvalheira, M.; Rodrigues, A. M.; Cardoso, V. V.; Benoliel, M. J.; Barros, M. T.; Morgado, M. J.; Soares, H. M. V. M.; Lemos, P. C.; Reis, M. A. M., Ethylenediamine-N,N'-Diglutamic Acid (EDDG) as a Promising Biodegradable Chelator: Quantification, Complexation and Biodegradation. *Journal of Environmental Science and Health Part A-Toxic/Hazardous Substances & Environmental Engineering* **2011**, 46 (6), 553-559.

Li, H.; Guo, A.; Wang, H., Mechanisms of Oxidative Browning of Wine. *Food Chemistry* **2008**, 108 (1), 1-13.

Lin, Y.-T.; Chien, Y.-C.; Liang, C., A Laboratory Treatability Study for Pilot-Scale Soil Washing of Cr, Cu, Ni, and Zn Contaminated Soils. *Environmental Progress & Sustainable Energy* **2012**, 31 (3), 351-360.

Lopez-Rayó, S.; Correias, C.; Lucena, J. J., Novel Chelating Agents as Manganese and Zinc Fertilisers: Characterisation, Theoretical Speciation and Stability in Solution. *Chemical Speciation and Bioavailability* **2012**, 24 (3), 147-158.

Lucena, J. J., Fe Chelates for Remediation of Fe Chlorosis in Strategy I Plants. *J. Plant Nutr.* **2003**, 26 (10-11), 1969-1984.

Martell, A. E.; Smith, R. M., *Nist Standard Reference Database 46 Version 8.0, Nist Critically Selected Stability Constants of Metal Complexes Database*. US Department of Commerce: National Institute of Standards and Technology, 2004.

Martins, J. G.; Pinto, R. M.; Gameiro, P.; Barros, M. T.; Soares, H. M. V. M., Aqueous Equilibrium and Solution Structural Studies of the Interaction of N,N'-Bis(4-

Imidazolymethyl)Ethylenediamine with Ca(II), Cd(II), Co(II), Cu(II), Mg(II), Mn(II), Ni(II), Pb(II) and Zn(II) Metal Ions. *Journal of Solution Chemistry* **2010a**, 39 (8), 1153-1167.

Martins, J. G.; Gameiro, P.; Teresa Barros, M.; Soares, H. M. V. M., Potentiometric and Uv-Visible Spectroscopic Studies of Cobalt(II), Copper(II), and Nickel(II) Complexes with N,N'-(S,S)-Bis 1-Carboxy-2-(Imidazol-4-yl)Ethyl Ethylenediamine. *Journal of Chemical and Engineering Data* **2010b**, 55 (9), 3410-3417.

Martins, J. G.; Teresa Barros, M.; Pinto, R. M.; Soares, H. M. V. M., Cadmium(II), Lead(II), and Zinc(II) Ions Coordination of N,N'-(S,S)Bis 1-Carboxy-2-(Imidazol-4-yl)Ethyl Ethylenediamine: Equilibrium and Structural Studies. *Journal of Chemical and Engineering Data* **2011**, 56 (3), 398-405.

Miyake, H.; Watanabe, M.; Takemura, M.; Hasegawa, T.; Kojima, Y.; Inoue, M. B.; Inoue, M.; Fernando, Q., Novel Optically-Active Bis(Amino Acid) Ligands and Their Complexation with Gadolinium. *Journal of the Chemical Society-Dalton Transactions* **2002**, (6), 1119-1125.

OECD, *Test No. 301: Ready Biodegradability, Oecd Guidelines for the Testing of Chemicals, Section 3*. OECD Publishing: 1992.

Pereira, F. V.; Alves Gurgel, L. V.; Gil, L. F., Removal of Zn<sup>2+</sup> from Aqueous Single Metal Solutions and Electroplating Wastewater with Wood Sawdust and Sugarcane Bagasse Modified with Edta Dianhydride (Edta). *Journal of Hazardous Materials* **2010**, 176 (1-3), 856-863.

Pinto, I.S.S., Ascenso, O.S., Barros, M.T., Soares, H.M.V.M. Pre-treatment of the paper pulp in the bleaching process using biodegradable chelating agents. *International Journal of Environmental Science and Technology*, **2014** (DOI 10.1007/s13762-013-0480-0).

Rudie, A.; Hart, P., Managing Calcium Oxalate Scale in the Bleach Plant. *Solutions : for people, processes and paper (June 2005)* **2005**, 45-46.

Salgueiro, M. J.; Zubillaga, M.; Lysionek, A.; Caro, R.; Weill, R.; Boccio, J., Fortification Strategies to Combat Zinc and Iron Deficiency. *Nutr. Rev.* **2002**, *60* (2), 52-58.

Schecher, W. D.; McAvoy, D. C. *Minql+, a Chemical Equilibrium Modeling System Version 4.5 for Windows*, Environmental Research Software, Hallowell: Maine, **2003**.

Sreeram, K. J.; Ramasami, T., Sustaining Tanning Process through Conservation, Recovery and Better Utilization of Chromium. *Resources Conservation and Recycling* **2003**, *38* (3), 185-212.

Sykora, V.; Pitter, P.; Bittnerova, I.; Lederer, T., Biodegradability of Ethylenediamine-Based Complexing Agents. *Water Research* **2001**, *35* (8), 2010-2016.

Tandy, S.; Bossart, K.; Mueller, R.; Ritschel, J.; Hauser, L.; Schulin, R.; Nowack, B., Extraction of Heavy Metals from Soils Using Biodegradable Chelating Agents. *Environ. Sci. Technol.* **2004**, *38* (3), 937-944.

Wuorimaa, A.; Jokela, R.; Aksela, R., Recent Developments in the Stabilization of Hydrogen Peroxide Bleaching of Pulps: An Overview. *Nordic Pulp & Paper Research Journal* **2006**, *21* (4), 435-443.

Xie, T.; Marshall, W. D., Approaches to Soil Remediation by Complexometric Extraction of Metal Contaminants with Regeneration of Reagents. *Journal of Environmental Monitoring* **2001**, *3* (4), 411-416.

Zeronian, S. H.; Inglesby, M. K., Bleaching of Cellulose by Hydrogen Peroxide. *Cellulose* **1995**, *2* (4), 265-272.

## Chapter 3

---

N,N'-Dihydroxy-N,N'-diisopropylhexanediamide,  
a siderophore analogue, as a possible iron chelating  
agent for hydroponic conditions:

metal equilibrium studies



**N,N'-Dihydroxy-N,N'-diisopropylhexanediamide, a siderophore  
analogue, as a possible iron chelating agent for hydroponic conditions:  
metal equilibrium studies\***

**Abstract**

Synthetic iron chelates are the most efficient iron fertilizers. The stability in solution of the iron chelates in the presence of other metal cations that may compete with iron for the chelating agent in nutrient solutions is crucial for its effectiveness in supplying iron to plants.

In this work, the chelating properties of N,N'-Dihydroxy-N,N'-diisopropylhexanediamide (DPH), a biological model of the natural siderophore rhodotorulic acid, were evaluated in order to assess its potentialities for being used, as iron chelate, in hydroponic cultures. For this purpose, the complexation for the metal [Ca(II), Cu(II), Mg(II), Mn(II) or Zn(II)]-DPH-OH systems has been studied using pH-potentiometry and the overall stability constants has been determined for the first time.

For all M-DPH-OH systems, MHL and ML species were identified. For [Cu(II), Mn(II) or Zn(II)]-DPH-OH systems, the  $M_2L_3$  species was detected, whereas the formation of ML(OH) species was found in the [Ca(II) or Mg(II)]-DPH-OH systems.

Finally, the chemical stability of iron chelated with DPH in hydroponic conditions was assessed by computer chemical simulations and compared with the one predicted when iron is chelated with ethylenediamine-N,N'-bis(o-hydroxyphenyl)acetic acid (o,o-EDDHA) in similar conditions.

---

\* N,N'-Dihydroxy-N,N'-diisopropylhexanediamide, a siderophore analogue, as a possible iron chelating agent for hydroponic conditions: metal equilibrium studies (Submitted for publication).

### 3.1 Introduction

The extreme insolubility of ferric hydroxides, that reduces the availability of iron (Fe) in soils, is the major cause of iron chlorosis in plants (Loper and Buyer, 1991).

The hydroxamate group, present in natural compounds is one of the most common found in the siderophores produced by molds, fungi, and yeast (Barclay, et al., 1984a; Farkas, et al., 1998). Hydroxamic acids take part in many types of biological systems and are also produced by several types of plants, mainly to inhibit plant pathogens. However, several authors have suggested that these compounds are also used by plants for metal ion uptake from soil (Barclay, et al., 1984a; Farkas, et al., 1998).

Naturally produced hydroxamates are usually trihydroxamic acids that form very stable 1:1 complexes with ferric ion. Desferrioxamine B (Figure 1.17, section 1.3.1) is a microbial hydroxamate siderophore that has been extensively studied and was found to be an efficient source of iron for many microorganisms and for a variety of plants (Barclay, et al., 1984a; Siebner-Freibach, et al., 2006).

In contrast to trihydroxamic acids, rhodotorulic acid (RA) is a dihydroxamic acid, (Barclay, et al., 1984a). This siderophore is a tetradentate ligand, which is unable to satisfy the octahedral coordination of ferric ion through the formation of a 1:1 complex. It has been found to form dimeric complexes with Fe(III), Al(III) and Cr(III) with the formula  $M_2-(RA)_3$  (Barclay, et al., 1984a). Although the preparation of several N-unsubstituted dihydroxamate ligands has been reported, they have not been used previously as siderophore analogues but rather were prepared as analytical reagents (Barclay, et al., 1984a; Barclay, et al., 1984b).

N,N'-Dihydroxy-N,N'-diisopropylhexanediamide (DPH) (Figure 3.1) is a biological and physicochemical model of rhodotorulic acid. DPH is constituted by two N-isopropylhydroxamic acid groups separated by a aliphatic chain of four methylene groups. In solution, besides the formation of  $[FeL]$  ( $\log \beta=22.3$ ) (Barclay, et al., 1984a), DPH is known to form a very stable dinuclear species  $[Fe_2L_3]$  with iron(III) ( $\log \beta=62.2$ ) (Barclay, et al., 1984a). A possible structure for the dimeric ferric dihydroxamate



complex formed by DPH was purposed by Barclay et al (1984a), and is represented in Figure 1.21D (section 1.31).

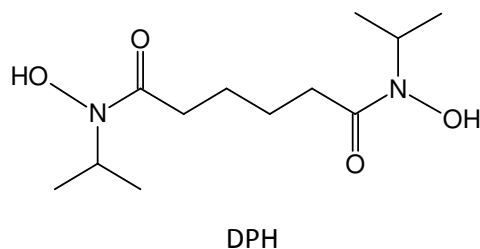


**Figure 3.1** Structure of N,N'-Dihydroxy-N,N'-diisopropylhexanediamide (DPH).

The chelating properties of hydroxamic acids are extremely important in the biological activity of hydroxamic acids and the knowledge of the stability in solution of new chelating agents is essential to predict their behavior as iron fertilizers in hydroponic culture but also for fertigation and soil applications (Farkas, et al., 1998; Lucena, et al., 2010).

In order to assess the behaviour of DPH, as an iron chelate, in micronutrient mixtures used in hydroponic cultures, the objective of this work was to study the interaction of DPH with different metal ions. For this purpose, overall protonation and metal formation stability constants of DPH with macro [Ca(II) and Mg(II)] and micronutrients [Cu(II), Mn(II) and Zn(II)], which are typically present in hydroponic solutions, were evaluated. Finally, the chemical stability of iron chelated with DPH in Hoagland nutrient solution was predicted by chemical simulations.

### 3.2 Materials and Methods

All reagents used in this work were of analytical grade. All aqueous solutions were prepared with deionized water.  $\text{CaCl}_2$ ,  $\text{CuCl}_2$ ,  $\text{MgCl}_2$ ,  $\text{MnCl}_2$  and  $\text{ZnCl}_2$  standard solutions, as well as KOH and HCl products, were obtained from Merck (Merck KGaA, Darmstadt, Germany). DPH was synthesized by the research group headed by

Professor Maria Teresa Barros, REQUIMTE, Faculdade de Ciências e Tecnologia, Universidade Nova de Lisboa. This compound was obtained using the method described by Smith and Raymond (1980), as a white powder, with an overall yield of 60% as its hydrochloride salt.

### 3.2.1 Potentiometric studies

The potentiometric titrations were performed with a PC-controlled system assembled from a Crison MicroPH 2002 meter, a Crison MicroBu 2030 microburette, and a Crison 52 09 pH electrode, or a Philips GAH 110 electrode and an Orion 90-02-00 (double junction) reference electrode with an outer chamber filled with  $0.1 \text{ mol.L}^{-1}$  KCl. Automatic acquisition of data was done using a home-made computer program, COPOTISY. All measurements were performed on solutions adjusted to an ionic strength of  $0.1 \text{ mol.L}^{-1}$  KCl in a Methrom (Herisau, Switzerland) jacketed glass vessel equipped with a magnetic stirrer and thermostatted at  $(25 \pm 0.1) ^\circ\text{C}$  using a water bath. The measurements were carried out under anaerobic conditions by bubbling purified nitrogen (99.9995 % purity) for ca. 15 min before starting the titration and during the titration in order to exclude oxygen and carbon dioxide from the reaction mixture in the titration cell.

The glass electrode calibration, in terms of hydrogen ion concentration, was accomplished by addition of a standardized solution of potassium hydroxide (KOH) to a standardized solution of hydrochloric acid (HCl) (both solutions adjusted to the ionic strength of  $0.1 \text{ mol.L}^{-1}$ ). From this potentiometric titration, the values of  $E^0$  and response slope were obtained by fitting a straight line to the experimental points collected around  $\text{pH} = 2$  and  $11$ .

The protonation and stability constants of DPH with the metal ions  $\text{Ca(II)}$ ,  $\text{Cu(II)}$ ,  $\text{Mg(II)}$ ,  $\text{Mn(II)}$  and  $\text{Zn(II)}$  were determined by direct potentiometric titrations. For all systems, monotonic additions of standardized KOH (titrant) were made, and the potential was recorded as a function of the added volume. For the determination of the protonation constants, pH potentiometric titrations were performed using a concentration of DPH of  $2 \times 10^{-3} \text{ mol.L}^{-1}$  (4 titrations). For all metal–DPH systems

studied, pH potentiometric titrations were performed using fixed ligand-to-metal ion  $[L_T]:[M_T]$  molar concentration ratios. For Cu(II)-DPH and Zn(II)-DPH systems, titrations were conducted with a  $[L_T]:[M_T]$  ratio of 2 (6 and 2 titrations for Cu and Zn, respectively) and 4 (2 and 5 titrations for Cu and Zn, respectively) with  $[M_T]=1.0 \times 10^{-3}$  mol.L<sup>-1</sup>. To study the Mn(II)-DPH system it was used a  $[L_T]:[M_T]$  ratio of 2 with  $[M_T]=1.25 \times 10^{-3}$  mol.L<sup>-1</sup> (2 titrations) and  $[M_T]=2.5 \times 10^{-3}$  mol.L<sup>-1</sup> (1 titration). For Ca(II)-DPH system, titrations were performed with a  $[L_T]:[Ca_T]$  ratio of 1 with  $[Ca_T]=4 \times 10^{-3}$  mol.L<sup>-1</sup> (2 titrations), and with a  $[L_T]:[Ca_T]$  ratio of 2,  $[M_T]=1.0 \times 10^{-3}$  mol.L<sup>-1</sup> (1 titration). Mg(II)-DPH system was studied with  $[L_T]:[Mg_T]$  ratio of 1 with  $[Mg_T]=4.0 \times 10^{-3}$  mol.L<sup>-1</sup> (4 titrations).

The simulation and optimization procedures of potentiometric data were performed using the Equilibrium Simulation for Titration Analysis (ESTA) program (May, et al., 1985; May, et al., 1988).

The refinement operations used in potentiometry involve solving mass-balance equations, including an equation for the total proton concentrations, in such way that the computed free proton concentration, when used by the equation describing the response of the calibrated glass electrode, reproduces the experimentally recorded potential of the glass electrode as accurately as possible. This is done by minimization of an objective function,  $U$ , defined in Equation 3.1:

$$U = (N - n_p)^{-1} \sum_{n=1}^N (E_n^{obs} - E_n^{calc})^2 \quad (3.1)$$

where  $U$  is the objective function to be minimized,  $N$  is the total number of experimental titration points;  $n_p$  represents the number of parameters simultaneously optimized,  $E_n^{obs}$  is the observed electrode potential at the  $n^{th}$  data point, and  $E_n^{calc}$  is defined by Equation 3.2,

$$E_n^{calc} = E^{o'} + k \log[H^+] \quad (3.2)$$

where  $E^{o'}$  is the electrode intercept and  $k$  the electrode calibration slope.

A Gauss-Newton method is the adopted approach by ESTA to minimize  $U$ . The Hamilton R-factor,  $R^H$ , is the statistical parameter used by ESTA to reflect the improved agreement between the calculated and the observed data. It is given by:

$$R^H = \left[ \frac{U}{\sum_{n=1}^N E_n^{obs}} \right]^{1/2} \quad (3.3)$$

The Hamilton R-factor does not have dimensions. The ESTA software includes a proton,  $Z_H$ , and a metal,  $Z_M$ , formation functions defined by

$$Z_H = \frac{[H_T] - [H^+] + [OH^-]}{[L_T]} \quad (3.4)$$

and

$$Z_M = \frac{[L_T] - L(1 + \sum_{n=1}^N \beta_{n01} [H^+]^n)}{[M_T]} \quad (3.5)$$

where

$$L = \frac{[H_T] - [H^+] + [OH^-]}{\sum_{n=1}^N \beta_{n01} [H^+]^n} \quad (3.6)$$

$[H_T]$ ,  $[L_T]$  and  $[M_T]$  represent the total concentration of proton, ligand, and metal, respectively;  $\beta_{n01}$  stands for the formation constants of  $M_nL_0H_l$  species.  $Z_H$  and  $Z_M$  functions are calculated for each datum point and are plotted against pH, and  $pL = -\log[L]$ , respectively, to aid in the modelling procedures.

It is important to stress that the  $Z_H$  or  $Z_M$  functions can only be generated for the assumed  $M-(L)_x-(OH)_y$  model. This implies that one has to investigate numerous possible models and generate  $Z_H$  or  $Z_M$  functions for all of them to select the most probable one, usually based on the observed fit of the theoretical function into the objective (experimental) one.

For each M-DPH system, several models were tested. When the final model was established, as the best one that fitted the experimental data, the overall stability constants were refined simultaneously by ESTA using the data obtained in all titrations. During the refinement operations, the water protonation constant and all known stability constants for metal hydroxide species were kept fixed (Table 3.1).

**Table 3.1** Protonation constants for water and overall stability constants for M(II) complexes with OH<sup>-</sup>, at 25.0 °C (Martell and Smith, 2004).

	Equilibrium	Log $\beta$	$\mu$ (mol L <sup>-1</sup> )
<b>Water</b>	$\text{H}_2\text{O} \leftrightarrow \text{H}^+ + \text{OH}^-$	-13.78	0.1
<b>Calcium</b>	$\text{Ca}^{2+} + \text{OH}^- \leftrightarrow \text{CaOH}^+$	0.96	0.1
	$\text{Ca}(\text{OH})_2(\text{s}) \leftrightarrow \text{Ca}^{2+} + 2\text{OH}^-$	-5.29	0.0
<b>Copper</b>	$\text{Cu}^{2+} + \text{OH}^- \leftrightarrow \text{CuOH}^+$	6.1	0.1
	$\text{Cu}^{2+} + 2\text{OH}^- \leftrightarrow \text{Cu}(\text{OH})_2$	11.8	0.1
	$\text{Cu}^{2+} + 3\text{OH}^- \leftrightarrow \text{Cu}(\text{OH})_3^-$	14.5	1.0
	$\text{Cu}^{2+} + 4\text{OH}^- \leftrightarrow \text{Cu}(\text{OH})_4^{2-}$	15.6	1.0
	$\text{Cu}(\text{OH})_2(\text{s}) \leftrightarrow \text{Cu}^{2+} + 2\text{OH}^-$	-18.9	1.0
<b>Magnesium</b>	$\text{Mg}^{2+} + \text{OH}^- \leftrightarrow \text{MgOH}^+$	1.87	0.1
	$4\text{Mg}^{2+} + 4\text{OH}^- \leftrightarrow \text{Mg}_4\text{OH}_4^{4+}$	16.1	3.0
	$\text{Mg}(\text{OH})_2(\text{s}) \leftrightarrow \text{Mg}^{2+} + 2\text{OH}^-$	-9.2	0.0
<b>Manganese</b>	$\text{Mn}^{2+} + \text{OH}^- \leftrightarrow \text{MnOH}^+$	2.7	0.1
	$\text{Mn}^{2+} + 4\text{OH}^- \leftrightarrow \text{Mn}(\text{OH})_4^{2-}$	7.7	0.0
	$2\text{Mn}^{2+} + \text{OH}^- \leftrightarrow \text{Mn}_2\text{OH}^{3+}$	3.4	0.0
	$2\text{Mn}^{2+} + 3\text{OH}^- \leftrightarrow \text{Mn}_2\text{OH}_3^{2+}$	18.1	0.0
	$\text{Mn}(\text{OH})_2(\text{s}) \leftrightarrow \text{Mn}^{2+} + 2\text{OH}^-$	-12.8	0.0
<b>Iron</b>	$\text{Fe}^{3+} + \text{OH}^- \leftrightarrow \text{FeOH}^{2+}$	11.24	3.0
	$\text{Fe}^{3+} + 2\text{OH}^- \leftrightarrow \text{Fe}(\text{OH})_2^+$	21.5	0.5
	$\text{Fe}^{3+} + 3\text{OH}^- \leftrightarrow \text{Fe}(\text{OH})_3$	30.2	0.0
	$\text{Fe}^{3+} + 4\text{OH}^- \leftrightarrow \text{Fe}(\text{OH})_4^-$	34.4	0.0
	$2\text{Fe}^{3+} + 2\text{OH}^- \leftrightarrow \text{Fe}_2(\text{OH})_2^{2-}$	24.5	0.1
	$3\text{Fe}^{3+} + 4\text{OH}^- \leftrightarrow \text{Fe}_3(\text{OH})_4^{5-}$	48.9	3.0
	$\text{Fe}(\text{OH})_3(\text{s}) \leftrightarrow \text{Fe}^{3+} + 3\text{OH}^-$	-38.6	0.0
<b>Zinc</b>	$\text{Zn}^{2+} + \text{OH}^- \leftrightarrow \text{ZnOH}^+$	4.6	0.1
	$\text{Zn}^{2+} + 2\text{OH}^- \leftrightarrow \text{Zn}(\text{OH})_2$	11.1	0.0
	$\text{Zn}^{2+} + 3\text{OH}^- \leftrightarrow \text{Zn}(\text{OH})_3^-$	16.3	0.0
	$\text{Zn}^{2+} + 4\text{OH}^- \leftrightarrow \text{Zn}(\text{OH})_4^{2-}$	14.8	0.0
	$2\text{Zn}^{2+} + \text{OH}^- \leftrightarrow \text{Zn}_2\text{OH}^{3+}$	5.0	0.0
	$4\text{Zn}^{2+} + 4\text{OH}^- \leftrightarrow \text{Zn}_4(\text{OH})_4^{4+}$	27.9	3.0
	$\text{Zn}(\text{OH})_2(\text{s}) \leftrightarrow \text{Zn}^{2+} + 2\text{OH}^-$	-15.52	0.0

### 3.2.2 Computer chemical simulations

Metal chemical speciation calculations between each chelating agent and metal(s) were performed using MINEQL+ Version 4.5 (Environmental Research Software, Hallowell, ME, USA) (Schecher and McAvoy, 2003), as previously described (section 2.2.3). Computational simulations were performed in aqueous medium in the pH range between 0 and 14.

Table 3.2 shows the stability constants for *o,o*-EDDHA with metal ions considered in chemical simulations in the Hoagland nutrient solution.

**Table 3.2** Protonation and overall stability constants (as  $\log \beta$ ) for *o,o*-EDDHA complexes formed with Ca(II), Mg(II), Cu(II) and Fe(III) (Yunta, et al., 2003).

Metal ion	Equilibrium	Log $\beta$
<b>Protonation</b>	$L + H \leftrightarrow HL$	11.18
	$L + 2H \leftrightarrow H_2L$	22.67
	$L + 3H \leftrightarrow H_3L$	31.33
	$L + 4H \leftrightarrow H_4L$	37.51
<b>Ca(II)</b>	$M + L \leftrightarrow ML$	7.29
	$M + L + H \leftrightarrow MHL$	16.77
	$M + L + 2H \leftrightarrow MH_2L$	25.95
<b>Mg(II)</b>	$M + L \leftrightarrow ML$	9.76
	$M + L + H \leftrightarrow MHL$	18.18
	$M + L + 2H \leftrightarrow MH_2L$	25.36
<b>Cu(II)</b>	$M + L \leftrightarrow ML$	25.13
	$M + L + H \leftrightarrow MHL$	32.61
	$M + L + 2H \leftrightarrow MH_2L$	37.31
<b>Fe(III)</b>	$M + L \leftrightarrow ML$	35.09
	$M + L + H \leftrightarrow MHL$	36.89
	$M + L + H \leftrightarrow ML(OH)$	23.66

### 3.3 Results and Discussion

#### 3.3.1 Protonation and metal-complexation of DPH

The dissociation constants of DPH and  $M_x\text{-DPH}_y\text{-(OH)}_z$  complex formation systems [ $M = \text{Ca(II)}, \text{Cu(II)}, \text{Mg(II)}, \text{Mn(II)}$  and  $\text{Zn(II)}$ ] have been studied by glass electrode potentiometry (GEP). Representative pH titration curves for DPH and for the different metal-ligand systems are shown in Figure 3.2, where  $a$  value is the ratio of moles of base added per mole of ligand present; at  $a=0$ , the ligand is in the  $\text{H}_2\text{L}$  form.

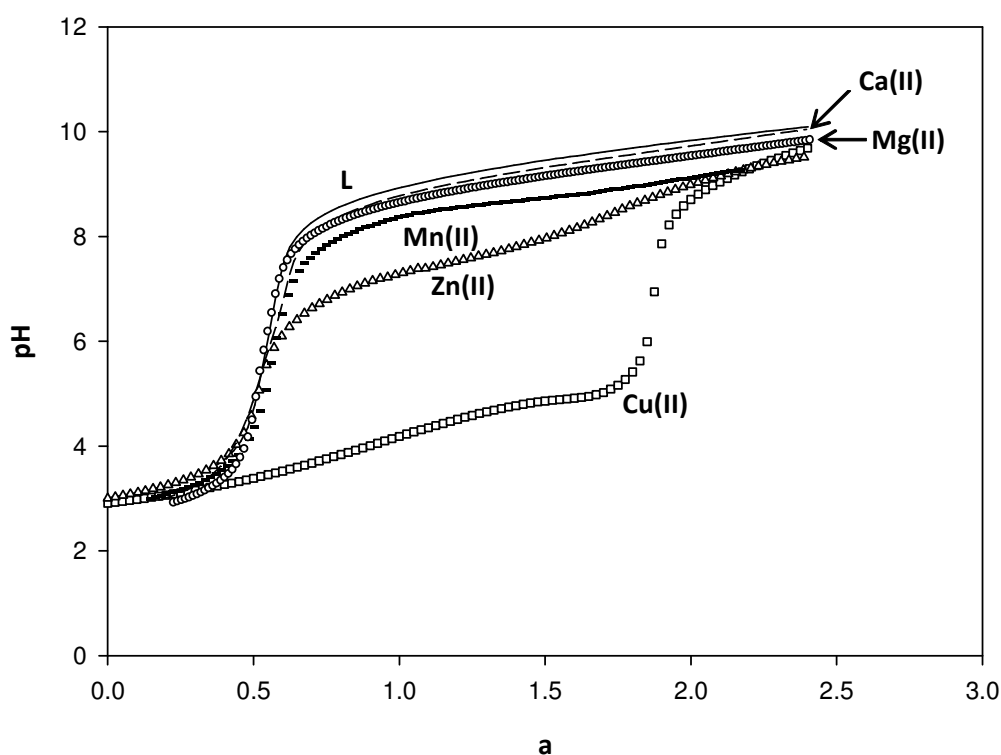


**Figure 3.2** Representative pH titration curves for DPH and metal [ $\text{Ca(II)}$ ,  $\text{Cu(II)}$ ,  $\text{Mg(II)}$ ,  $\text{Mn(II)}$  or  $\text{Zn(II)}$ ]-DPH-OH systems.  $\text{Ca(II)}$  and  $\text{Mg(II)}$ :  $[\text{L}_\text{T}]:[\text{M}_\text{T}]=2$  and  $1$ , respectively, with  $[\text{M}_\text{T}] = 4.0 \times 10^{-3} \text{ mol.L}^{-1}$ ;  $\text{Cu(II)}$  and  $\text{Zn(II)}$ :  $[\text{L}_\text{T}]:[\text{M}_\text{T}]=2$ ,  $[\text{M}_\text{T}] = 1.0 \times 10^{-3} \text{ mol.L}^{-1}$ ;  $\text{Mn(II)}$ :  $[\text{L}_\text{T}]:[\text{M}_\text{T}]=2$ ,  $[\text{Mn}_\text{T}] = 2.5 \times 10^{-3} \text{ mol.L}^{-1}$ ; For DPH alone:  $[\text{L}_\text{T}] = 2.0 \times 10^{-3} \text{ mol.L}^{-1}$ .  $\mu = 0.1 \text{ mol.L}^{-1}$  (KCl) and  $T = 25^\circ\text{C}$ ;  $a$  = moles of base (KOH) added per mole of ligand.



The overall refined protonation constants of DPH are listed in Table 3.3. The values determined in the present work ( $9.79 \pm 0.03$  and  $18.89 \pm 0.03$ ) are in very good agreement with those published by Barclay et al., (1984a).

The comparative analysis between the curves of pH *versus*  $\alpha$ , obtained in the different titrations of DPH alone and with each metal ion studied (Figure 3.2), evidences that complexation of DPH with the various metal ions follows different behaviours and reveals great differences in the stability of the M-DPH complexes. Whereas the complex formation of DPH with Cu(II) starts at very low pH values, no interaction between DPH and Ca(II) or Mg(II) occurs up to about pH 6. For Mn(II) and Zn(II) ions, pH *versus*  $\alpha$  curves evidence that DPH starts to complex with these metal ions in less acidic conditions than with Cu(II) ions, which evidence that DPH forms less stronger complexes with these two metal ions.

For Cu(II)-DPH system, the analysis of Figure 3.2 evidences that between pH 4 and 10, the pH *versus*  $\alpha$  curve draws an accentuated sigmoidal shape, which evidences the formation of a strong major species.

Furthermore, precipitation was observed at pH values higher than 5, most likely due to the formation of insoluble Cu(II) complexes (Farkas, et al., 1999); due to this fact, refinement operations were only performed over a narrow pH range (between 3.0 and 4.75), where no precipitation was experimentally observed.

**Table 3.3** Overall DPH protonation constants and stability constants (as  $\log \beta$ ) for DPH with Cu(II), Zn(II), Mn(II), Mg(II) and Ca(II), refined simultaneously for all titrations in ESTA, determined by GEP in 0.1 M KCl at 25 °C (charges were omitted for simplicity).

Equilibrium	DPH	Metal Ions				
		Cu(II)	Zn(II)	Mn(II)	Mg(II)	Ca(II)
$H + L \leftrightarrow HL$	$9.79 \pm 0.03$	-	-	-	-	-
$2H + L \leftrightarrow H_2L$	$18.89 \pm 0.03$	-	-	-	-	-
$M + H + L \leftrightarrow MHL$	-	$18.318 \pm 0.008$	$14.71 \pm 0.02$	$13.52 \pm 0.01$	$12.22 \pm 0.01$	$11.57 \pm 0.01$
$M + L \leftrightarrow ML$	-	$13.898 \pm 0.006$	$7.19 \pm 0.01$	$3.88 \pm 0.07$	$2.722 \pm 0.007$	$1.42 \pm 0.02$
$2M + 3L \leftrightarrow M_2L_3$	-	$43.11 \pm 0.03$	$22.18 \pm 0.04$	$16.87 \pm 0.04$	-	-
$M + L + OH \leftrightarrow ML(OH)$	-	-	-	-	$6.485 \pm 0.005$	$5.317 \pm 0.005$
Number of titrations/number of independent solutions	4/2	8/4	7/4	3/2	3/2	4/2
$[L_T]:[M_T]^*$	-	2 ; 4	2 ; 4	2	1	1 ; 2

\* For additional information, see section 3.2.1. Potentiometric studies.

Initially, two models were assumed: Model I [CuL] and Model II [CuHL and CuL]. Although ESTA refined both models (Table 3.4), the statistical  $R^H$  parameter evidences a better adjustment between the experimental and the calculated data in model II (Table 3.4). Moreover, for pH values lower than 4 ( $pL > 14$ ), the calculated  $Z_M$  functions for models I and II, in Figure 3.3, clearly evidence that CuHL species should be formed in this pH range. The possible formation of MHL species in the M-DPH systems arises from the fact that up to pH *ca* 10, DPH is in the form of  $H_2L$  (Figure 3.4).

However, Figure 3.3 evidences a mathematical difference between the complexation curves calculated for Models I or II and the experimental data obtained for the whole refined pH range. For higher pH values ( $pL$  values  $< 12.5$ ), the calculated  $Z_M$  function was below the experimental points, which evidences the possibility of other  $Cu_xL_y$  species.

The formation of  $M_2L_3$  species by dihydroxamic acids with some metal ions has already been reported (Farkas, et al., 1999; Farkas, et al., 2004); therefore, besides CuL and CuHL, also  $Cu_2L_3$  species was included in model III, which reproduces well the experimental results in the pH range considered (Figure 3.3).

To test model III, a species distribution diagram (SDD) was generated for  $[L_T]:[Cu_T] = 2$ ,  $[Cu_T] = 1 \times 10^{-3} \text{ mol.L}^{-1}$  (Figure 3.5). This figure shows that complexation starts at pH 1, as CuHL species, followed by the formation of CuL and  $Cu_2L_3$  species. From pH 4 to 5, both CuL and  $Cu_2L_3$  species are being formed at the same time, in agreement with the calculated  $Z_M$  function where CuL and  $Cu_2L_3$  individual slopes are indistinguishable from each other (Figure 3.3).

**Table 3.4** Overall stability constants (as  $\log \beta$  values) for M-DPH systems determined by GEP for one titration in 0.1 mol L<sup>-1</sup> KCl at 25° C;M = Cu(II) or Zn(II),  $[M_T] = 1.0 \times 10^{-3}$  mol.L<sup>-1</sup>.

$[L_T] / [M_T]$	Metal ion					
	Cu(II)			Zn(II)		
	2			2		
	Model I	Model II	Model III	Model I	Model II	Model III
<b>Complexes</b>						
<b>M + H + L <math>\leftrightarrow</math> MHL</b>	NI	17.89 $\pm$ 0.06	18.34 $\pm$ 0.01	NI	14.43 $\pm$ 0.09	14.68 $\pm$ 0.02
<b>M + L <math>\leftrightarrow</math> ML</b>	13.91 $\pm$ 0.04	14.03 $\pm$ 0.03	13.952 $\pm$ 0.004	7.18 $\pm$ 0.06	7.26 $\pm$ 0.06	7.27 $\pm$ 0.02
<b>2M + 3L <math>\leftrightarrow</math> M<sub>2</sub>L<sub>3</sub></b>	NI	NI	43.09 $\pm$ 0.01	NI	NI	22.38 $\pm$ 0.06
<b>Hamilton R-factor, R<sup>H</sup></b>	0.047	0.033	0.003	0.20	0.17	0.064
<b>Number of points</b>	57	57	57	61	61	61
NI- Not included						

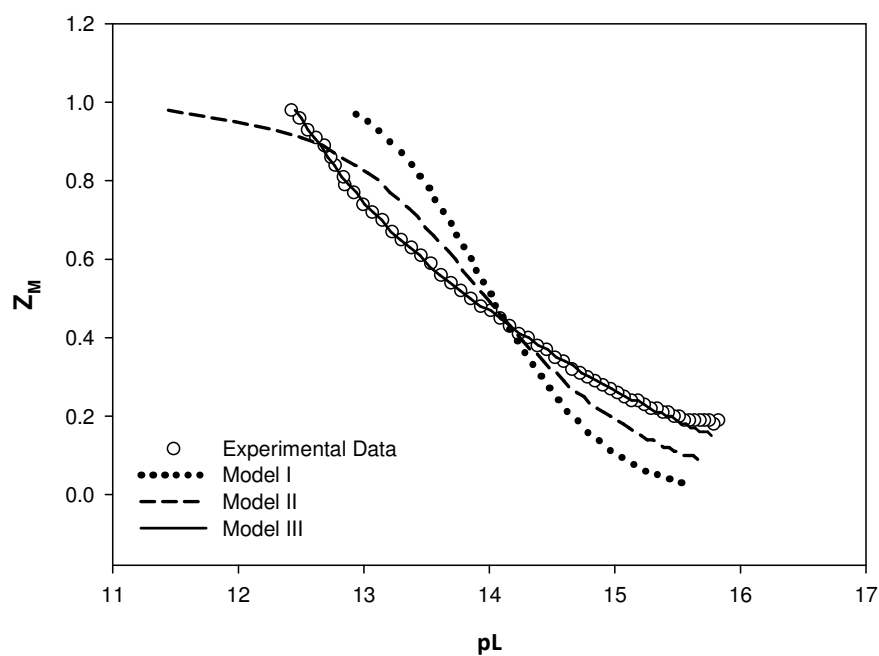


**Figure 3.3**  $Z_M$  function for Cu(II)-DPH-OH system. The computed function was calculated from the refinement operation performed for the models presented in Table 3.4.  $[L_T]: [Cu_T]=2$ ,  $[Cu]= 1.0 \times 10^{-3} \text{ mol.L}^{-1}$ .

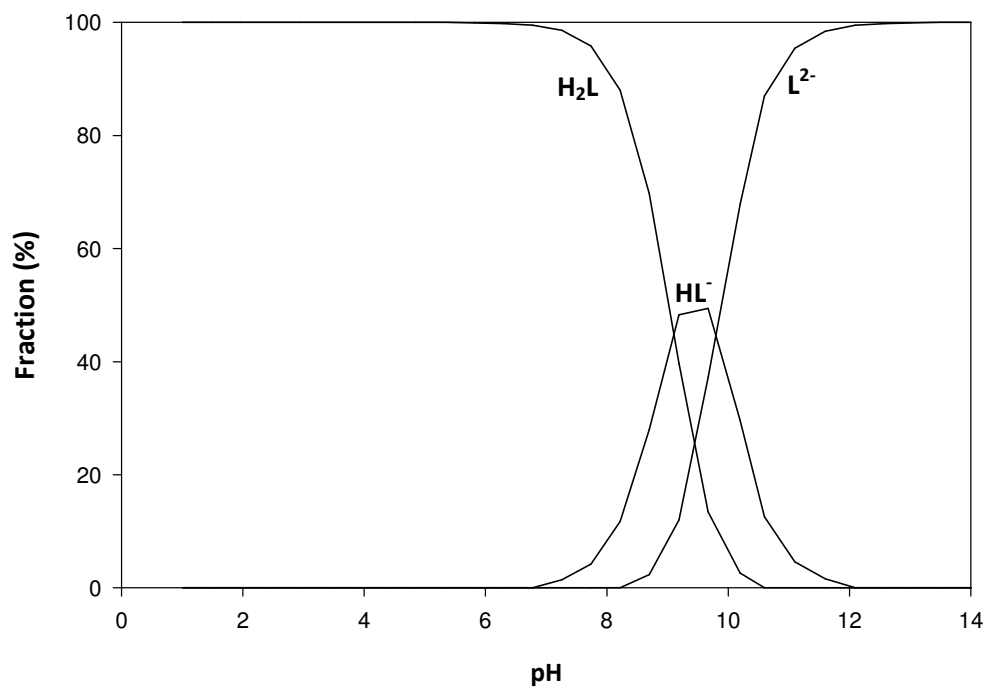


**Figure 3.4** Species distribution diagram computed for DPH;  $[L_T] \text{ } 2.0 \times 10^{-3} \text{ mol.L}^{-1}$ .

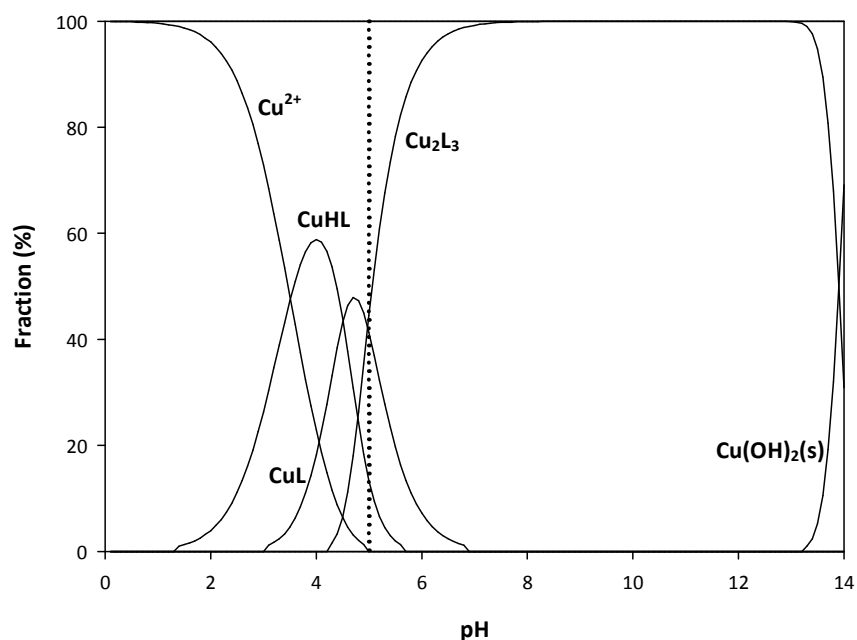


**Figure 3.5** Species distribution diagram computed, assuming the final model, for Cu(II)–DPH–OH system. Model III, Table 3.4,  $[L_T]: [M_T]=2$ ,  $[M_T]= 1.0 \times 10^{-3} \text{ mol.L}^{-1}$ . The dotted line indicates the pH value where precipitation was experimentally observed.

Additionally, SDD predicts precipitation of  $\text{Cu(OH)}_2(\text{s})$  for pH values higher than 13, which is not in agreement with our experimental observation. In Cu(II)-hydroxamic acid systems, it is frequent the formation of insoluble complexes (Farkas, et al., 1998). In our study, precipitation was observed at pH values higher than 5, after the formation of the  $\text{Cu}_2\text{L}_3$ ; this fact strongly suggests the formation of other, but insoluble, polynuclear complexes, already referred by other authors (Farkas et al., 1999), for copper(II)-dihydroxamic systems.

For Zn(II)-DPH system, the analysis of the pH *versus*  $\alpha$  curve (Figure 3.2) suggests the formation of at least one species, evidenced by the gentle sigmoidal shape between pH 6 and 9.5.

Because precipitation was observed at about pH 10, the refinement was restricted from pH 4 to 9. The first refinement attempts were performed with two models: Model I in which only ZnL was considered, and Model II in which ZnHL was also included. The stability constants obtained for ZnL in both models are similar (Table 3.4), however, in the lower pH range ( $\text{pH} < 7$ ) a better fitting to the experimental data

was observed with the inclusion of ZnHL in Model II. This is evidenced by the lower  $R^H$ , and also by the graphical representation of the  $Z_H$  function in Figure 3.6.

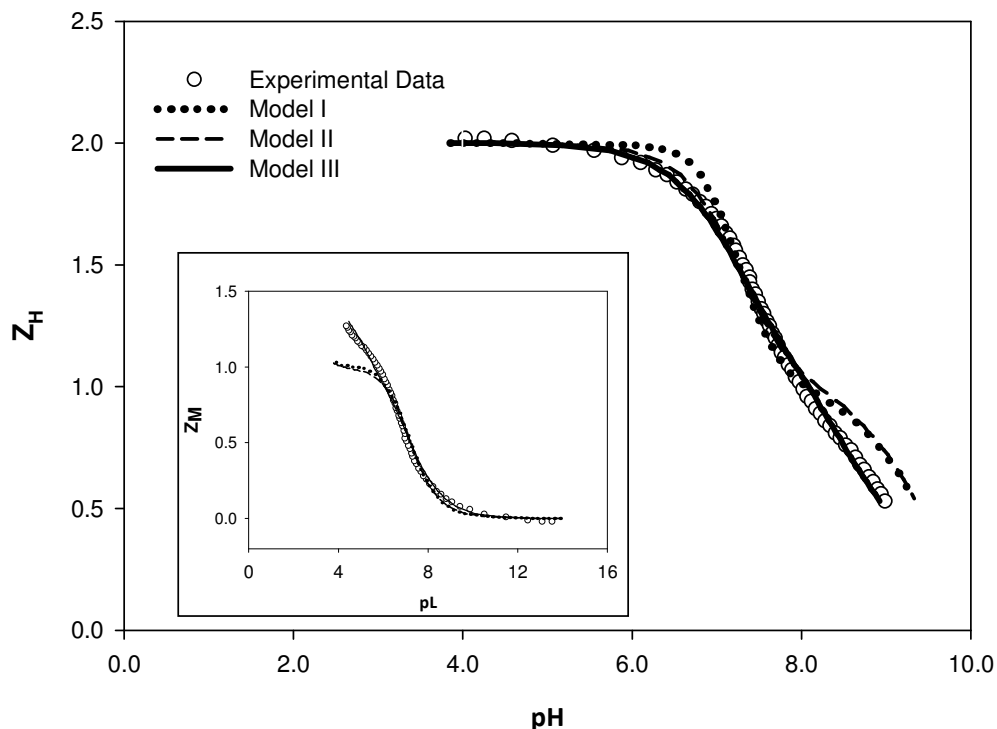


**Figure 3.6**  $Z_H$  and  $Z_M$  (insert) functions for Zn(II)-DPH-OH system computed from the refinement operation performed for the models presented in Table 3.4;  $[L_T]:[Zn_T] = 2$ ,  $[Zn_T] = 1.0 \times 10^{-3} \text{ mol.L}^{-1}$ .

At higher pH values ( $pH > 8$ ), the  $Z_M$  experimental data was trending to  $Z_M = 1.5$  (Figure 3.5, insert). This fact suggests the formation, at higher pH, of another species besides the mononuclear ML species. Therefore, the formation of  $Zn_2L_3$  species was also considered in model III. This model, which included  $ZnL$ ,  $ZnHL$  and  $Zn_2L_3$  species (Model III, Table 3.4), was able to reproduce well the experimental results in the pH range considered (Figure 3.6). Based on these results, model III was considered the final model for Zn(II)-DPH system.

To test the final model, the SDD was generated for  $[L_T]:[Zn_T] = 2$ ,  $[Zn_T] = 1 \times 10^{-3} \text{ mol.L}^{-1}$  (Figure 3.7).

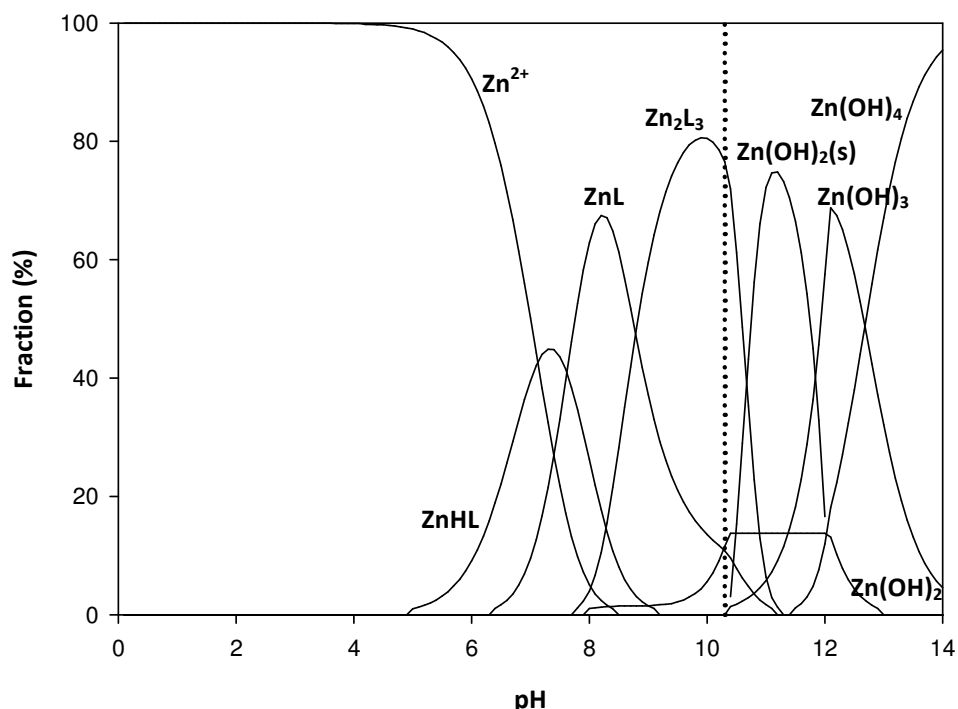


**Figure 3.7** Species distribution diagram computed, assuming the final model, for Zn(II)–DPH–OH system: Model III, Table 3.4,  $[L_T]: [M_T]=2$ ,  $[M_T]= 1.0 \times 10^{-3} \text{ mol.L}^{-1}$ ). The dotted line indicates the pH value where precipitation was observed.

The obtained SDD is in accordance with the observed in the pH versus  $\alpha$  plot (Figure 3.2) and  $Z_H$  function (Figure 3.6). ZnHL species starts to be formed at about pH 5 and is the predominant complex up to pH 7. ZnL and  $Zn_2L_3$  species predominate at pH from 7 to 8, and above 8.5, respectively. Additionally, the SDD predicts precipitation at pH = 10, which is in accordance with what was observed experimentally.

Experimentally, the study of the Mn(II)-DPH system was difficult to perform due to the oxidation of Mn(II) to Mn(III), even under oxygen free atmosphere maintained during the potentiometric titrations. Changes in the colour of the solution were monitored and a change in solution from colourless to brown was recorded at pH *ca.* 8.5. From this, the refinement exercises were only performed up to pH 8.4.



The oxidation kinetics of Mn(II) to Mn(III) depends on the denticity of the ligand and on the pH, being slower at lower pH ranges (Szabo and Farkas, 2011). The pH versus  $\alpha$  graph evidences the formation of Mn(II) complexes only at higher pH values ( $\text{pH} > 6$ ) (Figure 3.2). As the complexation begins at acidic pH and considering the behaviour of the previously studied metals, MnHL and ML species were included in the first model (Model I, Table 3.5). This model fitted properly the experimental data bellow pH 7.8, showing that MnHL and MnL species are indeed present (Figure 3.8), but not at higher pH values (lower pL values). Due to this fact and taking into account the complexation behaviour of the previous M-DPH-OH systems,  $\text{Mn}_2\text{L}_3$  species was included in Model II.

This model was able to fit the whole studied experimental data with a low Hamilton R-factor (Table 3.5). Although the SDD generated using  $[\text{L}_\text{T}]:[\text{Mn}_\text{T}] = 2$ ,  $[\text{Mn}_\text{T}] = 2.5 \times 10^{-3} \text{ mol.L}^{-1}$  (Figure 3.9) shows that in the pH range used during the refinement procedures MnL and  $\text{Mn}_2\text{L}_3$  species are only present in very low quantities, the adjustment to the experimental data was only possible with the inclusion of those species. The SDD shows that complexation starts at pH *ca.* 6, as MnHL, being this species the major one present up to pH *ca.* 8.3. Below pH 8.3, only a faint presence of MnL and  $\text{Mn}_2\text{L}_3$  species is predicted. Due to the observable oxidation of Mn(II) to Mn(III), no further conclusions can be taken for higher pH values.

**Table 3.5** Overall stability constants (as  $\log \beta$  values) for M-DPH systems determined by GEP for one titration in 0.1 mol L<sup>-1</sup> KCl at 25° C; M = Mn(II), Mg(II) or Ca(II).

[L <sub>T</sub> ] / [M <sub>T</sub> ] [M <sub>T</sub> ] (mol.L <sup>-1</sup> )	Metal ion							
	Mn(II)		Ca(II)			Mg(II)		
	2		2			1		
	2.5x10 <sup>-3</sup>		4.0x10 <sup>-3</sup>			4.0x10 <sup>-3</sup>		
Complexes	Model I	Model II	Model I	Model II	Model III	Model I	Model II	Model III
<b>M + H + L ↔ MHL</b>	13.45 ± 0.01	13.51 ± 0.01	NI	11.29 ± 0.04	11.39 ± 0.02	NI	12.17±0.02	12.06 ± 0.01
<b>M + L ↔ ML</b>	4.42 ± 0.02	3.85 ± 0.07	2.17 ± 0.15	NI	1.36 ± 0.03	2.99 ± 0.06	NI	2.54 ± 0.01
<b>2M + 3L ↔ M<sub>2</sub>L<sub>3</sub></b>	NI	16.82 ± 0.02	NI	NI	NI	NI	NI	NI
<b>M + L + OH ↔ ML(OH)</b>	NI	NI	NI	5.238±0.007	5.269 ± 0.006	NI	6.52±0.01	6.48 ± 0.01
<b>Hamilton R-factor</b>	0.013	0.005	0.102	0.005	0.004	0.097	0.02	0.004
<b>Number of points</b>	30	30	138	138	138	183	183	183

NI- Not included

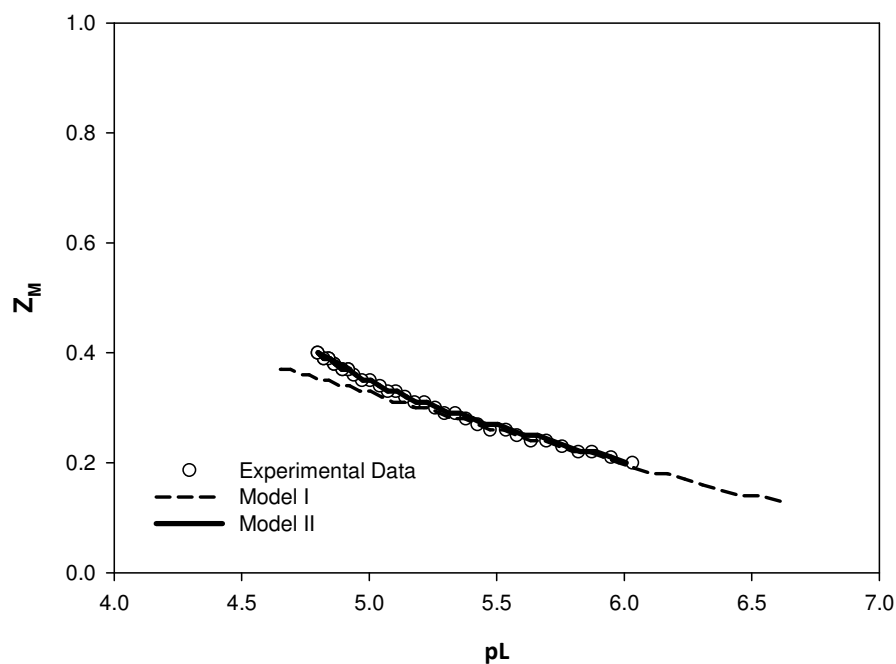


**Figure 3.8**  $Z_M$  function for Mn(II)–DPH–OH system. The computed function was calculated from the refinement operation performed for the models presented in Table 3.5:  $[L_T]:[Mn_T]=2$ ,  $[Mn]=2.5 \times 10^{-3} \text{ mol.L}^{-1}$ .

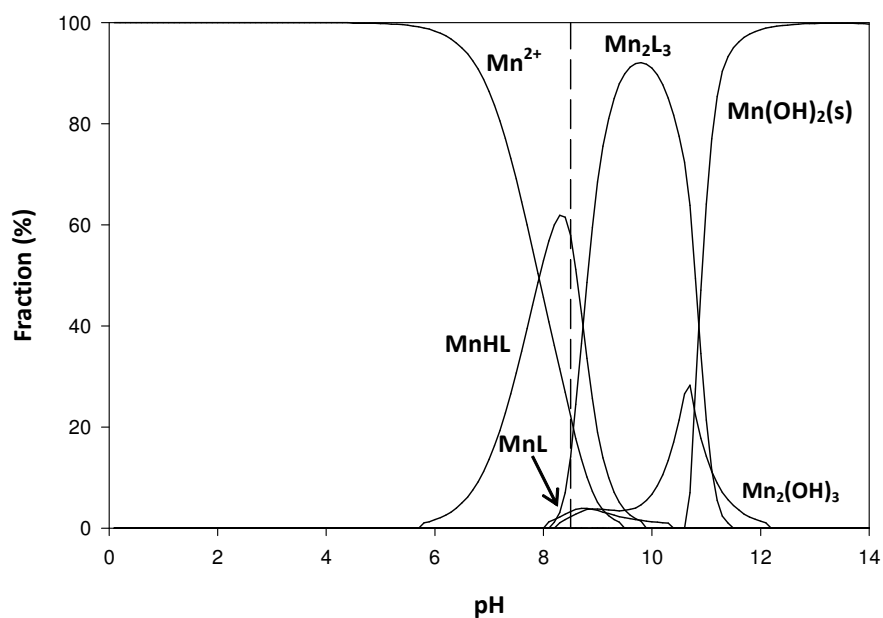


**Figure 3.9** Species distribution diagram computed, assuming the final model, for Mn(II)–DPH–OH system: Model II, Table 3.5,  $[L_T]:[Mn_T] = 2$ ,  $[M_T] = 2.5 \times 10^{-3} \text{ mol.L}^{-1}$ . The dashed line indicates Mn(II) oxidation.

For Ca(II)-DPH system, the analyses of the pH *versus*  $\alpha$  curve (Figure 3.2) hardly suggest complexation between Ca(II) and DPH as the curve almost superposes with the one of the DPH alone. Any complexation seems to occur until neutral to alkaline pH. Three models were tested (Table 3.5). Model I, containing CaL species, proved to be ineffective to replicate the experimental data (Figure 3.10).

The  $Z_M$  function (Figure 3.10) shows that model I failed to replicate the experimental data at in the whole pH range. The strong curving of  $Z_M$  function at higher pH values, and the poor fitting at lower ones, showed in Figure 3.10 suggested the presence of  $ML(OH)_x$  and MHL species. The formation of these two species was tested in Model II (Table 3.5). The  $Z_M$  function obtained for this model showed a slight deviation from the experimental data, that lead to the inclusion of CaL to the model (Model III, Table 3.5), which, upon refinement, fits well the experimental data (Table 3.5).

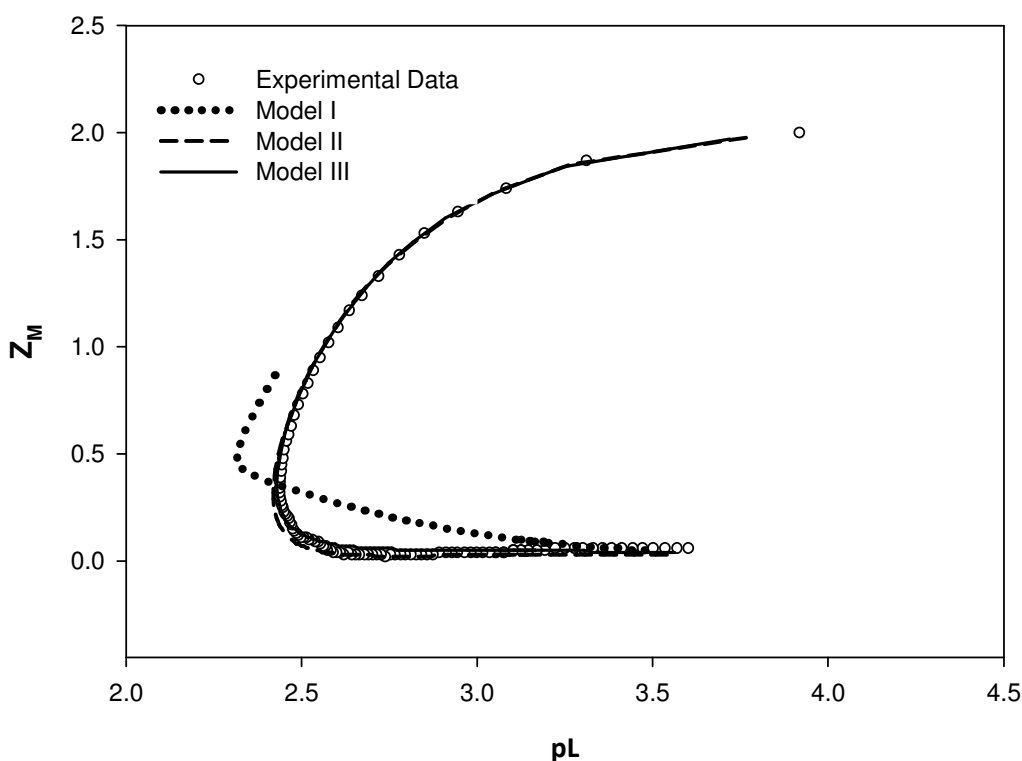


**Figure 3.10**  $Z_M$  function for Ca(II)-DPH-OH system. The computed  $Z_M$  function was calculated from the refinement operation performed for the models presented in Table 3.5: Ca(II):  $[L_T]$ :  $[Ca_T] = 2$ ,  $[Ca_T] = 4 \times 10^{-3} \text{ mol.L}^{-1}$ .

The SDD obtained for the final model (Model III, Table 3.5) with  $[L_T]:[Ca_T] = 2$ ,  $[Ca_T] = 4 \times 10^{-3} \text{ mol.L}^{-1}$  (Figure 3.11) shows that complexation starts above pH 8, as CaHL species, and at about pH 9.5, both CaL and CaLOH species start being formed simultaneously, being the later the predominant one. The SDD does not predict precipitation up to pH 14.

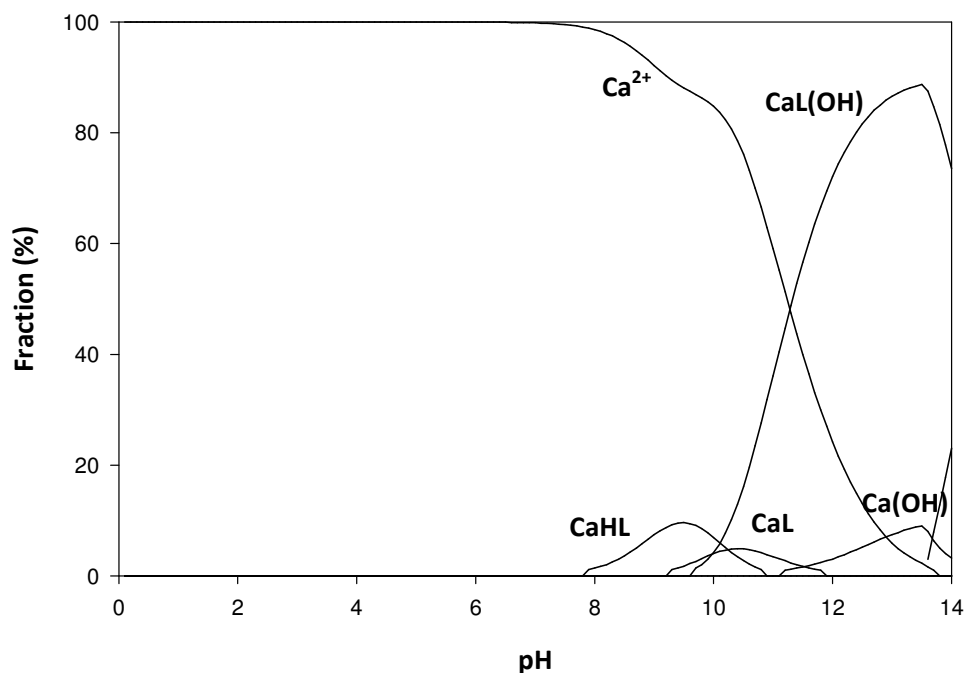


**Figure 3.11** Species distribution diagram computed, assuming the final model, for Ca(II)–DPH–OH system: Model III, Table 3.5,  $[L_T]:[M_T] = 2$ , with  $[M_T] = 4.0 \times 10^{-3} \text{ mol.L}^{-1}$ .

For Mg(II)-DPH system, the analyses of the pH *versus*  $\alpha$  curve (Figure 3.2) show that: (i) the shape of the pH *versus*  $\alpha$  curve is not very different from the one recorded with DPH alone and (ii) DPH starts to complex Mg(II) at pH *ca.* 7. As complexation starts at alkaline pH, the first model tested only included MgL species (Model I, Table 3.5). However, the  $Z_M$  calculated function showed a poor fitting of this model to the experimental  $Z_M$  data (Figure 3.12). Since Model I wasn't able to fit to the experimental data in the whole pH range used, the formation of MgLOH species, evidenced by the strong curving of the experimental  $Z_M$  function, and of MgHL species was tested, without success, in Model II. Only Model III, comprising MgHL, MgL and MgLOH species, was able to match the experimental data more precisely (Figure 3.12) and presenting a much lower Hamilton R-factor than models I and II (Table 3.5).

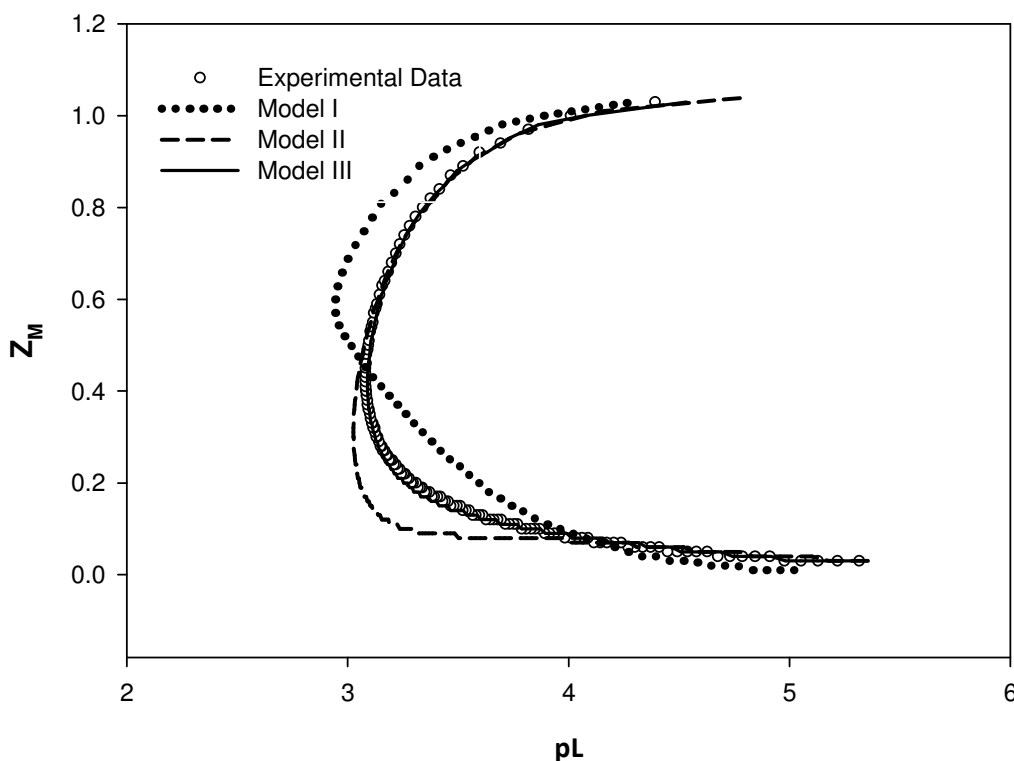


**Figure 3.12**  $Z_M$  function for Mg(II)–DPH–OH system. The computed function was calculated from the refinement operation performed for the models presented in Table 3.5:  $[L_T]:[Mg_T] = 1$ ,  $[Mg] = 4.0 \times 10^{-3} \text{ mol.L}^{-1}$ .

To further validate model III, as the final model, for the Mg-DPH system, a SDD was generated using  $[L_T]:[Mg_T] = 1$ ,  $[Mg_T] = 4 \times 10^{-3} \text{ mol.L}^{-1}$  (Figure 3.13). Analysis of the SDD shows that complexation begins approximately at pH 7 with the formation of MgHL species followed by MgL. MgLOH species is present in greater quantity from pH 10 on. This is in perfect agreement with the analyses of  $Z_M$  plot (Figure 3.12).

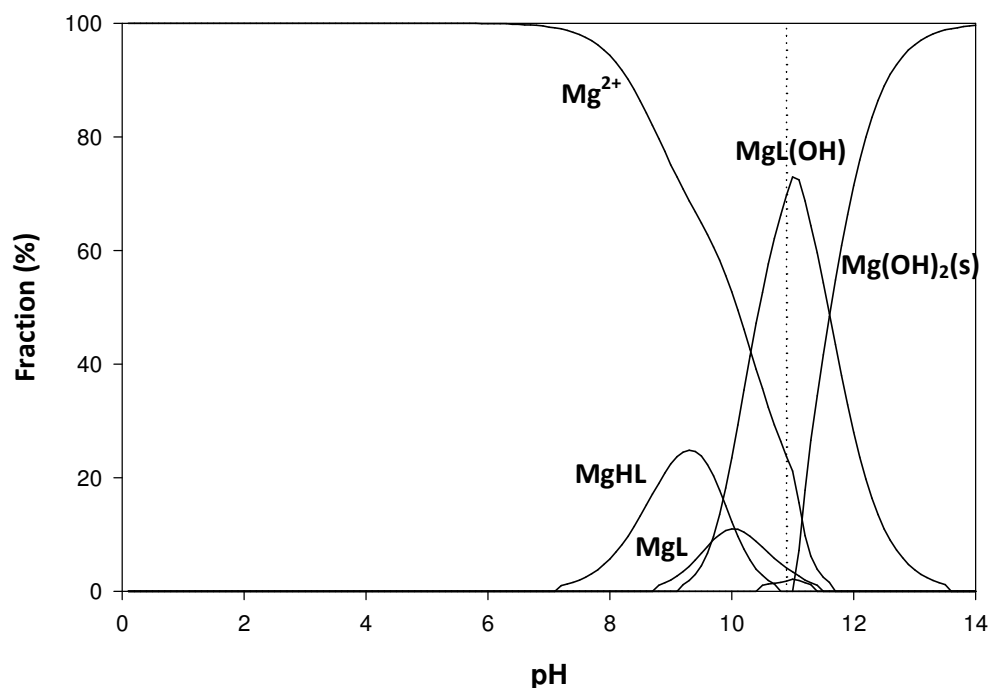


**Figure 3.13** Species distribution diagram computed, assuming the final model, for Mg(II)–DPH–OH system: Model III, Table 3.5,  $[L_T]:[M_T] = 1$  with  $[M_T] = 4.0 \times 10^{-3} \text{ mol.L}^{-1}$ . The dotted line indicates the pH value where precipitation was observed.

The SDD also predicts precipitation at pH around 11, which was observed experimentally. Finally, both MgL and MgLOH species are formed in the same range of pH ( $8.5 < \text{pH} < 9.5$ ), which is in line with the observation of  $Z_M$  function (Figure 3.12), where the curves from each species are barely distinguishable from each other.

Considering the final models, established above for each M-DPH system, the final overall stability constants obtained, after refining simultaneously all titrations of all  $[L_T]:[M_T]$  ratios, are presented in Table 3.3. The stability constants for CuL,  $\text{Cu}_2\text{L}_3$ , ZnL,  $\text{Zn}_2\text{L}_3$ , MnL,  $\text{Mn}_2\text{L}_3$ , MgL and MgLOH species, refined in this work, are in the same order of magnitude as those described by Farkas, et al. (1999) and Szabo et. al (2011) for similar dihydroxamic acids. However, all the stability constant values for MHL species, refined in this work, present about one log unit higher than those previously reported by the same authors. This may be due to higher basicity of the coordinating oxygen atoms as a consequence of the isopropyl groups attached to the hydroxamic

acid, whereas in the dihydroxamic acids studied by Farkas et. al (1999), methyl groups were bounded to the hydroxamic acid. Additionally, the CaL stability constant reported here (Table 3.5) was lower than those reported before. Again, the isopropyl groups may be responsible as Ca(II) has the larger ionic radius (100pm) and there may be repulsion between Ca(II) and the isopropyl groups whereas for other metals the effect is not so noticeable as the ionic radius are smaller (<70pm).

### 3.3.2 Stability of Fe-DPH complexes under hydroponic conditions

The ability of a chelating agent to maintain iron(III) in solution without being displaced by other cations is essential for its efficiency to remediate Fe chlorosis. To evaluate the ability of DPH, as a potential iron supplier to plants under hydroponic conditions, chemical simulations were performed considering the composition of the Hoagland nutrient solution ( $[\text{Fe(III)}]_{\text{T}} = 1 \times 10^{-4} \text{ mol.L}^{-1}$ ,  $[\text{Cu(II)}]_{\text{T}} = 3.15 \times 10^{-7} \text{ mol.L}^{-1}$ ,  $[\text{Mg(II)}]_{\text{T}} = 8.0 \times 10^{-4} \text{ mol.L}^{-1}$ ,  $[\text{Ca(II)}]_{\text{T}} = 1.6 \times 10^{-3} \text{ mol.L}^{-1}$ ,  $[\text{Zn(II)}]_{\text{T}} = 1.54 \times 10^{-6} \text{ mol.L}^{-1}$ ,  $[\text{Mn(II)}]_{\text{T}} = 4.36 \times 10^{-6} \text{ mol.L}^{-1}$ ). The concentration of ligand was calculated to be 10% in excess of the Fe(III) concentration. Thus, a DPH concentration of  $1.65 \times 10^{-4} \text{ mol.L}^{-1}$  (Figure 3.14) was used in order to satisfy the stoichiometry of the dinuclear  $\text{Fe}_2\text{L}_3$  species, to ensure total iron complexation;  $\text{Fe(OH)}_3(\text{s})$  equilibrium was also introduced as a solubility controller (Table 3.1). For comparative purposes, SDD was also generated for *o,o*-EDDHA (Figure 3.15) in nutrient solution assuming a  $[\text{L}_{\text{T}}]:[\text{Fe}_{\text{T}}]$  ratio of 1.1 ( $[\text{EDDHA}] = 1.1 \times 10^{-4} \text{ mol.L}^{-1}$ ) and the stability constants described in table 3.2 as well as the  $\text{Fe(OH)}_3(\text{s})$  equilibrium (Table 3.1).

Because  $\text{Mn(II)}-(\text{o,o-EDDHA})$  and  $\text{Zn(II)}-(\text{o,o-EDDHA})$  chelates do not form in the presence of Fe(III) (Yunta, et al., 2003), the equilibria between *o,o*-EDDHA and Mn(II) or Zn(II) were not considered.

The analysis of SDDs for EDDHA (Figures 3.15) reveals that, even though a minor complexation between EDDHA and Ca(II) and Mg(II) is predicted in the pH of interest (between pH 7.5 and 8.5) (Figure 3.15A), this fact does not disturb the efficacy of EDDHA for iron complexation (Figure 3.15B) for the  $[\text{L}_{\text{T}}]:[\text{Fe}_{\text{T}}]$  ratio evaluated. On the other hand, SDDs for DPH (Figures 3.14) evidence no appreciable complexation



between Ca(II) and Mg(II) and DPH and Fe(III)-DPH species predominate throughout the agronomic pH range.

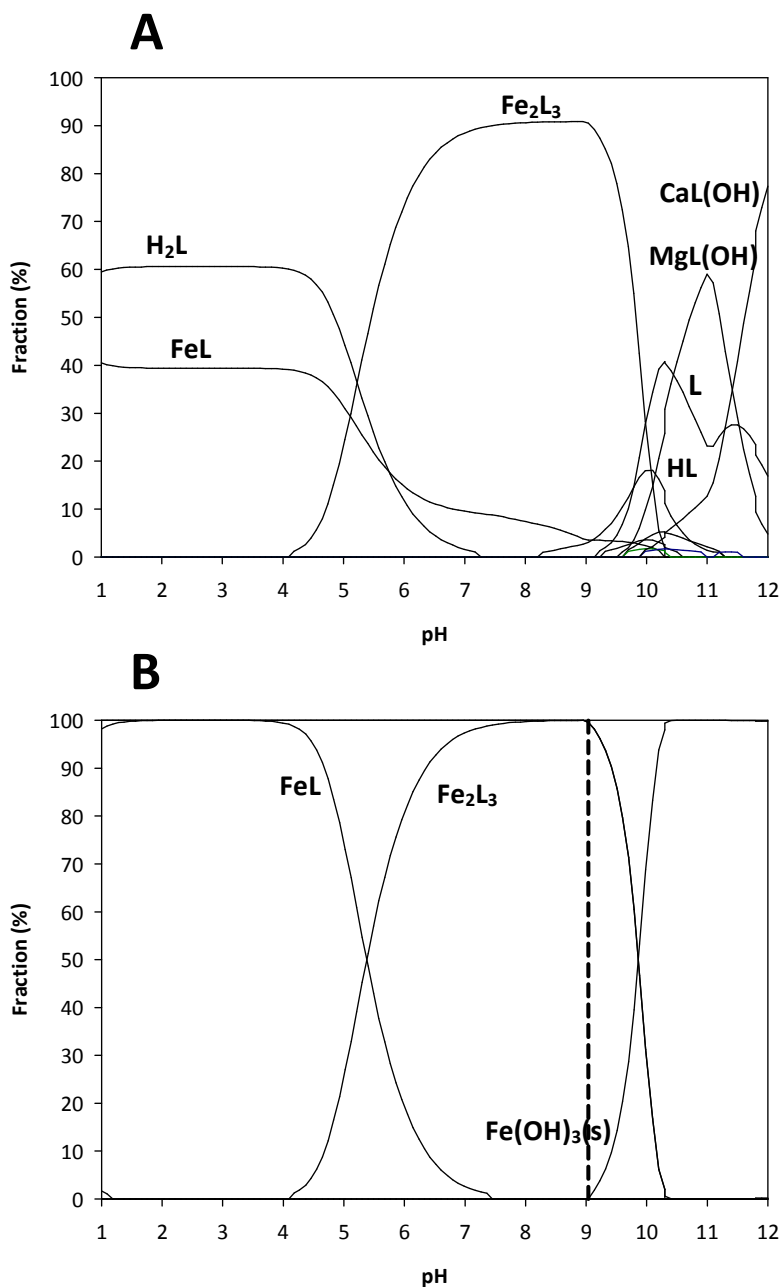


**Figure 3.14** Species distribution diagram of the DPH system in Hoagland nutrient solution (for detailed information about the composition of the solution see text):  $[L]=1.65 \times 10^{-4} \text{ mol.L}^{-1}$ ;  $[Fe^{3+}]=1.0 \times 10^{-4} \text{ mol.L}^{-1}$ . % is the percentage of species present, **(A)** with total ligand concentration set at 100%, or **(B)** with total Fe(III) concentration set at 100%; the dashed vertical line indicates  $Fe(OH)_3$  precipitation.

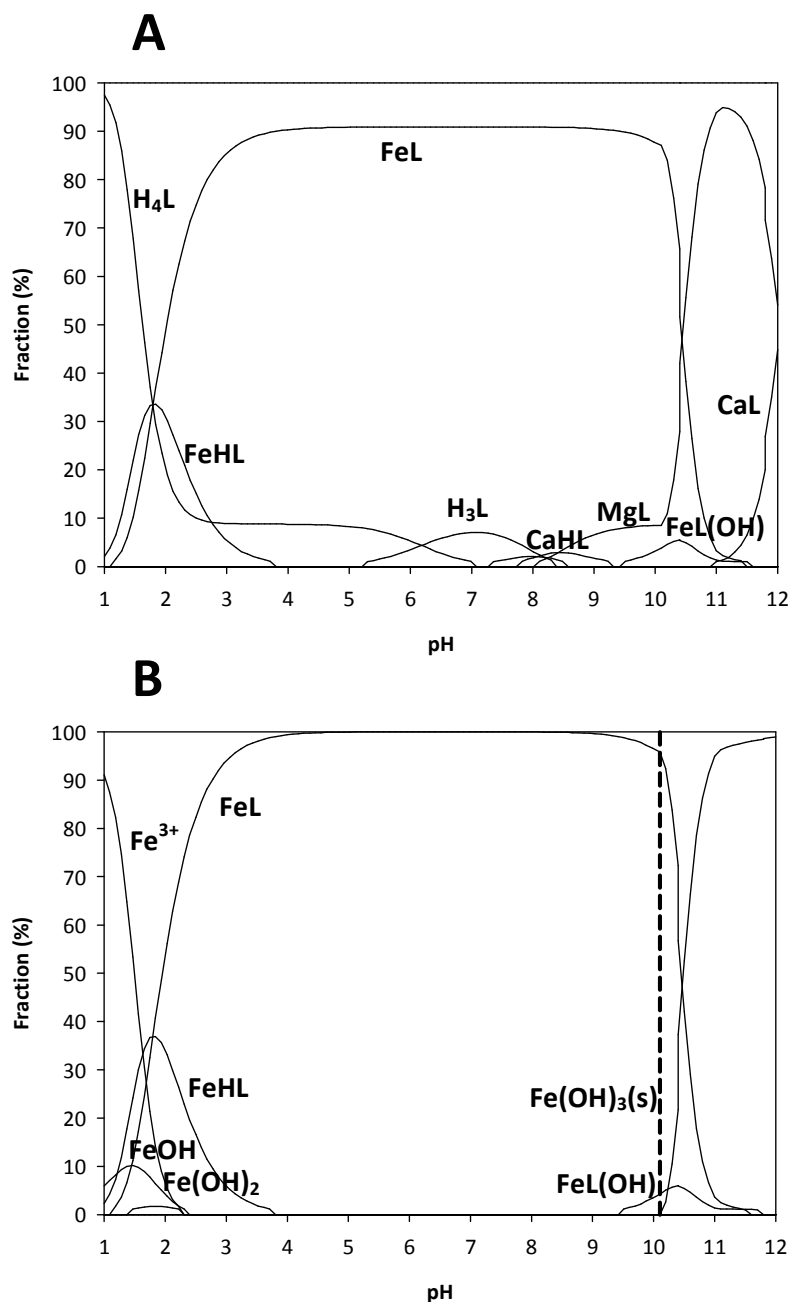


**Figure 3.15** Species distribution diagram of the *o,o*-EDDHA system in Hoagland nutrient solution (for detailed information about the composition of the solution see text):  $[L]=1.1 \times 10^{-4} \text{ mol.L}^{-1}$ ;  $[Fe^{3+}]=1.0 \times 10^{-4} \text{ mol.L}^{-1}$ . % is the percentage of species present (A) with total ligand concentration set at 100%, or (B) with total Fe(III) concentration set at 100%; the dashed vertical line indicates  $Fe(OH)_3$  precipitation.

These results suggest that DPH is more specific for Fe(III), under these conditions, than EDDHA. SDD also reveals that iron is chelated to *o,o*-EDDHA in a slightly wider pH range than DPH. Ca(II) and Mg(II) ions are present in Hoagland nutrient solution at greater quantity than Fe(III) and thus they can compete with Fe(III) for complexation sites. Because these ions form less stable complexes with DPH than Fe(III), both metals complex DPH at a higher pH range (pH >10), leaving iron(III) totally complexed with DPH up to pH 9.5. These results suggest that DPH fulfills the chelating properties to maintain iron in a soluble form over the agronomic pH range. Since DPH is a biological and physicochemical model of the natural siderophore, rhodotorulic acid, it can be considered a more environmental friendly alternative as iron fertilizer for chlorosis treatment.

### 3.4 References

Barclay, S. J.; Huynh, B. H.; Raymond, K. N., Coordination Chemistry of Microbial Iron Transport Compounds .27. Dimeric Iron(III) Complexes of Dihydroxamate Analogs of Rhodotorulic Acid. *Inorganic Chemistry* **1984a**, 23 (14), 2011-2018.

Barclay, S. J.; Riley, P. E.; Raymond, K. N., Coordination Chemistry of Microbial Iron Transport Compounds .26. Dimeric Dialkoxo-Bridged Iron(III) Complexes of Linear Dihydroxamate Ligands. *Inorganic Chemistry* **1984b**, 23 (14), 2005-2010.

Farkas, E.; Kozma, E.; Petho, M.; Herlihy, K. M.; Micera, C., Equilibrium Studies on Copper(II)- and Iron(III)-Monohydroxamates. *Polyhedron* **1998**, 17 (19), 3331-3342.

Farkas, E.; Enyedy, E. A.; Csoka, H., A Comparison between the Chelating Properties of Some Dihydroxamic Acids, Desferrioxamine B and Acetohydroxamic Acid. *Polyhedron* **1999**, 18 (18), 2391-2398.

Farkas, E.; Batka, D.; Pataki, Z.; Buglyo, P.; Santos, M. A., Interaction of Desferrioxamine B (DFB) Model Dihydroxamic Acids with Some Essential and Toxic Metal(II) Ions: Effects of the Structure and Length of Connecting Chains on the Metal Ion Selectivity. *Dalton Transactions* **2004**, (8), 1248-1253.

Loper, J. E.; Buyer, J. S., Siderophores in Microbial Interactions on Plant-Surfaces. *Mol. Plant-Microbe Interact.* **1991**, 4 (1), 5-13.

Lucena, J. J.; Garate, A.; Villen, M., Stability in Solution and Reactivity with Soils and Soil Components of Iron and Zinc Complexes. *J. Plant Nutr. Soil Sci.* **2010**, 173 (6), 900-906.

Martell, A. E.; Smith, R. M., *Nist Standard Reference Database 46 Version 8.0, Nist Critically Selected Stability Constants of Metal Complexes Database*. US Department of Commerce: National Institute of Standards and Technology, **2004**.

May, P. M.; Murray, K.; Williams, D. R., The Use of Glass Electrodes for the Determination of Formation Constants - II. Simulation of Titration Data. *Talanta* **1985**, 32 (6), 483-489.

May, P. M.; Murray, K.; Williams, D. R., The Use of Glass Electrodes for the Determination of Formation Constants - III. Optimization of Titration Data: The Esta Library of Computer Programs. *Talanta* **1988**, 35 (11), 825-830.

Schecher, W. D.; McAvoy, D. C. *Minql+, a Chemical Equilibrium Modeling System Version 4.5 for Windows*, Environmental Research Software, Hallowell: Maine, **2003**.

Siebner-Freibach, H.; Hadar, Y.; Yariv, S.; Lapidés, I.; Chen, Y., Thermos Pectroscopic Study of the Adsorption Mechanism of the Hydroxamic Siderophore Ferrioxamine B by Calcium Montmorillonite. *Journal of Agricultural and Food Chemistry* **2006**, 54 (4), 1399-1408.

Smith, W. L.; Raymond, K. N., Synthesis of Aliphatic Dimeric N-Isopropylhydroxamic Acids and the Crystal and Molecular-Structure of N,N'-Dihydroxy-N,N'-Diisopropylhexanediamide - Hydroxamic Acid in the Trans Conformation. *Journal of the American Chemical Society* **1980**, 102 (4), 1252-1255.

Szabo, O.; Farkas, E., Characterization of Mn(II) and Mn(III) Binding Capability of Natural Siderophores Desferrioxamine B and Desferricoprogen as Well as Model Hydroxamic Acids. *Inorganica Chimica Acta* **2011**, 376 (1), 500-508.

Yunta, F.; Garcia-Marco, S.; Lucena, J. J., Theoretical Speciation of Ethylenediamine-N-(o-Hydroxyphenylacetic)-N'-(p-Hydroxyphenylacetic) Acid (o,p-EDDHA) in Agronomic Conditions. *Journal of Agricultural and Food Chemistry* **2003**, 51 (18), 5391-5399.



## Chapter 4

---

The siderophore Azotochelin,  
and the siderophore mimic N,N'-Dihydroxy-N,N'-  
diisopropylhexanediamide as a Fe source to  
cucumber plants in hydroponic cultures





**The siderophore Azotochelin, and the siderophore mimic  
N,N'-Dihydroxy-N,N'-diisopropylhexanediamide as a Fe source to  
cucumber plants in hydroponic cultures\***

**Abstract**

Environmental concerns related to the use of synthetic iron chelates, usually non-biodegradable, for overcoming iron chlorosis motivates the search for alternatives compounds.

In view of more environmental friendly practices, the siderophore, azotochelin, and the siderophore mimic, DPH, were evaluated as potential sources of iron to cucumber plants grown in hydroponic cultures. The behavior of the iron chelates of azotochelin and DPH, as a substrate of ferric chelate reductase (FCR) and the ability as iron suppliers for chlorotic plants was studied and compared with *o,o*-EDDHA/Fe<sup>3+</sup> and EDTA/Fe<sup>3+</sup> chelates, traditionally used for these purposes. Both azotochelin/Fe<sup>3+</sup> and DPH/Fe<sup>3+</sup> chelates were effective in supplying iron to cucumber plants growing hydroponically.

---

\*The siderophore azotochelin, and the siderophore mimic N,N'-Dihydroxy-N,N'-diisopropylhexanediamide as a Fe source to cucumber plants in hydroponic cultures (Submitted for publication).

## 4.1 Introduction

The application of iron chelates is the most efficient remedy to overcome and control iron chlorosis, a common and complex nutritional disorder that affects plants growing with insufficient quantities of available iron. Most of those chelates are expensive and recently some environmental concerns about the environmental fate of the current nondegradable synthetic chelates raised.

Moreover, the risk of leaching out of the root zone in regimes of high water availability of highly efficient chelates, such as *o,o*-EDDHA/Fe<sup>3+</sup> (Figure 1.3 section 1.1.2) constitutes also an important constrain when synthetic chelates are applied to soils (Rodriguez-Lucena, et al., 2010). EDTA (Figure 1.2, section 1.1.1) is also used as a ligand for iron fertilization; due to the low stability of the EDTA/Fe<sup>3+</sup> chelate, it is used in hydroponics, fertigation, or other fertilization practices, where a thorough interaction between the chelate in high-pH soils is avoided. Besides the ability to maintain iron in the soil solution, the efficacy of an iron chelate depends on the ability of plant roots to take up iron (Villen, et al., 2007).

Siderophores (section 1.3) are a class of biogenic ligands that have evolved in nature to bind selectively to iron, and are traditionally associated with the mobilization and uptake of iron(III) (Crumbliss and Harrington, 2009; Harrington, et al., 2012). The use of natural compounds, as bio-fertilizers, can be a more environmental-friendly alternative to the synthetic chelates in use.

DPH (Figure 3.1, section 3.1), like rhodotorulic acid, was also found to form very stable dimeric iron(III) complexes, with Fe<sup>3+</sup>:L ratio of 2:3, containing pseudooctahedraltris(hydroxamate)iron(III) centers. In solution, besides the formation of this Fe<sub>2</sub>L<sub>3</sub> complex (log β=62.2), DPH also forms the 1:1 species [FeL] (log β=22.3) (Barclay, et al., 1984).

N, N'-2,6-bis(2,3-dihydroxybenzoyl)-L- lysine, usually named as azotochelin (Figure 4.1), is a bis(catecholamide) siderophore produced by the nitrogen-fixing soil bacterium *Azotobacter vinelandii* (Bellenger, et al., 2007). The high efficiency of azotochelin as iron chelator has already been reported (Duhme, et al., 1996; Duhme, et al., 1997; Cornish and Page, 1998).

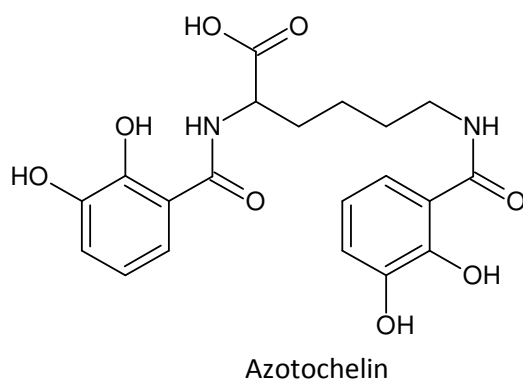


**Figure 4.1** Structure of N, N'-2,6-Bis(2,3-dihydroxybenzoyl)-L-lysine (azotochelin).

It is well known that Fe deficiency stimulates the exudation of organic compounds, including phenolic compounds, that already showed to play an important role, although still unclear, in the Fe mobilization from the rizosphere for utilization by plants (Fourcroy, et al., 2014; Schmid, et al., 2014). Recently, Schmid et al. (2014) observed the release, by Fe deficient plants, of coumarins that, once in the rizosphere may undergo modifications to become effective  $\text{Fe}^{3+}$  chelators, such as esculetin, a simple coumarine containing two adjacent hydroxyl groups in the 5'- and 6'- position of the benzene ring. Although the contribution of esculetin in the  $\text{Fe}^{3+}$  mobilization capacity of root exudates was not quantified, these observations evidence the importance of the catechol-type compounds, such as azotochelin, in plant nutrition.

These facts altogether point out that DPH and azotochelin can be used as potential iron chelating agents. Thus, in this chapter, the efficacy of the iron chelates of azotochelin and DPH to provide iron to cucumber (*Cucumis sativus*) (iron-efficient) plants in hydroponic cultures is studied. Because the reduction of iron(III) to iron(II) is an essential step for iron uptake by dicotyledonous plants, the ability of iron chelates of azotochelin or iron chelates of DPH, to act as substrates in enzymatic reduction, at pH 7.5, was also evaluated. In both experiments, the results were compared with the iron chelates of *o,o*-EDDHA and EDTA.

## 4.2 Materials and Methods

All chemicals were of analytical grade. The chelating agents, *o,o*-EDDHA, 94,49% (LGC Standards),  $\text{Na}_2\text{H}_2\text{EDTA}$  99% (86% as free acid) (Titriplex III, Merck), were purchased from the market. The titrimetric purity of *o,o*-EDDHA, expressed with respect to the acidic form, was determined as described in Yunta et al. (2003b).

Azotochelin, as well as DPH, as it was already mentioned in section 3.2, were synthesized by the research group headed by Professor Maria Teresa Barros, REQUIMTE, Faculdade de Ciências e Tecnologia, Universidade Nova de Lisboa. Azotochelin was synthesized based on the literature procedure (Leydier et al., 2008).

### 4.2.1 Preparation of Iron chelates

For the preparation of the Fe chelate solutions used in the hydroponic experiments (Figure 4.2), the amount of iron added was 5% in excess than the calculated in order to ensure a complete metalation of the ligand.

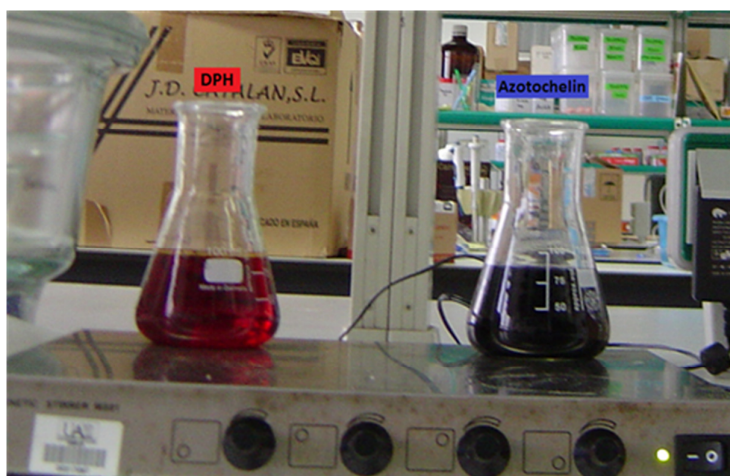


**Figure 4.2.** Fe chelate solutions formed with DPH and azotochelin, at pH 7.5.

For reductase experiments, 5% excess of ligand was used to ensure total metal complexation. The calculated amount of  $\text{Fe}(\text{NO})_3$  solution was added slowly to a solution of the ligand, previously dissolved in sufficient NaOH. The formation of 3:2 ligand to metal complexes was considered for the iron chelation with DPH (Barclay, et al., 1984) or with azotochelin (Duhme, et al., 1996; Cornish and Page, 1998). For EDTA and *o,o*-EDDHA the formation of 1:1 complexes was considered.

During the chelation, the pH was maintained between 6.0 and 8.0. At the end, the pH was adjusted to 7.5 for azotochelin/ $\text{Fe}^{3+}$  and DPH/ $\text{Fe}^{3+}$ , 7.0 for *o,o*-EDDHA/ $\text{Fe}^{3+}$  and 6.5 for EDTA/ $\text{Fe}^{3+}$ . Solutions were left to stand overnight to allow the precipitation of Fe in excess as (hydr)oxides. In the case of azotochelin/ $\text{Fe}^{3+}$  chelate, the solutions were stirred for 62h and then left to stand overnight. Final solutions were filtered through a 0.45- $\mu\text{m}$  cellulose membrane (Millipore) and made up to volume to obtain the desired concentration with type I water (electrical conductivity max:  $0.056 \mu\text{S} \cdot \text{cm}^{-1}$  at  $25^\circ\text{C}$ ; total organic C max:  $100 \mu\text{g} \cdot \text{L}^{-1}$ ;  $\text{Na}^+$  max:  $1 \mu\text{g} \cdot \text{L}^{-1}$ ;  $\text{Cl}^-$  max:  $1 \mu\text{g} \cdot \text{L}^{-1}$ ; total Si max:  $3 \mu\text{g} \cdot \text{L}^{-1}$ ). In order to prevent chelate photodecomposition, light exposure was avoided during preparation and storage of chelate solutions.

#### 4.2.2 Effect of pH on the stability of azotochelin/ $\text{Fe}^{3+}$ chelates, in $\text{Ca}^{2+}$ solutions

50 mL solutions of azotochelin/ $\text{Fe}^{3+}$  ( $[\text{Fe}] = 1.5 \times 10^{-4} \text{ mol} \cdot \text{L}^{-1}$ ), and  $\text{CaCl}_2$ ,  $1.6 \times 10^{-3} \text{ mol} \cdot \text{L}^{-1}$  were prepared in 100 mL plastic vessels, from a stock solution of the chelate prepared as described in section 4.2.1, using, 10% excess of ligand. The pH of each solution, between pH=4 and 10 was adjusted with HCl or NaOH solutions, as needed. Each solution was also buffered using a proper buffer (MES, HEPES or CAPSO), depending on the pH.

The samples were shaken at  $25^\circ\text{C}$  for 3 and 7 days and 56 rpm. At the end of this period, the pH of the solutions was measured using a Crison MicropH 2002 meter and a Crison 52 09 pH combined electrode, and the total soluble iron was determined by atomic absorption spectrometry with flame atomization (AAS-FA) using a Perkin-Elmer Analyst AA400 spectrophotometer. Two replicates per pH were performed.

### 4.2.3 Azotochelin/ $\text{Fe}^{3+}$ and DPH/ $\text{Fe}^{3+}$ as substrate for FCR activity in stressed cucumber plants

Cucumber seeds (*Cucumis sativus* L. cv. Ashley) were germinated using a standard seed-growing procedure in sterilized trays (Garcia-Marco, et al., 2006). The seeds were washed with water for 30 min and then placed in trays between two sheets of cellulose paper moistened with distilled water (Figure 4.3 A, B). The trays were kept in darkness at 28 °C for 4 days in a thermostated incubator.

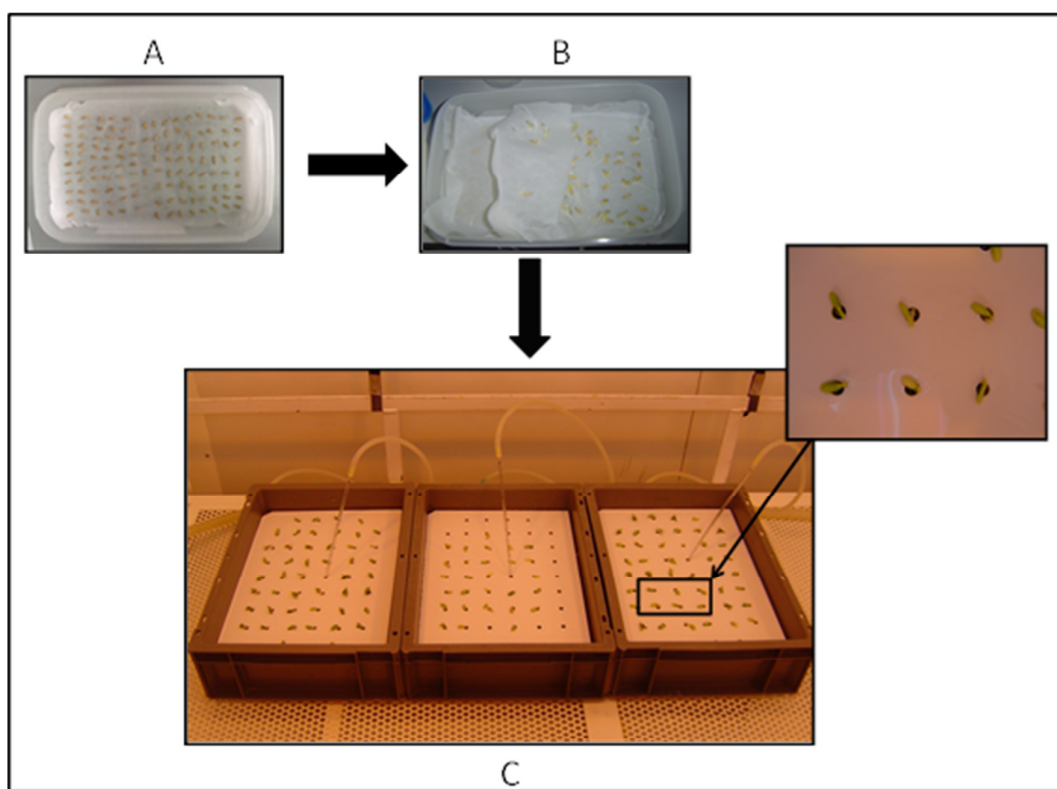


**Figure 4.3** Germination of cucumber seeds (*Cucumis sativus* L. cv. Ashley) (A, B). Seedlings in holed plates (C).

After germination (Figure 4.3B), seedlings were placed on a holed plate, floating in containers with a continuously aerated EDTA buffered (100  $\mu\text{M}$  excess) nutrient solution (Figure 4.3 C) with the following composition: macronutrients (mM) – 1.0  $\text{Ca}(\text{NO}_3)_2$ , 0.9  $\text{KNO}_3$ , 0.3  $\text{MgSO}_4$ , 0.1  $\text{KH}_2\text{PO}_4$ ; cationic micronutrients ( $\mu\text{M}$ ) – 5.0 HBED/ $\text{Fe}^{3+}$ , 2.5  $\text{MnSO}_4$ , 1.0  $\text{CuSO}_4$ , 10  $\text{ZnSO}_4$ , 1.0  $\text{CoSO}_4$ , 1.0  $\text{NiCl}_2$ , 115.5  $\text{EDTANa}_2$ ;

anionic micronutrients ( $\mu\text{M}$ ) – 35 NaCl, 10  $\text{H}_3\text{BO}_3$ , 0.05  $\text{Na}_2\text{MoO}_4$ ; and 0.1 mM HEPES as pH buffer.

The pH of the solution was adjusted to 7.5 with KOH 1M. Plants were grown in this nutrient solution for 6 days in a Dycometal-type CCKF 0/16985 growth chamber, where they were grown under controlled climatic conditions: day/night photoperiod, 16/8 h; temperature (day/night) 30/25 °C; relative humidity (RH) (day/night) 50/70%. The amount of Fe added ( $5\mu\text{M}$ ) was found by Lucena and Chaney (2006) to be the most adequate to produce green but stressed cucumber plants.

Then, uniform seedlings were selected and the stems of two individual plants were wrapped together with polyurethane foam and placed in a 12-L polypropylene bucket (12 pairs of plants per bucket) (Figure 4.4A) in a continuously aerated EDTA buffered nutrient solution, with the same composition as described above, but the amount of  $\text{Fe}^{3+}$  added was replaced by HBED/ $\text{Fe}^{3+}$   $2\mu\text{M}$ . The pH was buffered at 7.5 with HEPES 0,1 mM, and 2.4g  $\text{CaCO}_3$  per pot were added to simulate the conditions of calcareous soils. After 3 days, the plants were used for the reductase assay.

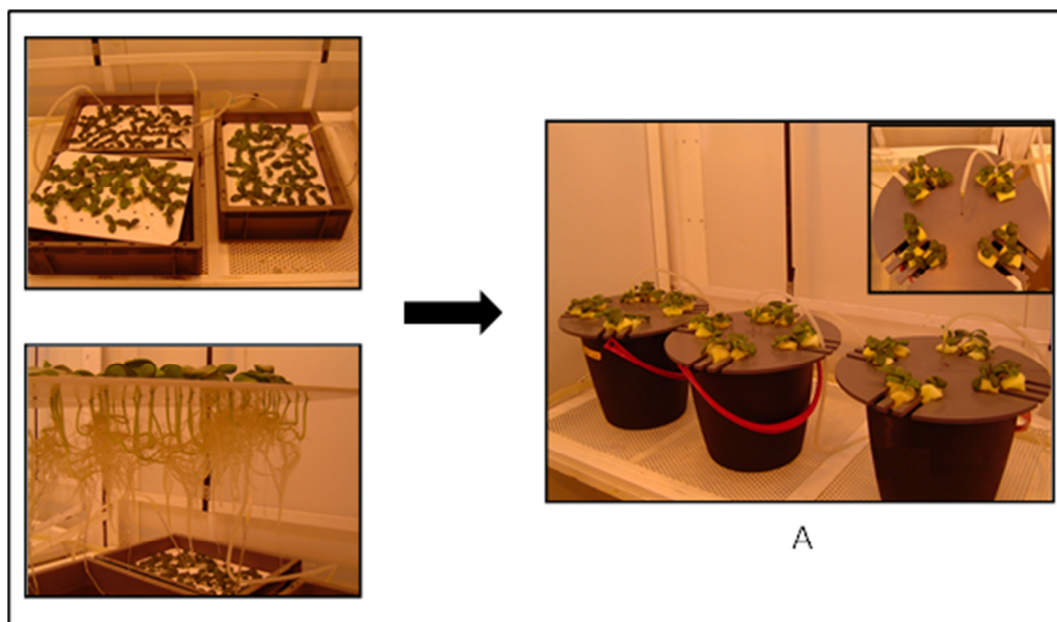


**Figure 4.4** Cucumber plants growing in 12-L polypropylene bucket (12 pairs of plants per bucket) (A).

The FCR activity measurement was made in accordance with Lucena and Chaney (2006) at pH 7.5. The experiment was initiated within the following 2 h after the day-light period. A bunch of two plants was transplanted into 200 mL assay solution (Figure 4.5) containing  $\text{Na}_2\text{BPDS}$  (300  $\mu\text{M}$ ), and 5 mL of the corresponding treatment solution ( $o,o$ -EDDHA/ $\text{Fe}^{3+}$ , EDTA/ $\text{Fe}^{3+}$ , azotochelin/ $\text{Fe}^{3+}$ , DPH/ $\text{Fe}^{3+}$ ) was added (time 0) so that the final concentration of iron was 100  $\mu\text{M}$ . For each treatment, six replicates were arranged. In addition, 2 blank replicates, per chelate, consisting of solutions without plants were included in order to correct reduction rates for slow photoreduction. Aliquots of 3 mL were sampled at 0, 10, 20, 60 and 120 min, and the fresh weight of the roots was quantified at the end of the experiment.

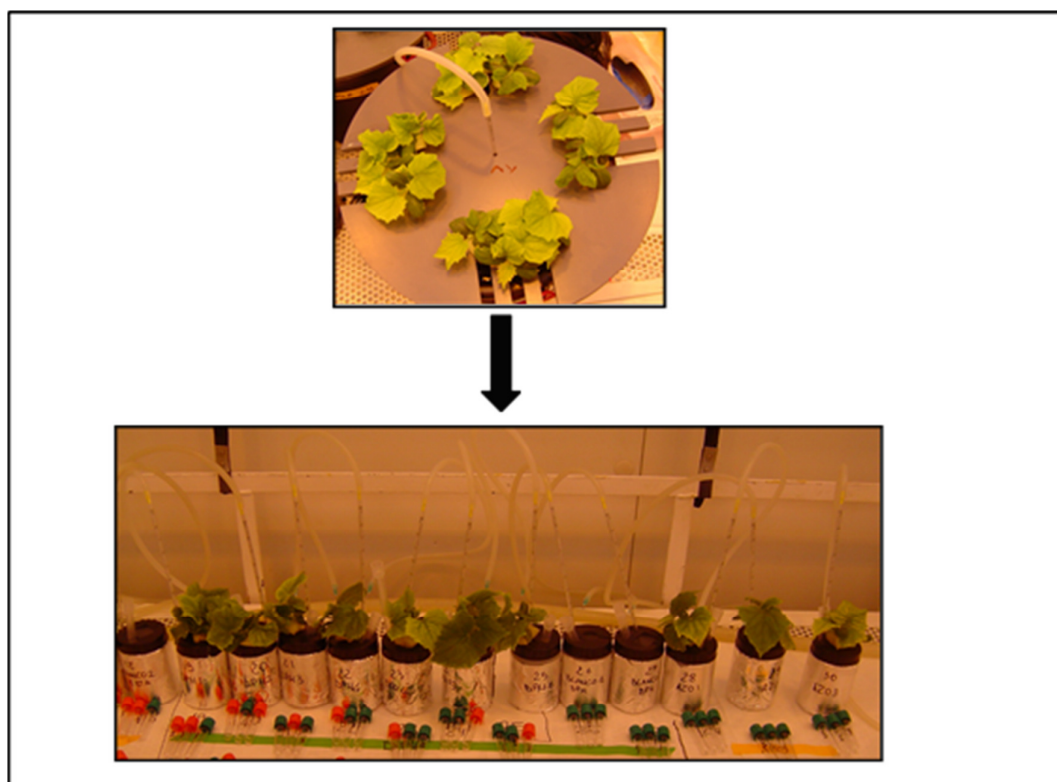


**Figure 4.5** Reductase assay.

The  $(\text{BPDS})_3/\text{Fe}^{2+}$  concentration was calculated as in Lucena and Chaney (2006) by determining the absorbance, using a JASCO V-650 UV-Vis spectrophotometer (JASCO Corporation, Tokyo, Japan), at 535 nm [maximum absorbance of the  $(\text{BPDS})_3/\text{Fe}^{2+}$  complex] and at 480 nm, 375 nm and 630nm for the treatments with  $o,o$ -



EDDHA/Fe<sup>3+</sup>, DPH/Fe<sup>3+</sup> and azotochelin/Fe<sup>3+</sup>, respectively, to consider the contribution of the applied treatments on the total absorbance. The concentration of each chelate was calculated by solving the two-equation system, exemplified below for the case of *o,o*-EDDHA/Fe<sup>3+</sup>.

$$A_{535} = a_{\text{FeBPDS}535} \times [\text{Fe}(\text{BPDS})_3] + a_{\text{o,oEDDHA/Fe}535} \times [\text{o,oEDDHA/Fe}] \quad (4.1)$$

$$A_{480} = a_{\text{FeBPDS}480} \times [\text{Fe}(\text{BPDS})_3] + a_{\text{o,oEDDHA/Fe}480} \times [\text{o,oEDDHA/Fe}] \quad (4.2)$$

where  $A_{535}$  and  $A_{480}$  are the absorbance measured for each sample at 535 and 480 nm, respectively;  $\alpha_{\text{FeBPDS}535}$ ,  $\alpha_{\text{FeBPDS}480}$ ,  $\alpha_{\text{o,oEDDHA/Fe}535}$  and  $\alpha_{\text{o,oEDDHA/Fe}480}$  are the molar absorption coefficients in the experimental conditions, and  $[\text{Fe}(\text{BPDS})_3]$  and  $[\text{o,oEDDHA/Fe}]$  are the concentration of the chelates.

The slope of the plots of produced Fe(II) [ $\mu\text{mol.g}^{-1}$  fresh root against time (h)] was used as the Fe(III) reduction rate for each pair of plants. Data was expressed as the mean reduction rates, including the standard deviation corresponding to 6 plants replicates per treatment.

#### 4.2.4 Efficacy of azotochelin/Fe<sup>3+</sup> and DPH/Fe<sup>3+</sup> to provide Fe to cucumber plants in hydroponic culture.

Cucumber seeds (*Cucumis sativus* L. cv. Ashley) were germinated using the same procedure as for reductase assays (section 4.2.3). After germination, seedlings of similar development were placed on a holed plate, floating in containers with a continuously aerated nutrient solution with the same composition as in the FCR assays, but 1/5 diluted, for 6 days, in the growth chamber, where they were grown under controlled climatic conditions: day/night photoperiod, 16/8 h; temperature (day/night), 28/20 °C; relative humidity (RH) (day/night) 40/60%.

After this time, the stems of two plants were wrapped together with foam, and placed in 2 L polyethylene vessels [three holes in the lid, six plants (3 pairs) per pot] containing 2 L of a continuously aerated full strength nutrient solution with the same

composition as in the reductase experiment (Figure 4.6A). Iron was not added to this nutrient solution. The pH was adjusted to 7.5 with KOH 1.0 mol.L<sup>-1</sup> and buffered with HEPES 0.1 mM, and 0.4 g of solid CaCO<sub>3</sub> per pot. The 2 L pots were covered with black plastic to avoid light exposure.

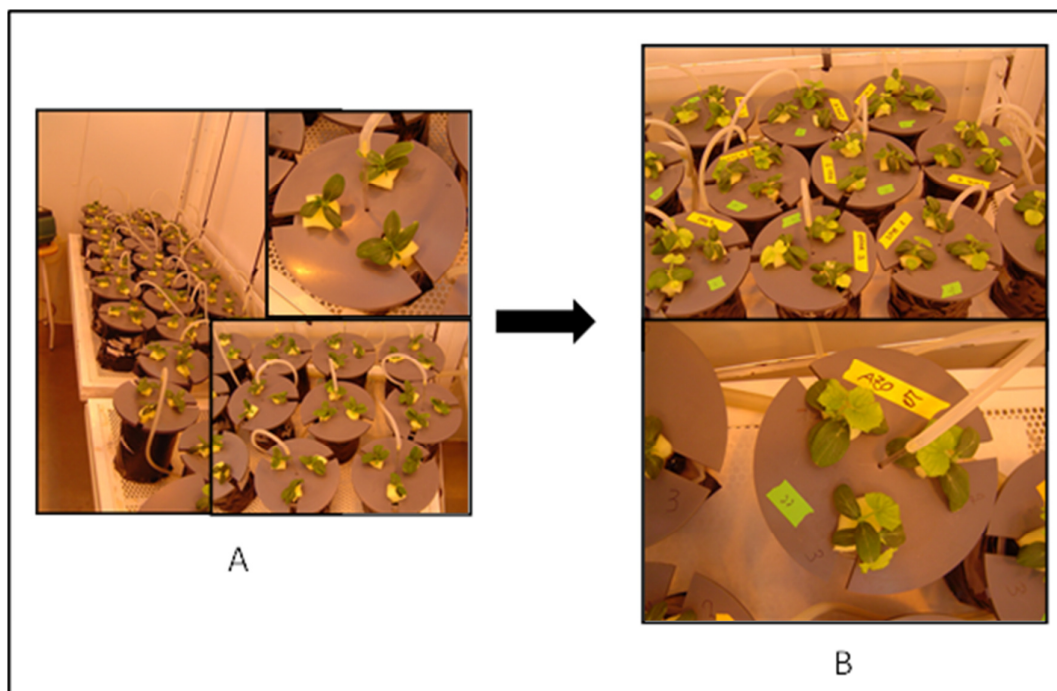


**Figure 4.6** Cucumber plants grown in hydroponic culture (**A;B**), showing visible symptoms of iron deficiency at the time of application of the treatments (0 DAT) (**B**)

Plants were grown under these conditions until symptoms of iron deficiency were observed (6 days), when treatments were applied (Figure 4.6B). The treatments with the iron (10  $\mu$ M) chelates of *o,o*-EDDHA, EDTA<sup>3+</sup>, DPH and azotochelin, respectively, as sources of iron were replicated five times in a completely randomized design, as well as the control containing 2 $\mu$ M HBED/Fe<sup>3+</sup> (3 replicates). The growth chamber conditions were the same as those described above. Water was added every 2 days and the solution renewed weekly. During the experiment, Soil-Plant Analysis Development (SPAD) index readings, with a chlorophyll-meter (Minolta SPAD-502) were taken for all the leaf stages (average of three readings per leaf) at several times. Whole plants were sampled 7 (two pairs of plants) and 21 (one pair of plants) days after application of the treatments. After sampling, plant nutritional status and Fe

redistribution were studied. The sampled roots, stems and leaves were separated, weighed and washed with a 0.01% non-ionic detergent (Tween 80) in 0.1% HCl solution for 30 seconds and rinsed twice with ultrapure water following the procedure of Garcia-Marco *et al.* (2006). Then, samples were dried in a forced air oven at 65° C for 3 days. Fresh and dry weights were determined. After dry digestion in a muffle furnace (480 °C), the ashes were dissolved in 6 M HCl. Micronutrients were determined in roots, stems and leaves. Fe, Mn, Cu were analysed by AAS-FA using a Perkin-Elmer Analyst 800 spectrophotometer.

#### **4.2.5 Statistical Analysis**

Statistical analyses were performed with SPSS statistical software (v.21; SPSS, Chicago, IL, USA). Differences among treatments were determined using a one-way analysis of variance (ANOVA). Significant differences were established at  $p < 0.05$  using the Duncan test.

#### **4.2.6 Computer chemical simulations**

Metal chemical speciation calculations were performed as described in Chapter 3 (section 3.2.2). The pFe values were calculated based on chemical speciation calculations that were executed using MINEQL+ Version 4.5 (Schecher and McAvoy, 2001). Chemical equilibrium concentrations of all species considered in the model by the program reactions were generated based on component stability constants and molar concentrations.

Table 4.1 shows the stability constants for EDTA with metal ions considered in the chemical simulations in the Hoagland nutrient solution.

**Table 4.1** Protonation and overall stability constants (as  $\log \beta$ ) for EDTA complexes formed with Ca(II), Cu(II), Mg(II), Mn(II) and Zn(II) (Martell and Smith, 2004).

Metal ion	Equilibrium	Log $\beta$
<b>Protonation</b>	$L + H \leftrightarrow HL$	10.984
	$L + 2H \leftrightarrow H_2L$	17.221
	$L + 3H \leftrightarrow H_3L$	19.911
	$L + 4H \leftrightarrow H_4L$	21.911
	$L + 5H \leftrightarrow H_5L$	23.411
	$L + 6H \leftrightarrow H_6L$	23.811
<b>Ca(II)</b>	$M + L \leftrightarrow ML$	9.68
	$M + L + H \leftrightarrow MHL$	12.78
<b>Mg(II)</b>	$M + L \leftrightarrow ML$	8.96
	$M + L + H \leftrightarrow MHL$	12.81
<b>Cu(II)</b>	$M + L + H \leftrightarrow MHL$	18.78
	$M + L + 2H \leftrightarrow MH_2L$	23.88
	$M + L + OH \leftrightarrow ML(OH)$	21.06
<b>Zn(II)</b>	$M + L \leftrightarrow ML$	16.5
	$M + L + H \leftrightarrow MHL$	19.5
	$M + L + OH \leftrightarrow ML(OH)$	18.68
<b>Mn(II)</b>	$M + L \leftrightarrow ML$	13.89
	$M + L + H \leftrightarrow MHL$	16.96

### 4.3 Results

#### 4.3.1 Azotochelin/ $\text{Fe}^{3+}$ and DPH/ $\text{Fe}^{3+}$ chelates as substrate for FCR activity in stressed cucumber plants

The ability of the iron chelates of azotochelin, DPH, EDDHA and EDTA to act as substrates in enzymatic reduction was evaluated; Fe-stressed, but still green, cucumber plants (Figure 4.5) were used in these experiments.

The Fe reduction rate ( $\mu\text{mol Fe(II)} \text{ g}^{-1} \text{ fresh root h}^{-1}$ ) using EDTA/ $\text{Fe}^{3+}$ , *o,o*-EDDHA/ $\text{Fe}^{3+}$  and DPH/ $\text{Fe}^{3+}$  chelates is shown in Figure 4.7. For azotochelin/ $\text{Fe}^{3+}$  chelate, it was not possible to determine the reduction rate.

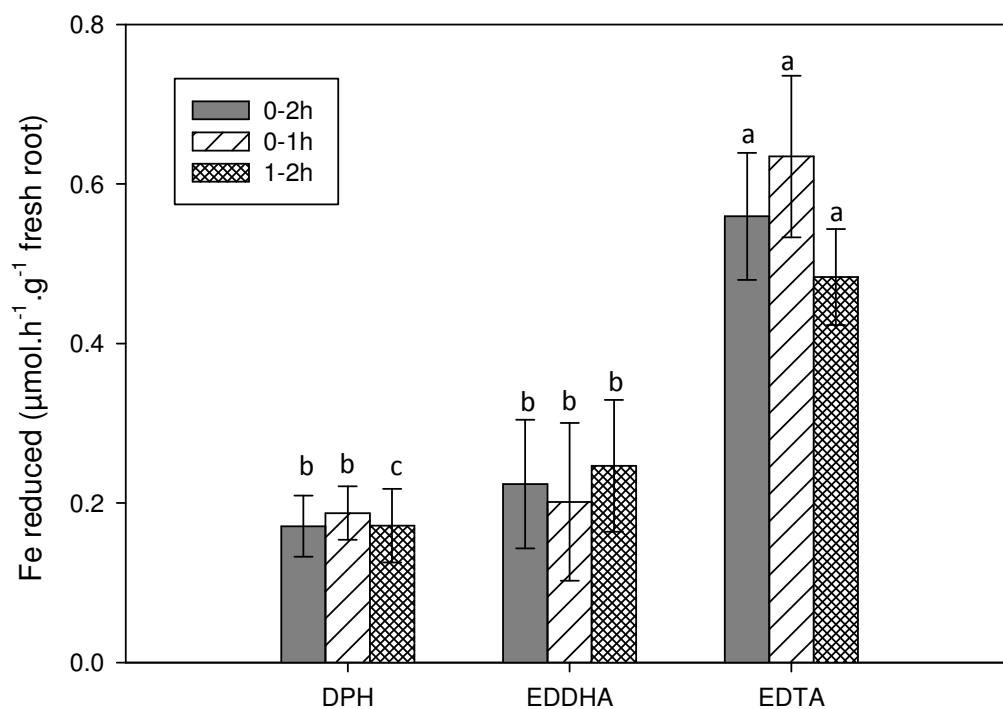


**Figure 4.7** Rate of  $\text{Fe}^{3+}$  reduction from the iron chelates of DPH, EDDHA and EDTA, used for cucumber plants. Error bars represent standard deviations (SD,  $n=6$ ). Different letters in the same period denotes significant differences among treatments for Duncan test ( $p<0.05$ ).

The reduction assays were conducted for 2 h. In the first hour, the reduction rate for EDTA/ $\text{Fe}^{3+}$  chelate was significantly higher than for the other iron chelates; DPH/ $\text{Fe}^{3+}$  chelate showed a similar activity to *o,o*-EDDHA/ $\text{Fe}^{3+}$  chelate. The levels of reductase activity with DPH/ $\text{Fe}^{3+}$  chelate did not suffer significant changes in the second hour.

Figure 4.8A shows the absorbance at both 535 and 630 nm in the FCR test samples (full lines) and in the blanks (dashed lines) for the reduction assay with azotochelin/ $\text{Fe}^{3+}$  chelate. During the first 20 minutes, a proportional decrease of the absorbance at 535 and 630 nm was observed in the FCR test samples. This behavior indicates changes in the azotochelin/ $\text{Fe}^{3+}$  chelate, which absorbs at both wavelengths.

The iron(III) reduction to iron(II) is shown by the variation at 535 nm, after the first 20 minutes of the experiment, due to the formation of the  $\text{Fe}^{2+}$  complex with the colorimetric indicator, BPDS. However, it was not possible to determine the rate of reduction of azotochelin/ $\text{Fe}^{3+}$  chelate due to non-negligible changes observed in the blanks, which would lead to misleading results. In the case of reductase assay with *o,o*-EDDHA/ $\text{Fe}^{3+}$ , DPH/ $\text{Fe}^{3+}$  and EDTA/ $\text{Fe}^{3+}$  (Figures 4.8 B,C and D, respectively), no changes were observed in the blanks, besides the initial variation (dashed lines), observed only in the case of *o,o*-EDDHA/ $\text{Fe}^{3+}$ , that was similar to the initial variation also observed in the FCR experiments (full lines).

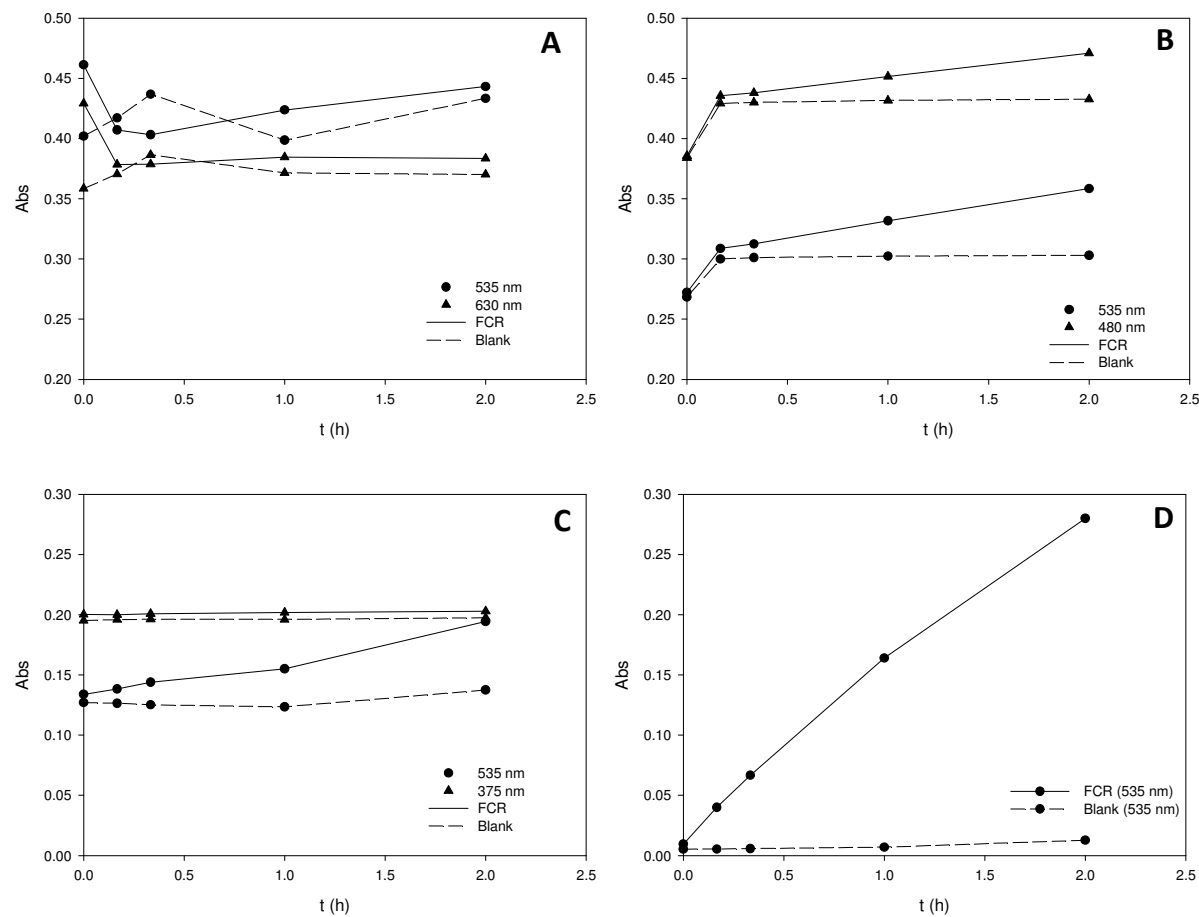


**Figure 4.8** Representative plots of the change of the absorbance over time, measured in the FCR assay with (A) azotochelin/ $\text{Fe}^{3+}$ , at 535 and 630 nm, (B) *o,o*-EDDHA/ $\text{Fe}^{3+}$ , at 535 and 480 nm, (C) DPH/ $\text{Fe}^{3+}$ , at 535 and 375 nm, (D) EDTA/ $\text{Fe}^{3+}$ , at 535 nm, and in blanks, respectively.

### 4.3.2 Efficacy of azotochelin/ $\text{Fe}^{3+}$ and DPH/ $\text{Fe}^{3+}$ chelates to provide iron to cucumber plants in hydroponic culture.

In this experiment, four different Fe ( $10\mu\text{M}$ ) chelate treatments were applied to Fe- efficient cucumber plants with visible chlorotic symptoms (Figure 4.6B). The effect of the iron chelates of azotochelin/ $\text{Fe}^{3+}$ , DPH/ $\text{Fe}^{3+}$ , EDDHA/ $\text{Fe}^{3+}$  and EDTA/ $\text{Fe}^{3+}$  was evaluated and the results were compared with the control ([Fe] limited:  $2\mu\text{M}$  Fe, HBED/ $\text{Fe}^{3+}$ ).

The SPAD index was measured in the following days after the application of the treatments (DAT) to estimate the chlorophyll concentration and recovery during the experiment.

Figure 4.9 shows the time course of the SPAD index, measured in the first leaf level (the first developed after the cotyledons) and Table 4.2 shows the SPAD readings for the most recently developed leaves, formed in different levels, after the application of the treatments.

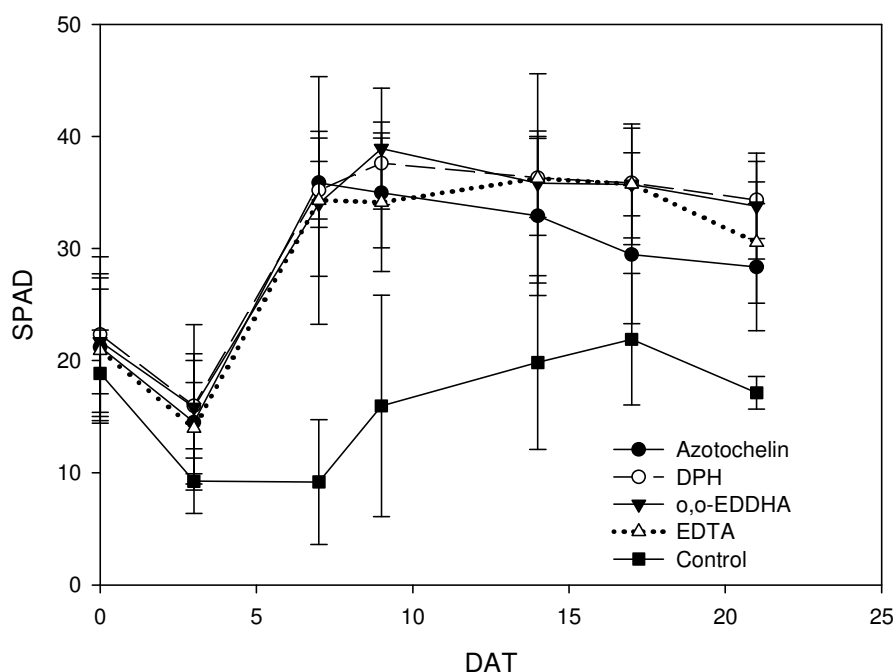


**Figure 4.9** Effect of the different Fe chelate treatments on the SPAD index ( $\pm$  standard deviation;  $n = 5$ ), measured in the first leaf level, of cucumber plants in hydroponic experiments.



After the application of the treatments, all four iron chelates showed significantly higher SPAD values than the control, in all leaf levels, and in all stages of the experiment. These results are in agreement with the visual symptoms of iron deficiency exhibited by the control plants during the experiment. In the leaves of the first level, a marked increase of the SPAD index was observed after the third day of treatment with all chelates (Figure 4.9), while in the control, only a slight increase of the SPAD index was observed after the day 7.

Table 4.2 shows the SPAD index for the most recently developed leaves formed in different levels after the application of the treatments (3 DAT, second level; 7 DAT, third level; 14 DAT, fourth level and 21 DAT on fifth level). At the end of the experiment (21 DAT), the SPAD measured in the upper leaf levels were similar in all the treated plants, with the exception of the fourth leaf level, where SPAD index in the leaves of the plants treated with EDTA/Fe<sup>3+</sup> was slightly higher than the plants treated with azotochelin/Fe<sup>3+</sup> and DPH/Fe<sup>3+</sup>. It must be noted that the leaves in the fifth level were small and were present only in few plants in each treatment.

In both samplings (7 and 21 DAT), the leaf dry weight (Table 4.3) of all treated plants was always greater than the control (HBED/Fe<sup>3+</sup>, 2μM) and followed the same trend than the SPAD index. In the case of root and stem dry weight (Table 4.3), the differences between the control and the treated plants were significant only at the end of the experiment (21 days). Only the stem dry weight of the plants treated with azotochelin/Fe<sup>3+</sup> showed a slightly higher value at DAT 7. Among the treated plants at DAT 21, it was observed that the dry weight of the leaves and stems of the plants treated with azotochelin/Fe<sup>3+</sup> and DPH/Fe<sup>3+</sup> was lower than EDTA/Fe<sup>3+</sup> treatments.

The iron concentration in leaves (μmol.g<sup>-1</sup> DW) and total content of iron in leaves (μmol plant<sup>-1</sup>) (Table 4.4) and the concentrations of Mn and Cu in leaves (Table 4.5) were determined to evaluate the mineral status of the plants. All iron (10μM) chelates tested increased the leaf Fe concentration. In the first sampling (7 DAT), the Fe concentration in leaves was similar in all plants treated with the iron chelates, and higher than in the control (HBED, 2μM).

**Table 4.2** Effect of the different Fe -chelate treatments on the SPAD index ( $\pm$  standard deviation; n = 5 for iron chelates tested and n=3 for control) in most recently developed leaves of cucumber plants formed in different levels after the application of the Fe-chelates treatments in hydroponic experiments.

Treatment	DAT						
	3	7	14	21			
	Level 2	Level 3	Level 4	Level 2	Level 3	Level 4	Level 5
Control	-*	16 $\pm$ 10 b	-*	15 $\pm$ 5 b	15 $\pm$ 5 b	15 $\pm$ 3 c	19 $\pm$ 8 b
Azotochelin	24 $\pm$ 3 a	37 $\pm$ 2 a	39 $\pm$ 4 ns	31 $\pm$ 2 a	31 $\pm$ 5 a	30 $\pm$ 2 b	30 $\pm$ 6 a
DPH	21 $\pm$ 4 a	37 $\pm$ 4 a	-*	33 $\pm$ 3 a	29 $\pm$ 3 a	32 $\pm$ 3 b	28 $\pm$ 3 a
EDDHA	19 $\pm$ 4 ab	37 $\pm$ 3 a	40 $\pm$ 5	35 $\pm$ 4 a	34 $\pm$ 5 a	33 $\pm$ 5 ab	37 $\pm$ 4 a
EDTA	12 $\pm$ 7 b	39 $\pm$ 1 a	39 $\pm$ 2	32 $\pm$ 2 a	31 $\pm$ 5 a	36 $\pm$ 2 a	34 $\pm$ 2 a

Different letters in the same column denotes significant differences among treatments for Duncan test ( $p < 0.05$ ). ns: no significant differences.

\* Not complete leaf development at this level and time.

**Table 4.3** Effect of the different Fe chelate treatments on the dry weight (g;  $\pm$  standard deviation; n = 5 for iron chelates tested and n=3 for control) of leaf, root and stem in cucumber plants grown in hydroponic experiments.

Treatment	Dry weight					
	leaves		roots		stems	
	7 DAT	21 DAT	7 DAT	21 DAT	7 DAT	21 DAT
<b>Control</b>	0.18 $\pm$ 0.05 b	0.53 $\pm$ 0.03 c	0.06 $\pm$ 0.02 ns	0.08 $\pm$ 0.01 b	0.04 $\pm$ 0.01 b	0.08 $\pm$ 0.01 c
<b>Azotochelin</b>	0.33 $\pm$ 0.07 a	1.41 $\pm$ 0.22 b	0.06 $\pm$ 0.02	0.31 $\pm$ 0.05 a	0.06 $\pm$ 0.01 a	0.36 $\pm$ 0.08 b
<b>DPH</b>	0.29 $\pm$ 0.10 a	1.41 $\pm$ 0.28 b	0.06 $\pm$ 0.02	0.29 $\pm$ 0.09 a	0.05 $\pm$ 0.01 ab	0.33 $\pm$ 0.04 b
<b>EDDHA</b>	0.29 $\pm$ 0.09 a	1.69 $\pm$ 0.44 ab	0.06 $\pm$ 0.02	0.31 $\pm$ 0.09 a	0.05 $\pm$ 0.01 b	0.41 $\pm$ 0.08 ab
<b>EDTA</b>	0.28 $\pm$ 0.06 a	1.95 $\pm$ 0.33 a	0.06 $\pm$ 0.02	0.31 $\pm$ 0.10 a	0.05 $\pm$ 0.01 ab	0.45 $\pm$ 0.09 a

Different letters in the same column denotes significant differences among treatments for Duncan test ( $p < 0.05$ ). ns: no significant differences.

The same behavior was observed, at day 21, for EDDHA/Fe<sup>3+</sup>, DPH/Fe<sup>3+</sup> and azotochelin/Fe<sup>3+</sup>, but not for EDTA/Fe<sup>3+</sup> treatments. At this time, the concentration of iron in plants treated with EDTA/Fe<sup>3+</sup> was lower and similar to the control.

**Table 4.4** Effect of the different Fe chelate treatments on the leaf Fe concentration ( $\mu\text{mol.g}^{-1}$  DW;  $\pm$  standard deviation;  $n = 5$  for iron chelates tested and  $n=3$  for control) and Fe content ( $\mu\text{mol plant}^{-1}$ ;  $\pm$  standard deviation;  $n = 5$  for iron chelates and  $n = 3$  for control) in cucumber plants grown in hydroponic experiments.

Treatment	Fe concentration in leaves		Fe content in leaves	
	$(\mu\text{mol g}^{-1} \text{ DW})$		$(\mu\text{mol plant}^{-1} \text{ DW})$	
	7 DAT	21 DAT	7 DAT	21 DAT
<b>Control</b>	$0.47 \pm 0.12 \text{ b}$	$0.97 \pm 0.17 \text{ b}$	$0.17 \pm 0.02 \text{ b}$	$0.51 \pm 0.06 \text{ c}$
<b>Azotochelin</b>	$0.80 \pm 0.04 \text{ a}$	$1.15 \pm 0.11 \text{ a}$	$0.52 \pm 0.10 \text{ a}$	$1.62 \pm 0.24 \text{ b}$
<b>DPH</b>	$0.86 \pm 0.09 \text{ a}$	$1.17 \pm 0.08 \text{ a}$	$0.45 \pm 0.10 \text{ a}$	$1.66 \pm 0.39 \text{ b}$
<b>EDDHA</b>	$0.83 \pm 0.13 \text{ a}$	$1.27 \pm 0.16 \text{ a}$	$0.50 \pm 0.13 \text{ a}$	$2.11 \pm 0.44 \text{ a}$
<b>EDTA</b>	$0.80 \pm 0.12 \text{ a}$	$0.94 \pm 0.11 \text{ b}$	$0.45 \pm 0.05 \text{ a}$	$1.79 \pm 0.10 \text{ a b}$

Different letters in the same column denotes significant differences among treatments for Duncan test ( $p < 0.05$ ).

Nevertheless, the SPAD index readings are in good agreement with the iron concentration measured in leaves. At day 7, all plants treated with the iron chelates showed similar SPAD values and similar iron concentration in leaves. Both parameters were significantly lower in the controls. At day 21, the SPAD index measured in the recent leaves (fifth level) is in straight agreement with the amount of iron measured in the leaves of plants treated with *o,o*-EDDHA/Fe<sup>3+</sup>, DPH/Fe<sup>3+</sup> and azotochelin/Fe<sup>3+</sup>. In the case of EDTA/Fe<sup>3+</sup>, a higher iron concentration in leaves was expected, due to the high SPAD values measured in all leaf levels.

**Table 4.5** Effect of the different Fe chelate treatments on leaf Mn and Cu concentrations ( $\mu\text{mol g}^{-1}$  DW;  $\pm$  standard deviation; n = 5 for iron chelates tested and n=3 for control) and Fe/Mn ratio in cucumber plants grown in hydroponic experiments.

Treatment	Concentration in leaves ( $\mu\text{mol.g}^{-1}$ DW)					
	Mn		Cu		Fe/Mn	
	7 DAT	21 DAT	7 DAT	21 DAT	7 DAT	21 DAT
<b>Control</b>	$3.3 \pm 0.4$ a	$4.4 \pm 0.5$ a	$0.25 \pm 0.02$ a	$0.30 \pm 0.02$ a	$0.15 \pm 0.04$ c	$0.22 \pm 0.04$ d
<b>Azotochelin</b>	$2.5 \pm 0.3$ b	$3.1 \pm 0.2$ b	$0.19 \pm 0.01$ c	$0.19 \pm 0.01$ c	$0.33 \pm 0.03$ ab	$0.37 \pm 0.03$ bc
<b>DPH</b>	$2.6 \pm 0.6$ b	$2.8 \pm 0.5$ b	$0.25 \pm 0.03$ a	$0.22 \pm 0.03$ b	$0.33 \pm 0.03$ ab	$0.43 \pm 0.03$ b
<b>EDDHA</b>	$2.3 \pm 0.4$ b	$1.9 \pm 0.1$ c	$0.18 \pm 0.01$ c	$0.18 \pm 0.03$ c	$0.35 \pm 0.03$ a	$0.64 \pm 0.03$ a
<b>EDTA</b>	$3.2 \pm 0.2$ a	$2.9 \pm 0.3$ b	$0.21 \pm 0.02$ b	$0.21 \pm 0.01$ b	$0.25 \pm 0.03$ b	$0.32 \pm 0.03$ c

Different letters in the same column denotes significant differences among treatments for Duncan test ( $p < 0.05$ ).

The effect of the application of iron chelates on the uptake of other nutrients is evidenced by the higher concentration of Mn and Cu (Table 4.5) measured in the leaves of the untreated plants, especially at day 21. For the treatments with DPH/Fe<sup>3+</sup>, azotochelin/Fe<sup>3+</sup>, EDTA/Fe<sup>3+</sup> and mainly EDDHA/Fe<sup>3+</sup>, the higher Fe concentration lead to lower Mn concentration in leaves.

The Fe/Mn ratio (Table 4.5) has been considered as an index of adequate iron nutrition for several crops mainly those grown in hydroponic conditions (Garcia-Marco, et al., 2006).

An increase of the Fe/Mn ratio implies a recovery from iron chlorosis. The Fe/Mn ratio was higher in the treatment with *o,o*-EDDHA/Fe<sup>3+</sup> than with EDTA/Fe<sup>3+</sup> even in the first sampling time and the highest at 21 DAT. Among the treatments, EDTA/Fe<sup>3+</sup> showed the lowest Fe/Mn ratio but higher than the control. At day 7, the Fe/Mn ratio values obtained for DPH/Fe<sup>3+</sup> and azotochelin/Fe<sup>3+</sup> treatments were similar and comparable to *o,o*-EDDHA/Fe<sup>3+</sup> but much lower than it at day 21.

The iron concentration in the stems (Table 4.6) and roots was also determined. However, due to the impossibility to ensure that the results obtained with the roots correspond to the absorbed iron, and not to iron in the surface of the root, which was not removed during the washings, these results were not considered. In the case of the iron concentration in the stems (Table 4.6), only the plants treated with *o,o*-EDDHA/Fe<sup>3+</sup> showed statistical differences from the other iron chelates, by showing a lower value at DAT 7, and a higher value at the end of the experiment. Surprisingly, the iron concentration in the stems of the plants treated with *o,o*-EDDHA/Fe<sup>3+</sup> was always similar to the controls, while the plants treated with the iron chelates of azotochelin, DPH and EDTA showed higher values than the control plants at DAT 7, but not at DAT 21.

**Table 4.6** Effect of the different Fe chelate treatments on the Fe concentration ( $\mu\text{mol g}^{-1}$  DW;  $\pm$  standard deviation;  $n = 5$  for iron chelates tested and  $n=3$  for control) in the stems at 7 and 21 DAT in cucumber plants grown in hydroponic experiments.

Treatment	Fe concentration in stems ( $\mu\text{mol g}^{-1}$ DW)	
	7 DAT	21 DAT
Control	$0.30 \pm 0.06\text{b}$	$0.54 \pm 0.05\text{ab}$
Azotochelin	$0.68 \pm 0.16\text{a}$	$0.45 \pm 0.05\text{b}$
DPH	$0.81 \pm 0.13\text{a}$	$0.43 \pm 0.05\text{b}$
EDDHA	$0.42 \pm 0.07\text{b}$	$0.72 \pm 0.32\text{a}$
EDTA	$0.74 \pm 0.14\text{a}$	$0.43 \pm 0.12\text{b}$

Different letters in the same column denotes significant differences among treatments for Duncan test ( $p < 0.05$ ).

The pFe values were determined to compare the iron stability of the different chelates used, and the values obtained are shown in Table 4.7.

**Table 4.7** Stability constants (as  $\log \beta$ ) of  $\text{Fe}^{3+}$  with DPH, *o,o*-EDDHA and EDTA and pFe calculated for  $[\text{L}_\text{T}] = 1.0 \times 10^{-5} \text{ mol.L}^{-1}$ ,  $[\text{Fe}_\text{T}] = 1.0 \times 10^{-6} \text{ mol.L}^{-1}$ , at pH 7.5.  $\text{Fe}(\text{OH})_3$  (s) ( $\log \beta = -2.74$ ) (Martell and Smith, 2004) was introduced as precipitation controller.

Ligand	equilibrium	$\log \beta$	pFe (pH=7.5)
DPH	$\text{Fe} + \text{L} \leftrightarrow \text{FeL}$	22.89 <sup>a)</sup>	20.8
	$2\text{Fe} + 3\text{L} \leftrightarrow \text{Fe}_2\text{L}_3$	62.20 <sup>a)</sup>	
<i>o,o</i> -EDDHA	$\text{Fe} + \text{L} \leftrightarrow \text{FeL}$	35.09 <sup>b)</sup>	27.2
	$\text{Fe} + \text{L} + \text{H} \leftrightarrow \text{FeL}$	36.89 <sup>b)</sup>	
	$\text{Fe} + \text{L} \leftrightarrow \text{FeL}(\text{OH}) + \text{H}$	23.66 <sup>b)</sup>	
EDTA	$\text{Fe} + \text{L} \leftrightarrow \text{FeL}$	25.10 <sup>a)</sup>	22.9
	$\text{Fe} + \text{L} + \text{H} \leftrightarrow \text{FeL}$	26.4 <sup>a)</sup>	
	$\text{Fe} + \text{L} \leftrightarrow \text{FeL}(\text{OH}) + \text{H}$	17.71 <sup>a)</sup>	
Azotochelin	-	-	23.1 (pH=7.4) <sup>c)</sup>

<sup>a)</sup> Martell and Smith (2004); <sup>b)</sup> Yunta, et al. (2003c); <sup>c)</sup> Cornish et al. (1988)

## 4.4 Discussion

The objective of this work was to evaluate the efficiency of two stable iron chelates, DPH/ $\text{Fe}^{3+}$  and azotochelin/ $\text{Fe}^{3+}$ , to supply iron to plants and to relate their efficiency to their chemical properties. Under hydroponic conditions, plants treated with DPH/ $\text{Fe}^{3+}$  chelate showed similar SPAD values and iron concentration in leaves as those treated with *o,o*-EDDHA/ $\text{Fe}^{3+}$  chelate (Tables 4.2 and 4.4); these results indicate the same level of recovery of the chlorosis symptoms.

Plants treated with EDTA/ $\text{Fe}^{3+}$  chelate showed at DAT21 lower values of iron concentration in leaves than those treated with EDDHA/ $\text{Fe}^{3+}$  chelate; these differences are in good agreement with published results (Nadal, et al., 2012). However, the SPAD values and the visible recovery observed in plants treated with EDTA (Figure 4.10) suggest that the total iron content ( $\mu\text{mol plant}^{-1}$ ), and not the leaf iron concentration ( $\mu\text{mol.g}^{-1}$  DW) (Table 4.4) is a more adequate parameter for comparing the iron uptake from the different treatments. Plants treated with DPH/ $\text{Fe}^{3+}$  showed a similar iron content than the plants treated with EDTA/ $\text{Fe}^{3+}$  at all sampling times.

The  $\text{pFe}^{3+}$  values express the amount of “free iron” present in equilibrium under particular set of conditions (section 1.3.1). Usually at a total ligand concentration of  $10^{-5}$  M, a total iron concentration of  $10^{-6}$  M, at pH 7.4, the  $\text{pFe}^{3+}$  values are used for a more direct comparison of the iron stability of the different chelates in solution (Zhang, et al., 2009; Hider and Kong, 2010) but also in nutrient solutions, as shown by Yunta et al. (2003b) that demonstrated that  $\text{pFe}^{3+}$  value is a good index to predict the behavior of iron chelates in agronomic pH range. Assuming these total concentrations of ligand and iron ( $10^{-5}$  and  $10^{-6}$  M, respectively), computer chemical simulations were performed to calculate  $\text{pFe}^{3+}$  values, in solution, at pH 7.5 (Table 4.7). The lower  $\text{pFe}^{3+}$  values indicate a lower stability of the DPH/ $\text{Fe}^{3+}$  chelate at pH 7.5 when compared with *o,o*-EDDHA/ $\text{Fe}^{3+}$  chelate, and explains the slightly lower iron content in plants treated with DPH/ $\text{Fe}^{3+}$  at the end of the experiment.





**Figure 4.10** Cucumber plants after 7 and 21 days of treatment, in hydroponic culture, with the iron chelates (10  $\mu$ M Fe) of Azotochelin, DPH, *o,o*-EDDHA, EDTA and control plants (2  $\mu$ M Fe).

The relationship between the efficiency of a chelate to deliver iron to plants and the reduction of iron(III) chelated by the reductase is not yet clear and is still in discussion (Lucena, et al., 2008; Escudero, et al., 2012). The behavior of a chelating agent when it is used as a substrate of the enzyme FCR is an important step in the evaluation of the efficiency of a new chelating agent to provide iron to plants.

However, several authors have already demonstrated that the amount of iron reduced by the plants gives only information about a part of the uptake process (Lucena and Chaney, 2006; Nadal, et al. 2012). In fact, a higher reduction rate observed with EDTA/Fe<sup>3+</sup> chelate did not result in a higher amount of iron in the leaves due to the high stability of the EDTA/Fe<sup>2+</sup> chelate that serves as an Fe<sup>2+</sup> trapping agent and prevents that most of the iron is taken up by the plants (Lucena and Chaney, 2006; Nadal, et al., 2012).

Siderophores possess a higher affinity for iron(III) than iron(II), which is one of the defining characteristics of a siderophore (Villen, et al., 2007; Hider and Kong, 2010). This fact contributes to the similar iron uptake by DPH/Fe<sup>3+</sup> and EDTA/Fe<sup>3+</sup> chelates despite the much higher reduction rate of the latter.

Another important characteristic of the siderophores is the high selectivity for iron (Hider and Kong, 2010) that ensures the stability of the iron chelates of DPH and azotochelin in the nutrient solution. The stability of the iron chelates of DPH was studied in Chapter 3, which were found to be stable in the conditions of Hoagland solutions up to pH 9. Moreover, since Mg and specially Ca cations are considered the main competitors for iron in calcareous conditions for chelating agents (Yunta, et al., 2003a), the stability of the iron chelates of DPH, especially in the presence of these metal cations, using the Hoagland solution conditions ( $[Ca^{2+}] = 1.6 \times 10^{-3} \text{ mol.L}^{-1}$ ;  $[Mg^{2+}] = 8 \times 10^{-4} \text{ mol.L}^{-1}$ ;  $[Fe^{3+}] = 1.0 \times 10^{-4} \text{ mol.L}^{-1}$ ), at pH 7.5 was previously demonstrated (Figure 3.14 section 3.3.2).

On the other hand, in the case of EDTA, the chelated iron can be displaced by other cations in solution that form stable complexes with EDTA and thus reduces the soluble Fe in solution available for the plants (Villen, et al., 2007). This is evidenced by the SDDs obtained for the chelation of EDTA with Fe(III) in aqueous (Figure 4.11 A) or in Hoagland nutrient (Figures 4.11 B and C) solutions. The stability constants for EDTA with the metal ions in Hoagland solution, or with Fe<sup>3+</sup> are shown in tables 4.1 and 4.7,

respectively. In the case of *o,o*-EDDHA/Fe<sup>3+</sup> chelate, the higher stability of the chelate minimizes the Fe displacement by other cations from the chelate in the nutrient solution (Villen, et al., 2007), as it was shown in Chapter 3 (Figure 3.15, section 3.3.2).

The plants treated with azotochelin/Fe<sup>3+</sup> chelate also showed an iron content in leaves similar to DPH/Fe<sup>3+</sup> and EDTA/Fe<sup>3+</sup> chelates (Table 4.4). Catechol-based siderophores, like azotochelin, are effective iron chelators. However, despite the importance of iron binding by polyphenols, very few stability constants are reported for catecholate complexes of Fe<sup>3+</sup>, mostly due to the specially variable coordination modes of polyphenols, that depends largely, not only on the pH but also on the ligand to metal ratio (Perron and Brumaghim, 2009). Figure 4.12 evidences the high stability of azotochelin/Fe<sup>3+</sup> between pH 6 and 10, in the presence of Ca(II), 1.6 x 10<sup>-3</sup> mol.L<sup>-1</sup>.

At pH 4, a decrease of the soluble iron is observed, as well as the formation of a dark/black precipitate, which redissolved at higher pH values, regenerating the original purple color solution at pH 7.5. The formation of reversible precipitate at low pH is often observed in iron(III)-catecholate solutions and is associated with formation of uncharged iron complex species (Dhungana, et al. 2001; Mies, et al. 2008).

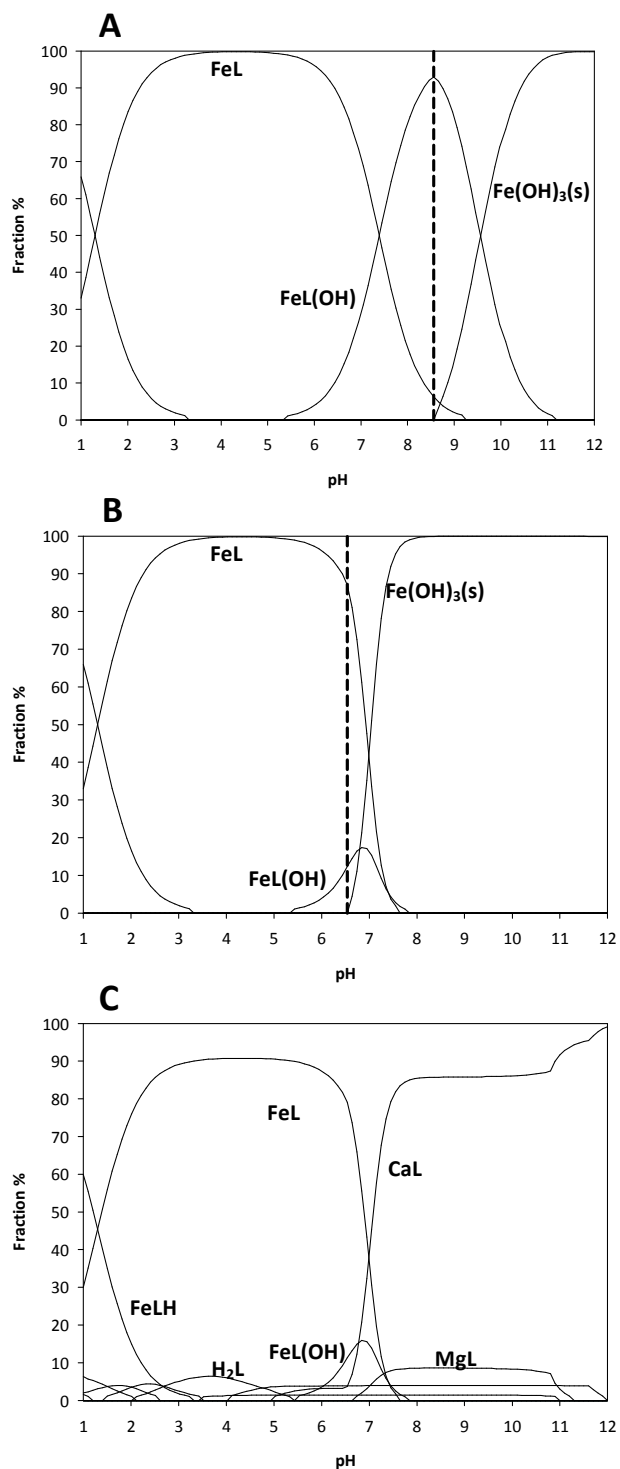


**Figure 4.11** Species distribution diagrams of the EDTA system in (A) aqueous and in (B,C) Hoagland nutrient solutions (for detailed information about the composition of the solution see Chapter 3):  $[L]=1.1 \times 10^{-4} \text{ mol.L}^{-1}$  ;  $[\text{Fe}^{3+}]=1.0 \times 10^{-4} \text{ mol.L}^{-1}$ . % is the percentage of species present (A,B) with total Fe(III) concentration set at 100% or (C) with total ligand concentration set at 100%; the dashed vertical line indicates  $\text{Fe}(\text{OH})_3$  precipitation.

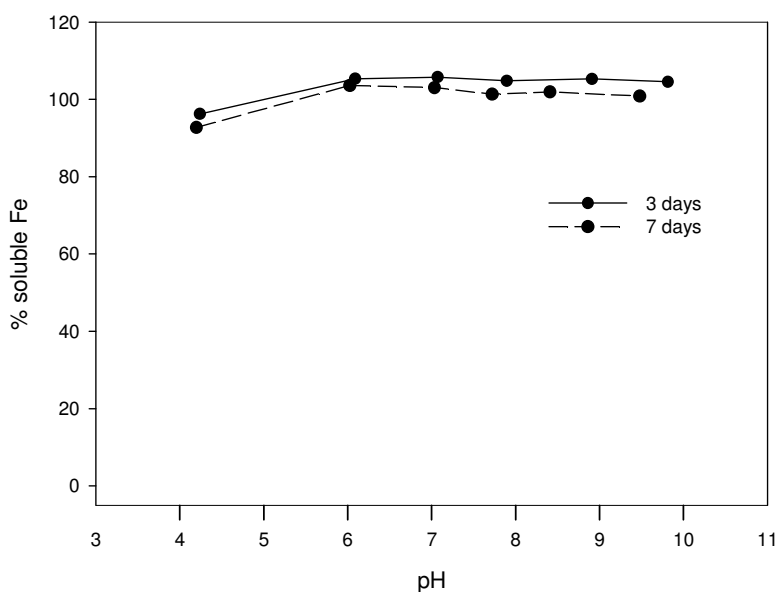


**Figure 4.12** Soluble Fe, at different pH, measured in Azotochelin/ $\text{Fe}^{3+}$  ( $[\text{Fe}^{3+}] = 1.5 \times 10^{-4} \text{ mol.L}^{-1}$ ) solutions after 3 and 7 days of interaction with  $\text{Ca}^{2+} 1.6 \times 10^{-3} \text{ mol L}^{-1}$ . Mean value from two replicates obtained at each pH.

UV-Vis spectrophotometry was used to study the complex formed in the preparation of the iron(III) chelate with azotochelin at pH 7.5, in aqueous solution (Figure 4.13). The formation of a bis(catecholate)-iron(III) complex (two catechol ligands coordinated to a single iron) was evidenced by the UV-Vis spectra with a  $\lambda_{\text{max}}$  at 560 nm, characteristic of this species, as well as the purple color of the chelate formed (Perron and Brumaghim, 2009; Hider et al., 1981; Duhme et al., 1996). Two possible bis(catecholate)-iron(III) species formed by azotochelin and iron(III) are represented in Figures 4.13 A and B.

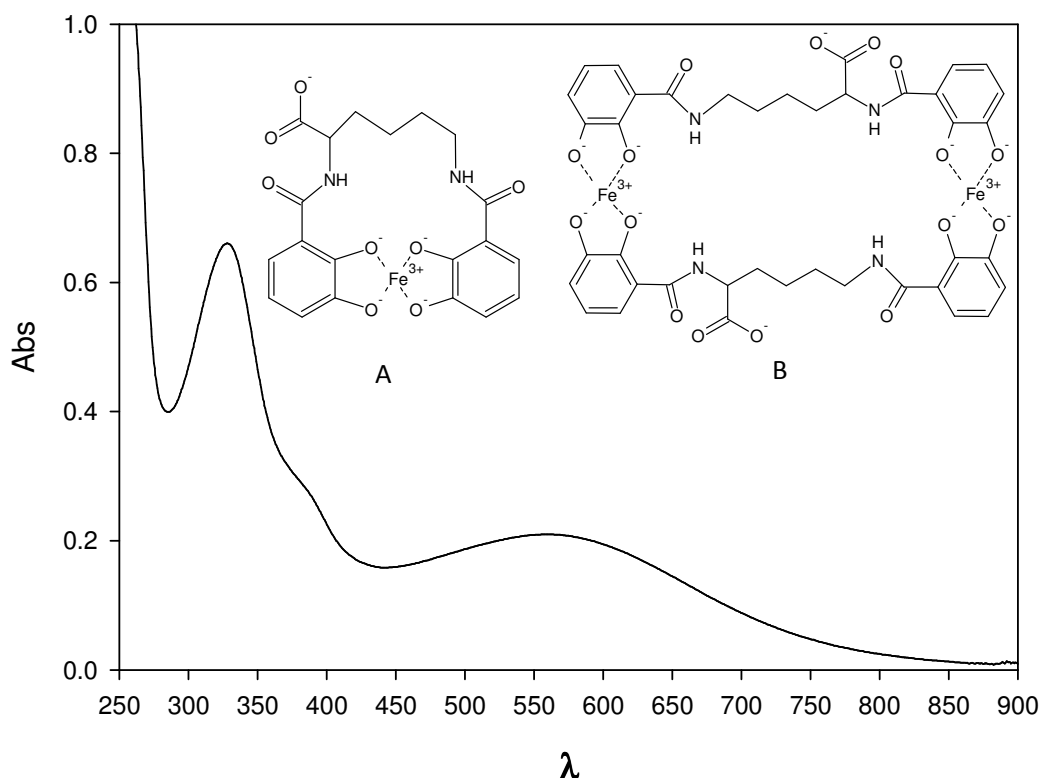


**Figure 4.13** Representative UV-Vis absorption spectra of a azotochelin/ $\text{Fe}^{3+}$  ( $[\text{Fe}^{3+}] = 50 \mu\text{M}$ ) solution at pH 7.5; and two proposed structures, for possible bis(catecholate)-iron(III) complex species,  $\text{FeL}$  (**A**) and  $\text{Fe}_2\text{L}_2$  (**B**) formed by azotochelin and iron(III) at pH 7.5.

Above pH 8, with the increase of the pH, a gradual change in the color of the solution was observed, with the formation, at pH 10 of a red-wine solution, characteristic of tris(catecholate)-iron(III) complexes (Hider et al. 1981), also observed by Duhme et al. (1996). Additionally Cornish & Page (1998) reported the formation of 3:2 ligand:metal complexes of azotochelin with iron(III).

The  $\text{pFe}^{3+}$  value of 23.1 for azotochelin, at pH 7.4 (Table 4.7), was also determined by Cornish et al. (1998). This value was calculated with the method described by Harris et. al. (1979), and is similar to the  $\text{pFe}^{3+}$  value calculated for EDTA, at pH 7.5.

However, the higher affinity for iron(III) over iron(II), and the more negative redox potential of the catechol-based siderophores, that can prevent the reduction by

most biological reductases (Hider and Kong, 2010) could limit the iron uptake by the plants treated with azotochelin/ $\text{Fe}^{3+}$ .

Nevertheless, azotochelin/ $\text{Fe}^{3+}$  was able to deliver iron to plants, but no correlation could be made with the results obtained in the FCR experiment, that were inconclusive.

On the other hand, the reduction and iron release from catecholamides siderophores, observed in several microorganisms, involves the shift of the binding mode of coordination from the catecholate to the salicylate mode, after the protonation of the distal hydroxyl donor at each catecholamide donor group as shown in Figure 4.14 (Abergel, et al., 2006; Harrington, et al., 2012).

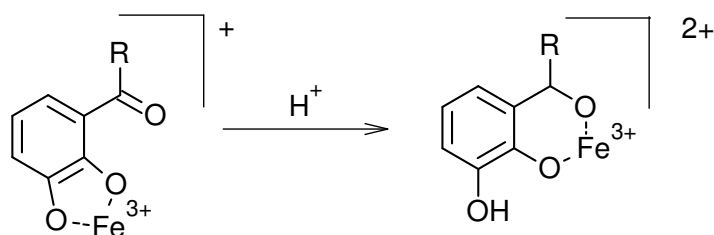


**Figure 4.14** Coordination shift from catecholate to the salicylate mode upon protonation.

In plants, it is possible that this shift of the binding mode occurs near the roots because it is known that a deficiency of iron increases the production and concentration of organic acids acidifying the rhizosphere (Marschner and Romheld, 1994). Additionally, Strategy I for iron uptake mainly used by dicots, involves the reduction by an iron(III) chelate reductase before the transport across the plasma, but also the generation of a proton gradient to facilitate iron(III) solubilization outside the cell (Bellenger, et al., 2007). Despite the use of 0.1 mM HEPES as pH buffer, the increased activity of  $\text{H}^+$ -ATPase in roots during iron deprivation acidifies the rhizosphere by excreting  $\text{H}^+$  and may decrease the pH of the rhizosphere by 0.5-1 pH units. This is consistent with the fact that the FCR activity decreases with increasing pH (Lucena and Chaney, 2007).

The shift from the catecholate to the salicylate mode not only lowers the affinity for binding trivalent metal cations but also shifts the redox potentials of

iron(III) complexes, moving them into the range where iron(III) can be reduced by biological reductants (Bellenger, et al., 2007; Harrington, et al., 2012).

Thus, the decrease of the absorbance at both 535 and 630 nm in the reductase assay with azotochelin (Figure 4.8A, full lines) may be due to the reduction of iron(III) to iron(II), after the shift to the salicylate coordination mode, with the formation of colorless Fe(II)-catechol complexes (Hider, et al., 1981). The increase of the absorbance at 535 nm after the first 20 minutes suggests the release of iron(II) from azotochelin by competition with BPDS. This affinity for iron(II) may lower the release efficiency of  $\text{Fe}^{2+}$  from azotochelin, with implications in the supply of iron to plants (Miethke, 2013). However, it must be noted that the uptake of intact  $\text{Fe}^{3+}$ -siderophore complexes without the requirement of a reduction step can also occur (Vansuyt, et al., 2007) and cannot be excluded.

The behavior of the azotochelin/ $\text{Fe}^{3+}$  chelate in the blanks (Figure 4.8A, dashed lines) suggest significant interactions of the chelate with the medium that would lead to misleading rates of reduction of the azotochelin/ $\text{Fe}^{3+}$  chelate. Initially, it was observed a proportional variation of the absorbance at 535 and 630 nm (Figure 4.8A, dashed lines), also observed in the case of *o,o*-EDDHA/ $\text{Fe}^{3+}$  at 535 and 480nm (Figure 4.8B, dashed lines). However, after this period, while the absorbance in the blanks of the FCR assay with *o,o*-EDDHA/ $\text{Fe}^{3+}$  remained constant until the end of the experiment, significant changes were observed in the case of azotochelin/ $\text{Fe}^{3+}$ , due most likely to the interaction between the azotochelin/ $\text{Fe}^{3+}$  chelate and BPDS. The possibility of interactions of azotochelin/ $\text{Fe}^{3+}$  with BPDS was beyond the scope of the present work.

The redox potential determined for rhodotorulic acid (-0.419 V vs NHE) (Crumbliss and Harrington, 2009) and for several dihydroxamic acids compounds at high-pH conditions (-0.261 to -0.446 V vs NHE) (Crumbliss and Harrington, 2009) suggest that the redox potential of DPH/ $\text{Fe}^{3+}$  chelate is higher than the redox potential of *o,o*-EDDHA/ $\text{Fe}^{3+}$  chelate (-0.560 V vs NHE) (Gomez-Gallego et al., 2005). From this, and due to the lower stability of the DPH/ $\text{Fe}^{3+}$  chelate, this complex was expected to be a better substrate for FCR than *o,o*-EDDHA/ $\text{Fe}^{3+}$  chelate. However, as in the case of azotochelin, a mechanism involving the changes in the coordination of the *o,o*-EDDHA/ $\text{Fe}^{3+}$  chelate at a more acidic pH in the vicinity of the roots, has already been



proposed (Gomez-Gallego, et al., 2005). This fact can probably explain the more effective reduction of *o,o*-EDDHA/Fe<sup>3+</sup> chelate (Figure 4.7) and the higher iron uptake from *o,o*-EDDHA/Fe<sup>3+</sup> chelate by plants (Table 4.4) despite the low redox potential of the very stable iron(III) chelate formed with *o,o*-EDDHA. Structural effects are also determinant in the interactions between each chelate and the FCR active site (Escudero et al., 2012) and further studies must be performed to evaluate the structure-activity relationship in the enzymatic processes.

The uptake of Cu and Mn by plants was affected by the uptake of iron in the different treatments. In fact, the leaf concentrations of Cu and Mn (Table 4.5) evidence the favored uptake of those cations under iron deficiency conditions. The higher concentration of Cu and Mn in the leaves of the untreated plants (Control, 2μM Fe) is related to the involvement of the Iron Regulated Transporter 1 (IRT1), not only in the uptake of iron, but also in the absorption of those cations, by the roots (Rodriguez-Lucena, et al., 2010). Moreover, the high affinity of *o,o*-EDDHA by Cu normally reduce Cu concentration in leaves when *o,o*-EDDHA/Fe<sup>3+</sup> is used in hydroponics (Yunta et al., 2003a). This behavior is shown in this work with azotochelin, suggesting also a high affinity of this siderophore by Cu.

The Fe/Mn ratio obtained with the treatments of DPH/Fe<sup>3+</sup> and azotochelin/Fe<sup>3+</sup> chelates were similar in both samplings (7 and 21 DAT) and much higher than those obtained in the untreated plants. These results indicate a good recovery from iron chlorosis. However, these results were worse than the ones obtained in the treatment with *o,o*-EDDHA/Fe<sup>3+</sup>, especially in the second sampling (21 DAT), when the Fe/Mn ratio showed by the treatment with DPH/Fe<sup>3+</sup> was slightly higher than the one obtained with EDTA/Fe<sup>3+</sup>.

The results obtained in this work suggest that the iron chelates of the siderophore azotochelin and the siderophore mimic DPH are able to supply iron to plants, in hydroponic solution at pH 7.5, to correct iron chlorosis and to maintain a good nutritional status of the plants. Taken into account the nature of these compounds, these results open the possibility of application of the iron(III) chelates of azotochelin and DPH for more environmental friendly iron fertilization.

## 4.5 References

Abergel, R. J.; Warner, J. A.; Shuh, D. K.; Raymond, K. N., Enterobactin Protonation and Iron Release: Structural Characterization of the Salicylate Coordination Shift in Ferric Enterobactin. *Journal of the American Chemical Society* **2006**, *128* (27), 8920-8931.

Barclay, S. J.; Huynh, B. H.; Raymond, K. N., Coordination Chemistry of Microbial Iron Transport Compounds .27. Dimeric Iron(III) Complexes of Dihydroxamate Analogs of Rhodotorulic Acid. *Inorganic Chemistry* **1984**, *23* (14), 2011-2018.

Bellenger, J. P.; Arnaud-Neu, F.; Asfari, Z.; Myneni, S. C. B.; Stiefel, E. I.; Kraepiel, A. M. L., Complexation of Oxoanions and Cationic Metals by the Biscatecholate Siderophore Azotochelin. *Journal of Biological Inorganic Chemistry* **2007**, *12* (3), 367-376.

Cornish, A. S.; Page, W. J., The Catecholate Siderophores of *Azotobacter Vinelandii*: Their Affinity for Iron and Role in Oxygen Stress Management. *Microbiology-(UK)* **1998**, *144*, 1747-1754.

Crumbliss, A. L.; Harrington, J. M., Iron Sequestration by Small Molecules: Thermodynamic and Kinetic Studies of Natural Siderophores and Synthetic Model Compounds. In *Advances in Inorganic Chemistry, Vol 61: Metal Ion Controlled Reactivity*, VanEldik, R.; Hubbard, C. D., Eds. Elsevier Academic Press Inc: San Diego, **2009**; Vol. 61, pp 179-250.

Dhungana, S.; Heggemann, S.; Heinisch, L.; Mollmann, U.; Boukhalfa, H.; Crumbliss, A. L., Fe(III) Coordination Properties of Two New Saccharide-Based Enterobactin Analogues: Methyl 2,3,4-Tris-O-{N-2,3-Di(Hydroxy)Benzoyl-Glycyl-Aminopropyl}-Alpha-D-Glu Copyranoside and Methyl 2,3,4-Tris-O-{N-2,3-Di-(Hydroxy)-Benzoyl - Aminopropyl}-Alpha-D-Glucopyr Anoside. *Inorganic Chemistry* **2001**, *40* (27), 7079-7086.

Duhme, A. K.; Hider, R. C.; Khodr, H., Spectrophotometric Competition Study between Molybdate and Fe(III) Hydroxide on N,N'-Bis(2,3-Dihydroxybenzoyl)-L-Lysine, a Naturally Occurring Siderophore Synthesized by *Azotobacter Vinelandii*. *Biometals* **1996**, *9* (3), 245-248.

Duhme, A. K.; Hider, R. C.; Khodr, H. H., Synthesis and Iron-Binding Properties of Protochelin, the Tris(Catecholamide) Siderophore of *Azotobacter Vinelandii*. *Chemische Berichte-Recueil* **1997**, *130* (7), 969-973.

Escudero, R.; Gomez-Gallego, M.; Romano, S.; Fernandez, I.; Gutierrez-Alonso, A.; Sierra, M. A.; Lopez-Rayó, S.; Nadal, P.; Lucena, J. J., Biological Activity of Fe(II) Aquo-Complexes Towards Ferric Chelate Reductase (FCR). *Organic & Biomolecular Chemistry* **2012**, *10* (11), 2272-2281.

Fourcroy, P.; Siso-Terraza, P.; Sudre, D.; Saviron, M.; Reyt, G.; Gaymard, F.; Abadia, A.; Abadia, J.; Alvarez-Fernandez, A.; Briat, J.-F., Involvement of the Abcg37 Transporter in Secretion of Scopoletin and Derivatives by *Arabidopsis* Roots in Response to Iron Deficiency. *New Phytologist* **2014**, *201* (1), 155-167.

Garcia-Marco, S.; Martinez, N.; Yunta, F.; Hernandez-Apaolaza, L.; Lucena, J. J., Effectiveness of Ethylenediamine-N(o-Hydroxyphenylacetic)-N'(p-Hydroxy-Phenylacetic) Acid (o,p-EDDHA) to Supply Iron to Plants. *Plant Soil* **2006**, *279* (1-2), 31-40.

Gomez-Gallego, M.; Pellico, D.; Ramirez-Lopez, P.; Mancheno, M. J.; Romano, S.; de la Torre, M. C.; Sierra, M. A., Understanding of the Mode of Action of Fe<sup>III</sup>-EDDHA as Iron Chlorosis Corrector Based on Its Photochemical and Redox Behavior. *Chem.-Eur. J.* **2005**, *11* (20), 5997-6005.

Harrington, J. M.; Bargar, J. R.; Jarzecki, A. A.; Roberts, J. G.; Sombers, L. A.; Duckworth, O. W., Trace Metal Complexation by the Triscatecholate Siderophore Protochelin: Structure and Stability. *Biometals* **2012**, *25* (2), 393-412.

Harris, W. R.; Carrano, C. J.; Cooper, S. R.; Sofen, S. R.; Avdeef, A. E.; McArdle, J. V.; Raymond, K. N., Coordination Chemistry of Microbial Iron Transport Compounds .19. Stability-Constants and Electrochemical Behavior of Ferric Enterobactin and Model Complexes. *Journal of the American Chemical Society* **1979**, *101* (20), 6097-6104.

Hider, R. C.; Mohdnor, A. R.; Silver, J.; Morrison, I. E. G.; Rees, L. V. C., Model Compounds for Microbial Iron-Transport Compounds .1. Solution Chemistry and Mossbauer Study of Iron(II) and Iron(III) Complexes from Phenolic and Catecholic Systems. *Journal of the Chemical Society-Dalton Transactions* **1981**, (2), 609-622.

Hider, R. C.; Kong, X., Chemistry and Biology of Siderophores. *Natural product reports* **2010**, *27* (5), 637.

Leydier, A.; Lecercle, D.; Pellet-Rostaing, S.; Favre-Reguillon, A.; Taran, F.; Lemaire, M., Sequestering Agent for Uranyl Chelation: A New Family of Cams Ligands. *Tetrahedron* **2008**, *64* (28), 6662-6669.

Lucena, J. J.; Chaney, R. L., Synthetic Iron Chelates as Substrates of Root Ferric Chelate Reductase in Green Stressed Cucumber Plants. *J. Plant Nutr.* **2006**, *29* (3), 423-439.

Lucena, J. J.; Chaney, R. L., Response of Cucumber Plants to Low Doses of Different Synthetic Iron Chelates in Hydroponics. *J. Plant Nutr.* **2007**, *30* (4-6), 795-809.

Lucena, J. J.; Sentis, J. A.; Villen, M.; Lao, T.; Perez-Saez, M., Idha Chelates as a Micronutrient Source for Green Bean and Tomato in Fertigation and Hydroponics. *Agronomy Journal* **2008**, *100* (3), 813-818.

Marschner, H.; Romheld, V., Strategies of Plants for Acquisition of Iron. *Plant Soil* **1994**, *165* (2), 261-274.

Martell, A. E.; Smith, R. M., *Nist Standard Reference Database 46 Version 8.0, Nist Critically Selected Stability Constants of Metal Complexes Database*. US Department of Commerce: National Institute of Standards and Technology, 2004.

Mies, K. A.; Gebhardt, P.; Moellmann, U.; Crumbliss, A. L., Synthesis, Siderophore Activity and Iron(III) Chelation Chemistry of a Novel Mono-Hydroxamate, Bis-Catecholate Siderophore Mimic: N-Alpha,-N-Epsilon-Bis 2,3-Dihydroxybenzoyl -L-Lysyl-(Gamma-N-Methyl-N-Hydroxyamido)-L-Glutamic Acid. *Journal of Inorganic Biochemistry* **2008**, *102* (4), 850-861.

Miethke, M., Molecular Strategies of Microbial Iron Assimilation: From High-Affinity Complexes to Cofactor Assembly Systems. *Metallomics* **2013**, *5* (1), 15-28.

Nadal, P.; Garcia-Marco, S.; Escudero, R.; Lucena, J. J., Fertilizer Properties of Dcha/Fe<sup>3+</sup>. *Plant Soil* **2012**, *356* (1-2), 367-379.

Perron, N. R.; Brumaghim, J. L., A Review of the Antioxidant Mechanisms of Polyphenol Compounds Related to Iron Binding. *Cell Biochemistry and Biophysics* **2009**, *53* (2), 75-100.

Rodriguez-Lucena, P.; Ropero, E.; Hernandez-Apaolaza, L.; Lucena, J. J., Iron Supply to Soybean Plants through the Foliar Application of IDHA/Fe<sup>3+</sup>: Effect of Plant Nutritional Status and Adjuvants. *J. Sci. Food Agric.* **2010**, *90* (15), 2633-2640.

Schecher, W. D.; McAvoy, D. C. *Minql+, a Chemical Equilibrium Modeling System Version 4.5 for Windows*, Environmental Research Software, Hallowell: Maine, **2001**.

Schmid, N. B.; Giehl, R. F. H.; Doell, S.; Mock, H.-P.; Strehmel, N.; Scheel, D.; Kong, X.; Hider, R. C.; von Wiren, N., Feruloyl-CoA 6'-Hydroxylase1-Dependent Coumarins Mediate Iron Acquisition from Alkaline Substrates in Arabidopsis. *Plant Physiol.* **2014**, *164* (1), 160-172.

Vansuyt, G.; Robin, A.; Briat, J.-F.; Curie, C.; Lemanceau, P., Iron Acquisition from Fe-Pyoverdine by Arabidopsis Thaliana. *Mol. Plant-Microbe Interact.* **2007**, *20* (4), 441-447.

Villen, M.; Garcia-Arsuaga, A.; Lucena, J. J., Potential Use of Biodegradable Chelate N-(1,2-Dicarboxyethyl)-D,L-Aspartic Acid/Fe<sup>3+</sup> as an Fe Fertilizer. *Journal of Agricultural and Food Chemistry* **2007**, *55* (2), 402-407.

Yunta, F.; Garcia-Marco, S.; Lucena, J. J.; Gomez-Gallego, M.; Alcazar, R.; Sierra, M. A., Chelating Agents Related to Ethylenediamine Bis(2-Hydroxyphenyl)Acetic Acid (Eddha): Synthesis, Characterization, and Equilibrium Studies of the Free Ligands and Their  $\text{Mg}^{2+}$ ,  $\text{Ca}^{2+}$ ,  $\text{Cu}^{2+}$ , and  $\text{Fe}^{3+}$  Chelates. *Inorganic Chemistry* **2003a**, 42 (17), 5412-5421.

Yunta, F.; Sierra, M. A.; Gomez-Gallego, M.; Alcazar, R.; Garcia-Marco, S.; Lucena, J. J., Methodology to Screen New Iron Chelates: Prediction of Their Behavior in Nutrient Solution and Soil Conditions. *J. Plant Nutr.* **2003b**, 26 (10-11), 1955-1968.

Yunta, F.; Garcia-Marco, S.; Lucena, J. J., Theoretical Speciation of Ethylenediamine-N-(o-Hydroxyphenylacetic)-N'-(p-Hydroxyphenylacetic) Acid (o,p-EDDHA) in Agronomic Conditions. *Journal of Agricultural and Food Chemistry* **2003c**, 51 (18), 5391-5399.

Zhang, G.; Amin, S. A.; Kuepper, F. C.; Holt, P. D.; Carrano, C. J.; Butler, A., Ferric Stability Constants of Representative Marine Siderophores: Marinobactins, Aquachelins, and Petrobactin. *Inorganic Chemistry* **2009**, 48 (23), 11466-11473.

## Chapter 5

---

Foliar application of iron chelates of the siderophores Azotochelin, and the siderophore mimic N,N'-Dihydroxy-N,N'-diisopropylhexanediamide as a Fe source to soybean plants growing in hydroponic cultures





**Foliar application of iron chelates of the siderophores Azotochelin, and the siderophore mimic N,N'-Dihydroxy-N,N'-diisopropylhexanediamide as a Fe source to soybean plants growing in hydroponic cultures\***

**Abstract**

In this work, the efficacy of the foliar application of the iron chelates of a siderophore, azotochelin, and a siderophore mimic, DPH, to deliver iron to soybean plants showing chlorotic symptoms, was studied. The nutritional status of the plants treated with azotochelin/ $\text{Fe}^{3+}$  and DPH/ $\text{Fe}^{3+}$  was evaluated and the results were compared with plants treated with EDTA/ $\text{Fe}^{3+}$  and *o,o*-EDDHA/ $\text{Fe}^{3+}$ . Foliar sprays of DPH/ $\text{Fe}^{3+}$ , EDTA/ $\text{Fe}^{3+}$  or *o,o*-EDDHA/ $\text{Fe}^{3+}$  were able to deliver Fe to soybean plants. However, only the translocation of Fe to the roots was observed in the plants treated with the iron chelates of DPH and *o,o*-EDDHA. The concentration of Mn in the roots of the plants was also affected by the foliar application of the iron chelates. No evidences were found for the Fe uptake by the plants treated with foliar sprays of azotochelin/ $\text{Fe}^{3+}$ .

---

\*Foliar Application of Iron Chelates of the Siderophore Azotochelin, and the Siderophore Mimic N,N'-Dihydroxy-N,N'-diisopropylhexanediamide as a Fe Source to Soybean Plants Growing in Hydroponic Cultures (In preparation).

## 5.1 Introduction

Fe fertilizers are usually applied to the soil, but can also be delivered to the foliage (Abadia et al. 2011). However, the effectiveness of foliar application of Fe is still controversial. Several authors evaluated this type of fertilization as a suitable technique to meet the demand of growing leaves in Fe-deficient plants, and to overcome iron chlorosis, although with variable results (Huve et al. 2003; Nikolic et al. 2003; Rodriguez-Lucena et al. 2010a).

Innumerable uncertainties remain and the response of plants to Fe fertilization, using synthetic Fe-chelates, Fe-complexes and inorganic Fe salts is still under investigation. Thus, new studies using different conditions and/or new chelating agents are useful to clarify the mechanism involved in the penetration and transport of Fe applied foliarly to plants. Nevertheless, foliar application of Fe-chelates is used as an alternative way to overcome Fe chlorosis and is usually considered when weak or moderate chelating agents are used (Rodriguez-Lucena et al. 2009; Rodriguez-Lucena et al. 2010a; Rodriguez-Lucena et al. 2010b; Abadia et al. 2011).

Natural occurring siderophores, and synthetic analogues, can constitute an environmental friendly alternative to the synthetic chelates, many nondegradable, usually used in iron fertilization. Also, treatment with foliar Fe sprays can lower the environmental impact of the use of synthetic chelates applied to soils (Fernandez et al. 2005).

The ability of the iron chelates of azotochelin (Figure 4.1, section 4.1) and DPH (Figure 3.1, section 3.1) to supply Fe to (cucumber) plants, in hydroponic conditions, have already been demonstrated in Chapter 4. In the present chapter, we studied the effectiveness of the foliar application of the Fe chelates of azotochelin and DPH, respectively, as Fe suppliers to soybean plants with visible chlorotic symptoms.

EDTA (Figure 1.2 section 1.1.1) and *o,o*-EDDHA (Figure 1.3 section 1.1.2), already showed to be effective in supplying Fe to plants by foliar application of their iron chelates (Modaihsh 1997; Ylivainio et al. 2004; Rodriguez-Lucena et al. 2009; Fernandez et al.

2008; Roosta & Mohsenian 2012), and were also tested in this work, under the same conditions, for comparative purposes.

## 5.2 Materials and Methods

The chelating agents used in the preparation of the iron(III) chelates for foliar application, *o,o*-EDDHA, Na<sub>2</sub>H<sub>2</sub>EDTA, azotochelin and DPH were previously described in section 4.7.

### 5.2.1 Preparation of Iron chelates

The Fe (III) chelate solutions for foliar application were prepared as in section 4.2.1, for hydroponic experiments.

### 5.2.2 Efficacy of Azotochelin/Fe<sup>3+</sup> and DPH/Fe<sup>3+</sup> to provide Fe to soybean plants by foliar application.

Soybean plants (*Glycine max* L. cv. Stine 0408) were used in the foliar application experiments.

After washing with distilled water (10 min), then twice with H<sub>2</sub>O<sub>2</sub>, 2% (10 min), seeds were rinsed with distilled water and germinated during 4 days.

After germination (Figure 5.1A), seedlings of similar development were placed on a holed plate, floating in 10 L containers (Figure 5.1B) with a continuously aerated 1/5 diluted nutrient solution [nutrient solution composition: macronutrients (mM) – 1.0 Ca(NO<sub>3</sub>)<sub>2</sub>, 0.9 KNO<sub>3</sub>, 0.3 MgSO<sub>4</sub>, 0.1 KH<sub>2</sub>PO<sub>4</sub>; cationic micronutrients (μM) – 1.0 HBED/Fe<sup>3+</sup>, 2.5 MnSO<sub>4</sub>, 1.0 CuSO<sub>4</sub>, 10 ZnSO<sub>4</sub>, 1.0 CoSO<sub>4</sub>, 1.0 NiCl<sub>2</sub>, 115.5 EDTANa<sub>2</sub>; anionic micronutrients (μM) – 35 NaCl, 10 H<sub>3</sub>BO<sub>3</sub>, 0.05 Na<sub>2</sub>MoO<sub>4</sub>; 0.1 mM HEPES.], for

7 days, in a Dycometal-type CCKF 0/16985 growth chamber, where they were grown under controlled climatic conditions: day/night photoperiod, 16/8 h; temperature (day/night), 28/20 °C; relative humidity (RH) (day/night) 40/60%.

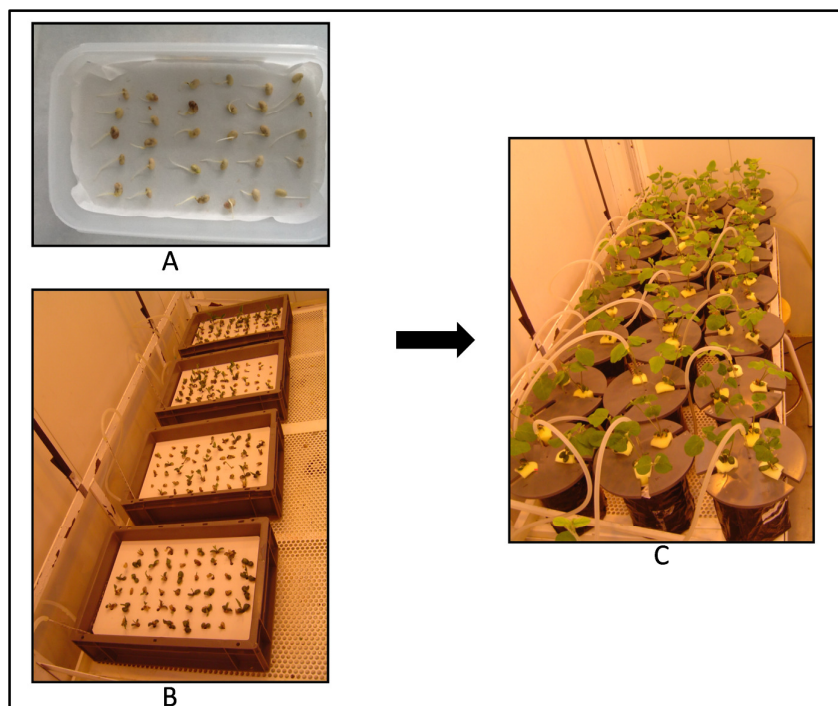


**Figure 5.1** Germination of soybean seeds (*Glycine max* L. cv. Stine 0408) (A). Seedlings in holed plates (B); Plants in 2 L vessels (C).

After this time, the stems of two plants were wrapped together with foam, and placed in 2 L polyethylene vessels [three holes in the lid, six plants (3 pairs) per pot] containing 2 L of a continuously aerated full strength nutrient (Figure 5.1C). 1.0  $\mu\text{M}$  of Fe (HBED/ $\text{Fe}^{3+}$ ) was added to the nutrient solution. The pH was adjusted to 7.5 with KOH 1.0 M and buffered with HEPES 0.1 mM, and 2 g of solid  $\text{CaCO}_3$  per pot. The 2L pots were covered with black plastic to avoid light exposure.

The plants were kept in this solution for 4 days. After this time, the solution was renewed, but no Fe was added to the nutrient solution, and the foliar treatments with Fe-chelates were applied.

Each treatment was replicated five times (two pairs of plants per replicate) in a completely randomized design. All the Fe chelate solutions were adjusted to pH 5.5 to avoid altering the ion exchange properties of the cuticle. Each pair of plants was sprayed with 2 mL of the treatment containing a Fe concentration of  $5.0 \text{ mmol L}^{-1}$ , using a nebulizer system (Figure 5.2A). The non-ionic surfactant Tween 80 (non-ionic surfactant; PROBUS, Barcelona, Spain) was added to the leaf sprays at 0.1% (v/v), and the treatments were applied in the first leaf level of each plant, both on the adaxial and abaxial leaf surface (Figure 5.2B). During the leaf spraying, the untreated parts of the plants and nutrient solution were covered with plastic sheet to avoid contamination. A control (5 replicates) was included in which no Fe supply was used. Water was added to the nutrient solution every 2 days, and during the experiments, SPAD readings were taken periodically, using a SPAD meter (Minolta 502, Osaka, Japan), to estimate leaf chlorophyll concentration.

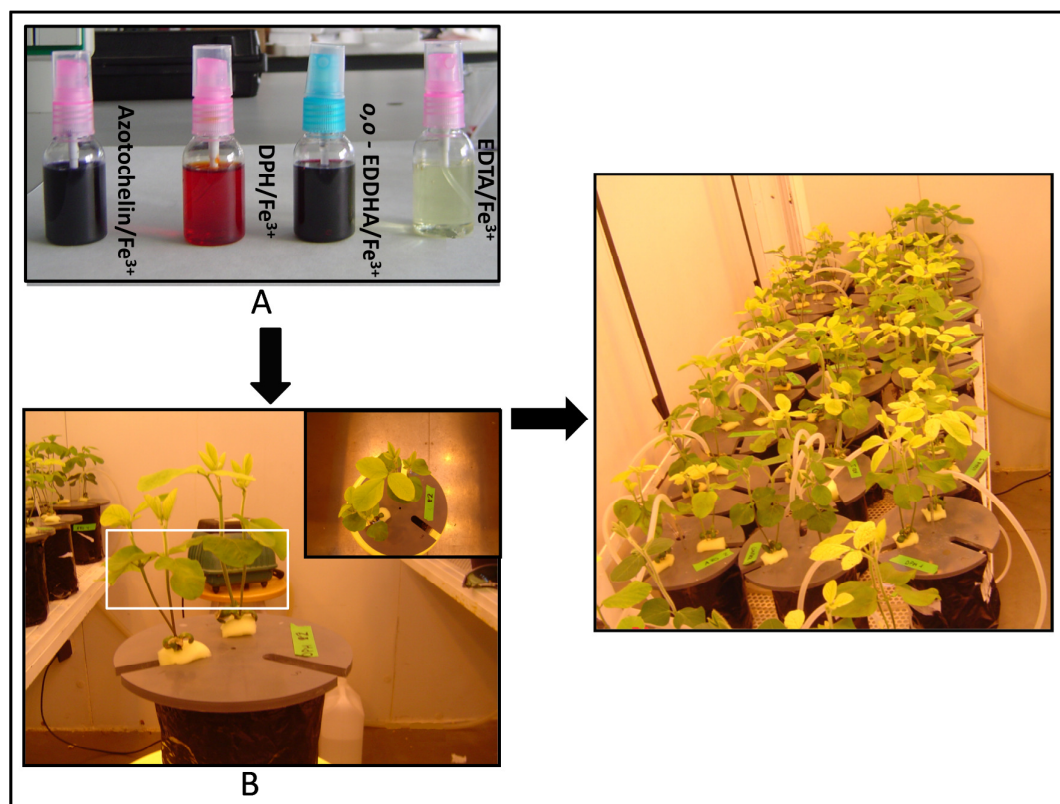


**Figure 5.2** Nebulizer system (A) used to spray first leaf level of each plant (B) in foliar application treatments.

Sampling was performed 7 days after the application of the treatments. The roots, stems, treated leaves (first leaf level) and untreated leaves (upper leaf levels) were separated, weighted, washed and dried at 65 °C for 3 days. After dry digestion in a muffle furnace (480 °C), the ashes were dissolved in 6 M HCl. Fe, Mn, Cu and Zn were analysed by AAS-FA using a Perkin-Elmer Analyst 800 spectrophotometer, to study the plant nutritional status and Fe redistribution.

### 5.3 Statistical Analysis

Statistical analyses were performed as it was described in section 4.2.5. Significant differences were established at  $p < 0.1$  using the Duncan test.

### 5.4 Results and Discussion

In this work, we studied the ability of foliar application of the Fe chelates of azotochelin and DPH, to deliver Fe to soybean plants with visible symptoms of Fe chlorosis. Foliar applications of EDTA/Fe<sup>3+</sup> and *o,o*-EDDHA/Fe<sup>3+</sup>, and control plants (-Fe) to which no Fe was added, were also performed for comparative purpose.

The SPAD index was measured in different leaf levels of the plants, and at different periods of the experiment, to measure leaf re-greening, associated with the increase of chlorophyll and Fe amount. In order to evaluate the Fe uptake and transport within the plant, Fe content was measured in several parts of the plants. Cu, Mn and Zn concentrations were also assessed to evaluate the influence of foliar application on different nutrient concentrations. Leaf, stems and root dry weight was also determined.

Generally, the Fe amount measured in the upper (untreated) leaf levels of the plants sprayed with the Fe chelates (Table 5.1) did not show significant differences from the control plants (-Fe), at the end of the experiment (DAT 7). Examples of the soybean plants at DAT 7 are shown in Figure 5.3.

**Table 5.1** Effect of the foliar application of the different Fe chelate treatments on the Fe content ( $\mu\text{mol plant}^{-1} \text{ DW}$ ;  $\pm$  SE,  $n=5$ ) in untreated leaves, stems and roots, of soybean plants grown in hydroponics conditions (DAT 7).

Treatment	Fe content ( $\mu\text{mol plant}^{-1} \text{ DW}$ )		
	Untreated (upper levels) leaves	stems	roots
Azotochelin	0.33 $\pm$ 0.05 ab	0.25 $\pm$ 0.05 a	0.15 $\pm$ 0.02 a
DPH	0.20 $\pm$ 0.05 a	0.34 $\pm$ 0.05 ab	0.23 $\pm$ 0.02 b
EDDHA	0.37 $\pm$ 0.06 b	0.27 $\pm$ 0.06 a	0.22 $\pm$ 0.02 b
EDTA	0.60 $\pm$ 0.06 c	0.29 $\pm$ 0.06 a	0.22 $\pm$ 0.02 b
Control	0.28 $\pm$ 0.06 ab	0.44 $\pm$ 0.06 b	0.15 $\pm$ 0.02 a

Different letters in the same column denotes significant differences among treatments for Duncan test ( $p<0.1$ ).

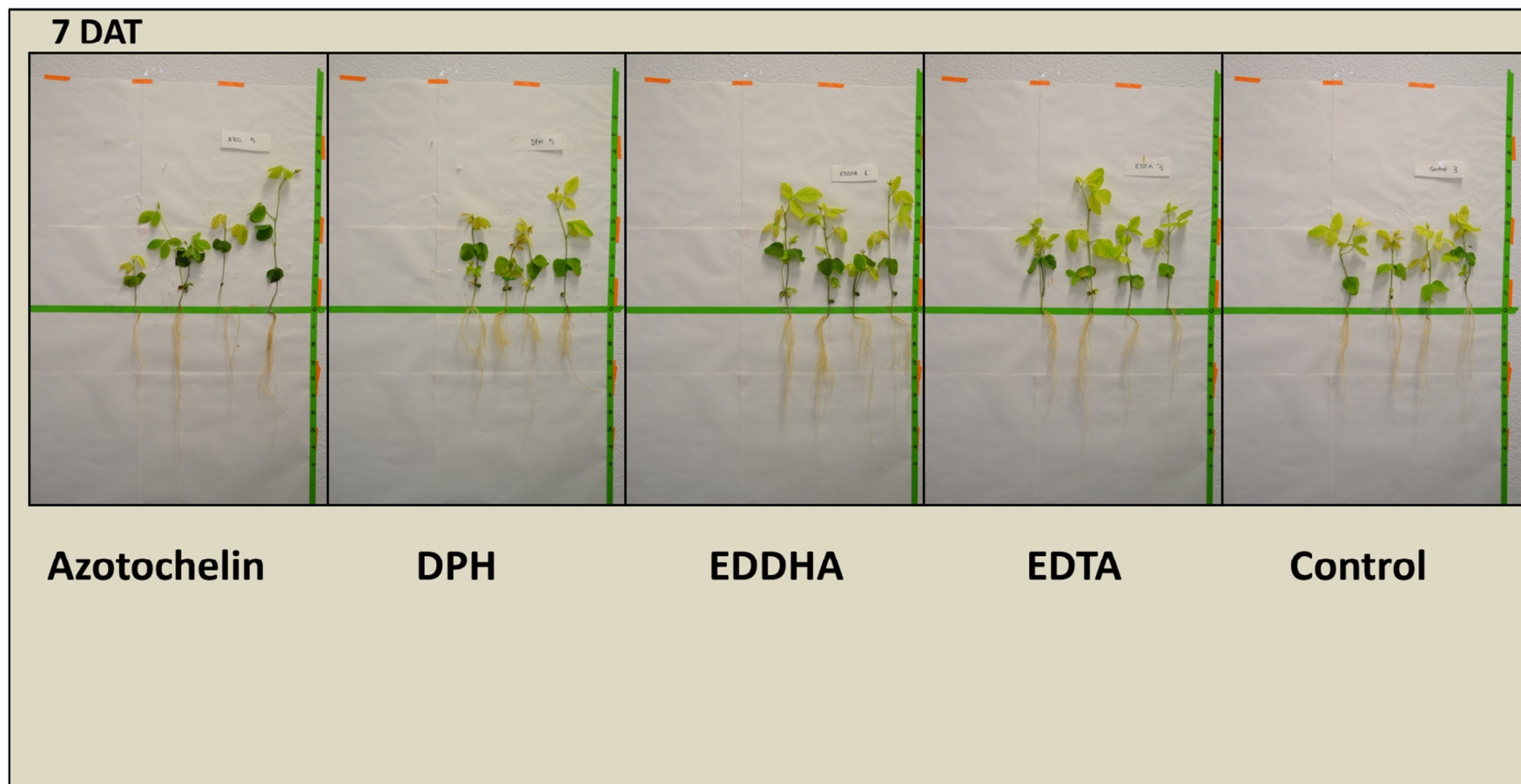


**Figure 5.3** Examples of soybean plants after 7 days after foliar application with the iron chelates ( $5 \text{ mmol.L}^{-1} \text{ Fe}$ ) of Azotochelin, DPH, *o,o*-EDDHA, EDTA and control plants ( $- \text{Fe}$ ).



Only the plants treated with EDTA/Fe<sup>3+</sup> showed significant higher Fe content, in the untreated leaves. Surprisingly, the Fe content measured in the stems of the control plants was higher than the treated ones. These results suggest that, with the exception of the treatments using EDTA/Fe<sup>3+</sup>, the Fe transport to growing leaves did not occur, which was already predicted by the SPAD values measured in the second leaf level, in different periods of the experiment, shown in Table 5.2. The SPAD index measured in the second leaf level of the treated plants did not show significant differences from the untreated ones, even in the case of EDTA/Fe<sup>3+</sup>, which was the only treatment that showed higher leaf Fe content than the control plants (Table 5.1). On the other hand, at the end of the experiment (DAT 6), the plants treated with EDTA/Fe<sup>3+</sup> and *o,o*-EDDHA/Fe<sup>3+</sup> showed higher SPAD values in the first leaf level, than the plants treated with the iron chelates of azotochelin or DPH, or than the untreated ones (Table 5.2). These results suggest a higher foliar Fe uptake by the plants treated with EDTA/Fe<sup>3+</sup> and *o,o*-EDDHA/Fe<sup>3+</sup> solutions. However, it was not possible to make a correlation with the iron concentration, since the foliar treatments were sprayed in this leaf level (first leaf level). Therefore, the Fe content was not considered due to the impossibility to ensure that the iron measured was in fact Fe absorbed and not Fe remaining in the surface of the leaves after washing.

It can be observed in Table 5.1 that the plants treated with EDTA/Fe<sup>3+</sup>, *o,o*-EDDHA/Fe<sup>3+</sup> or DPH/Fe<sup>3+</sup> showed significant higher Fe content in roots than the controls, which evidences the absorption of Fe through leaf surfaces, but also the translocation to the roots.

However, as already referred, only in the case of the plants treated with EDTA/Fe<sup>3+</sup>, the amount of iron measured in the untreated leaves suggests the transport to the upper leaf levels, which was not observed in the plants treated with DPH/Fe<sup>3+</sup> and *o,o*-EDDHA/Fe<sup>3+</sup>. No evidences were found for the iron uptake by the plants treated with foliar sprays of azotochelin/Fe<sup>3+</sup>.

**Table 5.2** Effect of the foliar application of the different Fe chelate treatments on the SPAD values ( $\text{SPAD} \pm \text{SE}$ ,  $n=5$ ) measured in the first and second leaf levels, in soybean plants grown in hydroponic conditions.

Treatment	SPAD					
	Level 1			Level 2		
	DAT 0	DAT3	DAT 6	DAT 0	DAT3	DAT 6
Azotochelin	$26.4 \pm 0.9$ ns	$28.0 \pm 1.1$ ab	$28.2 \pm 1.2$ ac	$7.9 \pm 1.3$ ns	$5.6 \pm 0.8$ ns	$7.1 \pm 1.1$ ns
DPH	$28.5 \pm 0.9$	$28.5 \pm 1.1$ ab	$28.4 \pm 1.1$ ac	$8.3 \pm 1.8$	$5.9 \pm 1.0$	$5.6 \pm 1.0$
EDDHA	$26.2 \pm 1.0$	$29.8 \pm 1.2$ a	$32.5 \pm 1.3$ b	$7.1 \pm 1.5$	$4.8 \pm 1.0$	$4.4 \pm 1.3$
EDTA	$26.7 \pm 0.9$	$28.3 \pm 1.2$ ab	$29.9 \pm 1.3$ ab	$7.5 \pm 2.0$	$5.9 \pm 1.0$	$6.1 \pm 1.1$
Control	$26.7 \pm 1.0$	$26.2 \pm 1.2$ b	$26.4 \pm 1.3$ c	$8.3 \pm 1.8$	$6.3 \pm 1.0$	$7.0 \pm 1.2$

Different letters in the same column denotes significant differences among treatments for Duncan test ( $p < 0.1$ ). ns: no significant differences.

Only the plants treated with *o,o*-EDDHA showed a slightly higher root dry weight than the control plants (Table 5.3), and thus it was not possible to correlate the iron content with the dry weight of the roots. Also, no significant differences were observed between the leaf and stem dry weight of the treated plants when compared with the untreated ones.

Foliar applications of EDTA/Fe<sup>3+</sup> and *o,o*-EDDHA already showed to be effective in treating chlorosis in different plants, under appropriate conditions, and are used in foliar-spray treatments (Fernandez, et al., 2008; Rodriguez-Lucena, et al., 2009; Rodriguez-Lucena, et al., 2010b). Nevertheless, in the particular case of foliar application of EDTA/Fe<sup>3+</sup> to soybean plants, the preferential translocation towards the roots was also observed by Rodriguez-Lucena, et al. (2010b). On the other hand, Rodriguez-Lucena et al. (2009) observed the translocation toward the leaves formed after the Fe application to tomato plants, but not to cucumber leaves, in which <sup>59</sup>Fe translocation to untreated plant tissues was not clearly directed toward a specific sink. Nikolic et al. (2003) also observed the translocation of <sup>59</sup>Fe to untreated leaves, although 50% of the <sup>59</sup>Fe supplied foliarly to sunflower leaves was found in the roots. Thus, the higher Fe concentration in roots observed with DPH/Fe<sup>3+</sup> may indicate that this chelating agent is a potential chelating agent to provide Fe to soybean when applied through foliar sprays. Further experiments must be performed in order to confirm these results, but also to evaluate the possibility of Fe transport to other parts of the plant.

The mechanisms involved in the uptake and translocation of Fe from the treated leaves to other parts of the plants are diverse and not well understood. Additionally, the effectiveness of foliar application of chelates depends on several factors involved in the process of leaf penetration, plant translocation and cell Fe uptake (Fernandez, et al., 2005). Suitable foliar fertilizer formulations, which may be different for each chelating agent, are difficult to specify, due to the lack of understanding of such processes (Schoenherr, 2006; Fernandez, et al., 2008; Rodriguez-Lucena, et al., 2009; Rodriguez-Lucena, et al., 2010a; Rodriguez-Lucena, et al., 2010b).

**Table 5.3** Effect of the foliar application of different Fe chelate treatments on leaves, stems and roots dry weight ( $\pm$  SE,  $n=5$ ), in soybean plants grown in hydroponic conditions.

Treatment	Dry weight, g <sup>-1</sup>					
	Leaves			stems	Roots	Plant (whole)
	level 1	Untreated (upper levels)	All leaves			
<b>Azotochelin</b>	0.39 $\pm$ 0.03 ns	0.50 $\pm$ 0.07 a	0.90 $\pm$ 0.08 a	0.67 $\pm$ 0.06 a	0.26 $\pm$ 0.02 a	1.8 $\pm$ 0.1 a
<b>DPH</b>	0.40 $\pm$ 0.03	0.53 $\pm$ 0.07 a	0.94 $\pm$ 0.08 ab	0.81 $\pm$ 0.06 ab	0.31 $\pm$ 0.02 ab	2.1 $\pm$ 0.1 ab
<b>EDDHA</b>	0.35 $\pm$ 0.03	0.76 $\pm$ 0.08 b	1.11 $\pm$ 0.09 ab	0.84 $\pm$ 0.07 ab	0.34 $\pm$ 0.02 b	2.3 $\pm$ 0.2 b
<b>EDTA</b>	0.35 $\pm$ 0.03	0.80 $\pm$ 0.08 b	1.15 $\pm$ 0.09 b	0.85 $\pm$ 0.07 b	0.31 $\pm$ 0.02 ab	2.3 $\pm$ 0.2 b
<b>Control</b>	0.34 $\pm$ 0.03	0.62 $\pm$ 0.08 ab	0.96 $\pm$ 0.09 ab	0.78 $\pm$ 0.07 ab	0.27 $\pm$ 0.02 a	2.0 $\pm$ 0.2 ab

Different letters in the same column denotes significant differences among treatments for Duncan test ( $p<0.1$ ); ns: no significant differences.

All these uncertainties led to variable results regarding to the uptake and the redistribution of Fe from the treated leaves, reported by several authors (Alvarez-Fernandez, et al., 2004; Fernandez, et al., 2006; Fernandez, et al., 2008; Rodriguez-Lucena, et al., 2009). Besides the type of plant used, other factors, such as the surfactant used, type of molecule applied, characteristics concerning to the treated leaf are known to be determinant to the effectiveness of an Fe chelate to prevent or cure Fe chlorosis (Rodriguez-Lucena, et al., 2009; Rodriguez-Lucena, et al., 2010b).

The application of Fe chelates, or other agrochemical active ingredient, to leaves is usually ineffective unless provided with an appropriate surfactant (Perkins, et al., 2005). In addition, the type of surfactant used has a major importance in the composition of the foliar sprays, as it was already reported by other authors (Fernandez, et al., 2008). The use of surfactants lowers the surface tension, which increases the spray retention and wetting. Thus, the use of a suitable surfactant can increase the permeability of the leaf membranes and accelerate cuticular and foliar penetration (Liu, 2004; Schonherr, et al., 2005). Non-ionic surfactants, as the one used in this work, are the most commonly used in the foliar applications, since interaction with the active ingredient is minimised (Fernandez, et al., 2008; Rodriguez-Lucena, et al., 2010a; Rodriguez-Lucena, et al., 2010b).

Due to the nature of each Fe-containing compound, different leaf Fe penetration, translocation and cell uptake can be expected (Ylivainio, et al., 2004; Fernandez, et al., 2005). However, it is known that not only the Fe-source (independently), but also the interaction with the surfactant is determinant for the efficiency of a Fe-chelate to deliver Fe to plants by foliar applications (Fernandez, et al., 2008; Rodriguez-Lucena, et al., 2010a; Rodriguez-Lucena, et al., 2011). Thus, different surfactants must be tested in further experiments with azotochelin, but also with DPH/Fe<sup>3+</sup>, since not only the Fe uptake, but also the transport to untreated parts of the plant is affected by the type of chelating agents and/or surfactant used (Fernandez, et al., 2008).

Because foliar treatments with Fe-containing solutions may influence the uptake of other nutrients (Fernandez, et al., 2008), the concentrations of Mn, Zn and Cu was also measured (Table 5.4).

**Table 5.4** Effect of the foliar application of the different Fe chelate treatments on the concentration of Fe, Mn, Zn and Cu ( $\mu\text{mol.g}^{-1}$  DW  $\pm$  SE, n=5) measured in the roots of soybean plants grown in hydroponic conditions.

Treatment	Concentration in roots ( $\mu\text{mol.g}^{-1}$ DW)			
	Fe	Mn	Zn	Cu
Azotochelin	0.57 $\pm$ 0.05 a	0.48 $\pm$ 0.04 a	0.48 $\pm$ 0.05 ns	0.15 $\pm$ 0.05 ns
DPH	0.74 $\pm$ 0.05 b	0.41 $\pm$ 0.04 a	0.58 $\pm$ 0.05	0.25 $\pm$ 0.05
EDDHA	0.62 $\pm$ 0.06 ab	0.50 $\pm$ 0.05 a	0.51 $\pm$ 0.06	0.17 $\pm$ 0.06
EDTA	0.73 $\pm$ 0.06 b	0.45 $\pm$ 0.05 a	0.48 $\pm$ 0.06	0.14 $\pm$ 0.06
Control	0.53 $\pm$ 0.06 a	0.66 $\pm$ 0.05 b	0.58 $\pm$ 0.06	0.14 $\pm$ 0.06

Different letters in the same column denotes significant differences among treatments for Duncan test ( $p < 0.1$ ). ns: no significant differences.

It was found that all the treated plants with foliar application of the iron chelates showed significant lower Mn concentration than the untreated plants. It has already been reported that the affinity of the roots for Mn is reduced by the translocation of Fe to the roots (Ylivainio, et al., 2004; Rodriguez-Lucena, et al., 2010b). Therefore, the results obtained in this work were expected for the plants treated with EDTA/Fe<sup>3+</sup>, o,o-EDDHA/Fe<sup>3+</sup> and DPH/Fe<sup>3+</sup>, which showed significant higher Fe content in roots, but not with azotochelin/Fe<sup>3+</sup>. Nevertheless, it was evident the higher Mn concentration in the roots of the control plants. On the other hand, no differences were found in the concentration of Zn and Cu measured in the treated plants or in the controls.

## 5.5 Conclusions

Although the results obtained in this work evidence Fe uptake by soybean plants, when supplied with foliar applications of DPH/Fe<sup>3+</sup>, further experiments are required to evaluate the possible translocation of the Fe towards untreated and growing leaves, which was only observed in plants treated with EDTA/Fe<sup>3+</sup>.

As expected, the type of ligand used plays an important role in the foliar application of the Fe chelates, and it was not possible to confirm the Fe uptake in plants treated with azotochelin/Fe<sup>3+</sup>, suggesting that the ideal composition of the formulation differs with the nature of the compound. Different conditions must also be tested to study the effect of this type of fertilization using azotochelin.

Several factors, such as the pH, number, frequency and timing of the applications, level of severity of chlorosis at the time of application, concentration of Fe chelate, plant species may affect foliar application experiments (Tagliavini and Rombola, 2001; Alvarez-Fernandez, et al., 2004; Fernandez, et al., 2005; ; Fernandez and Ebert, 2005; Schonherr, et al., 2005; Rodriguez-Lucena, et al., 2011) and must be considered in further experiments to understand and optimize the process. Also, foliar application of Fe chelates can be used as a complementary source of Fe, to

conventional supply of Fe chelates into soil or to nutrient solution and should also be considered.

## 5.6 References

Abadia, J.; Vazquez, S.; Rellán-Alvarez, R.; El-Jendoubi, H.; Abadia, A.; Alvarez-Fernandez, A.; Flor Lopez-Millan, A., Towards a Knowledge-Based Correction of Iron Chlorosis. *Plant Physiology and Biochemistry* **2011**, *49* (5), 471-482.

Alvarez-Fernandez, A.; Garcia-Lavina, P.; Fidalgo, C.; Abadia, J.; Abadia, A., Foliar Fertilization to Control Iron Chlorosis in Pear (*Pyrus Communis* L.) Trees. *Plant Soil* **2004**, *263* (1-2), 5-15.

Fernandez, V.; Ebert, G.; Winkelmann, G., The Use of Microbial Siderophores for Foliar Iron Application Studies. *Plant Soil* **2005**, *272* (1-2), 245-252.

Fernandez, V.; Ebert, G., Foliar Iron Fertilization: A Critical Review. *J. Plant Nutr.* **2005**, *28* (12), 2113-2124.

Fernandez, V.; Del Rio, V.; Abadia, J.; Abadia, A., Foliar Iron Fertilization of Peach (*Prunus Persica* (L.) Batsch): Effects of Iron Compounds, Surfactants and Other Adjuvants. *Plant Soil* **2006**, *289* (1-2), 239-252.

Fernandez, V.; Del Rio, V.; Pumarino, L.; Igartua, E.; Abadia, J.; Abadia, A., Foliar Fertilization of Peach (*Prunus Persica* (L.) Batsch) with Different Iron Formulations: Effects on Re-Greening, Iron Concentration and Mineral Composition in Treated and Untreated Leaf Surfaces. *Scientia Horticulturae* **2008**, *117* (3), 241-248.

Huve, K.; Remus, R.; Luttschwager, D.; Merbach, W., Transport of Foliar Applied Iron ( $^{59}\text{Fe}$ ) in *Vicia Faba*. *J. Plant Nutr.* **2003**, *26* (10-11), 2231-2242.



Liu, Z. Q., Effects of Surfactants on Foliar Uptake of Herbicides - a Complex Scenario. *Colloids and Surfaces B-Biointerfaces* **2004**, 35 (3-4), 149-153.

Modaihsh, A. S., Foliar Application of Chelated and Non-Chelated Metals for Supplying Micronutrients to Wheat Grown on Calcareous Soil. *Experimental Agriculture* **1997**, 33 (2), 237-245.

Nikolic, M.; Cesco, S.; Romheld, V.; Varanini, Z.; Pinton, R., Uptake of Iron ( $^{59}\text{Fe}$ ) Complexed to Water-Extractable Humic Substances by Sunflower Leaves. *J. Plant Nutr.* **2003**, 26 (10-11), 2243-2252.

Perkins, M. C.; Roberts, C. J.; Briggs, D.; Davies, M. C.; Friedmann, A.; Hart, C.; Bell, G., Macro and Microthermal Analysis of Plant Wax/Surfactant Interactions: Plasticizing Effects of Two Alcohol Ethoxylated Surfactants on an Isolated Cuticular Wax and Leaf Model. *Applied Surface Science* **2005**, 243 (1-4), 158-165.

Rodriguez-Lucena, P.; Tomasi, N.; Pinton, R.; Hernandez-Apaolaza, L.; Lucena, J. J.; Cesco, S., Evaluation of  $^{59}\text{Fe}$ -Lignosulfonates Complexes as Fe-Sources for Plants. *Plant Soil* **2009**, 325 (1-2), 53-63.

Rodriguez-Lucena, P.; Hernandez-Apaolaza, L.; Lucena, J. J., Comparison of Iron Chelates and Complexes Supplied as Foliar Sprays and in Nutrient Solution to Correct Iron Chlorosis of Soybean. *J. Plant Nutr. Soil Sci.* **2010a**, 173 (1), 120-126.

Rodriguez-Lucena, P.; Ropero, E.; Hernandez-Apaolaza, L.; Lucena, J. J., Iron Supply to Soybean Plants through the Foliar Application of IDHA/ $\text{Fe}^{3+}$ : Effect of Plant Nutritional Status and Adjuvants. *J. Sci. Food Agric.* **2010b**, 90 (15), 2633-2640.

Rodriguez-Lucena, P.; Benedicto, A.; Lucena, J. J.; Rodriguez-Castrillon, J. A.; Moldovan, M.; Alonso, J. I. G.; Hernandez-Apaolaza, L., Use of the Stable Isotope  $^{57}\text{Fe}$  to Track the Efficacy of the Foliar Application of Lignosulfonate/ $\text{Fe}^{3+}$  Complexes to Correct Fe Deficiencies in Cucumber Plants. *J. Sci. Food Agric.* **2011**, 91 (3), 395-404.

Roosta, H. R.; Mohsenian, Y., Effects of Foliar Spray of Different Fe Sources on Pepper (*Capsicum Annum* L.) Plants in Aquaponic System. *Scientia Horticulturae* **2012**, *146*, 182-191.

Schoenherr, J., Characterization of Aqueous Pores in Plant Cuticles and Permeation of Ionic Solutes. *Journal of Experimental Botany* **2006**, *57* (11), 2471-2491.

Schoenherr, J.; Fernandez, V.; Schreiber, L., Rates of Cuticular Penetration of Chelated Fe-III: Role of Humidity, Concentration, Adjuvants, Temperature, and Type of Chelate. *Journal of Agricultural and Food Chemistry* **2005**, *53* (11), 4484-4492.

Tagliavini, M.; Rombola, A. D., Iron Deficiency and Chlorosis in Orchard and Vineyard Ecosystems. *European Journal of Agronomy* **2001**, *15* (2), 71-92.

Ylivainio, K.; Jaakkola, A.; Aksela, R., Effects of Fe Compounds on Nutrient Uptake by Plants Grown in Sand Media with Different Ph. *Journal of Plant Nutrition and Soil Science-Zeitschrift Fur Pflanzenernahrung Und Bodenkunde* **2004**, *167* (5), 602-608.

# **Chapter 6**

---

Main Conclusions and Future Work



## 6.1 Main Conclusions and Future Work

The main objective of the present work was the evaluation of potential chelating agents for more environmental friendly practices.

Nowadays, biodegradability is an important topic regarding to the chelating agents presently used, as well as in the research of new compounds. The ready biodegradability of four chelating agents (BCIEE, EC, EMI and PDA) was evaluated according to the OECD criteria (Chapter 2). Only PDA was found to be ready biodegradable. Therefore, this compound can be considered for applications where high amounts of chelating agents are required. Since PDA is a good chelating agent for Ca, it can be used in industrial cleaning agents, cooling waters and desalination systems to inhibit scale formation. Moreover, PDA can also be used when chelation to Cd, Cu, Ni, Zn, Co and Pb is advantageous, as well as for Fe under acidic conditions.

None of the other three chelating agents (BCIEE, EC and EMI) passed the ready biodegradation test. Furthermore, all the compounds showed to be non-toxic to microorganisms (Chapter 2). Therefore, these compounds should be considered for applications in which the environmental damage that occurs from their use is low (for example when they are part of a final product, e.g., food fortification) or when the persistence of these compounds in the environment for longer periods of time is required in order to carry out the tasks for which they are used (e.g., soil remediation, fertilization). Based on this, several applications for these three chelating agents are presented and discussed in Chapter 2. All these compounds are good chelators for Cd,

Cu, Ni and Zn. Additionally, EC can be considered for chelation with Co, Ca, Mg, Mn and Pb, BCIEE for Co, and EMI for Mn ions.

A particular attention for searching for alternative chelating agents for agriculture application, as iron fertilizers, has been devoted in this Thesis. The search for potential iron chelators that could serve as iron sources to plants involved a profound evaluation of several compounds commercially available or others that based on the information given in the literature would have good iron(III) chelating properties. This evaluation was conducted either by computational methods, when the stability constants of the chelating agents in question was available, or by determination of the iron(III) solubility, in aqueous solution, in the pH range of interest. A great number of compounds were considered. As expected, azotochelin, a siderophore, and DPH, a siderophore mimic of rhodotorulic acid, were found to form stable Fe chelates, at a wide range of pH, including in the pH range of alkaline and calcareous soils.

While azotochelin is a siderophore produced by *Azotobacter vinelandii*, under iron deficiency conditions, DPH is not produced biologically. Therefore, the chelating properties of DPH, with several metal ions that can potentially interfere with the chelating agent performance as an iron fertilizer, were studied. The overall stability constant for all M-DPH-OH [M=Ca(II), Cu(II), Mg(II), Mn(II), or Zn(II)] systems were determined in aqueous solution (Chapter 3).

DPH was found to form MHL [Log  $\beta$  = 11.57, Ca(II); 18.318, Cu(II); 12.22, Mg(II); 13.52, Mn(II); 14.71, Zn(II)] and ML [Log  $\beta$  = 1.42, Ca(II); 13.898, Cu(II); 2.722, Mg(II); 3.88, Mn(II); 7.19, Zn(II)] species with all the metal ions studied. The formation of  $M_2L_3$  species was observed with Cu(II) (Log  $\beta$  = 43.11), Mn(II) (Log  $\beta$  = 16.87) and with Zn(II)

(Log  $\beta$  = 22.18). With Ca(II) and Mg(II) ions, the formation of ML(OH) species [Log  $\beta$  = 5.317, Ca(II); 6.485, Mg(II)] was also observed. Computational calculations were performed in order to evaluate the stability of the iron chelates of DPH in the presence of such metal ions, under hydroponic conditions. The iron chelates of DPH were found to be the predominant species until pH 9.5, when Hoagland solution conditions were simulated.

The ability of the iron chelates of azotochelin and DPH to supply iron to plants was assessed in hydroponic cultures (Chapter 4) or by foliar application (Chapter 5).

Azotochelin and DPH were able to supply iron to chlorotic cucumber plants, a Strategy I species, under hydroponic cultures, at the pH of calcareous soils (Chapter 4). The plants treated with the iron chelates of both compounds evidenced a clear recovery of the chlorosis symptoms. SPAD measurements during the period of the experiments corroborate the visual observations of recovery. For all samplings, the dry weight of the leaves of the treated plants with the iron chelates (10  $\mu$ M Fe) was also higher than in the untreated ones (2  $\mu$ M Fe). The iron content measured in the leaves of the plants treated with the iron chelates of azotochelin and DPH was always similar to the plants treated with EDTA/Fe<sup>3+</sup>. This value was also similar to the one measured in the plants treated with EDDHA/Fe<sup>3+</sup> in the first days after the application of the treatments (7 DAT). At the end of the experiment (21 DAT) the plants treated with *o,o*-EDDHA/Fe<sup>3+</sup> showed the highest leaf Fe content of all treatments.

Besides the environmental advantages, which may arise from the use of natural products or analogues, azotochelin and DPH should be considered as potential iron chelators to be used as iron fertilizers, due to their siderophore properties. The high selectivity of siderophores for iron(III), provides advantages over other ligands that,

like EDTA and many APCAs, show high affinity for other metal ions besides  $\text{Fe}^{3+}$ . The stability of  $\text{EDTA/Fe}^{3+}$  is affected by the presence of other metal ions (e.g.,  $\text{Ca}^{2+}$  and  $\text{Mg}^{2+}$ ), and the effectiveness of the iron chelates of EDTA is reduced due to the displacement of  $\text{Fe}^{3+}$  by other metal ions.

On the other hand, the reduction of iron(III) to iron(II) is considered an important step in the Strategy used by these plants to acquire iron from the environment. Since EDTA shows high affinity for  $\text{Fe(II)}$ , it serves as an  $\text{Fe}^{2+}$  trapping agent, preventing that most of the iron is taken by the plants. This fact was evidenced by the FCR assays (Chapter 4). When  $\text{EDTA/Fe}^{3+}$  chelate was used as substrate for the enzyme FCR, it showed much higher reduction rates than  $\text{DPH/Fe}^{3+}$  and *o,o*- $\text{EDDHA/Fe}^{3+}$  chelates. However, the iron content in the leaves of the plants treated with  $\text{EDTA/Fe}^{3+}$  was similar to the plants treated with  $\text{DPH/Fe}^{3+}$  and lower than with plants treated with *o,o*- $\text{EDDHA/Fe}^{3+}$ .

The study of azotochelin and DPH was preferred over hexadentate chelating agents, based on the assumption that tetradentate ligands, although forming less stable chelates with iron(III), are also thermodynamically easier to reduce than hexadentate siderophores commonly produced by microorganisms.

In the case of azotochelin/ $\text{Fe}^{3+}$ , it was not possible to determine the rate of reduction by FCR, although the FCR assays provided evidences that the reduction occurred.

The determination of Cu and Mn concentration in the leaves of the plants treated with the iron chelates (10  $\mu\text{M}$  Fe) and the control plants (2  $\mu\text{M}$  Fe) revealed that the uptake of those cations was affected by the uptake of iron by the plants. In the control plants, the uptake of Cu and Mn was favored. Such results suggest the



involvement of the Iron Regulated Transporter 1 (IRT1), not only in the uptake of iron, but also in the absorption, by the roots, of other cations. However, since the way how plants use iron from siderophores is not fully understood, other mechanisms for the iron uptake from these compounds, (e.g., the direct uptake of the iron chelate), specially by different plant species, must not be discarded and should be considered/evaluated in further studies.

The effectiveness of the foliar application of the iron chelates of azotochelin and DPH, as a Fe source to soybean plants grown in hydroponic cultures, was also studied (Chapter 5). The foliar sprays of DPH/Fe<sup>3+</sup> chelate were able to deliver Fe to soybean plants showing chlorotic symptoms but it was only observed the translocation of Fe to the roots and not to the growing leaves. The same results were observed in the plants treated with foliar sprays of EDTA/Fe<sup>3+</sup> chelate and with *o,o*-EDDHA/Fe<sup>3+</sup>, but not with azotochelin/Fe<sup>3+</sup> chelates, for which no evidences of Fe uptake by the plants were observed.

The lower concentration of Mn in the roots of the plants treated with the iron chelates of DPH, EDTA and *o,o*-EDDHA, also suggested the uptake and translocation of iron to the roots, when those treatments were used.

Further studies must be conducted, under different conditions, in order to evaluate the potential use of the chelating agents under consideration in this Thesis as sources of Fe by foliar application. The effectiveness of foliar application of Fe chelates depends on several factors involved in the processes of leaf penetration, plant translocation and uptake of Fe by the cell, which are not well understood. Moreover, the suitable foliar fertilizer formulations are difficult to specify and are certainly different for each compound used. The results obtained in this work suggest that

different conditions might be required for each DPH and azotochelin. Among others, the adjuvant used, the pH, number and time of foliar applications, concentration of the iron chelates, plant species, and level of severity of chlorosis at the time of the application are known to be determinant to the effectiveness of foliar applications of iron chelates. Further work must be conducted in order to evaluate if azotochelin is able to deliver iron to plants by foliar application of its iron chelate. In the case of the foliar application of DPH/ $\text{Fe}^{3+}$ , the translocation of iron to growing leaves, either than to the roots, must be verified.

